SKB

TECHNICAL REPORT 97-33

Determination of radionuclide solubility limits to be used in SR 97

Uncertainties associated to calculated solubilities

Jordi Bruno[1], Esther Cera[1], Joan de Pablo[2],
Lara Duro[1], Salvador Jordana[1], David Savage[3]

1 QuantiSci S.L., Barcelona, Spain
2 DEQ-UPC, Barcelona, Spain
3 QuantiSci, Henley, UK

December 1997

SVENSK KÄRNBRÄNSLEHANTERING AB
SWEDISH NUCLEAR FUEL AND WASTE MANAGEMENT CO

P.O.BOX 5864 S-102 40 STOCKHOLM SWEDEN
PHONE +46 8 665 28 00
FAX +46 8 661 57 19

DETERMINATION OF RADIONUCLIDE SOLUBILITY LIMITS TO BE USED IN SR 97

UNCERTAINTIES ASSOCIATED TO CALCULATED SOLUBILITIES

Jordi Bruno[1], Esther Cera[1], Joan de Pablo[2], Lara Duro[1], Salvador Jordana[1], David Savage[3]

1 **QuantiSci S.L., Barcelona, Spain**
2 **DEQ-UPC, Barcelona, Spain**
3 **QuantiSci, Henley, UK**

December 1997

DETERMINATION OF RADIONUCLIDE SOLUBILITY LIMITS TO BE USED IN SR 97.

UNCERTAINTIES ASSOCIATED TO CALCULATED SOLUBILITIES

Jordi Bruno[1], Esther Cera[1], Joan de Pablo[2], Lara Duro[1], Salvador Jordana[1], David Savage[3]

[1]QuantiSci S.L., Barcelona, Spain [2] DEQ-UPC, Barcelona, Spain
[3]QuantiSci, Henley, UK

December 1997

Keywords: Solubilities, Radionuclides, Uncertainties

ABSTRACT

The thermochemical behaviour of 24 critical radionuclides for the forthcoming SR97 PA exercise is discussed. The available databases are reviewed and updated with new data compiled by Nagra and SKB, and an extense database for aqueous and solid species of the radionuclides of interest is proposed.

We have performed speciation calculations for the studied radionuclides under different groundwater composition. We have identified the most important aqueous ligands for each radionuclide and in this report we present the study of their relative importance by using conditional stability constants.

We have calculated solubility limits for the radionuclides of interest under different groundwater compositions. With this aim, three groundwater compositions: Äspö, Gidea and Finnsjon, as well as a bentonite porewater have been selected. A sensitivity analysis of the calculated solubilities with the composition of the groundwater is presented. Besides selecting the most likely solubility limiting phases, in this work we have used coprecipitation approaches in order to calculate more realistic solubility limits for minor radionuclides, such as Ra, Am and Cm.

The comparison between the calculated solubilities and the concentrations measured in relevant natural systems (NA) and in spent fuel leaching experiments helps to assess the validity of the methodology used and to derive source term concentrations for the radionuclides studied.

The uncertainties associated to the solubilities of the main radionuclides involved in the spent nuclear fuel have been also discussed in this work. The variability of the groundwater chemistry; redox conditions and temperature of the system have been considered the main factors affecting the solubilities. In this sense, a sensitivity analysis has been performed in order to study solubility changes as a function of these parameters. The uncertainties have been calculated by including the values found in a major extent in typical granitic groundwaters.

The results obtained from this analysis indicate that there are some radionuclides which are not affected by these parameters, i.e. Ag, Pa, Pd, Ra, Th and Zr, but in general most of these radionuclides are strongly affected by at least one of the parameters considered, i.e. Am, Cm, Ho, Nb, Ni, Np, Pu, Se, Sm, Sn, Sr, Tc and U.

SAMMANFATTNING

I den här rapporten diskuteras de termokemiska egenskaperna hos 24 kritska radionuklider, som ett bakgrundsmaterial inför säkerhestanalysen SR 97. De tillgängliga databaserna har granskats och en ny omfattande databas med lösta specier och fasta faser för de aktuella radionukliderna har producerats.

Specieringsberäkningar har genomförts för de studerade radionukliderna för olika grundvattensammansättningar. De viktigaste liganderna för varje radionuklid har identifierats och deras relativa betydelse har jämförts med hjälp av konditionella stabilitetskonstanter.

Lösligheterna för radionukliderna har beräknats för olika grundvatten-sammansättningar. Tre naturliga sammansättningar har valts: typiska vatten från Äspö, Finnsjön och Gideå tillsammans med ett antaget bentonitporvatten. I rapporten presenteras också en känslighetsstudie för lösligheterna som funktion av grundvattnens sammansättning. Förutom urvalet av de mest troliga löslighetsbegränsande fasta faserna, diskuteras också medfällningprocesser som ett medel att beräkna mer realistiska lösligheter för nuklider med små inventarier, t ex Ra, Am och Cm.

En jämförelse mellan de beräknade lösligheterna och mätta koncentrationer från relevanta naturliga system och bränslelakförsök har gjorts för att bedöma metodikens validitet och för att bestämma källtermskoncentrationer för de studerade nukliderna.

Osäkerheterna kopplade till radionuklidernas lösligheter diskuteras också i rapporten. Grundvattensammansättningens variabilitet, redoxförhållanden och temperatur har identifierats som de faktorer som har störst betydelse för lösligheten. En sensitivtetsanalys har genomförts för att visa hur lösligheten påverkas av förändringar i dessa parametrar. Känslighetsstudien visar att vissa radionuklider är i stort sett opåverkade av förändringar, men de flesta är mycket känsliga för förändringar av åtminstone en av parametrarna.

TABLE OF CONTENTS

1 INTRODUCTION

SKB is at present preparing a Performance Assessment exercise of its HLNW repository concept. The calculation of solubility limits for the main radionuclides of the spent fuel is necessary to constrain the possible migration of these radionuclides in the near and far fields.

There have been previous efforts in order to stablish source term radionuclide concentrations by using chemical equilibrium calculations (Bruno and Sellin, 1992, Berner, 1994).

In this work we attempt to build on recent developments in the determination of radionuclide solubility limits by incorporating:

a) Recently selected thermodynamic data for critical radionuclides. The original thermodynamic data used has been taken from the NTB91-17 and 91-18 databases, plus iron minerals and magnesite. Uranium data from Puigdomenech & Bruno (1988); plutonium data from Puigdomenech & Bruno (1991); technetium data from Puigdomenech & Bruno (1995); REE data from Spahiu & Bruno (1995) and neptunium data from Spahiu (1996). However, some modifications have been done, after checking the thermodynamic databases available (Hatches v.7.0) and according to a review exercise of the concerning literature (Baes and Mesmer, 1976, Lemire and Garisto, 1989, Puigdomènech and Bruno, 1991, Grenthe et al., 1992, Eriksen et al., 1993, Östhols, 1994, Silva et al., 1995, Spahiu and Bruno,1995). We have called this database as Nagra/SKB-97-TDB. See also chapter 10.

b) The experiences extracted from trace element geochemical investigations and modelling at various Natural System Studies, i.e. Poços de Caldas (Bruno et al., 1992), Cigar Lake (Bruno and Casas, 1994), El Berrocal (Bruno et al., 1996) and others.

c) To incorporate for minor elements like Cm and Ra the conditional solubilities approach recently developed (Bruno et al., 1995).

Furthermore, the uncertainties associated to groundwater chemical parameters as well as their associated thermodynamic data are discussed and calculated.

2 METHODOLOGY

The following table (Table 2-1) includes the radionuclides selected for this study (SR 95). Radionuclides have been ordered by increasing atomic number.

Table 2-1. List of radionuclides studied in this exercise.

Carbon	Technetium	Radium
Choride	Palladium	Thorium
Nickel	Silver	Protactinium
Selenium	Tin	Uranium
Kripton	Iodine	Neptunium
Strontium	Caesium	Plutonium
Zirconium	Samarium	Americium
Niobium	Holmium	Curium

The procedure followed to perform this work is as follows.

First, we have attempted to rank the different radionuclide natural water ligand interactions by comparing their relative strength. This has been done by applying the conditional constant approach developed by Ringbom (1963). This approach originally developed for analytical chemistry applications has been adapted to our specified purposes.

The information obtained in this part of the work has been completed and contrasted with the results obtained from sensitivity analysis calculations. They have been performed in order to study the effect of the main chemical parameters on radionuclide solubilities and speciation by using computer aided chemical equilibrium calculations (Puigdomènech, 1983).

Secondly, an extensive literature study of the occurrence and concentration of radionuclides in natural systems has been carried out to provide information of radionuclide contents and occurrence in natural waters as reference to our calculations.

Thirdly, we have done a summary of spent fuel dissolution experiments performed in the recent years with radionuclide concentrations determined in such tests. This information provides another reference level to the present calculations.

Finally, radionuclides solubility limits have been calculated by using the EQ3NR (Wolery, 1992) code package. Three different groundwaters have been studied, two typical granitic groundwaters and a bentonite pore water which simulates groundwater composition after entering in contact with the

bentonite buffer in a repository system. Thermodynamic databases have been checked and updated to perform the calculations.

The calculated solubility values have been discussed and compared with both measured values in natural systems and determined radionuclide concentrations in spent fuel dissolution experiments in order to check the sanity of the calculations performed and to provide realisticaly conservative values to the Performance Assessment exercise.

In a first step we have established the radionuclide solubility uncertainty ranges associated to the determination of the main groundwater parameters, pH, Eh and bicarbonate content.

At the end, we have established the uncertainty ranges associated to the main parameters affecting radionuclide solubilities, these parameters have been, chemical composition of the groundwater, i.e. pH and carbonate content and redox conditions and temperature of the system.

3 CONDITIONAL CONSTANTS

The conditional constant approach was introduced by Ringbom in 1963 (Ringbom, 1963) in order to study the effect of side reactions in analytical determinations. In this sense, the equilibrium constant of the main reaction which allows the analite determination is recalculated taking into account the stability constants of side reactions as well as the ionic medium.

This methodology can be applied in multicomponent systems to evaluate the relevant species (complexes and solids) which have to be considered in the performance assessment.

The calculations of conditional constants have been performed by using the Äspö groundwater composition given in Table 7-1, with a moderate salinity and a relatively low carbonate content (SR 95, 1995).

The databases considered to perform the calculations have been the same as in the equilibrium calculations (Section 4).

The procedure followed to calculate the conditional constants is illustrated in the next example. In such case, we describe the calculation of the conditional constants for complex and solid formation in the system Americium Äspö groundwater.

By considering this system, the main aqueous complexes to take into account are:

$AmOH^{2+}$, $Am(OH)_2^{+}$, Am(OH) (aq), $AmCl^{2+}$, $AmSO_4^{+}$, $Am(SO_4)_2^{-}$, $AmCO_3^{+}$, $Am(CO_3)_2^{-}$, $Am(CO_3)_3^{3-}$, $AmH_2PO_4^{2+}$, $AmHPO_4^{+}$

If we take the reaction:

$$Am^{3+} + CO_3^{2-} = AmCO_3^{+} \qquad 3\text{-}1$$

We can writte its conditional constant (K') as:

$$\log K' = \log K - \log \alpha_{Am} - \log \alpha_{CO3} \qquad 3\text{-}2$$

where:

$$\alpha_{Am}=\{[Am^{3+}] + [AmOH^{2+}] + [Am(OH)_2^{+}] + [Am(OH)_3(aq)] + [AmCl^{2+}] + [AmSO_4^{+}] + [Am(SO_4)_2^{-}] + [Am(CO_3)_2^{-}] + [Am(CO_3)_3^{3-}] + [AmH_2PO_4^{2+}] + [AmHPO_4^{+}]\} / [Am^{3+}]$$

and

$$\alpha_{CO3}=\{[CO_3^{2-}] + [HCO_3^{-}] + [H_2CO_3] + [CaCO_3] + [CaHCO_3] + [MgCO_3] + [MgHCO_3]\} / [CO_3^{2-}]$$

In the same way, the main solid phases considered in this system are:

$Am(OH)_3(am)$, $Am(OH)_3(s)$, $AmPO_4(s)$, $Am_2(CO_3)_3(s)$, $AmOHCO_3(s)$

and by taking for instance the dissociation reaction:

$$AmPO_4(s) = Am^{3+} + PO_4^{3-} \qquad 3\text{-}3$$

we can write the conditional constant (K'_{so}) as

$$\log K'_{so} = \log K_{so} + \log\alpha_{Am} + \log \alpha_{PO4} \qquad 3\text{-}4$$

where:

$\alpha_{PO4}=\{[PO_4^{3-}] + [HPO_4^{2-}] + [H_2PO_4^{-}] + [H_3PO_4] + [MgPO_4^{-}] + [MgHPO_4] + [MgH_2PO_4^{+}]\} / [PO_4^{3-}]$

This approach can be applied to all the soluble complexes and solids.

In the following sub-sections the results of these calculations for aqueous and solid speciation are given in different graphs for each element.

The ligands involved in the aqueous species taken into account in the calculations are numbered in the X axis. The Y axis gives the logarithm of the conditional constant calculated. The conditional constants are named with a subindex. The first number of this subindex indicates the number of metals and the second one gives the number of ligands, all of them involved in the species defined.

Dotted lines give a range of three logarithmic units in the conditional constants values in order to constrain an area as an easier way to compare the values obtained. Complexes included in this area can be considered dominant species in the system under study.

Following the graphs, a brief comment of the results is given for each element studied.

3.1 NICKEL

Aqueous speciation.

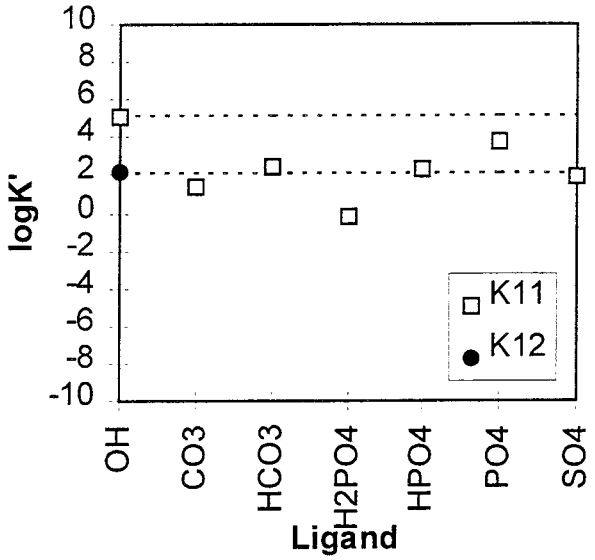

Solid phases.

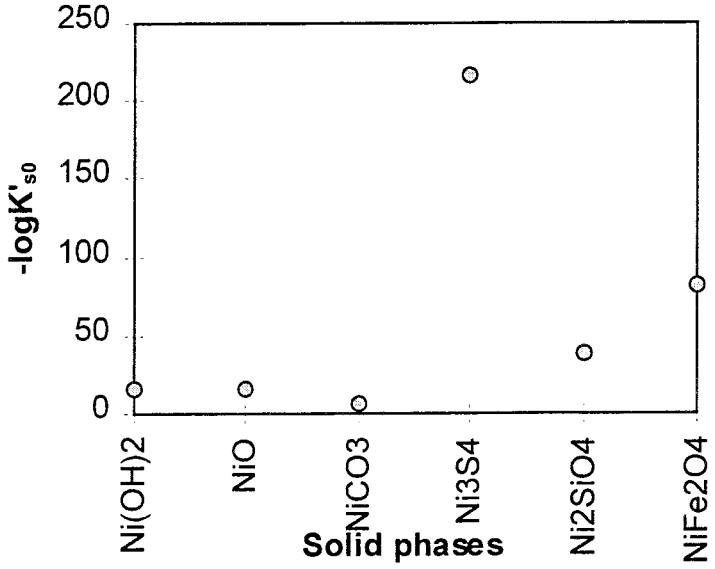

The low stability constants of the aqueous species imply similar conditional constants, therefore, we can expect that this radionuclide will be sensitive to changes in groundwater composition.

Under reducing conditions the conditional constant of Ni_3S_4 determines the system while under oxidising conditions the system seems less defined, in such case trevorite ($NiFe_2O_4$) would be a priori the most stable solid phase (if formed at low temperatures).

3.2 STRONTIUM

Aqueous speciation.

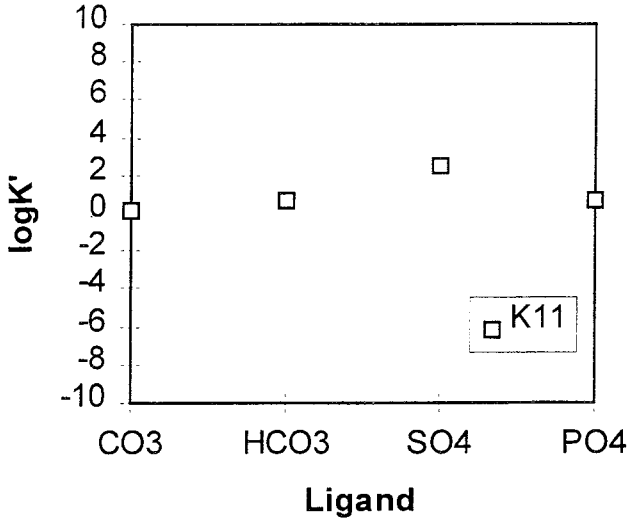

Solid phases.

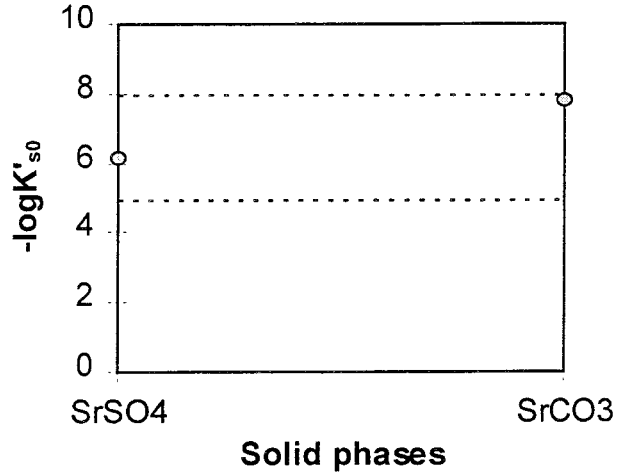

The stability constants of aqueous species are also very low, conditional constants indicate the strontium sulphate as the predominant aqueous species.

Both carbonate and sulphate solid phases are important depending on the sulphate/carbonate ratio.

3.3 ZIRCONIUM

Aqueous speciation.

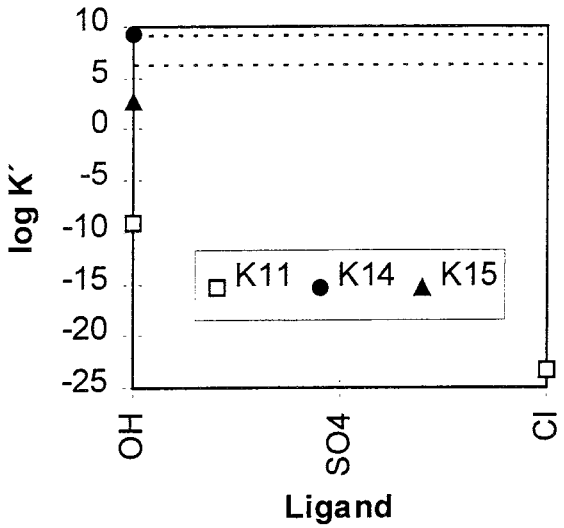

The relative strength of Zr(IV)-hydroxo complexes would indicate that these are the dominant aqueous species.

ZrO_2(c) is the predominant solid phase according to the conditional constants calculation.

3.4 TECHNETIUM

Aqueous speciation.

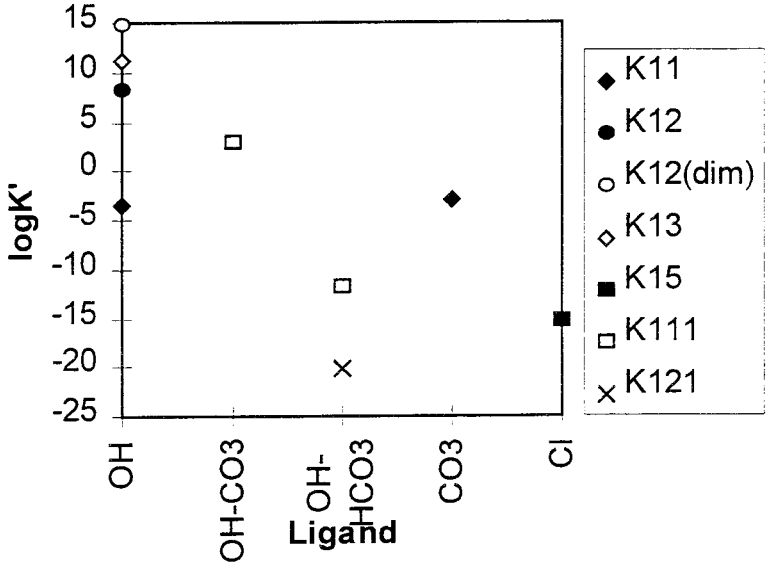

The high stability constants of the hydroxo complexes dominate the values of the conditional constants.

The large value for the conditional constant of the $[TcO(OH)_2]_2(aq)$ complex indicates its predominance.

$TcO_2(s)$ is the dominant solid phase according to the conditional constants calculation.

3.5 PALLADIUM

Aqueous speciation.

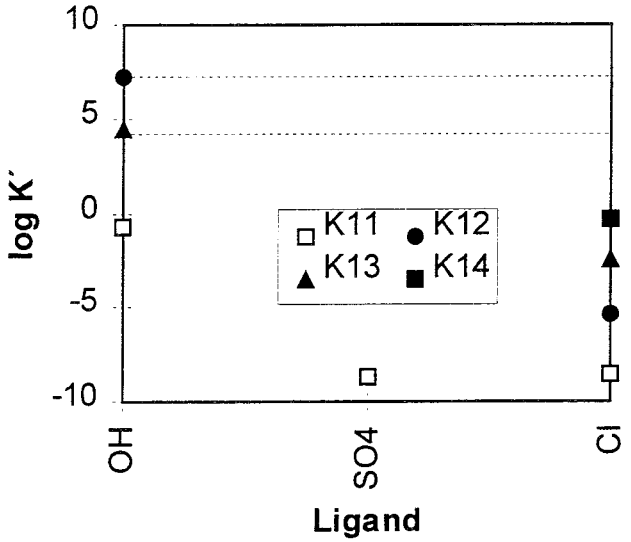

Solid phases.

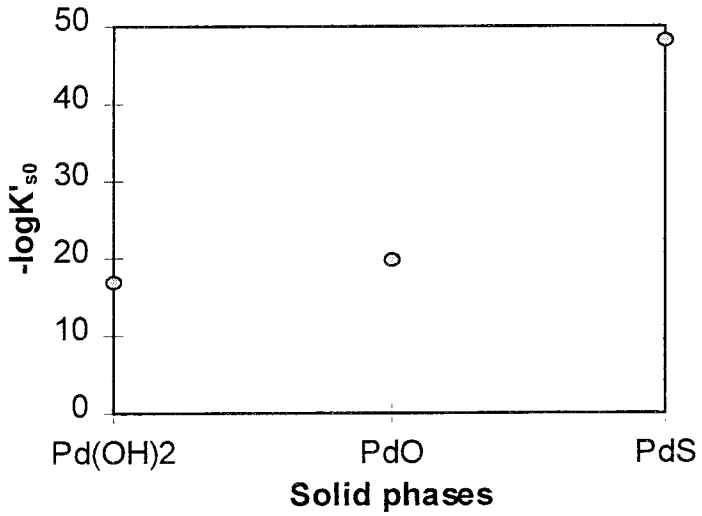

The hydroxocomplexes have the higher conditional constants and consequently, these species dominate under the present conditions.

Under reducing conditions PdS is the predominant solid phase while the Pd(II)-hydroxide/oxide are the predominant ones under oxidising conditions.

3.6 SILVER

Aqueous speciation

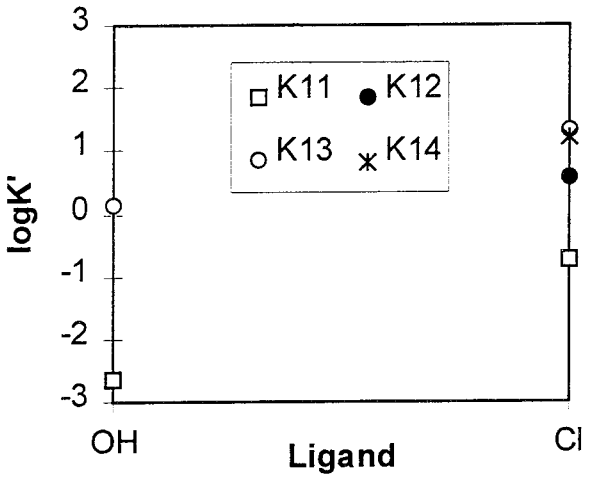

Solid phases.

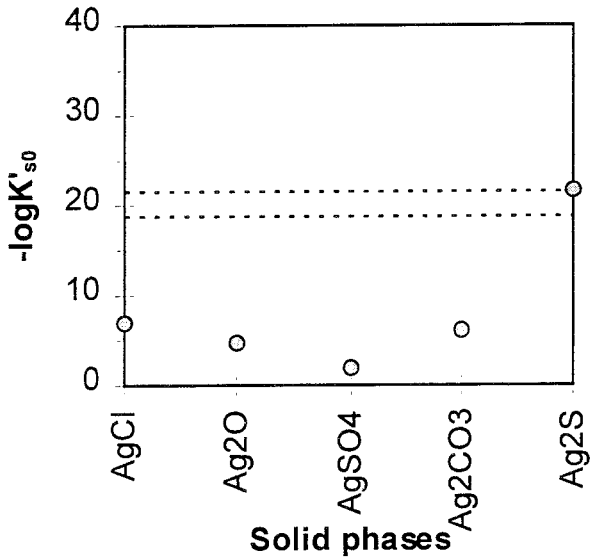

The relative high content of chloride in the reference groundwater results on a large conditional constant for the tetrachlorocomplex.

Under reducing conditions Ag_2S is the predominant solid while AgCl is the predominant one under oxidising conditions.

3.7 TIN

Tin aqueous speciation has been studied separately depending on the oxidation state due to the difficulties to calculate the conditional constants including redox processes. According to the sensitivity analysis performed in the next section (Section 4), the predominant aqueous speciation in the Äspö groundwater will be dominated by the IV-valence state.

Aqueous speciation.

Tin (II)

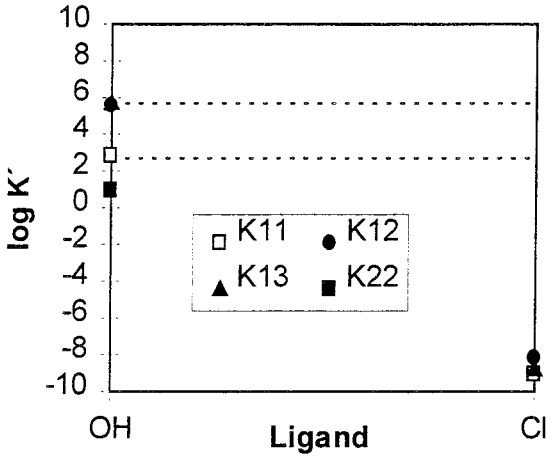

Tin (IV)

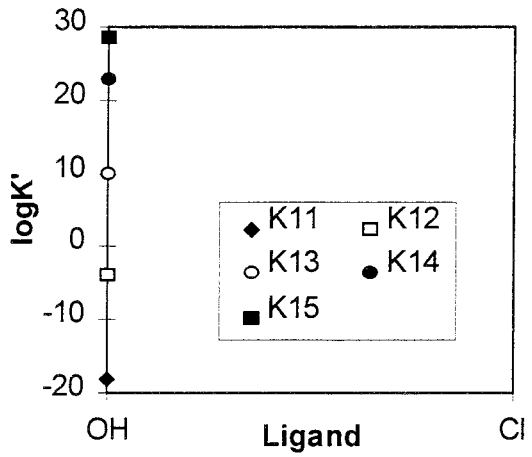

Solid phases.

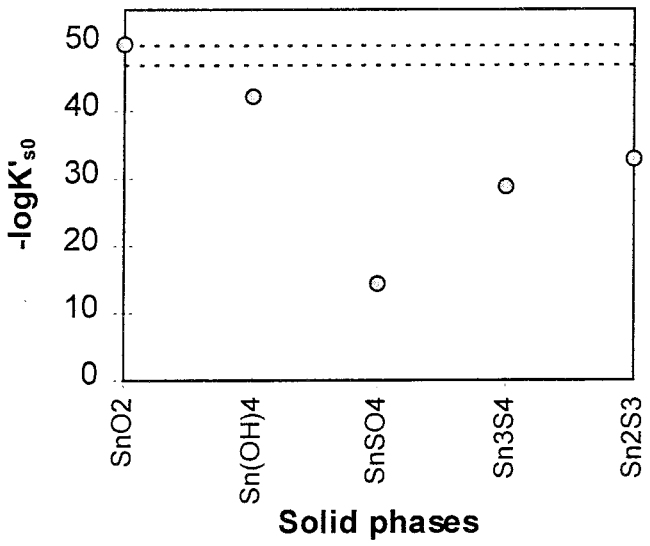

Sn(II) and Sn(IV)-hydroxo complexes are the predominant aqueous species according to the conditional constant calculations made.

Under reducing conditions sulphides are the predominant solid phases while Sn(IV) oxide is the predominant one under oxidising conditions.

3.8 SAMARIUM

Aqueous speciation.

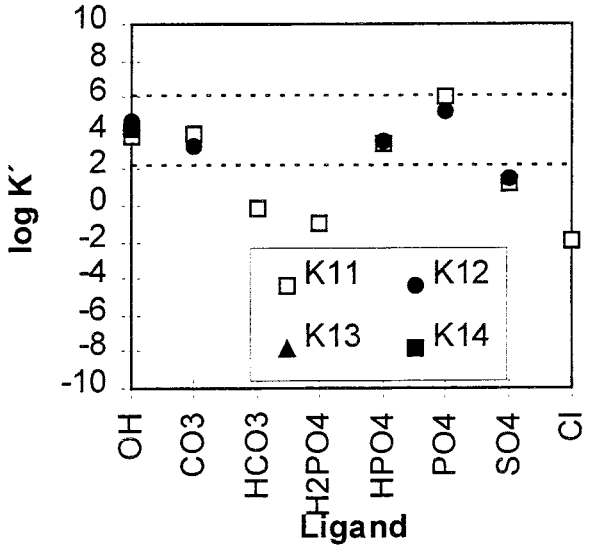

Solid phases.

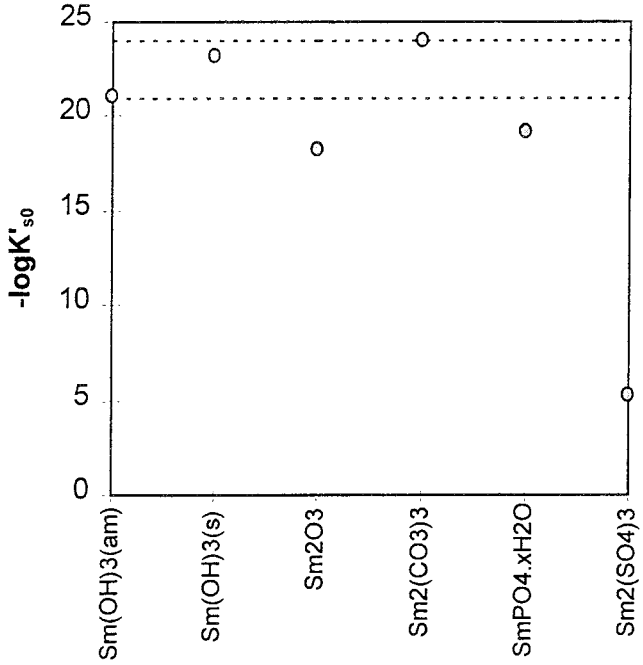

The conditional constant calculations reflect the fact that Sm(III) complexes with groundwater ligands are of similar strength. This would imply that this radionuclide is sensitive to groundwater compositional changes.

Sm(III)-hydroxide and carbonate are the predominant solid phases according to the calculations performed.

3.9 HOLMIUM

Aqueous speciation.

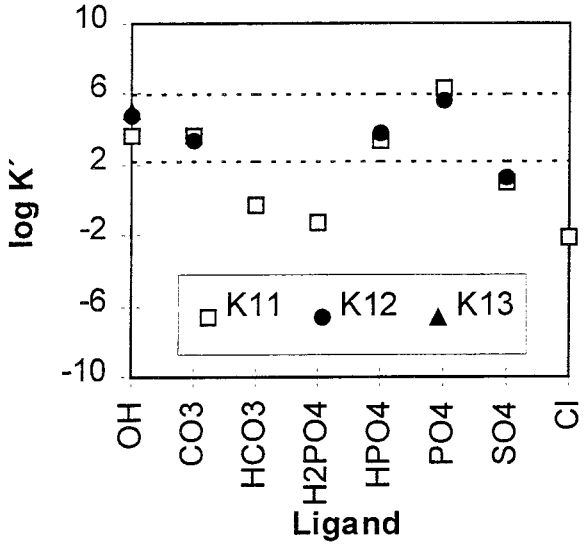

Solid phases.

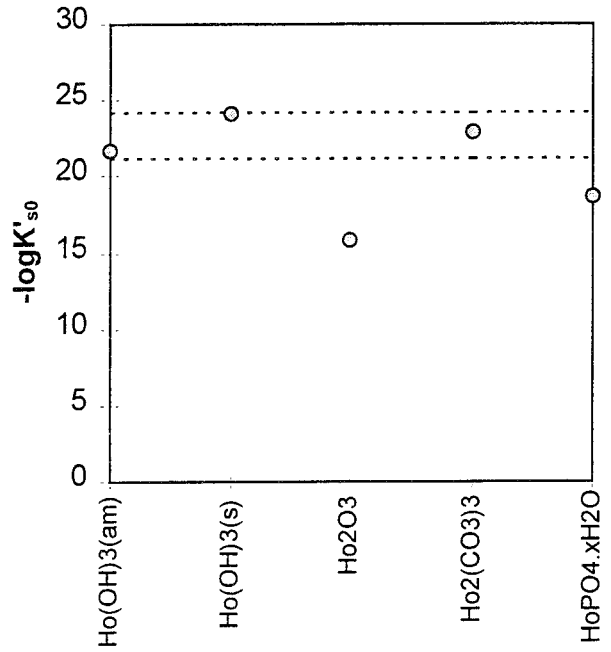

The conditional constant calculations reflect the fact that Ho(III) complexes with groundwater ligands are of similar strength. This would imply that this radionuclide is sensitive to groundwater compositional changes.

Ho(III)-hydroxide and carbonate are the predominant solid phases as in the previous case under study.

3.10 RADIUM

Aqueous speciation.

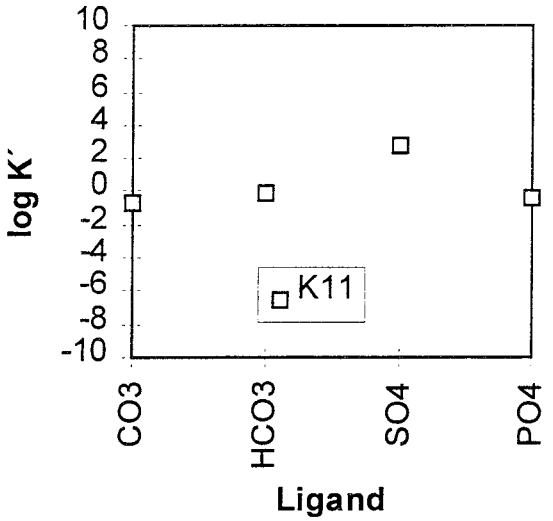

Solid phases.

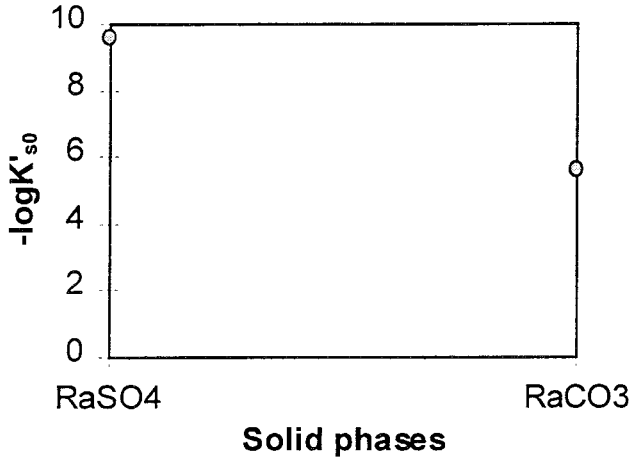

The calculated conditional constants are small. This implies the predominance of the free Ra^{2+} cation and that radium sulphate would be the dominant portion of the complexed Ra(II).

As in the case of strontium, both Ra(II)-carbonate and sulphate solid phases could be important depending on the groundwater composition under study. Therefore, this radionuclide is also sensitive to groundwater compositional changes.

3.11 THORIUM

Aqueous speciation.

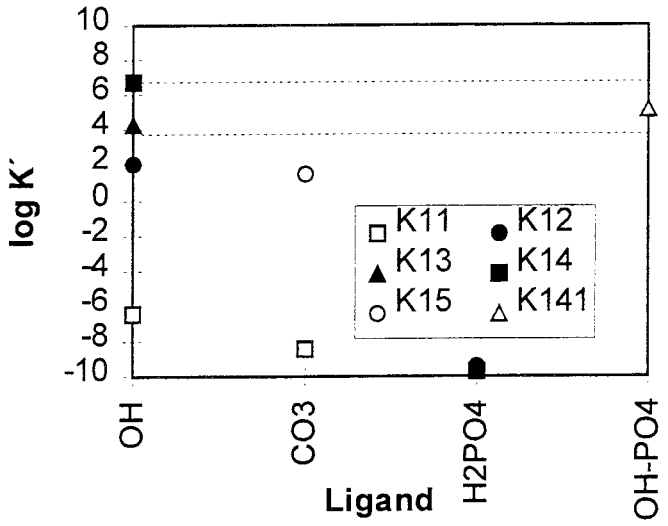

Conditional constants indicate the predominance of hydroxocomplexes. At higher phosphate content in the groundwater, hydroxophosphate complexes could be important.

ThO_2 is the predominant solid phase according to these calculations.

3.12 URANIUM

Uranium has been studied separately depending on the oxidation state in order to distinguish between predominant aqueous and solid phases under reducing and oxidising conditions.

Aqueous speciation.

Uranium (IV)

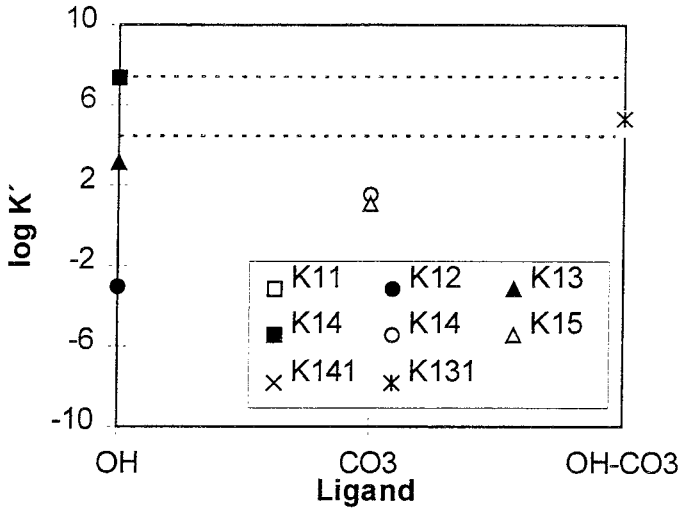

Uranium (VI)

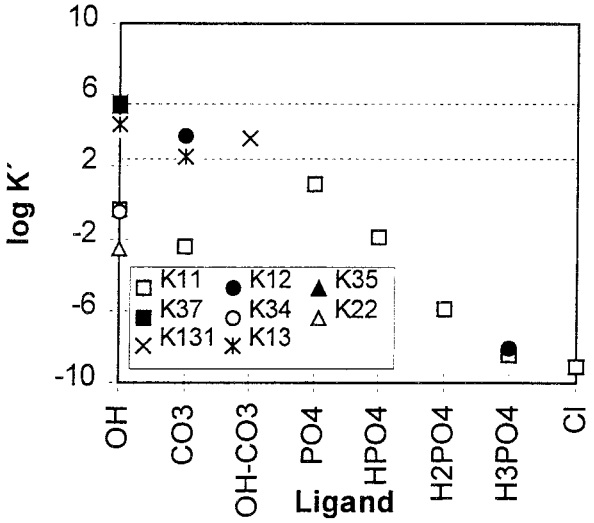

According to the conditional constant calculations, the aqueous speciation of uranium is dominated by $U(OH)_4(aq)$ under reducing conditions, while OH^- and CO_3^{2-} complexes dominate the aqueous speciation under oxic conditions.

Solid phases.

Uranium (IV)

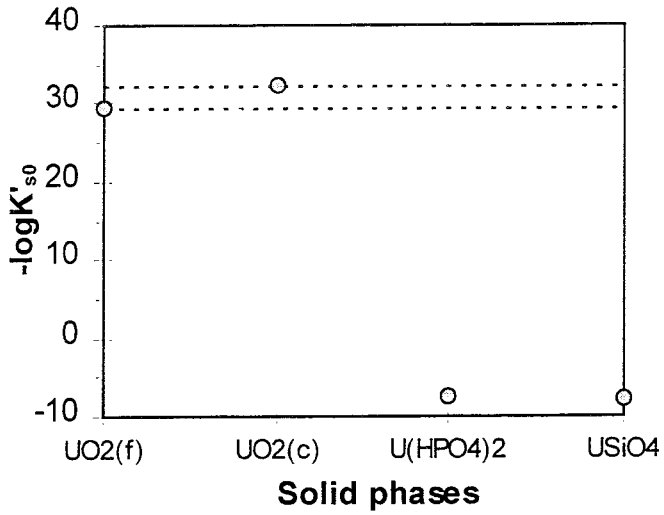

Uranium (VI)

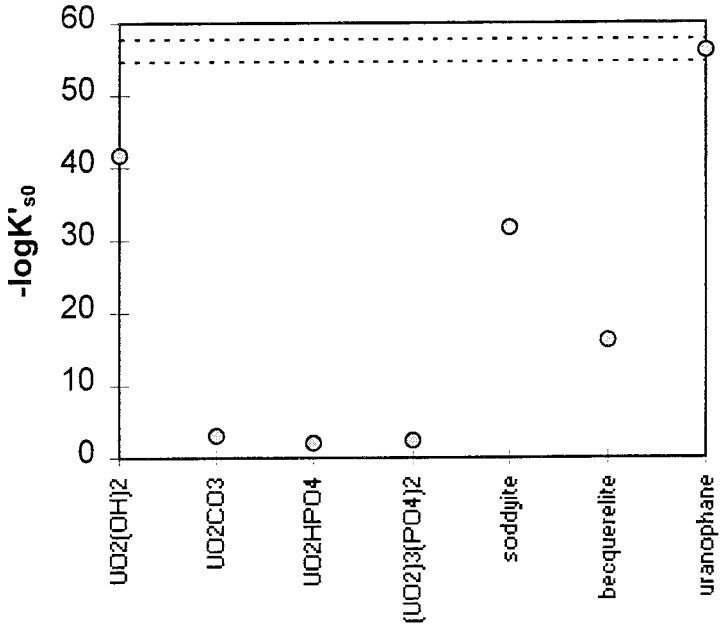

The various UO_2 morphologies dominate the solid speciation of uranium under reducing conditions. The conditional constant calculations would indicate that $UO_2(OH)_2$, soddyite and uranophane are the dominant U(VI) solid phases under oxic conditions.

3.13 NEPTUNIUM

As in the case of uranium, this element has been studied separately depending on the oxidation state considered.

Aqueous speciation.

Neptunium (IV)

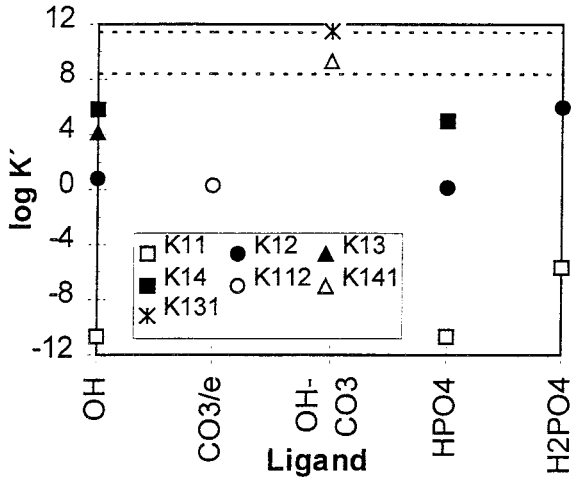

Neptunium (V)

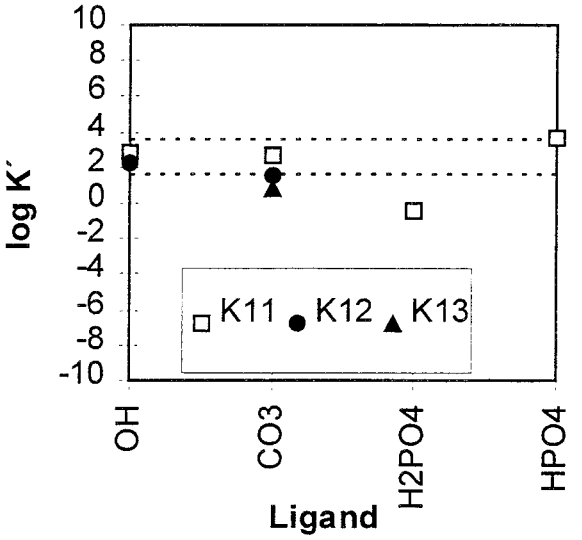

According to the conditional constant calculations Np(IV) hydroxo-carbonato complexes dominate the aqueous speciation under reducing conditions. The relatively similar and small conditional constant values for Np(V) would imply that this radionuclide is sensitive to groundwater compositional changes under oxic conditions.

Solid phases.

Neptunium (IV)

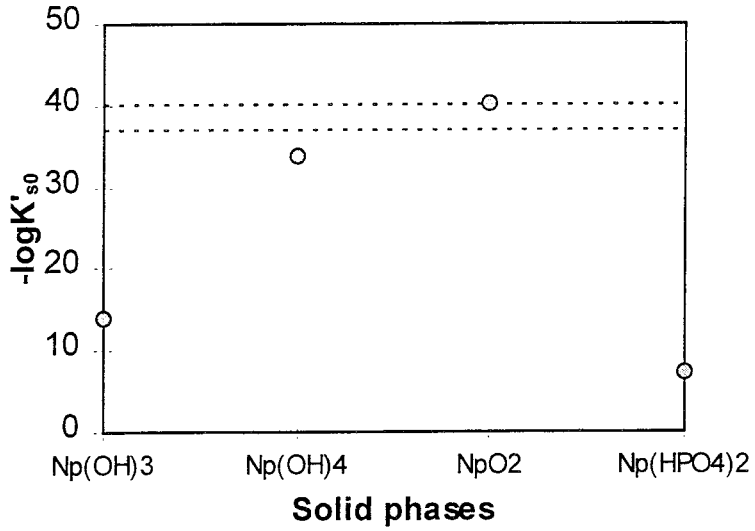

Neptunium (V)

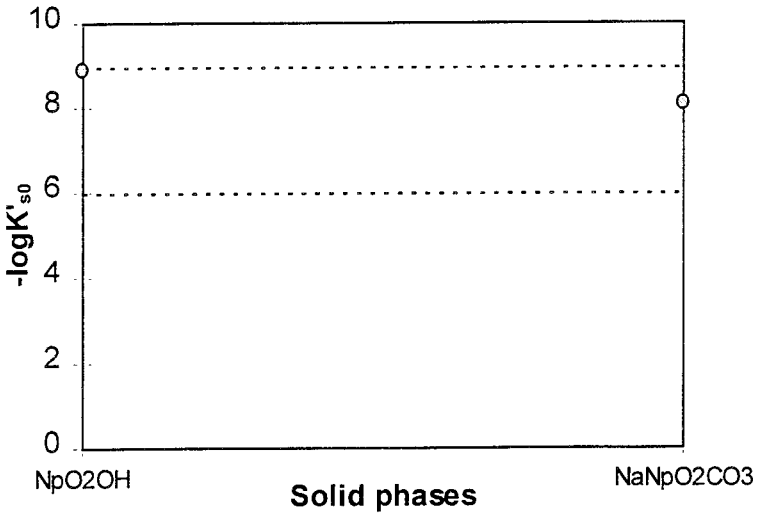

In anoxic conditions Np(IV)-oxide and hydroxide solid phases are the predominant while Np(V)-hydroxide and carbonate solid phases are the dominant under oxic conditions.

3.14 PLUTONIUM

Aqueous speciation.

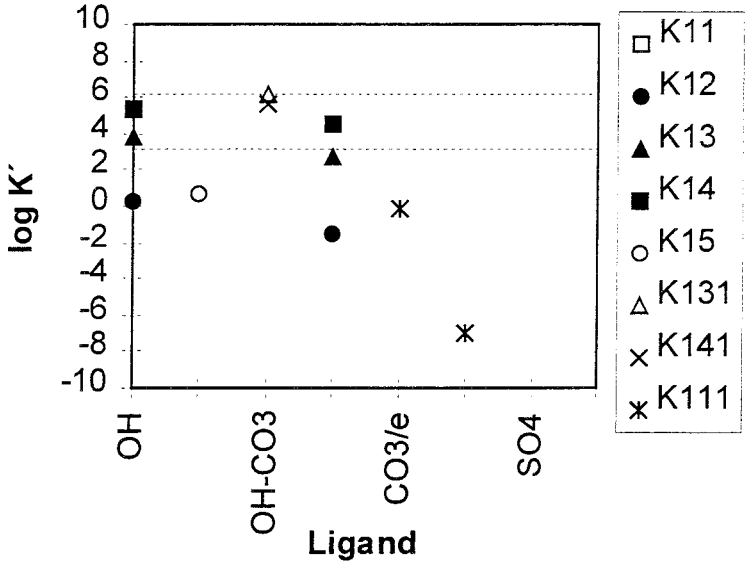

Solid phases.

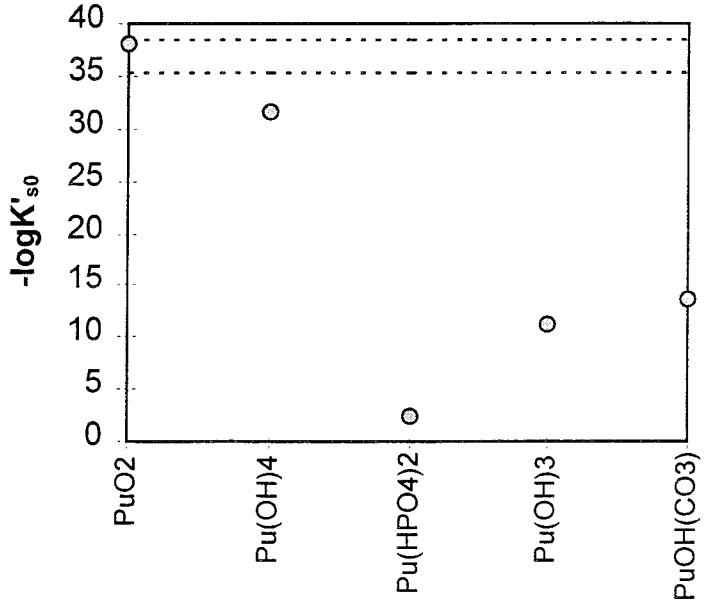

Pu(IV) hydroxo and hydroxo-carbonato complexes are the dominant aqueous species in the redox range considered in the conditional constant calculations.

Pu(IV) oxide and hydroxide are the dominant solid phases according to the results obtained from the calculations.

3.15 AMERICIUM

Aqueous speciation.

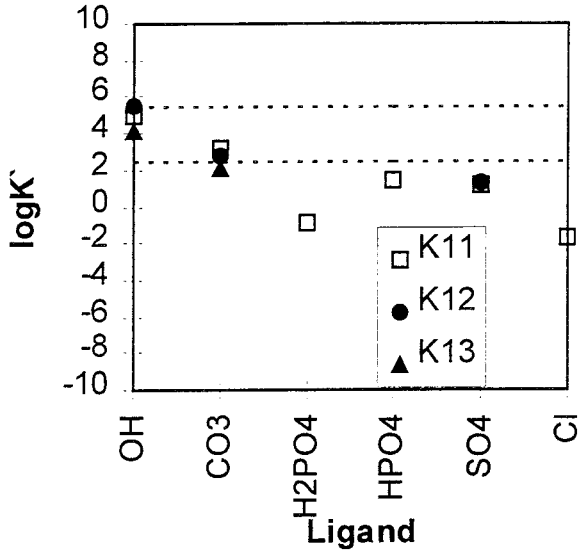

Solid phases.

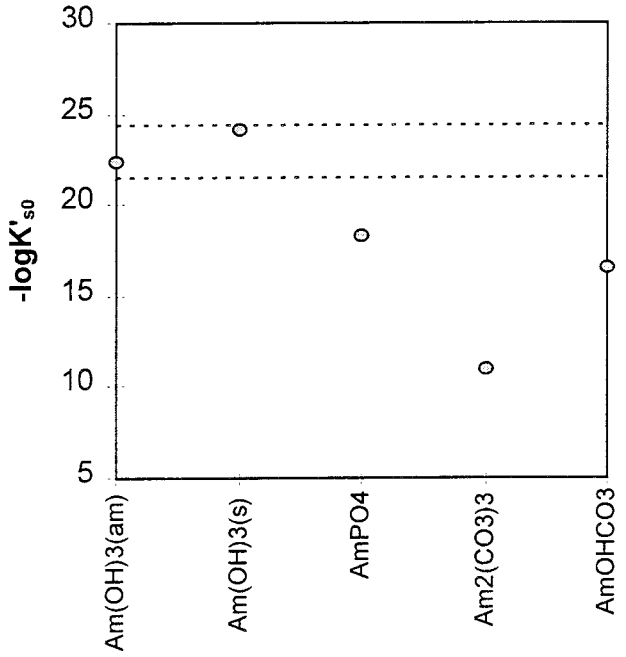

Am(III)-hydroxide and carbonate aqueous complexes and Am(III)-hydroxide solid phases dominate in this system within the present groundwater composition. However, the similarity between calculated aqueous conditional constants would imply that Am(III) speciation is sensitive to groundwater compositional changes.

3.16 CURIUM

Aqueous speciation can be considered similar to Am and Eu and therefore we expect the same predominant aqueous species due to the analogies in chemical behaviour.

Solid speciation.

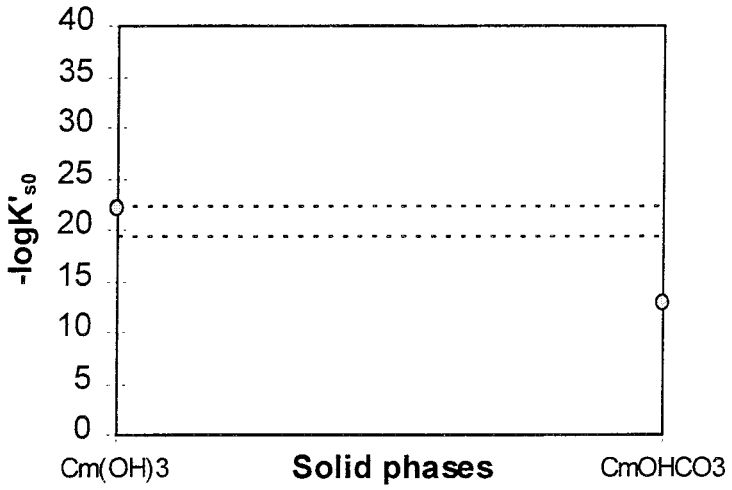

The predominant solid phases will be $Cm(OH)_3$ and $CmOHCO_3$ in analogy with americium.

4 SENSITIVITY ANALYSIS ON RADIONUCLIDE AQUEOUS AND SOLID SPECIATION DEPENDING ON GROUNDWATER COMPOSITION

To complement the calculation of the conditional constants performed in the previous section, a sensitivity analysis of the effect of the main physico-chemical parameters on radionuclide solubilities and speciation has been done by using chemical equilibrium calculations.

For this purpose, both fractional and predominance diagrams, as a function of pH and pe master variables, as well as the groundwater chemical composition have been calculated by using the HALTAFALL based INPUT/SED/PREDOM code package developed by Puigdomènech (1983). The main thermodynamic database used has been selected from the Nagra reports NTB91-17 and 91-18, and data for iron minerals and magnesite has been added.

The groundwater composition used in these calculations corresponds to the Äspö groundwaters (SR 95), which is a water composition of a typical granitic environment and has been previously used to perform conditional constants calculations. Their composition is given in Table 7-1.

Input metal concentrations have been set at 10^{-6} mol·dm^{-3} or close to their solubility limits, these cases are specified in the diagrams. No activity factor corrections have been done in these calculations.

In general, we have a good agreement between results obtained from conditional constants and chemical equilibrium calculations. However, some discrepancies have been detected concerning the stability of some hydroxocarbonate aqueous and solid species of some elements studied, i.e., Np, Am and Cm. One of the reasons for these discrepancies might be the different calculation methodology since the sensitivity of the conditional constants approach to multiple side reactions is lower than the one of the computer aided equilibrium calculations.

In the following sub-sections aqueous and solid speciation are given for each element, some comments are reported concerning the selection of the database which arised during the calculations.

Consequently, this exercise with the calculation of conditional constants presented in the previous section has been used to check thermodynamic databases available (EQ3/NTB91-17, 91-18 and Hatches v.7.0 (Cross and Ewart, 1989) as well as to perform a review exercise of the concerning literature. Finally, we have updated the NTB thermodynamic database according to the whole information collected, to perform the final solubility

calculations with the EQ3NR code (Wolery, 1992). As we mentioned before, the Nagra/SKB-97-TDB is used for all elements and is described in chapter 10.

4.1 CARBON

Not solubility limited.

4.2 CHLORIDE

Not solubility limited.

4.3 NICKEL

Sulphide solid phases have not been considered in the calculations since it is not possible to guarantee a sufficient supply of sulphides to the system.

Aqueous speciation.

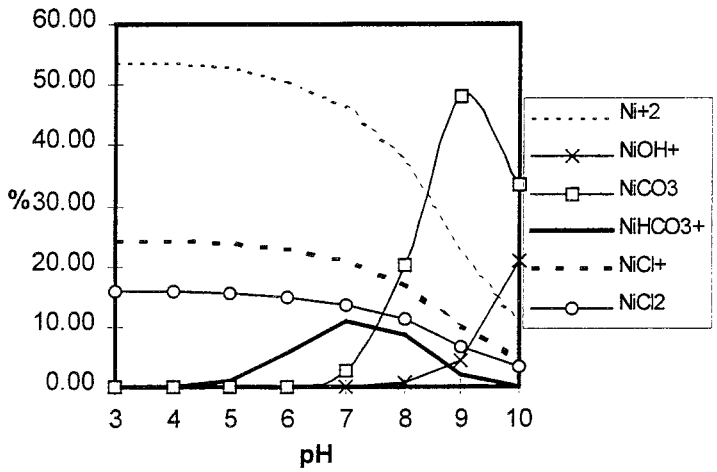

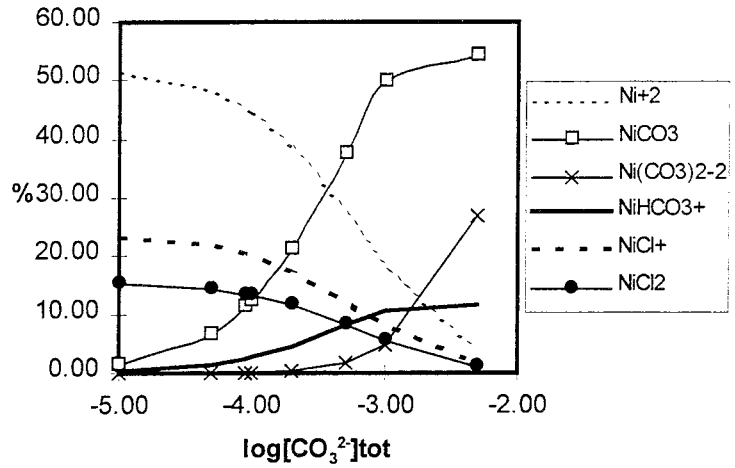

As we can see in the figures the aqueous speciation is very sensitive to both pH and carbonate content, around the Äspö average groundwater composition (pH=8.3 and $[CO_3^{2-}]_{tot.}= 3.37 \cdot 10^{-4}$ mol·dm^{-3}).

Predominant solid phases.

In the pH and pe ranges studied (pH 5 to 10 and pe -5 to 5), the solubility limiting solid phase is **NiO**. Other limiting solid phases, nickel silicates sulphides have been also considered in the later calculations although as we will discuss, these phases are not expected to control the solubility of this radionuclide since nickel silicates will not precipitate at low temperatures and due to iron competition for the limited sulphide supply.

4.4 SELENIUM

Aqueous speciation.

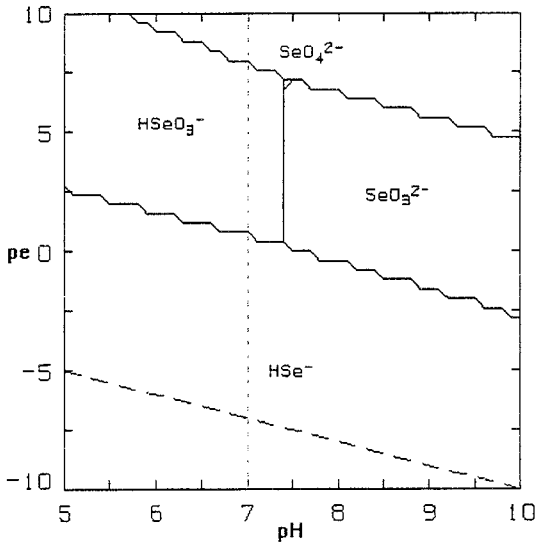

Predominant solid phases.

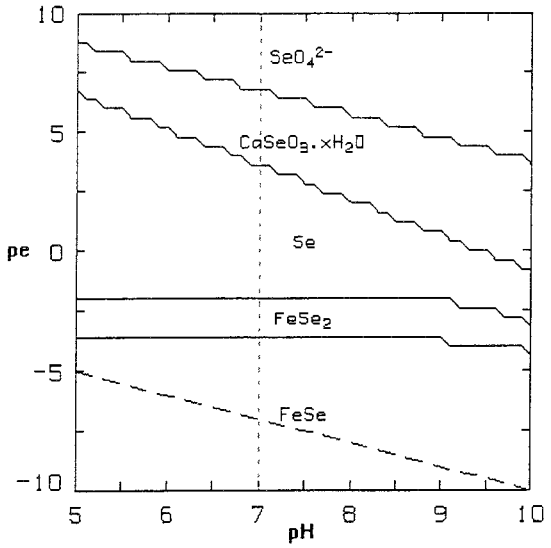

The previous figures show that both aqueous and solid speciation are basically dependent on the pe of the system.

4.5 KRYPTON

This element will not be solubility limited.

4.6 STRONTIUM

Aqueous speciation.

The cation Sr^{2+} is the dominant species in the whole pH range.

Predominant solid phases. (calculated by assuming $[Sr]_{tot} = 10^{-3}$ mol·dm^{-3})

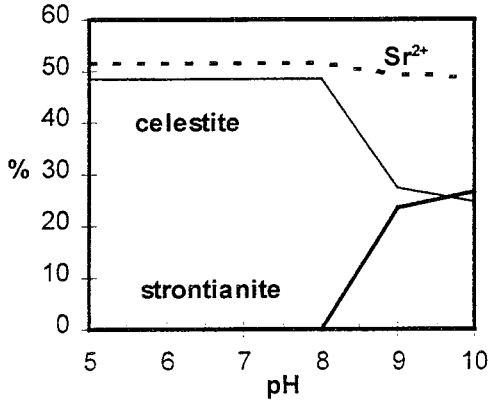

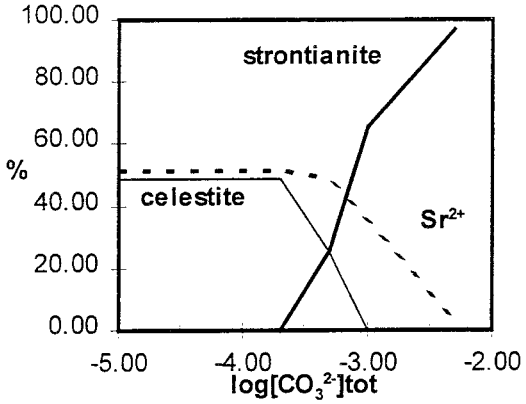

At lower carbonate content, and by taking into account that the Äspö groundwater contains sulphate with a concentration around $5 \cdot 10^{-3}$ mol·dm^{-3}, the predominant solid phase is celestite. However, if we slightly increase the carbonate content (see the last figure), the predominant solid phase becomes strontianite. Therefore, the predominant solid phase will mainly depend on the sulphate/carbonate ratio of the system under study.

The carbonate content of the Äspö groundwater ($[CO_3^{2-}]_{tot.}=3.37 \cdot 10^{-4}$ mol·dm^{-3}) is low in comparison with most typical groundwaters, therefore, it is expected that strontianite will be the predominant solid phase in most of the cases studied as we will see in the following sections (Section 7).

4.7 ZIRCONIUM

Aqueous speciation.

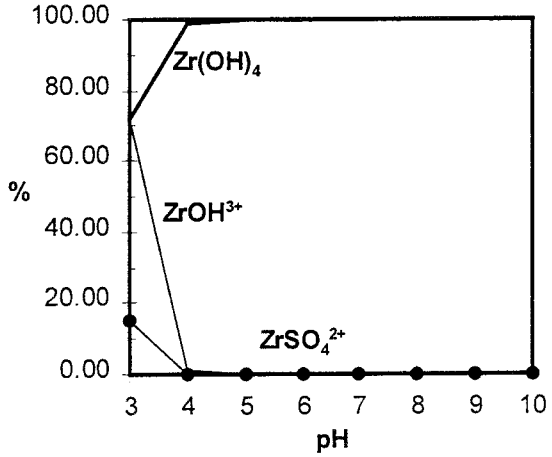

Predominant solid phases.

In the pH range studied (pH 5 to 10), the solubility limiting solid phase is **ZrO_2(am)**. We have assumed the precipitation of the amorphous phase prior

to the more crystalline following the Ostwald's step rule (Stumm and Morgan, 1996).

4.8 NIOBIUM

Initially and due to the lack of thermodynamic data for this element, we attempted some trial calculations by considering stability constants from vanadium species by analogy in behaviour with niobium. These data have been extracted from Baes and Mesmer (1976), the complexes added were: $NbOH^{2+}$, $Nb_2(OH)_2^{4+}$,NbO_2^+, $NbO(OH)_3(aq)$, $NbO_2(OH)_2^-$, NbO_3OH^{2-}, NbO_4^{3-}.

These calculations lead to very large Nb_2O_5 solubilities ($\approx 6 \cdot 10^{-3}$ mol·dm^{-3}) which are unrealistic. This is a consequence of the different redox behaviour of Nb with respect to V, as indicated by the redox half-cells (Stability Constants, 1964):

$$1/2Nb_2O_5(s) + 5H^+ + 2e^- \Rightarrow Nb^{3+} + 5/2H_2O \quad Eh = 0.05\ V \qquad 4\text{-}1$$

$$1/2V_2O_5(c) + 5H^+ + 2e^- \Rightarrow V^{3+} + 5/2H_2O \quad Eh = 0.65\ V \qquad 4\text{-}2$$

Therefore, the use of vanadium as a chemical analogue to niobium is not recommended. Consequently, we have only used the known niobium data for these solubility calculations.

Aqueous speciation.

(a) By using niobium species.

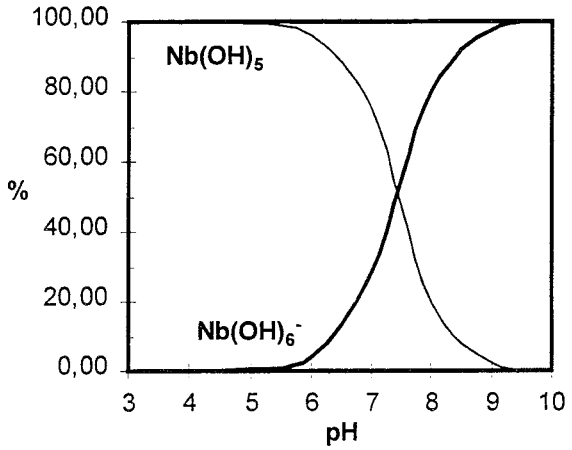

(b) Extended database by considering analogy with vanadium.

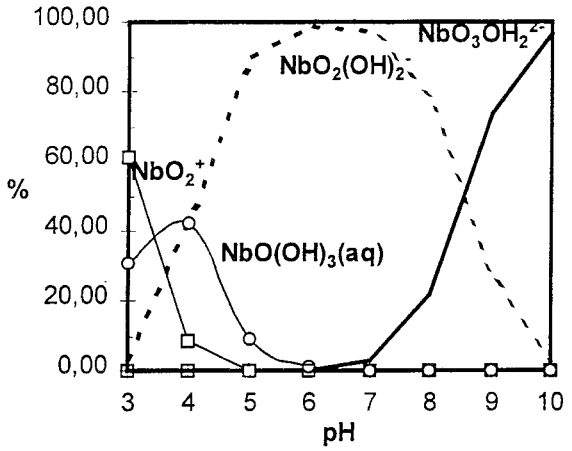

Figures **a** and **b** show the different speciation obtained depending on the database considered and consequently the different solubility of the solid phase as it has been explained before.

Predominant solid phases.

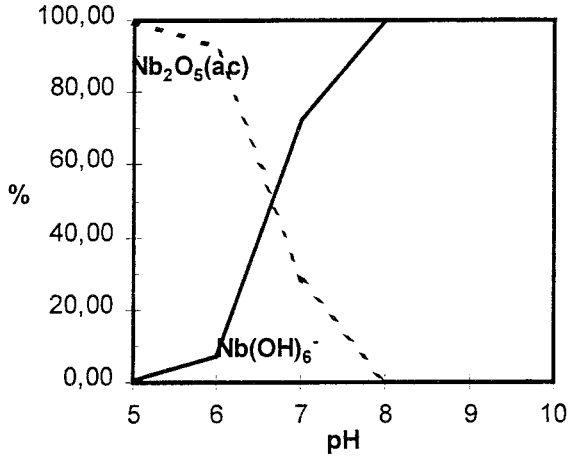

As it is shown in this figure the only predominant solid phase which will limit the solubility of this element is the Nb_2O_5(ac). Again, we have selected the reported "active" solid phase from Baes and Besmer (1976) in contrast to the more stable one, as a consequence of the Ostwald's step rule.

4.9 TECHNETIUM

Aqueous speciation.

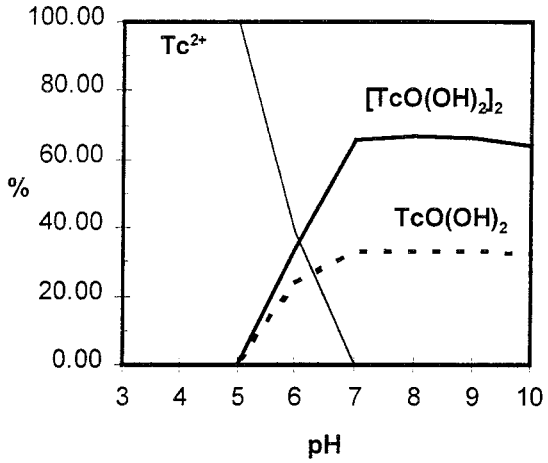

$[Tc(OH)_2]_2$ and $Tc(OH)_2$ are the predominant aqueous complexes in the granitic groundwaters pH range. Their relative percentage will depend on the total concentration of this element in the groundwater. Carbonate and hidroxocarbonate complexes become predominant at higher pH and carbonate concentrations.

Predominant solid phases.

In the pH range studied (pH 5 to 10), the predominant solid phase obtained has been $\mathbf{TcO_2 \cdot xH_2O}$. However, this solid phase is unstable at pe>0.

4.10 PALLADIUM

Aqueous speciation.

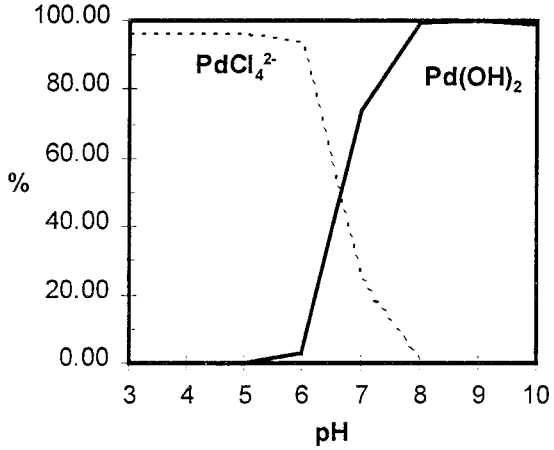

The palladium hydroxide is the predominant aqueous species at neutral and alkaline pH values, although chloride complexes play a role in this moderately saline water.

Predominant solid phases.

In the pH range studied (pH 5 to 10), the solubility limiting solid phase is **PdO**. No variation has been observed depending on the pe of the system (-5<pe<5).

The potential precipitation of metallic palladium has been supressed due to the slow kinetics of reduction of Pd(II) → Pd°.

4.11 SILVER

Aqueous speciation.

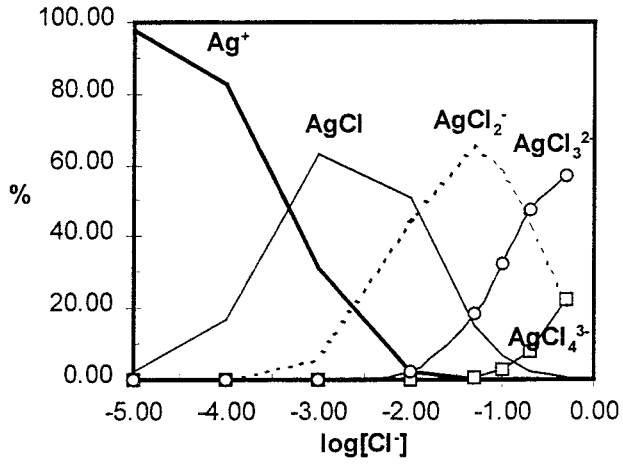

Aqueous speciation depends basically on the chloride content as we can see in the previous figure.

Predominant solid phases.

In the pH range studied (pH 5 to 10), the predominant solid phase obtained has been **Ag(s)**. No variation has been observed by changing the pe of the system (-5.07<pe<3.38). At higher redox potentials, i.e. pe>5.07, **AgCl(s)** becomes the predominant solid phase.

4.12 TIN

Sulphide solid phases have not been considered in the calculations since it is not possible to guarantee a sufficient supply of sulphides to the system.

Aqueous speciation.

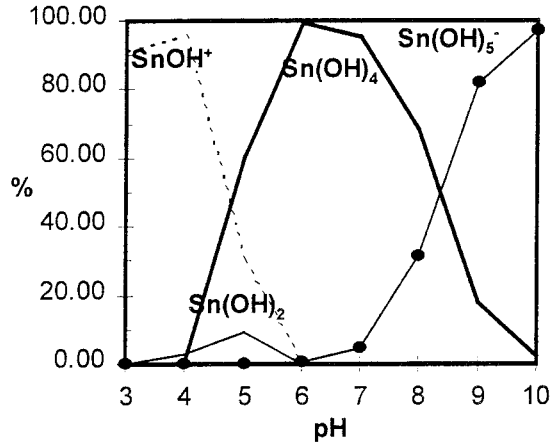

The aqueous speciation depends mainly on pH, as it is shown in the figure. At pH around 8, the predominant aqueous complex is $Sn(OH)_4$, but a slight pH increase (i.e. 0.7 units) makes $Sn(OH)_5^-$ the predominant one.

Predominant solid phases.

In the pH and pe ranges studied (pH 5 to 10 and pe -5 to 5), the solubility limiting solid phase is **SnO_2**.

4.13 IODINE

Not solubility limited.

4.14 CAESIUM

This element is not solubility limited.

Aqueous speciation.

The cation Cs^+ is the dominant species in the whole pH range.

4.15 SAMARIUM

Aqueous speciation.

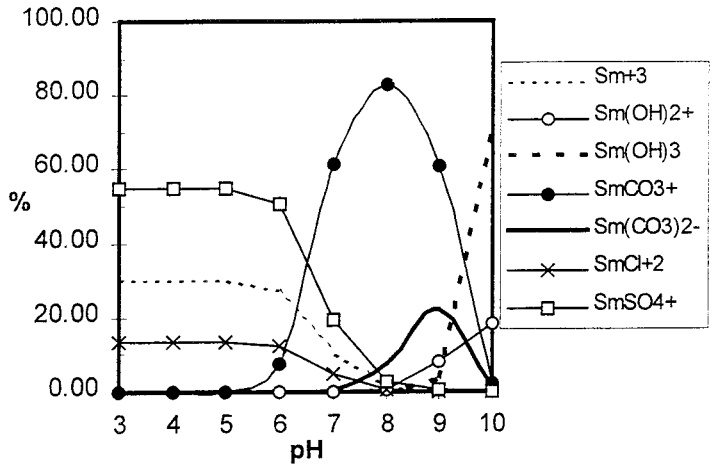

Samarium carbonate is the predominant aqueous species in the pH range of typical granitic groundwaters (7<pH<9), even in the relatively low carbonate content of the Äspö groundwater, as it is shown in the previous figure.

Predominant solid phases.

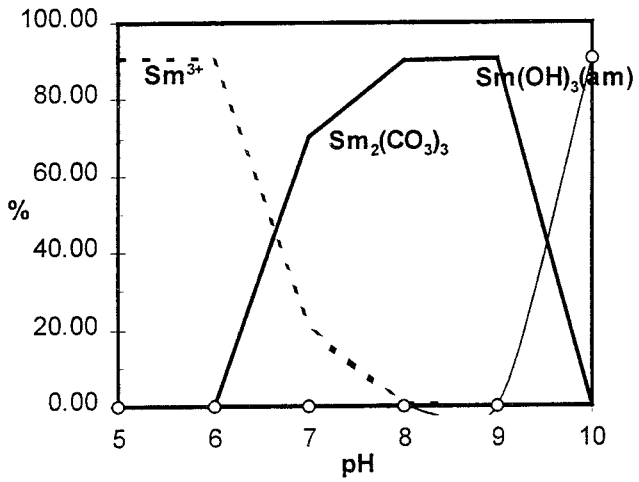

The solubility limiting solid phase will be the $Sm_2(CO_3)_3(s)$ under average groundwater conditions. Samarium phosphates do not predominate with the low phosphate content of this groundwater, which is limited by the solubility of apatite (see Figure 4-1, Section 4.18).

4.16 HOLMIUM

Aqueous speciation.

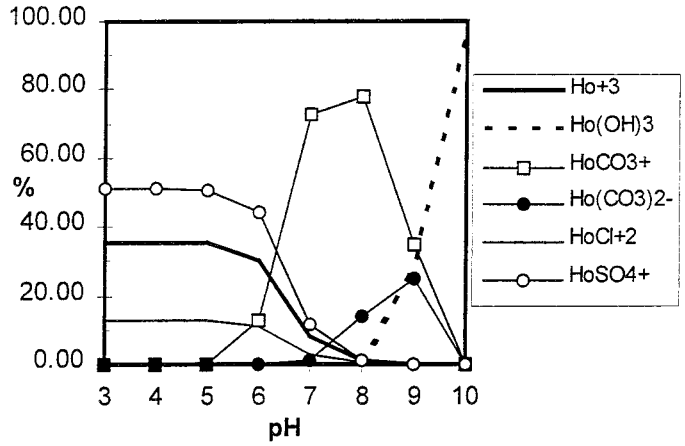

Predominant solid phases.

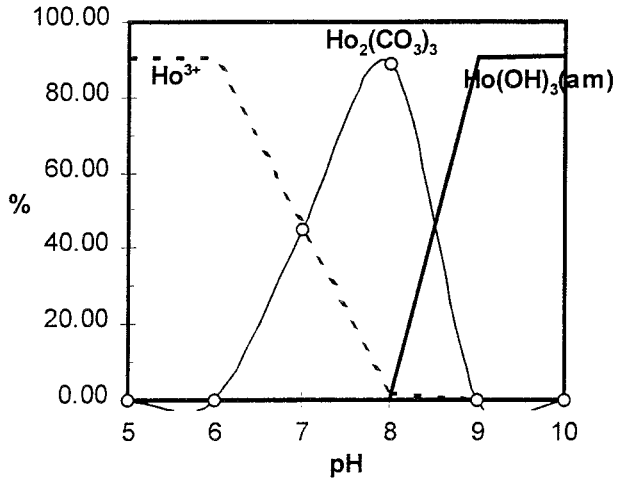

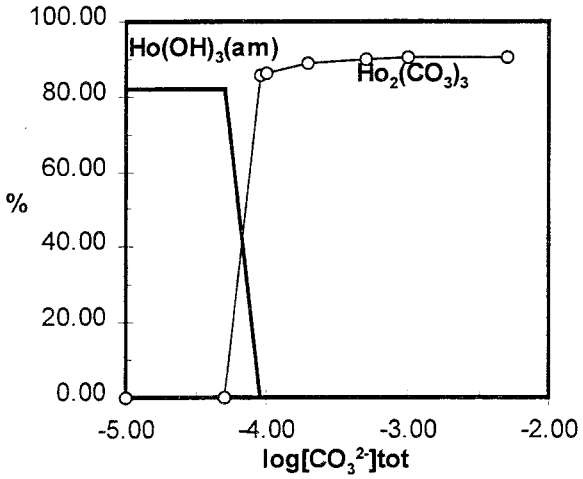

Not unexpectedly, samarium and holmium have similar chemical behaviour, as shown by the calculations.

4.17 RADIUM

Aqueous speciation.

As in the case of strontium, the cation Ra^{2+} is the dominant species throughout the whole pH range.

Predominant solid phases.

In the pH range studied (pH 5 to 10), the solubility limiting solid phase is **$RaSO_4(s)$**.

4.18 THORIUM

Aqueous speciation.

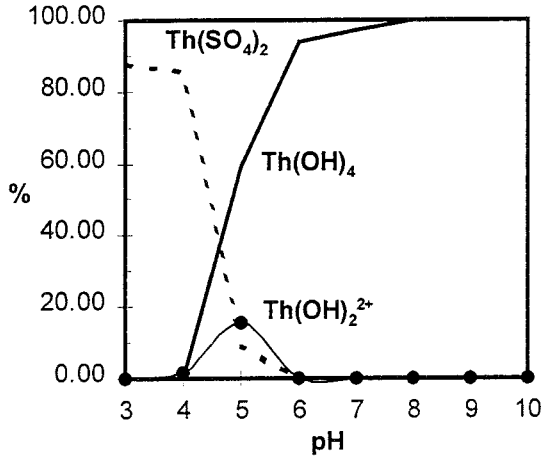

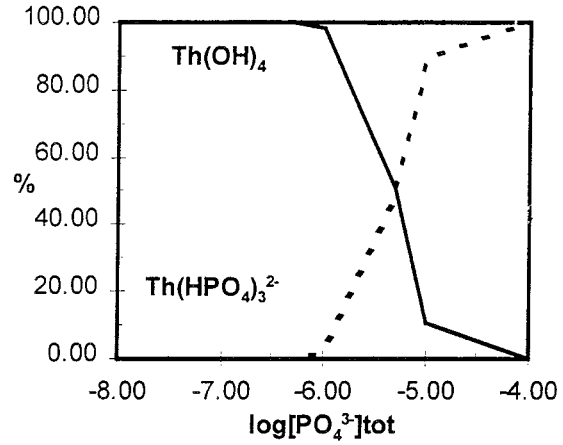

As it was expected, $Th(OH)_4(aq)$ is the predominant aqueous phase obtained from the calculations. However, if phosphate concentration increases then the $Th(HPO_4)_3^{2-}$ complex could become important. Nevertheless, this is highly improbable in granitic groundwaters where phosphate content is limited by the solubility of apatite, $[PO_4^{3-}]_{tot.} \leq 10^{-7}$ mol·dm^{-3} (see Figure 4-1).

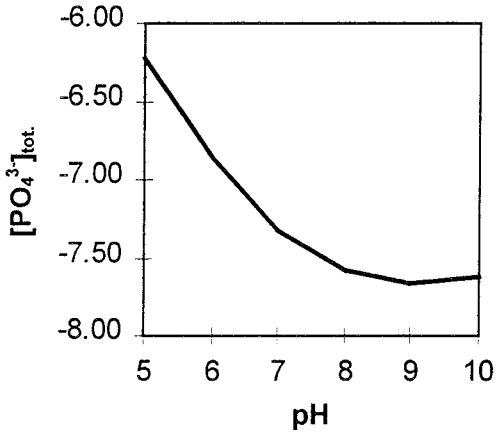

Figure 4-1. Solubility curve of apatite (fluorapatite) as a function of pH by taking the Äspö groundwater composition.

Predominant solid phases.

In the pH range studied (pH 5 to 10), the solubility limiting solid phase is **$Th(OH)_4$(am)**.

4.19 PROTACTINIUM

$PaO_2(aq)$ has not been included in the calculations as thermodynamic data for this species is not available.

Aqueous speciation.

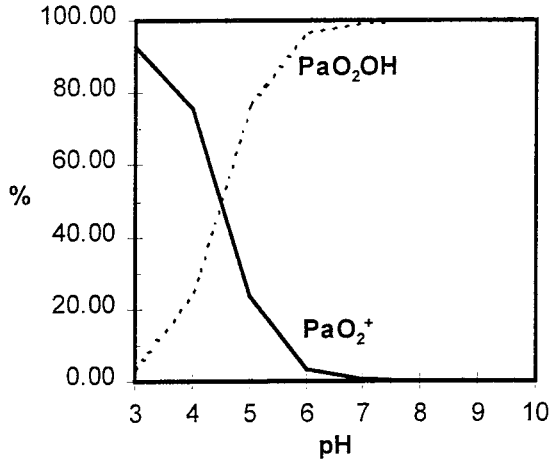

PaO_2OH is the predominant aqueous phase in the pH range expected in typical granitic groundwaters.

Predominant solid phases.

In the pH range studied (pH 5 to 10), the predominant solid phase obtained has been $\mathbf{Pa_2O_5}$. No variation has been observed by changing the pe of the system.

4.20 URANIUM

Aqueous speciation.

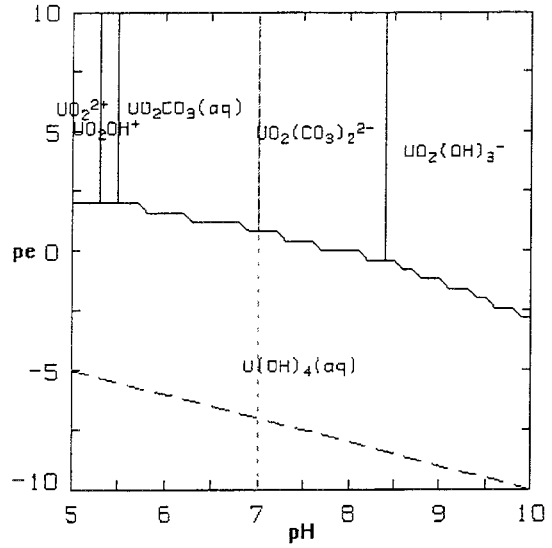

As it was expected, aqueous speciation depends mainly on the pe of the system and on the pH and carbonate content if we move on the oxidising area.

Predominant solid phases.

In the pH range studied (pH 5 to 10), the solubility limiting solid phase is **UO_2(fuel)** under reducing conditions. We have selected this phase according to experimental results obtained in a large number of uranium dioxide dissolution studies. In oxic conditions, the thermodynamically most stable solid phase under these average groundwater conditions is uranophane. However, according to experimental results (Forsyth et al., 1986) and the observations in natural systems (Finch and Ewing, 1991), the solubility limiting phase will be **schoepite** as the kinetically most favoured solid phase in a short-term. This is another application of Ostwald's step rule.

4.21 NEPTUNIUM

The database contains the complex $Np(OH)_5^-$, the results indicate that this species is very predominant in all the pH range considered even by considering a large pe range of work. The stability of this complex has given a solubility of the $Np(OH)_4$ solid phase ($\approx 3 \cdot 10^{-5}$ mol·dm^{-3}) higher than the one expected according to previous works (Bruno and Sellin, 1992, Cera et al., 1995). By analogy with Th(IV), U(IV) and Pu(IV), we advise to remove this species from the database.

Aqueous speciation.

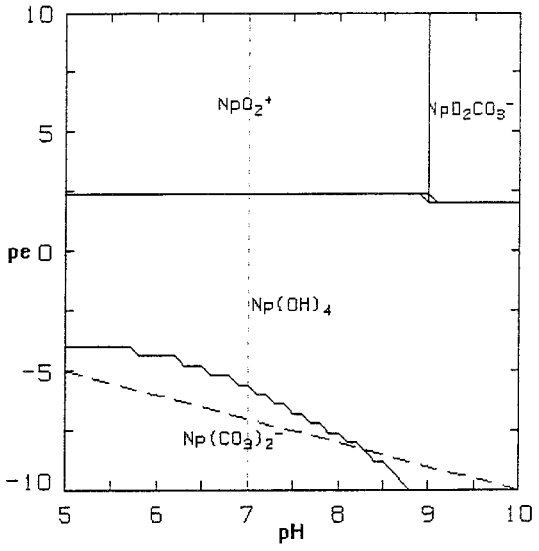

In the pe and pH ranges of natural granitic groundwaters, the predominant aqueous species is $Np(OH)_4(aq)$.

Predominant solid phases.

In the pH and pe ranges studied (pH 5 to 10 and pe -5 to 5), the solubility limiting solid phase is **$Np(OH)_4$(am)**. This phase has been selected according to the Ostwald's step rule as in the case of Th(IV), Zr(IV) and Nb(IV).

4.22 PLUTONIUM

Sensitivity calculations have shown that the inclusion of the $PuCO_3^+$ aqueous complex increases in one order of magnitude the calculated solubility of $Pu(OH)_4(s)$ at Äspö groundwater ($1.5 \cdot 10^{-10}$ mol·dm^{-3} versus $1.8 \cdot 10^{-9}$ mol·dm^{-3}). However, the effect on the Finnsjön groundwater (a higher carbonate content), is an increase on Pu solubilities of approximately three orders of magnitude, if the $PuCO_3^+$ is considered ($2.0 \cdot 10^{-8}$ mol·dm^{-3} vs. $1.0 \cdot 10^{-5}$ mol·dm^{-3}). Therefore, the inclusion of this species with such a large stability gives unrealistically high solubilities.

The stability constant of the $PuCO_3^+$ aqueous complex as stated in Bruno and Puigdomènech (1991) has a value of logK=-1.33 for the following reaction:

$$Pu^{3+} + HCO_3^- \Rightarrow PuCO_3^+ + H^+ \qquad 4\text{-}3$$

However, the solubility constant of this complex has been considered to be speculative by the same authors.

By taking the value given by the HATCHES v.7.0 database, logK=-3.83 for the same reaction (4-3) (Allard, 1982), the solubilities obtained are more realistic and agree with previous solubility calculations (Bruno and Sellin, 1992).

The constant value taken from Allard (1982) agree with the value reported for $NpCO_3^+$ (logK= -3.79) for the same reaction. This agreement gives us confidence in this constant because of the similar chemical behaviour of these actinides.

The similarities in chemical behaviour of the actinide (III) group is shown in the following figure (Figure 4-2), where we have plotted the stepwise formation constants for the Np(III) and Pu(III) aqueous carbonate complexes. The agreement between the two actinides ions indicate that the estimates are reasonable.

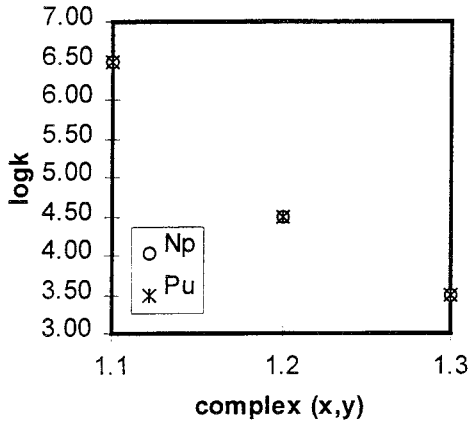

Figure 4-2. Correlation of the aqueous carbonate complexes for Np(III) and Pu(III). x stands for the number of metals and y is the number of ligands.

Aqueous speciation. (calculated by assuming $[Pu]_{tot} = 10^{-8}$ mol·dm^{-3})

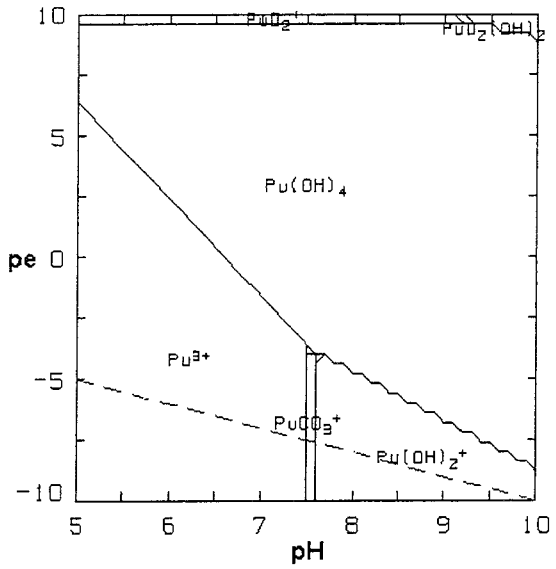

Predominant solid phases.

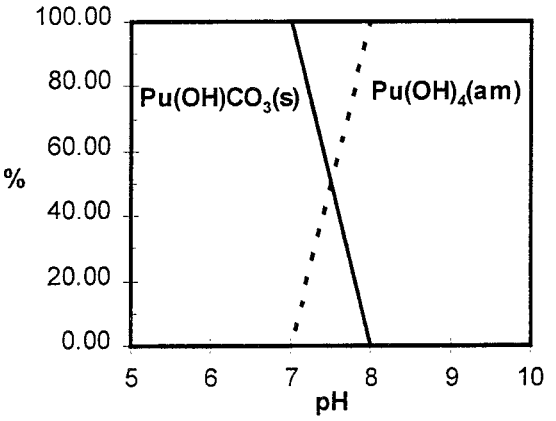

The predominant solid phase in the whole pe range studied (-5.07<pe<5.07) is the $Pu(OH)_4$(am) according to the Ostwald step rule. As we can see in the Figure this phase will be the solubility limiting one at neutral and alkaline pH values, this pH range can be considered the most commonly found in natural waters.

$Pu(OH)CO_3$(s) has been also considered the solubility limiting solid phase at low pe values although this phase has never been observed (Spahiu, personnal communication). However the solubility of this phase is slightly higher than $Pu(OH)_4$(am) solubility at these pe levels, i.e. Äspö groundwater conditions, pH=7.7 and pe=-5.21, the solubilities of $Pu(OH)_4$(am) and of $Pu(OH)CO_3$(s) are $6.56 \cdot 10^{-9}$ and $1.14 \cdot 10^{-8}$ mole·dm^{-3} respectively. Therefore we have considered only $Pu(OH)_4$(am) in the further calculations.

The $Pu(OH)_4$(am) can be considered the solubility limiting solid phase which better describes the Pu(IV) behaviour according to experimental results obtained by Rai and Swanson (1981) and Rai and Ryan (1982).

These authors observed in their work that the $PuO_2(c)$ converted gradually to an hydrated or amorphous material due to interaction with the radiolysis products of water, arriving to an steady state material having properties between the crystalline and the fresh hydrated phase.

4.23 AMERICIUM

Aqueous speciation.

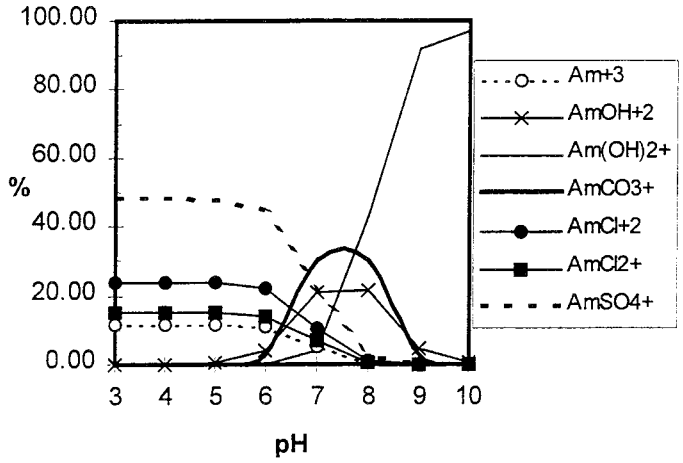

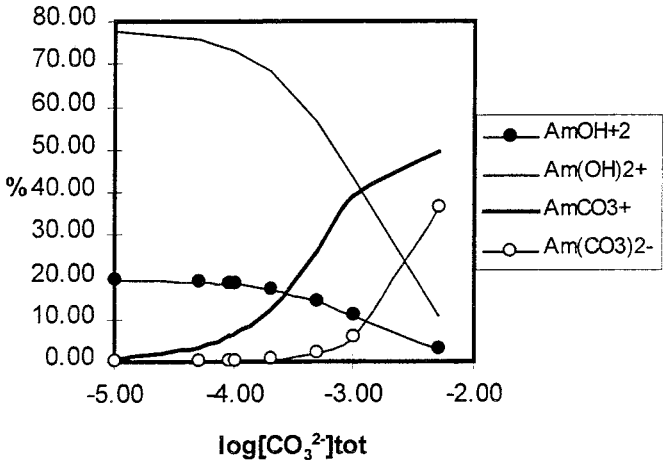

As we can see in the previous figures the aqueous speciation mainly depends on pH and carbonate content of the water. In the Äspö groundwater, the predominant aqueous complex is $Am(OH)_2^+$. However, if we increase the total carbonate concentration to 10^{-3} mol·dm^{-3} by fixing the pH, $AmCO_3^+$ becomes the predominant aqueous complex.

Predominant solid phases.

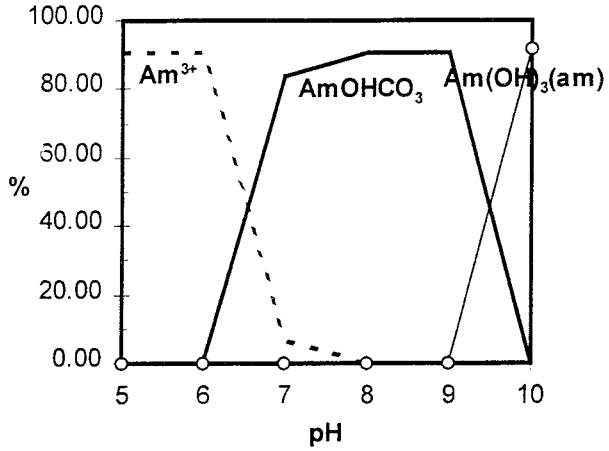

The solubility limiting solid phase in the pH range of granitic groundwaters is $AmOHCO_3$. Americium phosphates do not predominate due to the low phosphate content in granitic groundwaters where its concentration is limited by the solubility of apatite as it has been shown in Figure 4-1.

4.24 CURIUM

Aqueous speciation.

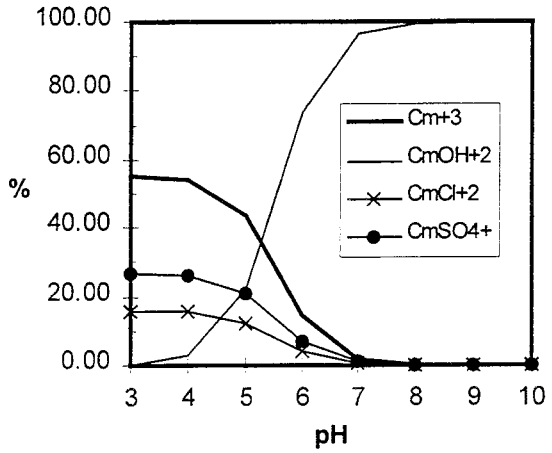

Predominant solid phases.

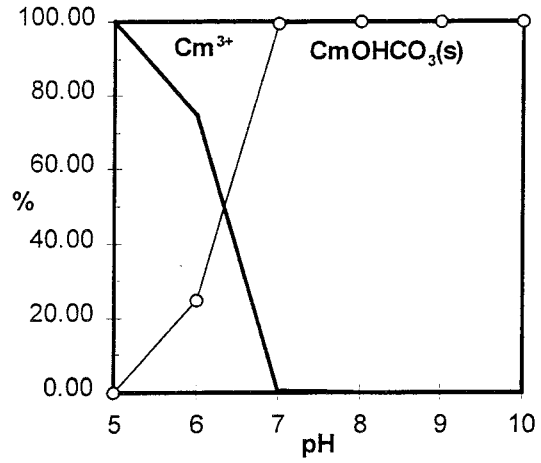

Based on the results, there are no changes in aqueous and solid speciation associated to the main parameters of the groundwaters studied (ie. pH and carbonate content).

5 THE NATURALLY-OCCURRING PA-RELEVANT TRACE ELEMENTS

5.1 NICKEL

Ni is concentrated in ultramafic and mafic rocks in the Earth's crust, with typical abundances in these rock types of 2000 and 200 ppm, respectively. In comparison, granite and shale contain only 0.5 and 95 ppm, respectively.

Nickel is present in sandstones on average at concentrations rather less than 20 ppm but like many others metals is higher than this in clays and shales up to 100 ppm. Ni is strongly associated geochemically with manganese and also with iron oxides. In most aquifer environments nickel is present as Ni^{2+} which is stable at pHs up to about 9. At higher pHs nickel solubility might be limited by $Ni(OH)_2$ (Edmunds et al., 1989).

The normal Ni contents of the rock samples from Poços de Caldas is below 10 ppm but at the redox front it can reach 60 ppm (MacKenzie et al., 1991).

In igneous rocks, Ni partitions into ferromagnesian minerals such as olivine, pyroxene, amphibole and spinel, whereas at lower temperatures it will be incorporated into a variety of silicates and hydroxides, such as smectite clay, sepiolite, talc and brucite (Decarreau, 1985; Velde, 1988). Ni does not form a discrete pure carbonate mineral and is the least stable of the M^{2+} ions in $Ca^{2+}M^{2+}(CO_3)_2$ (dolomite) compounds. Ni has appreciable chalcophilic behaviour, and in the presence of HS^- will form sulphides, either substituting for Fe^{2+} in pyrite, FeS_2 (there is almost complete solid solution in the FeS_2-NiS_2 system), co-precipitating with Fe^{2+} in pentlandite (Fe, Ni_9S_8), with Fe^{2+} and Cu^{2+} in chalcopyrite ($CuFeS_2$), or as discrete Ni-sulphides, such as the pyrite-structured vaesite (NiS_2) or millerite (NiS).

Nickel is enriched up to a factor of 4 during lateritic weathering of ultramafic rocks, so that such soils may be commercially-mined deposits of Ni (Golightly, 1981) Si and Mg are preferently removed in weathering solutions, but Ni is concentrated in solid products such as (with Ni end-member in parenthesis) sepiolite ("falcandoite", $Ni_4Si_6O_{15}(OH)_2.6H_2O$), talc ("kerolite", $Ni_3Si_4O_{10}(OH)_2$), serpentine ("nepouite", $Ni_3Si_2O_5(OH)_4$), and saponite ("pimelite", $Ni_3Si_4O_{10}(OH)_2$). The solubilities of the Ni end-member minerals are considerably less than those of other metals except Al (Golightly, 1981). Although nickel may be sorbed strongly by goethite, there is no apparent incorporation of nickel into this mineral. At higher temperatures, NiO is the least soluble of a range of divalent metal (Ca, Mg, Mn, Fe) oxides in the temperature range 400-700 ° C (Lin and Popp, 1984). This concurs with the low mobility of Ni relative to Ca, Mn, Fe, Zn, Cu

exhibited in hydrothermal (>300 ° C) water-rock systems, both experimentally (Seyfried and Dibble, 1980; Seyfried and Bischoff, 1981) and in natural systems (Humphris and Thompson, 1978).

The average Ni contents of the groundwaters from Poços de Caldas is about 0.6 μM.

Ni contents in sea water ranges between $2 \cdot 10^{-9}$ M and $10 \cdot 10^{-9}$ M, and the average residence time is 80000 years (Whitfield and Turner, 1987).

The average Ni contents of stream water is $3 \cdot 10^{-9}$ M (Wedepohl, 1978).

5.2 SELENIUM

Selenium has a crustal abundance of 0.05 ppm and is thus a comparatively rare element. Selenium has an order of magnitude higher concentration in shales (0.6 ppm) than in igneous rocks such as granite or basalt (Krauskopf, 1967). An estimate of the ratio of sulphur to selenium in igneous rocks is 6000 to 1. In seleniferous soils, selenium contents may be as high as 80 ppm.

Concentrations of selenium in coal and fuel oil range from 1.47 to 8.1 and 2.4 to 7.5 ppm, respectively. The combustion of fossil fuels mobilises ~4.5 10^8 g of selenium annually, whereas the annual flux from river discharges to the oceans is $7.2 \cdot 10^9$ g (Siu and Berman, 1989). Because of the similarity of ionic radius between sulphur (S^{2-} = 1.84 Å) and selenium (Se^{2-} = 1.91 Å), selenium will substitute readily for sulphur in solid sulphides and occurs in varying proportions in pyrite, chalcopyrite, pyrrhotite, galena, sphalerite, cinnababar, stibnite, molybdenite, arsenopyirte and others. Native Se occurs in nature only rarely. Selenium is a major component of 40 minerals and a minor constituent of 37 others (Elkin, 1982). Some selenium-bearing minerals are: ferroselite ($FeSe_2$); clausthalite (PbSe), stilleite (ZnSe), cadmoselite (CdSe), berzelianite (Cu2Se) and eucairite (AgCuSe). Galena (PbS) and clausthalite (the most abundant Se-mineral) form an isomorphous series. Se also occurs as selenites (cf. sulphites, which do not occur in nature). Selenates are very rare minerals, many selenates are isostructural with their corresponding sulphates (e.g. $PbSO_4$ is isostructural with $PbSeO_4$, kerstenite). Silicates of Se are not known. Typical Se contents in minerals are (Wedepohl, 1978); galena - 0-20%; molybdenite - 0-1000 ppm; pyrite - 0-3%; pyrrhotite - 1-60 ppm; pentlandite - 27-67 ppm; sphalerite - 1-120 ppm; millerite - 5-10 ppm; marcasite - 3-80 ppm.

Ferroselite occurs in roll front-type uranium deposits in sandstones and occurs at the interface between oxidised sandstone (containing goethite, limonite and hematite) and reduced pyritic uranium ore (Howard, 1977). This implies that selenium and ferrous iron in aqueous solution produced by the oxidation of seleniferous pyrite have combined to form ferroselite.

Therefore, ferroselite is stable under conditions more oxidising than those required for pyrite.

The normal Se contents of the rock samples from Poços de Caldas ranges between 0 and 10 ppm but at the redox front it can surpass 120 ppm (MacKenzie et al., 1991).

In aqueous systems, selenium may occur as one of three oxidation states (-II, IV, VI). Only two oxidation states of selenium are thought to be important in seawater: +4 and +6.

Se contents in sea water ranges between 0.2 and $2.4 \cdot 10^{-9}$ M, and the average residence time is 30000 years (Whitfield and Turner, 1987).

The total selenium content of rivers world-wide is in the range $0.2\text{-}9 \cdot 10^{-9}$ M (Cutter, 1989). Selenium concentrations in the Truckee, Walker, and Carson River systems which drain the eastern slope of the low Se content Sierra Nevada, California and Nevada, are low, ranging from less than $0.3 \cdot 10^{-9}$ M to about $16 \cdot 10^{-9}$ M (Doyle et al., 1995).

The Se concentration in dilute oxigenated groundwater at pH 7 range between $1.2 \cdot 10^{-9}$ and $1.2 \cdot 10^{-8}$ (Edmunds et al., 1989).

The amount of Se in Cigar Lake groundwater never reaches the limit of detection 0.38 μM (Cramer et al., 1994).

5.3 STRONTIUM

The average abundance of strontium in soils, earth crust, sediments and igneous rocks is 300, 385, 450 and 350 ppm respectively (Bockris, 1977).

The samples of the massive U-ore from Cigar Lake site have a Sr content which reach 1680 ppm (Smellie et al., 1994).

The normal Sr contents of the rock samples from Poços de Caldas ranges between 100 and 350 ppm (MacKenzie et al., 1991).

The Sr contents of the reference granite from El Berrocal can reach 6.85 ppm (Pérez del Villar et al., 1995).

Its valence and ionic size (1.12 Å) indicate that strontium will substitute for a variety of elements, such as Pb, Ca and Ba. Celestine is the principal mineral source of Sr and is found in evaporite deposits or in hydrothermal veins. There is complete solid-solution between $SrCO_3$ and $BaCO_3$. Strontianite most commonly occurs as hydrothermal veins, often in association with lead mineralisation.

Strontium is divalent and Sr^{2+} is the dominant aqueous specie in most natural waters.

The abundance of Sr in UK grounwaters (Edmunds et al., 1989) ranges from below 0.22 μM to about 80 μM.

Reduced groundwaters from Cigar Lake have around 2.3 μM, whereas oxidised waters have 3.4 μM in average (Cramer et al., 1994).

Sr contents in sea water ranges between 89 and 90 μM and the average residence time is 4 10^6 years (Whitfield and Turner, 1987).

5.4 ZIRCONIUM

Zirconium is a refractory lithophile element and occurs predominantly in the 4+ valence state with an ionic radius of 0.78 Å.

The average abundance of zirconium in soils, earth crust, sediments and igneous rocks is 300, 190, 200 and 170 ppm respectively (Bockris, 1977).

The most abundant Zr minerals are zircon ($ZrSiO_4$) and baddeleyite (ZrO_2). Zr forms a range of oxides, silicates ,halides, oxyhalides and chalcogenides. Zr will substitute for a range of elements of similar ionic radius, such as: Mg^{2+} (0.80 Å); Fe^{2+} (0.86 Å); Y^{3+} (0.98 Å); Ti^{4+} (0.69 Å); Nb^{5+} (0.72 Å); and Ta^{5+} (0.72 Å). Ilmenite, rutile and perovskite can contain up to 0.1% Zr. Varying, but significant amounts of Zr can be found in clinopyroxene, amphibole, mica and garnet. Concentrations of ~100 ppm in these minerals are frequently encountered. These substitutions may be of the type: $Zr^{4+}=Na^{+}+Fe^{3+}$. There are ~10 oxides, 2 carbonates and sulphates and ~20 silicates listed in Wedepohl (1978).

The samples of the massive U-ore from Cigar Lake site have a Zr content who reach 2740 ppm (Smellie et al., 1994). The Zr contents of the reference granite from El Berrocal ranges between 50 and 65 ppm (Pérez del Villar et al., 1995). The normal Zr contents of the rock samples from Poços de Caldas ranges between 100 and 2500 ppm (MacKenzie et al., 1991).

In seawater, Zr is predicted to occur as $Zr(OH)_5^-$ and is rapidly removed from seawater on the surfaces of sinking particles (McKelvey and Orians, 1993). These authors measured a dissolved Zr content of seawater varying from $12\text{-}95 \cdot 10^{-12}$ M in surface waters to $300 \cdot 10^{-12}$ M in deep water. This suggests that there is both a detrital and a sea-floor source of Zr in the oceans. Ferromanganese nodules in the equatorial by iron/manganese oxyhydroxides (Calvert and Piper, 1984). Phosphatic fish debris can act as a major sink for Zr and REE dissolved in seawater, suggesting strong complexation of Zr by phosphate ligands (Oudin and Cocherie, 1988).

Salvi and Williams-Jones (1990) inferred from fluid inclusion compositions that hydrothermal solutions (~100 ° C) transporting Zr in an altered peralkaline granite were of low-salinity and fluorine-rich.

Only in a few groundwater samples from Poços de Caldas, Zr contents surpass 1.1 μM (Nordstrom et al., 1991).

In a survey of alkaline thermal waters in granites in southern europe, Alaux-Negrel et al. (1993) concluded that zirconium (along with other tri- and tetravalent elements) was associated with a particulate fraction (<450 mm) in the groundwaters. This indicates that Zr was sorbed on the particulate fraction in the groundwaters and not in true solution. In a survey of over 400 groundwater compositions in a variety of rocks in the U.K., Edmunds et al. (1989) detected Zr in only one sample of groundwater ($34 \cdot 10^{-9}$ M). Elsewhere, Zr was below detection limits ($2.1\text{-}7.7 \cdot 10^{-9}$ M). Zr in oilfield waters of the U.S.A. are in the range $0.11\text{-}0.22 \cdot 10^{-9}$ M (Rittenhouse et al., 1969).

5.5 NIOBIUM

Niobium is a refractory lithophilic element (like zirconium) and has an identical abundance of 20 ppm in the crust, granite, basalt and shale (Krauskopf, 1967). The greatest abundance of Nb is in syenites and alkalic rocks (~100 ppm). The lowest abundance is in peridotittes (1.5 ppm).

Niobium minerals are almost exclusively oxides. Niobite, (F, Mn)(Nb, $Ta)_2O_6$ shows continuous solid solution with tantalite, thus forming the columbite suite of minerals. The chief hosts for Nb in most rocks are ferromagnesian minerals such as pyroxene, amphibole, biotite, muscovite, sphene, ilmenite and magnetite. Nb contents in these minerals may be up to a few 1000 ppm. Approximately 50 oxides/hydroxides, 1 borate and 10 silicates of Nb are listed in Wedepohl (1978) as occurring in nature. ~30 minerals are listed as containing up to 5% Nb.

Considerable amount of Nb may be found in natural cassiterites (SnO_2) of magmatic and hydrothermal origin, suggesting possible coherence of geochemical behaviour with tin under hydrothermal conditions (Möller et al., 1988).

The average abundance of niobium in soils is 115 ppm (Bockris, 1977).

The samples of the massive U-ore from Cigar Lake site have a Nb content who reach 50 ppm (Smellie et al., 1994). The normal Nb contents of the rock samples from Poços de Caldas ranges between 30 and 320 ppm (MacKenzie et al., 1991).

Nb(V) is the dominant redox state under natural water conditions (Baes and Mesmer, 1976). Its abundance in seawater is 10^{-10} M.

5.6 TECHNETIUM

The maximum ^{99}Tc contents of one sample from Cigar Lake ore is $0.85 \cdot 10^{-6}$ ppm (Fabryka-Martin et al., 1994).

Tc has since been decayed to be detectec under natural water conditions. Layer concentrations in natural systems are due to recent anthropogenic inputs.

In Cigar Lake site, the bounding concentrations for nuclear reaction products in groundwaters had been calculated. The maximum calculated ^{99}Tc concentrations in those waters is 10^{-9} M (Fabryka-Martin et al., 1994).

5.7 PALLADIUM

Palladium is a platinum metal and its behaviour is strongly linked with other elements of this kind (platinum, ruthenium, osmium, rhodium, iridium), and is thus strongly siderophilic. These metals have a crustal abundance of <0.05 ppm (Krauskopf, 1967). There are 6 naturally-occurring isotopes of Pd: ^{102}Pd (0.96%), ^{104}Pd (10.97%), ^{105}Pd (22.2%), ^{106}Pd (27.3%), ^{108}Pd (26.7%), ^{110}Pd (11.8%).

Pd may occur in olivine (50 ppb), bronzite (10 ppb), diopside (20 ppb) and serpentine (80 ppb). Zircone may contain 5000 ppb Pd. The average Pd content of rock-forming minerals is <10 ppb. Accessory minerals such as gadolinite and columbite may be enriched in Pd. Major ore deposits are associated with dunitic ultrabasic rocks and gabbros containing Cu-sulphides. Ni-sulphides are much higher in Pd than non Ni-sulphides. Platinum metals are also found indunites as discrete native metal occurrences. Platinum metals are strongly enriched in so-called "black (bituminous) shales", along with elements such as arsenic, silver, zinc, cadmium, lead, uranium, vanadium, molybdenum, antimony and bismuth. Although these rocks are organic-rich, the presence of high concentrations of rare metals are more likely due to deposition from oxidising chloride-rich fluids at a redox front.

The normal Pd contents of the rock samples from Poços de Caldas ranges between 0.4 and 3 ppm but at the redox front 26 ppm can reached (MacKenzie et al., 1991).

The Pd concentration in seawater ranges between 0.18 and $0.66 \cdot 10^{-12}$ M, and the residence time in the ocean is 50000 years (Whitfield and Turner, 1987).

McKinley et al. (1988) determined concentrations of Pd in hyperalkaline groundwaters of Oman in the range $3\text{-}7 \cdot 10^{-9}$ M.

Pd concentrations in the Salton Sea geothermal brines have been determined in the range $0.2\text{-}20 \cdot 10^{-9}$ M by McKibben et al. (1990) at 300 ° C and pH = 5.4 and log f_{O2} = -30 bars (sulphate-sulphide boundary).

5.8 SILVER

The average abundance of silver in soils, earth crust, sediments and igneous rocks is 1, 0.06, 0.5 and 0.2 ppm respectively (Bockris, 1977).

The most important Ag-ore minerals are found in hydrothermal zones. Galena is one of the most abundant sources og Ag at trace amounts. The sedimentary galena from Oklo site can content between 6 and 40 ppm of Ag (Gauthier-Lafaye, 1995).

The normal Ag contents of the rock samples from Poços de Caldas ranges between 0.2 and 3 ppm but at the redox front it can reach 10 ppm (MacKenzie et al., 1991).

The major inorganic species in natural waters for that element are Ag^+, AgCl (aq), $AgCl^{2-}$, AgCl. In sea water the Ag(I) form complexes with Cl^- (Stumm and Morgan, 1996).

The system Ag-Cl-S-O-H in Eh-pH space (Brookins, 1988) show the importance of dissolved Cl on Ag transport under oxidising, acidic conditions. The mobility of the Ag is relatively high in acidic conditions (Bockris, 1977).

In sea water the principal forms in which silver occur are $AgCl_2^-$ and $AgCl_3^{2-}$ (Bockris, 1977). The silver concentration in the Pacific Ocean ranges between 10^{-12} M at surface and $23 \cdot 10^{-12}$ M at depht. The residence time is 5000 years (Whitfield and Turner, 1987).

In several goundwater samples from Poços de Caldas the content of Ag reach 0.5 μM (Nordstrom et al., 1991).

In dilute oxygenated groundwater the concentration of Ag ranges between 92.6 and $926 \cdot 10^{-12}$ M (Edmunds et al., 1989).

5.9 TIN

The average abundance of tin in soils, earth crust, sediments and igneous rocks is 10, 40, 16 and 32 ppm respectively (Bockris, 1977).

The principal economic source of tin is the oxide, cassiterite (SnO_2) which is associated with granitic magmatism. Sn will also form solid solutions with various ferromagnesian silicates such as pyroxenes, micas and amphiboles. This relates to the substitution of Sn (ionic radius 0.71Å) for Ti (ionic radius 0.68 Å) and Fe^{3+} (ionic radius 0.64 Å). Sn in biotite and muscovite may be as high as 1250 ppm. Tin will also occur in sulphides such as stannite, Cu_2FeSnS_4, canfieldite, Ag_8SnS_6 and teallite, $PbSnS_2$. Tin minerals are comparatively few.

In the reference granite from El Berrocal the contents of tin can reach 30 ppm (Pérez del Villar et al., 1995).

The normal Sn contents of the rock samples from Poços de Caldas ranges between 5 and 20 ppm (MacKenzie et al., 1991).

The oxidation state of tin in seawater is IV, and the content range between 5 and $20 \cdot 10^{-12}$ M (Whitfield and Turner, 1987).

Byrd and Andreae (1986) measured an arithmetic mean for dissolved tin in the world's rivers of $20.5 \cdot 10^{-12}$ M and estimated a dissolved flux of tin to the oceans of $0.76 \cdot 10^{6}$ mol yr^{-1} and $300\text{-}600 \cdot 10^{6}$ mol yr^{-1} for the particulate fraction.

Edmunds et al. (1989) measured tin concentrations in groundwaters in various aquifers of the U.K. Values in the range $2.5\text{-}8.4 \cdot 10^{-9}$ M were found in groundwaters in the Millstone Grit and Carboniferous Limestone of Derbyshire, the Old Red Sandstone of Moray, the Trias of Shropshire, the Wealden and Lower Greensand. In only one sample was tin above $8.4 \cdot 10^{-9}$ M. 19 Bulgarian saline deep groundwaters have Sn concentrations in the range 0-5.6 μM (Pentcheva, 1965). The abundance of tin in hot springs (16-92 °C) in Japan was in the range $0.84\text{-}8.4 \cdot 10^{-9}$ M (Ikeda, 1955).

5.10 IODINE

The average ^{129}I contents of eight samples from Cigar Lake ore is $1.4 \cdot 10^{-6}$ ppm (Fabryka-Martin et al., 1994).

Iodine is the only halide which has several stable redox states unders natural water conditions.

In natural waters the majors species for the iodine are the iodide (I^-) and the iodate (IO_3^-); other species are I_2 , I_3^-, HIO, IO^-, and HIO_3. The concentration in sea water ranges between 0.2 and 0.5 μM and its oceanic residence time is 300000 years (Whitfield and Turner, 1987).

The majority of the samples of groundwaters from Cigar Lake have less than 0.078 μM of Iodine (Cramer et al., 1994).

The average iodine contents of several aquifers of the UK ranges between 0.016 and 0.26 μM (Edmunds et al., 1989). The iodine exists mainly as iodate but it is reduced to iodide towards anaerobic conditions. Total iodine increases in the deeper confined aquifer. Iodine may be formed by the oxidation of organic matter or during the mobilisation of Fe^{2+}. The release of iodine could also be the result of codissolution for fluorapatites, as indicated by the correlation between both anions in natural waters.

Iodine, a halogen, occurs sparingly in the form of iodides in sea water from which it is assimilated by seaweed, in brines from old sea deposits, and in brackish waters from oil and salt wells (Weast, 1975).

5.11 CAESIUM

The average abundance of caesium in soils, earth crust, sediments and igneous rocks is 5, 1, 10 and 10 ppm respectively (Bockris, 1977).

Pollucite (Cs and Na aluminosilicate) is the Cs bearing mineral with the highest grade of Cs, and it is found in pegmatitic rocks.

Studies on bentonites from Cabo de Gata (Spain), result of the alteration of volcanic rocks, show that the Cs is the less mobile element of all the trace element studied (Caballero et al., 1986).

Cs concentration for rocks from Äspö site is 3.3 ppm whereas the average contents of the groundwaters is 1.9 10^{-8} M (Miller et al., 1994).

The normal Cs contents of the rock samples from Poços de Caldas is about 0.5 ppm but at the redox front it can exceed 5 ppm (MacKenzie et al., 1991). The samples of the massive U-ore from Cigar Lake site have a Cs content who can reach 1.3 ppm (Smellie et al., 1994).

Cs is a cation with a low polarising power that is so weakly complexed in both freshwater and seawater that its speciation is dominated by the free cation (Turner et al., 1981).

Cs concentration in sea water ranges between $2.3 \cdot 10^{-9}$ M (Whitfield and Turner, 1987) and $3.7 \cdot 10^{-9}$ M (Lloyd and Heathcote, 1985) and the principal form in which cesium occurs is Cs^{+}. The residence time of Cs in the ocean is 6 10^{5} years (Whitfield and Turner, 1987).

Only in one sample of groundwater from Cigar Lake it had been found a Cs content of 0.52 μM (Cramer et al., 1994).

5.12 SAMARIUM

Sixteen isotopes of samarium exist. Natural samarium is a mixture of seven isotopes, three of which are unstable with long half-lives (Weast, 1975).

Samarium has a crustal abundance of 7.3 ppm, being concentrated in granitic rocks (9.4 ppm) (Krauskopf, 1967).

Grauch (1989) made a comprensive review of the samarium contents in metamorphic rocks. McLennan (1989) studied the contents and processes related with the LREE occurrence in sedimentary rocks.

Samarium is found along with other members of the REE in many minerals, including monazite (to the extent of 2.8%) and bastnasite (Weast, 1975).

~200 minerals are known which contain up to 0.01 % lanthanides. Highest concentrations are in bastnaesite (64 wt%), monazite (60 wt%) and cerite (59 wt%). 3 fluorides, 10 oxides, 10 carbonates, 1 borate, 1 sulphate, 8 phosphates and 20 silicate minerals containing REE are listed in Wedepohl (1978). REE contents of basalts and gabbros are concentrated in clinopyroxene rather than plagioclase. Biotites from granites contain more REE than feldspars and quartz.

The natural Sm contents of the reactor zone of Oklo ranges between 1.7 and 24 ppm (Gauthier-Lafaye, 1995).

The samples of the massive U-ore from Cigar Lake site have a Sm content which reach 48.2 ppm (Smellie et al., 1994). The normal Sm contents of the rock samples from Poços de Caldas ranges between 3 and 10 ppm (MacKenzie et al., 1991). The Sm average contents of the reference granite samples from El Berrocal is around 2 ppm (Pérez del Villar et al., 1995).

Sm contents in sea water ranges between 2.7 and 6.·8 10^{-12} M, and the average residence time is 200 years (Whitfield and Turner, 1987).

In North Atlantic ocean the Sm content increase slightly with depth and its around $4.5 \cdot 10^{-12}$ M (Elderfield and Greaves, 1989).

Elderfield et al. (1990) report REE analyses of rivers and seawaters. Sm values in river waters are in the range $46\text{-}810 \cdot 10^{-12}$ M.

Sm concentrations in the range $9\text{-}239 \cdot 10^{-12}$ M are reported by Michard et al. (1987) in CO_2-rich groundwaters in granites from Vals-les Bains, France. Their enrichment of heavy REE in these waters is ascribed to carbonate complexing. REE abundances in alkaline groundwaters in granites in southern Europe were associated with colloids (Alaux-Negrel et al., 1993). Smedley (1991) measured samarium concentrations in shallow groundwaters in the Carnmenellis granite and surrounding metasedimentary rocks in the range $0.3\text{-}66 \cdot 10^{-9}$ M. Gosselin et al. (1992) investigated concentrations of REE in chloride-rich groundwater in the Palo Duro Basin, Texas. These authors noted Sm concentrations in the range $0.035\text{-}48 \cdot 10^{-9}$ M. They concluded that chloride complexes dominated the REE speciation with only minor contributions from carbonate and sulphate species. Fresh groundwaters from wells in the schists of the Virginia Piedmont area of the U.S.A. have 60 ppb REE (Wedepohl, 1978).

Michard (1989) has reported REE analyses in waters from geothermal systems in Italy, Valles Caldera, Salton Sea and mid-Atlantic Ridge. Sm contents are in the range $0.0053\text{-}107 \cdot 10^{-9}$ M. REE concentrations of these fluids increases as pH decreases.

In deep groundwater from Poços de Caldas the average contents of Sm is below $6.6 \cdot 10^{-9}$ M (Miekeley et al., 1991).

In the Garone and Dordogne rivers the Sm contents is $0.051 \cdot 10^{-12}$ M (Brookins, 1989).

5.13 EUROPIUM

Grauch (1989) made a comprensive review of the europium contents in metamorphic rocks. McLennan (1989) studied the contents and processes related with the LREE occurrence in sedimentary rocks.

Europium is the most reactive of the rare earth metals, quickly oxidising in air. It resembles calcium in its reaction with water. Bastnasite and monazite are the principal minerals containing Eu (Weast, 1975).

The average Eu_2O_3 contents for carbonatite-derived and placer monazites is about 0.10 and 0.05 wt%, respectively, whereas for dark monazites the world-wide average is 0.36 wt% (Mariano, 1989).

The natural Eu contents of the reactor zone of Oklo ranges between 0.5 and 41 ppm (Gauthier-Lafaye, 1995).

The samples of the massive U-ore from Cigar Lake site have a Eu content who reach 3 ppm (Smellie et al., 1994). The average contents of the reference granite samples from El Berrocal is about 0.06 ppm (Pérez del Villar et al., 1995). The normal Eu contents of the rock samples from Poços de Caldas is about 2.5 ppm (MacKenzie et al., 1991).

Most REE do not readily substitute in minerals. Europium is an exception, because it substitutes Ca, it is preferentially absorbed, relative to other rare earth elements, by crystallising plagioclases. The rock containing the fractionated plagioclase will tend to be relatively enriched in Eu (Raymond, 1995).

Europium is the only lanthanide than under natural conditions, has a (II) valence, and this readily explains the segregation of Eu from the other lanthanides under reducing conditions (Brookins, 1989). Under such conditions, Eu^{2+} is almost identically to Sr^{2+} in its geochemical characteristics. Mixing of Eu^{2+} and Sr^{2+} in Ca^{2+}-sites during rock genesis is well documented. Like the alkaline earths, then, Eu^{2+} does not hydrolyse readily.

At low temperatures, near earth surface conditions, the aqueous geochemistry of europium should be dominated by the trivalent state, except possibly in the most reducing, alkaline pore waters of anoxic marine sediments. However, at temperatures greater than about 250°C and elevated pressures, divalent europium could predominate (Sverjensky, 1984).

Eu contents in sea water ranges between 0.6 and $1.8 \cdot 10^{-12}$ M, and the average residence time is 500 years (Whitfield and Turner, 1987). In North Atlantic ocean the Eu contents increases with depth (Elderfield and Greaves, 1989). In the Garone and Dordogne rivers the contents is $0.01 \cdot 10^{-12}$ M (Brookins, 1989).

In deep groundwater from Poços de Caldas the average contents of Eu is below $2 \cdot 10^{-9}$ M (Miekeley et al., 1991).

Elderfield et al. (1990) studied the REE in surface waters and says than the concentration of Eu in 15 rivers ranges between 7 and $208 \cdot 10^{-12}$ M. In 6 estuarine waters ranges between 2 and $80 \cdot 10^{-12}$ M and in 5 coastal sea water ranges between 2 and $10 \cdot 10^{-12}$ M. In oceanic water Eu can have an hydrothermal origin.

Gosselin et al. (1992) investigated concentrations of REE in chloride-rich groundwater in the Palo Duro Basin, Texas. These authors noted Eu concentrations in the range 10^{-11} - 10^{-9} M. They concluded that chloride complexes and free-ions dominated the REE speciation with only minor contributions from carbonate and sulphate species.

Smedley (1991) measured europium concentrations in shallow groundwaters in the Carnmenellis granite and surrounding metasedimentary rocks in the range 40 - $0.16 \cdot 10^{-9}$ M.

The Eu contents of the water from the nine springs at Val-les-Bains ranges between 0.26 and $8.2 \cdot 10^{-9}$ M (Michard et al., 1987).

The Eu contents of the hydrothermal fluids from seven geothermal fields ranges between $1.31 \cdot 10^{-12}$ M and $1.7 \cdot 10^{-8}$ M (Michard, 1989).

5.14 HOLMIUM

Grauch (1989) made a comprensive review of the holmium contents in metamorphic rocks. McLennan (1989) studied the contents and processes related with the LREE occurrence in sedimentary rocks.

Holmium occurs in gadolinite, monazite (to the extend of about 0.05%) and in others rare-earth minerals (Weast, 1975).

The normal Ho contents of the rock samples from Poços de Caldas is about 2 ppm (MacKenzie et al., 1991). The average Ho contents of the reference

granite samples from El Berrocal is about 0.3 ppm (Pérez del Villar et al., 1995).

Gosselin et al. (1992) investigated concentrations of REE in chloride-rich groundwater in the Palo Duro Basin, Texas. These authors noted Ho concentrations below $8.5 \cdot 10^{-9}$ M. They concluded that chloride complexes and the free-ion dominated the REE speciation with only minor contributions from carbonate and sulphate species.

Ho contents in sea water ranges between 1 and $3.6 \cdot 10^{-12}$ M (Whitfield and Turner, 1987).

Smedley (1991) measured holmium concentrations in shallow groundwaters in the Carnmenellis granite and surrounding metasedimentary rocks in the range $5.5 \cdot 10^{-9}$ M and below the detection limit ($0.3 \cdot 10^{-9}$ M).

In deep groundwater from Poços de Caldas the average contents of Ho is below $3.7 \cdot 10^{-9}$ M (Miekeley et al., 1991).

Brookins (1989) gives a Ho contents in the Garone and Dordogne rivers of $8.7 \cdot 10^{-15}$ M.

5.15 RADIUM

Radium is isovalent (+2), with an ionic radius of 1.43 Å. ^{226}Ra is the dominant isotope and exceeds 99% of total Ra.

Trace radium concentrations in groundwaters will tend to coprecipitate with barium to form barite solid solutions (Doernier and Hoskins, 1925), and is the basis for the removal of radium from mine waters and uranium mill tailings solutions (Sebesta et al., 1981; Paige et al., 1993). The calculated partition coefficient for Ra in alkaline-earth sulphates is greatest in celestite, $SrSO_4$(280), decreasing through anglesite, $PbSO_4$(11) to barite (1.8) (Langmuir and Riese, 1985). Ra-Ba sulphates and carbonates should behave as ideal solid solutions.

Radium concentrations are often high in saline waters (Kraemer and Reid, 1984; Dickson, 1985; Laul et al., 1985a, b), geothermal waters (Mazor, 1962; Wollenberg, 1975), but relatively low in low-temperature, low salinity groundwaters (Michel and Moore, 1980; Krishnaswami et al., 1982).

The behaviour of radium in sedimentary brines of the Palo Duro Basin in Texas has been investigated by Langmuir and Melchior (1985). All brines were undersaturated with respect to pure $RaSO_4$, but concentrations of ^{226}Ra ($0.2\text{-}5 \cdot 10^{-12}$ M) were probably limited by solid solutions of Ra in barite and celestite. The brines were saturated with respect to gypsum, anhydrite, celestite and barite.

Radium isotope activities in thermal waters of Yellowstone National Park have been investigated by Sturchio et al. (1993). They found that radium concentrations / activities in the waters were inversely correlated with temperature and that controls on these concentrations were either the solubility of a Ra-barite solid solution o in some instances, ion exchange of Ra with zeolites.

Rock / brine concentration ratios for Ra in high temperature (300 ° C) brines from the Salton Sea geothermal field are approximately unity (Zukin et al., 1987). The high Ra solubility in these brines is attributed to chloride complexing and reducing conditions which prevent $RaSO_4$ from forming.

Radium concentrations in natural water rarely exceed 10^{-12} M (Langmuir and Melchior, 1985). Ra contents in sea water ranges between 1.6 10^{-16} and 7 10^{-16} M (Whitfield and Turner, 1987).

The groundwaters from Cigar Lake have a content of Ra between 0.012 and 0.5 10^{-12} M (Cramer et al., 1994).

5.16 THORIUM

The actinides thorium and uranium are ubiquitous in nature with concentrations in soils, sediments and rocks as high as several tens of parts per million (Choppin and Stout, 1989).

Thorium is lithophilic element and has a crustal abundance of 9.6 ppm (Krauskopf, 1967). The average granite, basalt and shale contain 17, 2.2 and 11 ppm, respectively. The ionic radius of Th^{4+} is 1.02 Å. Similarities in ionic size and bond character link thorium, cerium, uranium and zirconium.

^{232}Th is the dominant isotope of thorium (~100% of natural abundance) and has half-life of $1.4 \cdot 10^{10}$ years.

Thorium is found in natural systems as the tetravalent cation only. It occurs as a major mineral only in rare phases such as thorianite (ThO_2) and thorite ($ThSiO_4$). The former mineral is isomorphous with uraninite, the latter with zircon. Consequently, a large part of naturally-occurring Th is in zircon. The chief source of Th is in monazite (Ce, La, Y, Th)PO_4 which usually contains 3-9% and up to 20% ThO_2. There are many examples of isostructural compounds of Th, Ce, U and Zr: ThS, US, CeS and ZrS; ThO_2, CeO_2, ZrO_2; $ThSiO_4$, $USiO_4$, $ZrSiO_4$; $ThGeO_4$, $UGeO_4$, $CeGeO_4$, $ZrGeO_4$; $BaThO_3$, $BaUO_3$, $BaCeO_3$, $BaZrO_3$. However, there are only a few Th silicates known as compared with the large number of Zr-silicates. A large number of Th-sulphides, selenides and tellurides is known. Th is a major cation in only a few minerals, none of which is common. Feldspars, biotites and amphiboles may contain only 0.5-50 ppm Th.

Most Th host minerals are refractory to weathering so that Th is considered a poorly soluble and immobile element. Th is usually fractionated from U during weathering because of the solubility of U(VI). Th is strongly adsorbed by clays and oxyhydroxides so that relatively high concentrations of Th occur in bentonites, marine pelagic clays, manganese nodules and bauxites.

Th in fresh surface waters ranges from 0.043 to $4.3 \cdot 10^{-9}$ M. Th concentrations in natural waters are more likely to be limited by mineral dissolution kinetics and sorption than by true mineral-fluid equilibria (Langmuir and Heman,1980).

Copenhaver et al. (1993) investigated retardation of ^{232}Th decay chain radionuclides in aquifers in Long Island and Connecticut. They measured retardation coefficients of the order 10^4-10^5 for Th. Rock/brine concentration ratios of ~$5 \cdot 10^5$ were observed for ^{232}Th in high temperature (300 ° C) brines of the Salton Sea geothermal field, indicating immobility of Th (Zukin et al., 1987).

The Th content of the reference granite from El Berrocal is about 7 ppm (Pérez del Villar et al., 1995).

The samples of the massive U-ore from Cigar Lake site have a Th content who reach 141 ppm (Smellie et al., 1994).

In natural waters, their concentrations are lower and it is often uncertain how the measured concentrations are distributed between species in true solution and those sorbed on suspended material. Uranium is rather abundant in surface sea water, $12 \cdot 10^{-9}$ M, while thorium is present only at $2.5 \cdot 10^{-12}$ M (Choppin and Stout, 1989).

In oceanic water the contents of Th ranges between 5 and $148 \cdot 10^{-14}$ (Whitfield and Turner, 1987). The residence time is 50 years.

The groundwaters from Cigar Lake have a contents of Th below $1.5 \cdot 10^{-9}$ M (Cramer et al., 1994).

Th in alkaline groundwaters in granites in southern europe was found to be associated with particulate material and not contained in true solution (Alaux-Negrel et al., 1993). McKinley et al. (1988) measured a concentration of $<0.2 \cdot 10^{-9}$ M in hyperalkaline groundwaters in Oman. Th concentrations of 0.06-$0.14 \cdot 10^{-9}$ M were measured in groundwaters in altered phonolites at Poços de Caldas (Bruno et al., 1992). Th was significantly associated with colloids in groundwaters in contact with uranium ore bodies at Nabarlek and Koongarra in the Alligator Rivers region, Northern Territory, Australia (Short and Lowson, 1988).

Only in two water samples from El Berrocal the ^{232}Th contents is over than $1.75 \cdot 10^{-11}$ M (Gómez et al., 1995).

5.17 PROTACTINIUM

The concentration of Pa in marine sediments is 10^{-5} ppm and in the continental earth crust 10^{-6} ppm (Fukai and Yokoyama, 1982). The same study gives the concentrations of U, Th and Ra.

Protactinium occurs in pitchblende to the extent of about 0.1 ppm. Ores from Congo have about 3 ppm. Protactinium has thirteen isotopes, the most common of which is ^{231}Pa with a half-life of 32500 years (Weast, 1975). Protactinium is one of the rarest natural occurring elements.

In sea water the concentration of Pa ranges between 10^{-14} M (Lloyd and Heathcote, 1985) and 10^{-17} M (Fukai and Yokoyama, 1982).

5.18 URANIUM

Uranium is a lithophilic element whose geochemistry is intimately linked with that of thorium. Uranium has a crustal abundance of 2.7 ppm, concentrated in granite (4.8 ppm) and shale (3.2 ppm) (Krauskopf, 1967).

Naturally-occurring uranium consist of three isotopes: ^{238}U, ^{235}U, and ^{234}U. ^{238}U and ^{235}U are parent isotopes for 2 separate radioactive decay series. No natural fractionation of ^{238}U and ^{235}U has been observed and all materials have a $^{238}U/^{235}U$ ratio of 137.5.

Although valence states between +3 and +6 could exist in nature, only the +4 and +6 valence states are of geochemical relevance.

Uranium occurs in a variety of minerals, but is concentrated in only a few. The most abundant uranium mineral is uraninite with a formula from UO_2 to U_3O_8. Well-crystallised UO_2 is described as uraninite and the microcrystalline form, pitchblende. Typical uranium contents of rock-forming minerals are as follows: feldspar - 0.1-10 ppm; biotite - 1-60 ppm; muscovite - 2-8 ppm; hornblende - 0.2-60 ppm; pyroxene - 0.1-50 ppm; olivine ~0.05 ppm; allanite - 30-1000 ppm; apatite - 10-100 ppm. In Wedepohl (1978) the following uranium minerals are listed: 15 oxides, 12 carbonates, 6 sulphates, 30 phosphate-arsenates, 10 vanadates, 15 silicates, 4 niobates and 5 molybdates.

Under oxidising conditions, pitchblende and uraninite are converted to bright-coloured minerals such as carnotite, $K_2(UO_2)_2(VO_4)_2.3H_2O$, tyuyamunite, $Ca(UO_2)_2(VO_4)_2.nH_2O$, autunite, $Ca(UO_2)_2(PO_4)_2nH_2O$, and rutherfordine, $UO_2.CO_3$. These minerals are soluble so that uranium may be transported by oxidising groundwater to be re-deposited under more reducing conditions.

The granite reference of El Berrocal has a U contents of about 16.5 ppm (Pérez del Villar et al., 1995).

The samples of the massive U-ore from Cigar Lake site have a U content who reach 220 ppm (Smellie et al., 1994).

Seawater contains $13.5 \cdot 10^{-9}$ M of uranium, mainly in the VI oxidation state. The ocean residence time is $3 \cdot 10^{5}$ years (Whitfield and Turner, 1987).

Edmuns et al., (1989) noted that most analyses of uranium in groundwaters in aquifers in the UK were below 10^{-7} M, although several anomalous values up to 10^{-5} M were observed. Uranium concentrations in alkaline-thermal waters in granites in southern Europe were limited by uraninite solubility (Alaux-Negrel et al., 1993). Bruno et al. (1992) concluded that waters in the alkaline rocks at Poços de Caldas were in equilibrium with pitchblende co-precipitated with Fe(III) oxy-hydroxides, with concentrations in the range: $1.7 \cdot 10^{-7}$ - $1.7 \cdot 10^{-8}$ M. A similar behaviour across the redox transition was observed in waters in contact with deep seabed sediments of the North Atlantic Abyssal Plain (Santschi et al., 1988), with concentrations ranging from 0.4 to $8 \cdot 10^{-9}$ M. In CO_2-rich waters from Vals-Bains (France), uranium concentrations are in the range 1-$3.5 \cdot 10^{-9}$ M (Michard et al., 1987).

Edmunds et al. (1987), measured uranium concentrations in deep groundwaters of the Carnmenllis granite in the range: $8 \cdot 10^{-11}$-$1.8 \cdot 10^{-7}$ M. Uranium concentrations in Stripa are in the range: $4 \cdot 10^{-8}$ to $3.7 \cdot 10^{-7}$ M. In the Cigar Lake uranium deposit uranium concentrations in the reduced zone are in the range $6 \cdot 10^{-9}$ to 10^{-7} M, indicating that the waters are in equilibrium with a slightly oxidised uraninite, represented by the stoichiometry $U_3O_7(s)$ (Bruno and Casas, 1994). In the oxidised part of Cigar Lake, the uranium concentrations range between 10^{-9} and $2 \cdot 10^{-6}$ M. This would suggest a control by the association of U(VI) to Fe(III) oxyhydroxides, present in this zone. Uranium concentrations associated with the uranium deposit at Crawford (Nebraska), have been reported by Spalding et al. (1984), in the range 20 to $300 \cdot 10^{-9}$ M.

In the hyperalkaline conditions encountered in Oman and Maqarin, the uranium concentrations are of the order of 10^{-11} M. This is in good agreement with the calculated solubility of Ca-uranates, the most stable phase under these conditions.

At higher temperatures and under reducing conditions the concentrations of uranium appear to be controlled by the uraninite-coffinite transition. Kraemer and Kharaka (1986) measured uranium concentrations in saline waters in geo-pressured aquifers (T:109-166 °C), in the US Gulf Cost , in the range 0.1-$2 \cdot 10^{-10}$ M.

The groundwaters from Cigar Lake have under 0.24 μM of U (Cramer et al., 1994).

5.19 NEPTUNIUM

In Cigar Lake site, the bounding concentrations for nuclear reaction products in groundwaters had been calculated. The maximum ^{237}Np concentrations in those waters is 10^{-10} M (Fabryka-Martin et al., 1994).

5.20 PLUTONIUM

Plutonium exists in trace quantities in naturally-occurring uranium ores. It is formed in much the same manner as neptunium, by irradiation of natural uranium with the neutrons which are present (Weast, 1975). The average ^{239}Pu contents of three samples from Cigar Lake ore is $1.2 \cdot 10^{-6}$ ppm (Fabryka-Martin et al., 1994).

The Pu and U release from the reaction zone of Oklo had been incorporated into the framework of the newformed chlorite (Gauthier-Lafaye, 1995).

Fifteen isotopes of plutonium are known. By far of greatest importance is the isotope ^{239}Pu, with a half-life of 24360 years, produced in extensive quantities in nuclear reactors from natural uranium (Weast, 1975).

Of the synthetic transuranium elements, plutonium and, to a lesser extent, americium are detectable in ecosystems (Choppin and Stout, 1989). Plutonium is found in relatively higher concentrations in the soil and water near the nuclear test sites and reprocessing facilities, primarily associated with subsurface soils, sediments or suspended particulates in water columns. When vegetation, animals, litter, and soils are compared, more than 99% of the plutonium is found in the sediments. Pu is transported mainly in ground water in the form of soluble species.

Very little plutonium is found in natural aquatic systems ($2.89 \cdot 10^{-17}$ M), making it difficult to obtain reliable values for the concentration (Choppin and Stout, 1989). Moreover, the amount of plutonium associated with suspended particulates may be more than an order of magnitude greater than that in true solution. In the Mediterranean, the plutonium activity in sea water was reduced 25-fold by passage the sample though a 0.45 μm filter.

The Pu concentrations in sea water, rivers and fresh water ranges between $2.6\ 10^{-18}$ M in the Mediterranean Sea and $1.6\ 10^{-14}$ M in the Irish Sea, near to Windscale (Choppin and Stout, 1989).

In the laboratory, the solubility of plutonium added to filtered sea water was measured to be $1.3\ 10^{-11}$ M after 30 days with 40% in ionic form (Choppin and Stout, 1989). The inclusion of humic material in these sea water samples increased the solubility of Pu six-fold after a month. Humic material are believed to be responsible for the higher concentrations of plutonium in organic-rich rivers and lakes.

In marine sediments from Palomares (Spain), plutonium was found to be associated mainly with organic mater and sesquioxides (Anton et al., 1994).

In marine natural waters, the limiting solubility of actinides is usually associated with either carbonate or hydroxide compounds. The insolubility of $Pu(OH)_4$ determines the amount of plutonium in solution, even if Pu(V) or Pu(VI) are the more stable states (Choppin and Stout, 1989).

In Cigar Lake site, the bounding concentrations for nuclear reaction products in groundwaters had been calculated. The maximum ^{239}Pu concentrations in those waters is 10^{-9} M (Fabryka-Martin et al., 1994).

5.21 AMERICIUM

Among the three isotopes of americium, ^{243}Am is the most stable with a half-life of 8800 years, compared to 470 years for ^{241}Am (Weast, 1975).

Trans-plutonium actinides (Am, Cm) have important III valences analogous to the lanthanides, at least, through Bk. The only important Am (IV) aqueous species may be $Am(OH)_5^-$ (Brookins, 1989). The same author gives stability constants for carbonate complexes of trivalent Am and Cm.

The stability fields for the Am species with and without C (Brookins, 1988) shows than the most important valence is III.

Observations of the distribution of ^{241}Am in marine environments indicate that Am has a high affinity for solid surfaces (Shanbhag and Morse, 1982).

5.22 CURIUM

Thirteen isotopes of curium are known. The most stable, ^{247}Cm, with a half-life of 16 millions years, is so short compared to the earth's age at any primordial curium must have disappeared. Natural curium has never been detected, not even in natural deposits of uranium (Weast, 1975).

The trivalent oxidation state is by far the most stable one for the curium element (Baes and Mesmer, 1976).

The stability constants for carbonate complexes of trivalent Cm are given by Brookins (1989).

5.23 NATURAL CONTENTS OF SEVERAL SOURCES AND SINKS FOR SOME TRACE ELEMENTS

	Stab. Isot.	Rocks Contents (ppm)	Minerals	Ocean Contents (M)	Resid. Time (years)	Fresh W.* Contents (M)	Ground Water Contents (M)
Ni		ultramaphic r. 200-2000 granite, shale 0.5-95	olivine, pyroxene, anphibole, spinel (clay minerals)	$2 - 10\ 10^{-9}$	$8\ 10^{4}$	$3\ 10^{-9}$	Poços $6\ 10^{-7}$
Se	79	shales 0.6	clausthalite (PbSe), galena (pyrite, sphalerite, ...)	$0.2 - 2.4\ 10^{-9}$	$3\ 10^{4}$	$0.2 - 9\ 10^{-9}$	Cigar Lake $<3.8\ 10^{-7}$ diluted $1.2 - 12\ 10^{-9}$
Sr		Poços 100-350 Berrocal <7	celestine, strontianite	$9\ 10^{-5}$	$4\ 10^{6}$		$0.2\text{-}80\ 10^{-6}$
Zr		Poços 100-2500 Berrocal 50-65	zircon, baddeleyite (ilmenite, rutile, perovskite)	$1.2 - 30\ 10^{-11}$			Poços $<1.1\ 10^{-6}$ UK $<8\ 10^{-9}$
Nb	93	syenites 100 Poços 30-320	niobite (pyroxene, anfivoles, micas, cassiterite)	10^{-10}			
Tc	99	Cigar Lake ore $8.5\ 10^{-7}$					Cigar Lake calculated $<10^{-9}$
Pd		Poços 0.4-26	olivine, bronzite, diopside, serpentine, zircon	$1.8 - 6.6\ 10^{-13}$	$5\ 10^{4}$		Oman $3 - 7\ 10^{-9}$ brines $0.2 - 20\ 10^{-9}$
Ag		Poços 0.2-10	blende, pyrite, galena (40 ppm)	$1 - 23\ 10^{-12}$	$5\ 10^{3}$		Poços $5\ 10^{-7}$ UK $< 10^{-9}$
Sn		Poços 5-20 Berrocal <30	cassiterite (pyroxenes, micas, anphiboles, sulphides)	$5 - 20\ 10^{-12}$		$2\ 10^{-11}$	UK $2.5 - 8.4\ 10^{-9}$
I	129	Cigar Lake ore $1.4\ 10^{-6}$	iodates, fluorapatite	$2 - 5\ 10^{-7}$	$3\ 10^{5}$		Cigar Lake $< 7.8\ 10^{-8}$ UK $1.6 - 26\ 10^{-8}$
Cs		Äspö 3 Poços 0.5	polucite	$2.3 - 3.7\ 10^{-9}$	$6\ 10^{5}$		Äspö $1.9\ 10^{-8}$ Cigar Lake $<5.2\ 10^{-7}$
Sm		granites 9.4 Poços 3-10, Berrocal 2	monazite, bastnasite, cerite	$2.7 - 6.8\ 10^{-12}$	200	$5\ 10^{-14} - 8\ 10^{-10}$	geothermal 10^{-7}, brines $4\ 10^{-8}$, other $10^{-11} - 10^{-7}$
Eu		Poços 2.5 Berrocal 0.06	monazite, bastnasite, cerite, plagioclase	$0.6 - 1.8\ 10^{-12}$	500	$10^{-14} - 2\ 10^{-10}$	$0.16\text{-}40\ 10^{-9}$
Ho		Poços 2 Berrocal 0.3	monazite, gadolinite	$1 - 3.6\ 10^{-9}$		$8.7\ 10^{-15}$	$<8.5\ 10^{-9}$
Ra	226		barite, celestine, anglesite	$1.6 - 7\ 10^{-16}$		$<10^{-12}$	$<5\ 10^{-12}$
Th	232	granite 17 Berrocal 7	thorianite,thorite, (uraninite, zircon, monazite)	$0.5 - 15\ 10^{-13}$	50	$4\ 10^{-11} - 4\ 10^{-9}$	$0.17\text{-}20\ 10^{-10}$
Pa	231		pitchblende (0.1 ppm)	$10^{-17} - 10^{-14}$			
U		Berrocal 16.5	uraninite, pitchblende, allanite, apatite,...	$1.4\ 10^{-8}$	$3\ 10^{5}$		Oman $4\ 10^{-11}$ other $10^{-9} - 4\ 10^{-7}$
Np							Cigar Lake calculated $<10^{-10}$
Pu	239	Cigar Lake ore $1.2\ 10^{-6}$		$2.9\ 10^{-17}$		$2\ 10^{-18} - 2\ 10^{-14}$	Cigar Lake calculated $<10^{-9}$
Am	243						
Cm	247						

Poços: subvolcanic phonolite strongly altered by hydrothermal and supergene processes
Berrocal: two mica alkaline feldspar granite
Äspö: porphyritic granite-granodiorite with fine lenses of metabasalts, metavolcanites and pegmatites
Cigar Lake: water saturated sandstone at the unconformity contact with the high-grade metamorphic rocks
UK: chalk, limestonne and sandstone of several aquifers

* Rivers and lakes

6 MEASURED RADIONUCLIDE CONCENTRATIONS FROM SPENT FUEL DISSOLUTION EXPERIMENTS. APPARENT SOLUBILITY LIMITS.

Spent fuel dissolution (leaching) experiments are in principle designed to obtain data concerning the dissolution rates and/or apparent solubility limits for relevant radionuclides in a variety of solvents, under different experimental conditions. The experiments are not designed *a priori* to obtain equilibrium radionuclide solubilities, but because of the long experimental periods involved steady state concentrations are reached which can be interpreted in terms of apparent solubilities (Bruno et al., 1985).

Different experimental procedures are used and this has an impact on the comparability of the reported data, although the conditions normally mimic those expected in the various repositories. Among the different parameters, the redox condition, the chemical composition of the leaching solutions, the Surface/Volume ratio and the saturation effects have been identified as the most significant. In spite of this, spent fuel dissolution data constitute an excellent test-bed to compare with the calculated solubilities, particularly for the transuranium radionuclides, where Natural System data is not existing.

In this chapter we will present reported experimental results concerning measured radionuclide concentrations from long-term spent fuel dissolution test performed within the various national programs. The reported results have been obtained in different laboratories: AECL in Canada (Tait et al., 1991 and Stroes-Gascoyne, 1992), PNL in USA (Wilson and Shaw, 1987, Gray, 1987, Wilson, 1990a, Wilson, 1990b), Studsvik in Sweden (Forsyth and Werme, 1992, Forsyth and Eklund, 1995) and FZK in Germany (Grambow et al., 1996).

The various sets of data are presented including a brief description of the experimental procedure:

6.1 AECL

CANDU fuel,	2-cm segments
Contact time:	30 days
Leachant:	DI water, Granitic GW, NaCl brine
Redox conditions:	Ar-3%H2, Ar, Air

Table 6-1. Radionuclides concentration from spent fuel dissolution experiments performed in AECL, contact time 30 days.

Redox conditions	Leaching solution	log solution concentration (mol/kg)				
		U	Tc	Pu	Am	Cm
Ar-3%H_2	DIW	-5.90	-8.45	-9.20	-11.16	-13.26
Ar-3%H_2	DIW	-6.40	-7.69	-9.01	-10.95	-13.08
Ar-3%H_2	DIW	-6.65	-8.14	-9.09	-10.95	-13.08
Ar-3%H_2	DIW	-8.44	-10.02	-10.49	-12.06	nm
Ar-3%H_2	DIW	-8.06	-9.77	-11.65	-13.27	nm
Ar-3%H_2	DIW	-7.11	-9.80	-8.90	-11.14	nm
Ar	DIW	-6.99	-9.05	-10.36	-12.13	-13.62
Ar	DIW	nm	nm	-9.63	-11.25	-13.40
Air	DIW	-4.82	nm	-8.97	-10.99	-13.26
Air	DIW	-6.64	nm	-9.65	-11.00	-12.54
Air	DIW	-3.43	-5.81	-7.14	-7.64	-9.46
Air	DIW	-3.38	nm	-7.04	-7.44	-9.40
Ar-3%H_2	NaCl	-5.75	-9.02	-8.15	-9.76	nm
Ar-3%H_2	Granitic [HCO^-_3] 0.005 M	-5.44	-7.55	-8.03	-9.92	nm
Ar-3%H_2	Granitic [HCO^-_3] 0.0011M	-6.51	-8.20	nm	nm	nm
Air	Granitic [HCO^-_3] 0.005 M	-6.40	nm	-9.37	-11.06	-12.99
Air	Granitic [HCO^-_3] 0.0011M	-6.43	nm	nm	nm	nm

nm = not measured

Table 6-2. Radionuclides concentration from spent fuel dissolution experiments performed in AECL. Contact time 500 days.

Redox conditions	Leaching solution	log solution concentration (mol/kg)			
		Cs	Sr	Tc	U
Ar-3%H_2-0.02%CO_2	DIW	-8.00	-9.70	-9.22	-7.40
	NaCl	-6.22	-7.40	-8.22	-6.70
	Granitic [HCO^-_3] 0.0011 M	-6.22	-7.40	-8.22	-7.10

A large number of leaching experiments by using CANDU (CANada Deuterium Uranium) fuel samples have been performed in this laboratory to determine fission product and actinide release and to establish the main factors which affect their release. Tables 6-1 and 6-2 show some of the results obtained in a short and in a long leaching period respectively.

Measured uranium concentrations range between $10^{-8.5}$ to $10^{-3.4}$ $mol \cdot dm^{-3}$. According to the authors, the fact that the values obtained are higher than the expected radionuclide concentrations (Lemire and Garisto, 1989) indicate that the redox condition of the system is more oxidising than expected due to the combination of radiolysis and high temperatures effects.

The measured uranium concentrations were in general lower in bidistilled water than in granitic groundwaters. However, the investigators did not observe any correlation as a function of the different groundwater compositions used as a solvent.

Measured Pu concentrations were in general lower than Pu concentrations predicted by the model of Lemire and Garisto. The authors attributed these differences to the fact that Pu concentrations in solution were limited by the quantity released from the fuel and not by the solubility due to the short time period of leaching (30 days).

Plutonium concentrations did not show a clear correlation with the composition of the contacting solution.

The technetium concentrations obtained in the experiments, indicated a redox control of this element, as expected from the redox behaviour of Tc.

Am and Cm concentrations appear to be , to some extent, dependent on the redox condition. As we can see in Table 6-1, the oxidising conditions caused an increase in the concentrations in solution, compared to the measured levels under reducing conditions. Because of the insensitivity of these elements to redox state, it has been postulated that the release of these radionuclides is controlled by the dissolution of the UO_2 matrix.

The increase of these radionuclides concentration in solution depending on the redox conditions seems to indicate the release of these elements according to the dissolution of the UO_2 matrix.

Bearing in mind the objective of our work, we have only selected the 500 day contact time data (Table 6-2), for the purpose of our comparisons.

6.2 PNL & YUCCA MOUNTAIN PROJECT

Several dissolution tests have been performed by using oxidised PWR spent fuel specimens, under different experimental conditions, temperature, solvent and fuel samples. Some of the leaching results obtained are given in

Table 6-3. These results are taken from Wilson, 1990a, 1990b and Gray, 1988.

By looking into the data from Table 6-3, we observe that the concentrations of the different radionuclides determined in solution decrease with the temperature of the system. This decrease in radionuclide concentrations at higher temperatures has been attributed to the precipitation of secondary solid phases. In this context, Wilson (1990b) identified uranophane, a calcium-uranium-silicate solid phase, in the experiments carried out at 85°C.

The fuel type used in the experiments had a slight effect on the measured U, Am and Np concentrations, whilst Pu did not show this dependence. The direct dependence of americium release on the fuel type used indicated that the release of Am is controlled by the UO_2 matrix dissolution. On the other hand and as it is shown in Table 6-3, the measured concentration of this radionuclide is strongly dependent on the filtration process.

When the experiments were performed in the presence of iron and by using NaCl brines (Gray, 1988) a decrease on the U and specially of Pu releases (approximately two orders of magnitude) was observed. This is due to the more reducing conditions imposed by the corrosion of iron in the system under study.

Table 6-3. Radionuclides concentration from spent fuel dissolution experiments obtained from PNL & Yucca Mountain project.

Solid	Redox conditions	Leaching solution	T (°C)	Contact time (days)	log solution concentration (mol/L)					
					U	Pu	Am	Np	Cm	Tc
Bare fuel series 2	Air	J-13	25	200	-5.39 ↓ -5.1	-9.1 ↓ -8.35	-9.82	-8.62	-11.6	
Bare fuel series 3	Air	J-13	25	200	-5.9	-8.4	-9.8	-8.9	-11.3	
Bare fuel series 3	Air	J-13	85	200	-6.18	-10.38	-12.38	-9.17	-14.3	-5.94 ↓ -5.22
mean value YM project					-5.22	-9.1 ↓ -8.4	-9.8 (0.4μm filt. sol.) -11.3 (1.8μm filt. sol.)	-8.6		
Fragments	Iron	NaCl brine	30	180	-7 ↓ -6.3	-9.8 ↓ -9				-7.8 ↓ -6.8
Fragments	no Iron	NaCl brine	30	180	-4.9 ↓ -4.2	-9 ↓ -7.3				-7.4 ↓ -6

6.3 STUDSVIK

BWR and PWR fuel, 2-cm segments, 21-49 Mwd/kg U local burnup

Temperature: 20-25 °C

Contact time: 500-1000 days

Solvent: DI water, Granitic GW

Redox conditions: oxic (air), anoxic (Ar + 5% H_2)

Table 6-4. Measured radionuclide concentrations from spent fuel dissolution experiments performed in Studsvik.

Redox conditions	Leaching solution	log solution concentration (mole/L)			
		U	Pu	Np	Tc
oxic	granitic	-5.22	-9.15	-9.41	
	GW	↓	↓	↓	
		-4.99	-8.27	-8.96	
oxic	DI water	-8.00	-7.7	-8.6	
anoxic	granitic	-7.22	-11.20	-11.37	-8.22
	GW	↓	↓	↓	
		-6.67	-10.09	-10.41	

Several long-term spent fuel leaching tests have been performed in this laboratory by using BWR and PWR specimens, under different experimental conditions.

The measured uranium, neptunium and plutonium are higher under oxidising conditions than under reducing ones.

The effect of the solution composition on the measured uranium and plutonium concentrations differs. Lower uranium concentrations are measured in distilled water than in synthetic granitic groundwater, whilst the measured plutonium concentrations are one order of magnitude larger in distilled water than in granitic groundwater. This effect has been recently rationalised in terms of solubility controls on Pu(IV) in granitic groundwater by the precipitation of $Pu(OH)_4(am)$, following the release of metastable Pu(IV) colloids (Bruno and Duro, 1996). This precipitation is not apparent when spent fuel is dissolved in distilled water. In such case, Pu concentrations remain around 10^{-8} mole·dm^{-3}, while in groundwater, Pu concentrations reach an steady state level ranging between 10^{-9} and 10^{-10} mole·dm^{-3}. The different solubility may be explained in terms of the stabilisation of suspensions in different solutions. First of all we can consider that a lower solubility may imply a larger particle size. On the

other hand, the coagulation of suspensions is favoured at higher ionic strengths (Stumm and Morgan, 1996), this could be the case of this radionuclide in groundwater. Finally, according to Rai and Swanson (1981), colloids tend to destabilise, and therefore, coagulate and precipitate when increasing pH, which is the case of groundwater with respect distilled water.

6.4 FZK-INE

PWR fuel, 50.4 Mwd/kg U

Temperature: 25 °C

Contact time: 400 days

Solvent: NaCl 95%

Redox conditions: Ar, iron, carbonate free

Table 6-5. Radionuclides concentration from spent fuel dissolution experiments performed in FZK.

Redox Conditions	log solution concentration (mole/kg)											
	U	Pu	Am	Np	Cm	Tc	Sr	Cs	Sb	Ag	Eu	Ru
Ar, iron	-7.0	-9.3	-10.4									
Ar	-6.0	-8.5	-10.4	-8.0	-9.4	-7.0	-8.0	-5.2	-8.1	-7.0	-8.1	-8.0
Ar	-4.2	-7.1	-8.0	-8.0	-7.5	-7.0	-6.0	-5.0	-6.5	-7.0	-8.1	-8.0

Spent fuel leaching studies performed in FZK have been carried out in brines.

The main trend in the results presented in Table 6-5 is an increase in the concentration of dissolved radionuclides as a function of the surface area/volume ratio, indicating a clear kinetic control.

Plutonium and uranium concentrations decrease in the presence of iron in the system due to the higher reducing conditions caused by the corrosion of Fe.

The lower uranium concentrations measured in comparison with results from other laboratories are attributed to the absence of carbonates in their system.

6.5 COMPARISON OF THE RESULTS OBTAINED IN THE DIFFERENT PROJECTS.

The following tables show the different results grouped as a function of the redox conditions, i.e. oxic and anoxic and as a function of the type of water used as leachant, i.e. distilled water, granitic ground water and brines.

Table 6-6. Results obtained in granitic groundwater and oxic conditions.

Granitic GW	Oxic	log solution concentration (mole/L)					
		U	Pu	Am	Np	Cm	Tc
AECL	Air	-6.43 ↓ -6.40	-9.37	-11.06		-12.99	
PNL	Air	-6.18 ↓ -5.10	-10.38 ↓ -8.35	-12.38 ↓ -9.80	-9.17 ↓ -8.62	-14.30 ↓ -11.30	-5.94 ↓ -5.22
STU	Air	-5.22 ↓ -4.99	-9.15 ↓ -8.27		-9.41 ↓ -8.96		

Table 6-7. Results obtained in granitic groundwater and anoxic conditions.

Granitic GW	Anoxic	log solution concentration (mol/L)					
		U	Pu	Am	Np	Cm	Tc
AECL	Ar 3%H_2	-6.51 ↓ -5.44	-8.03	-9.92			-8.2 ↓ -7.55
STU	Ar (Pd)	-7.22 ↓ -6.67	-11.20 ↓ -10.09		-11.37 ↓ -10.41		-8.22

Table 6-8. Results obtained in bidistilled water and oxic conditions.

DIW	Oxic	log solution concentration (mole/L)					
		U	Pu	Np	Am	Cm	Tc
AECL	Air	-6.64 ↓ -3.38	-9.65 ↓ -7.04		-11.00 ↓ -7.44	-13.26 ↓ -9.40	-5.81
STU	Air	-8.00	-7.7	-8.6			

Table 6-9. Results obtained in bidistilled water and anoxic conditions.

DIW	Anoxic	log solution concentration (mole/L)						
		U	**Pu**	**Am**	**Cm**	**Tc**	**Sr**	**Cs**
AECL	Ar 3%H_2	-8.44 ↓ -5.90	-11.65 ↓ -8.9	-13.27 ↓ -10.95	-13.26 ↓ -13.08	-10.02 ↓ -7.69	-9.70	-8.00
FZK-INE	Ar	-5.95	-7.48	-8.00	-10.47			

Table 6-10. Results obtained in brines and anoxic conditions.

Brine	Anoxic	log solution concentration (mol/L)											
		U	**Pu**	**Am**	**Np**	**Cm**	**Tc**	**Sr**	**Cs**	**Sb**	**Ag**	**Eu**	**Ru**
AECL	Ar 3%H_2	-5.75	-8.15	-9.76			-9.02						
PNL	Iron	-7.0 ↓ -6.3	-9.8 ↓ -9.0				-7.8 ↓ -6.8						
	No iron	-4.9 ↓ -4.2	-9 ↓ -7.3				-7.4 ↓ -6.0						
FZK-INE	Ar iron	-7.0	-9.3	-10.4									
	Ar	-6.0	-8.5	-10.4	-8.0	-9.40	-7.0	-8.0	-5.22	-8.09	-7.0	-8.09	-8.0

The concentrations of radionuclides measured in spent fuel leaching experiments are dependent on redox conditions as it is expected for sensitive redox actinides. In this sense for Uranium, Plutonium and Neptunium, the concentrations measured under anoxic conditions are 1 and 2 orders of magnitud lower than the ones measured under oxic conditions. In the case of Americium and Curium similar concentrations are measured independent on redox conditions.

The comparison of the results obtained under similar redox conditions but in brine or in granitic groundwater seems to indicate that actinides concentrations in brines are higher than those obtained in granitic groundwater.

7 SOLUBILITY CALCULATIONS

Solubility calculations have been performed by using the code EQ3NR (Wolery, 1992). The database used has been the Nagra/SKB-97-TDB and is described in chapter 10.

The correction of the ionic strength of the system has been performed by using the b-dot equation (Helgeson, 1969). This equation is an extended Debye-Hückel model which add the b°×I term, the b-dot parameter depends on the electrical charge of the species in question. This approach is used by default by the EQ3NR code. Due to the relatively low ionic strength of the granitic groundwaters, we judged this correction to be sufficiently accurate for the purpose of the calculations.

The calculations have been performed by using three water compositions. Their compositions are given in Tables 7-1, 7-2 and 7-3 respectively.

These waters correspond to three different environments, the first one is the Äspö groundwater, with a low carbonate content (SKB, TR SR-95). This water has been used in the previous sections as a reference water to calculate both the conditional constants and the speciation and to perform the sensitivity analysis (Section 8). The second one is a typical Finnsjön fresh groundwater, with a high carbonate content (Ahlbom and Smellie, 1989) and the last one corresponds to a bentonite pore water based on the work performed by Wanner and co-workers (1992) which simulates groundwater composition after saturating and equilibrating with the bentonite barrier in a repository system. The result is a higher pH, and a larger carbonate and sulphate contents.

While this work was in progress, SKB changed the composition of the reference Äspö and Finnsjön waters and added a third reference water; Gideä. The solubilities obtained according to these reference waters will be discussed later (Section 9).

Table 7-1. Composition of the Äspö water used in the calculations.

Component	Concentration ($mol \cdot dm^{-3}$)	$\pm\sigma$
Na	$9.13 \cdot 10^{-2}$	$9 \cdot 10^{-3}$
Ca	$4.75 \cdot 10^{-2}$	$5 \cdot 10^{-3}$
Mg	$1.73 \cdot 10^{-3}$	$8 \cdot 10^{-4}$
Fe	$4.12 \cdot 10^{-6}$	$4 \cdot 10^{-6}$
H_4SiO_4	$1.46 \cdot 10^{-4}$	$2 \cdot 10^{-5}$
HCO_3^- (free)	$1.64 \cdot 10^{-4}$	$8 \cdot 10^{-5}$
Cl^-	$1.80 \cdot 10^{-1}$	$2 \cdot 10^{-2}$
SO_4^{2-}	$5.73 \cdot 10^{-3}$	$6 \cdot 10^{-4}$
S^{2-}	$5.63 \cdot 10^{-6}$	$5 \cdot 10^{-6}$
PO_4^{3-}	$9.47 \cdot 10^{-8}$	$9 \cdot 10^{-8}$
pH	8.3	0.1
pe	-5.07	0.4

Table 7-2. Composition of the Finnsjön fresh water used in the calculations.

Component	Concentration ($mol \cdot dm^{-3}$)
Na	1.00E-03
K	8.21E-05
Ca	1.90E-03
Mg	2.59E-04
Fe	1.61E-04
H_4SiO_4	2.14E-04
HCO_3^- (free)	3.61E-03
F^-	3.16E-05
Cl^-	1.72E-03
Br^-	3.75E-06
SO_4^{2-}	9.27E-05
NO_3^-	8.06E-06
pH	6.9
pe	-3.38

Table 7-3. Composition of the bentonite water used in the calculations.

Component	Concentration ($mol \cdot dm^{-3}$)
Na	9.13E-02
Ca	1.00E-04
Mg	4.12E-05
HCO_3^- (free)	4.75E-03
Cl^-	1.92E-03
SO_4^{2-}	3.54E-02
pH	9.21

Calculations have been also performed by equilibrating these waters with magnetite and hematite in order to simulate redox conditions after groundwater gets in contact with the canister corrosion products in the repository system.

The solubilities have been calculated by taking into account the solubility limiting solid phases obtained in the solid speciation.

A basic principle in our calculations has been to assume that the less crystalline metal hydroxide phases are kinetically favoured (Ostwald Principle), and consequently they constitute the initial solubility limiting phases. In spite of the fact, that more stable phases could form in the system.

We have also assumed for radium the possibility that its solubility is limited by co-precipitation with other alkaline-earth-elements, and for curium and americium that their solubilities are limited by co-dissolution from the fuel according to the lower concentrations measured in spent fuel leching tests.

If nuclides are released due to a failure in the repository system radium could co-precipitate with strontium carbonate under groundwater conditions. By using the molar fraction reported in a previous work (Cera et al., 1995) based on natural systems determinations, we have calculated the corresponding conditional solubility constant (K_s*) according to the co-precipitation approach (Bruno et al., 1995).

$$\log K_s^* = \log K_s + \log \chi \qquad 7\text{-}1$$

Under the same conditions, curium and americium will co-dissolve with uranium. By taking measured values of nuclides in fuel samples (Guenther et al., 1989) we have calculated the molar fractions (χ) of Cm and Am with respect to U. The solubilities have been calculated according to the co-dissolution approach.

$$[TE] = \chi \times [Me] \qquad 7\text{-}2$$

where [TE] is the concentration of the trace element (Cm or Am), χ is the molar fraction and [Me] is the concentration of the major element.

The molar fractions considered in the calculations as well as the conditional solubility constant for radium are given in the following table.

	χ	logK_s	logK_s*
Cm	$2.88 \cdot 10^{-5}$		
Am	$4.32 \cdot 10^{-4}$		
Ra	0.001	-10.26	-13.26

The results of the solubility calculations as well as the aqueous speciation are given in Tables 7-4 and 7-5 respectively.

Table 7-4. Calculated solubilities and limiting solid phases.

	ÄSPÖ (old)		FINNSJÖN(old)		BENTONITE	
pH	**8.30**		**6.90**		**9.21**	
$[HCO_3^-]_{free}$	**$1.64 \cdot 10^{-4}$**		**$3.54 \cdot 10^{-3}$**		**$4.75 \cdot 10^{-3}$**	
pe	**-5.07**	**-5.60***	**-3.38**	**-4.20***	**-3.38**	**-6.51***
ELEMENT	*Solubility (mole·dm^{-3}) / Limiting Solid Phase*					
Ni	$3.68 \cdot 10^{-4}$ NiO	$3.68 \cdot 10^{-4}$ NiO	high NiO	high NiO	high NiO	high NiO
Se	$1.97 \cdot 10^{-10}$ FeSe	$3.42 \cdot 10^{-10}$ FeSe	$1.37 \cdot 10^{-10}$ $FeSe_2$	$1.08 \cdot 10^{-11}$ FeSe		$2.59 \cdot 10^{-9}$ FeSe
Sr	$2.31 \cdot 10^{-4}/8.51 \cdot 10^{-4}$ strontianite/celestite	$2.31 \cdot 10^{-4}/8.51 \cdot 10^{-4}$ strontianite/celestite	$7.05 \cdot 10^{-4}$ strontianite	$7.61 \cdot 10^{-4}$ strontianite	$1.21 \cdot 10^{-4}$ strontianite	$1.21 \cdot 10^{-4}$ strontianite
Zr	$2.49 \cdot 10^{-9}$ ZrO_2(am)	$2.49 \cdot 10^{-9}$ ZrO_2(am)	$2.51 \cdot 10^{-9}$ ZrO_2(am)	$2.51 \cdot 10^{-9}$ ZrO_2(am)	$2.50 \cdot 10^{-9}$ ZrO_2(am)	$2.50 \cdot 10^{-9}$ ZrO_2(am)
Nb	$1.96 \cdot 10^{-4}$ Nb_2O_5(ac)	$1.96 \cdot 10^{-4}$ Nb_2O_5(ac)	$2.14 \cdot 10^{-5}$ Nb_2O_5(ac)	$2.14 \cdot 10^{-5}$ Nb_2O_5(ac)	$1.37 \cdot 10^{-3}$ Nb_2O_5(ac)	$1.37 \cdot 10^{-3}$ Nb_2O_5(ac)
Tc	$7.14 \cdot 10^{-9}$ $TcO_2 \cdot xH_2O$	$7.14 \cdot 10^{-9}$ $TcO_2 \cdot xH_2O$	$1.18 \cdot 10^{-8}$ $TcO_2 \cdot xH_2O$	$1.18 \cdot 10^{-8}$ $TcO_2 \cdot xH_2O$	$7.57 \cdot 10^{-9}$ $TcO_2 \cdot xH_2O$	$7.67 \cdot 10^{-9}$ $TcO_2 \cdot xH_2O$
Pd	$4.15 \cdot 10^{-9}$ PdO	$4.15 \cdot 10^{-9}$ PdO	$4.17 \cdot 10^{-9}$ PdO	$4.17 \cdot 10^{-9}$ PdO	$4.17 \cdot 10^{-9}$ PdO	$4.17 \cdot 10^{-9}$ PdO
Ag	$5.28 \cdot 10^{-15}$ Ag(s)	$1.56 \cdot 10^{-15}$ Ag(s)	$5.79 \cdot 10^{-17}$ Ag(s)	$8.72 \cdot 10^{-17}$ Ag(s)	$6.28 \cdot 10^{-17}$ Ag(s)	$4.64 \cdot 10^{-20}$ Ag(s)
Sn	$9.48 \cdot 10^{-10}$ SnO_2	$9.48 \cdot 10^{-10}$ SnO_2	$4.41 \cdot 10^{-10}$ SnO_2	$4.41 \cdot 10^{-10}$ SnO_2	$4.49 \cdot 10^{-9}$ SnO_2	$4.49 \cdot 10^{-9}$ SnO_2
Sm	$7.00 \cdot 10^{-7}$ $Sm_2(CO_3)_3$	$7.00 \cdot 10^{-7}$ $Sm_2(CO_3)_3$	$4.17 \cdot 10^{-7}$ $Sm_2(CO_3)_3$	$4.20 \cdot 10^{-7}$ $Sm_2(CO_3)_3$	$8.03 \cdot 10^{-7}$ $Sm_2(CO_3)_3$	$8.03 \cdot 10^{-7}$ $Sm_2(CO_3)_3$
Ho	$2.48 \cdot 10^{-6}$ $Ho_2(CO_3)_3$	$2.48 \cdot 10^{-6}$ $Ho_2(CO_3)_3$	$1.61 \cdot 10^{-6}$ $Ho_2(CO_3)_3$	$1.62 \cdot 10^{-6}$ $Ho_2(CO_3)_3$	$5.58 \cdot 10^{-6}$ $Ho_2(CO_3)_3$	$5.58 \cdot 10^{-6}$ $Ho_2(CO_3)_3$

Table 7-4. Calculated solubilities and limiting solid phases (Cont.)

	ÄSPÖ (old)		FINNSJÖN (old)		BENTONITE	
pH	**8.30**		**6.90**		**9.21**	
$[HCO_3^-]_{free}$	**$1.64 \cdot 10^{-4}$**		**$3.54 \cdot 10^{-3}$**		**$4.75 \cdot 10^{-3}$**	
pe	**-5.07**	**-5.60***	**-3.38**	**-4.20***	**-3.38**	**-6.51***
ELEMENT	*Solubility (mole·dm^{-3}) / Limiting Solid Phase*					
Ra	$2.95 \cdot 10^{-7}$	$2.95 \cdot 10^{-7}$	$1.76 \cdot 10^{-6}$	$1.91 \cdot 10^{-6}$	$4.57 \cdot 10^{-8}$	$4.57 \cdot 10^{-8}$
	$RaSO_4$		$RaSO_4$		$RaSO_4$	
Ra-copret.	$2.95 \cdot 10^{-10}$	$2.95 \cdot 10^{-10}$	$1.76 \cdot 10^{-9}$	$1.91 \cdot 10^{-9}$	$4.57 \cdot 10^{-11}$	$4.57 \cdot 10^{-11}$
$\chi=10^{-3}$	Ra-copret		Ra-copret		Ra-copret	
Th	$2.40 \cdot 10^{-10}$	$2.40 \cdot 10^{-10}$	$2.40 \cdot 10^{-10}$	$2.40 \cdot 10^{-10}$	$1.22 \cdot 10^{-9}$	$1.22 \cdot 10^{-9}$
	$Th(OH)_4$		$Th(OH)_4$		$Th(OH)_4$	
Pa	$3.15 \cdot 10^{-7}$	$3.15 \cdot 10^{-7}$	$3.17 \cdot 10^{-7}$	$3.17 \cdot 10^{-7}$	$3.16 \cdot 10^{-7}$	$3.16 \cdot 10^{-7}$
	Pa_2O_5		Pa_2O_5		Pa_2O_5	
U	$1.27 \cdot 10^{-7}$	$1.27 \cdot 10^{-7}$	$1.29 \cdot 10^{-7}$	$1.29 \cdot 10^{-7}$	$1.34 \cdot 10^{-5}$	$1.28 \cdot 10^{-7}$
	UO_2(fuel)		UO_2(fuel)		UO_2(fuel)	
Np	$6.99 \cdot 10^{-9}$	$6.99 \cdot 10^{-9}$	$4.88 \cdot 10^{-8}$	$9.39 \cdot 10^{-8}$	$5.83 \cdot 10^{-8}$	$5.87 \cdot 10^{-8}$
	$Np(OH)_4$		$Np(OH)_4$		$Np(OH)_4$	
Pu	$1.92 \cdot 10^{-10}$	$4.05 \cdot 10^{-10}$	$6.07 \cdot 10^{-8}$	$4.07 \cdot 10^{-7}$	$1.04 \cdot 10^{-10}$	$1.38 \cdot 10^{-10}$
	$Pu(OH)_4$(am)		$Pu(OH)_4$(am)		$Pu(OH)_4$(am)	
Am	$2.37 \cdot 10^{-7}$	$2.37 \cdot 10^{-7}$	$6.37 \cdot 10^{-7}$	$6.40 \cdot 10^{-7}$	$9.34 \cdot 10^{-8}$	$9.34 \cdot 10^{-8}$
	$AmOHCO_3$		$AmOHCO_3$		$AmOHCO_3$	
Am-codiss.	$5.49 \cdot 10^{-11}$	$5.49 \cdot 10^{-11}$	$5.57 \cdot 10^{-11}$	$5.57 \cdot 10^{-11}$	$5.79 \cdot 10^{-9}$	$5.53 \cdot 10^{-11}$
$\chi=4.32 \cdot 10^{-4}$	Am-codiss.		Am-codiss.		Am-codiss.	
Cm	$5.52 \cdot 10^{-8}$	$5.52 \cdot 10^{-8}$	$2.07 \cdot 10^{-8}$	$2.12 \cdot 10^{-8}$	$1.66 \cdot 10^{-10}$	$1.66 \cdot 10^{-10}$
	$CmOHCO_3$		$CmOHCO_3$		$CmOHCO_3$	
Cm-codiss.	$3.66 \cdot 10^{-12}$	$3.66 \cdot 10^{-12}$	$3.71 \cdot 10^{-12}$	$3.71 \cdot 10^{-12}$	$3.86 \cdot 10^{-10}$	$3.69 \cdot 10^{-12}$
$\chi=2.88 \cdot 10^{-5}$	Cm-codiss.		Cm-codiss.		Cm-codiss.	

* pe assuming equilibrium with magnetite (constraint assigned to O_2 fugacity) and hematite (constraint assigned to iron concentration)

Table 7-5. Aqueous speciation.

	ÄSPÖ (old)	FINNSJÖN (old)	BENTONITE
pH	**8.30**	**6.90**	**9.21**
$[HCO_3^-]_{free}$	**$1.64 \cdot 10^{-4}$**	**$3.54 \cdot 10^{-3}$**	**$4.75 \cdot 10^{-3}$**
pe	**-5.07** **-5.60***	**-3.38** **-4.20***	**-3.38** **-6.51***
ELEMENT	*Aqueous speciation*		
Ni	Ni^{2+} $NiCO_3(aq)$ $NiCl^+$		
Se	HSe^-	HSe^-	HSe^-
Sr	Sr^{2+} $SrSO_4(aq)$	Sr^{2+}	$SrSO_4(aq)$ Sr^{2+}
Zr	$Zr(OH)_4(aq)$	$Zr(OH)_4(aq)$	$Zr(OH)_4(aq)$
Nb	NbO_3^- $Nb(OH)_5(aq)$	$Nb(OH)_5(aq)$	NbO_3^-
Tc	$TcO(OH)_2(aq)$	$TcO(OH)_2(aq)$ $TcOCO_3(aq)$ $Tc(OH)_2CO_3(aq)$	$TcO(OH)_2(aq)$
Pd	$Pd(OH)_2(aq)$	$Pd(OH)_2(aq)$	$Pd(OH)_2(aq)$
Ag	$AgCl_3^{2-}$ $AgCl_4^{3-}$ $AgCl_2^-$	$AgCl(aq)$ Ag^+ $AgCl_2^-$	$AgCl(aq)$ Ag^+ $AgCl_2^-$
Sn	$Sn(OH)_5^-$ $Sn(OH)_4(aq)$	$Sn(OH)_4(aq)$	$Sn(OH)_5^-$ $Sn(OH)_4(aq)$
Sm	$SmCO_3^+$ Sm^{3+}	$SmCO_3^+$ $Sm(CO_3)_2^-$	$Sm(CO_3)_2^-$
Ho	$HoCO_3^+$ $Ho(CO_3)_2^-$ Ho^{3+}	$HoCO_3^+$ $Ho(CO_3)_2^-$	$Ho(CO_3)_2^-$

Table 7-5. Aqueous speciation (Cont.)

	ÄSPÖ (old)	FINNSJÖN (old)	BENTONITE
pH	**8.30**	**6.90**	**9.21**
$[HCO_3^-]_{free}$	**$1.64 \cdot 10^{-4}$**	**$3.54 \cdot 10^{-3}$**	**$4.75 \cdot 10^{-3}$**
pe	**-5.07** **-5.60***	**-3.38** **-4.20***	**-3.38** **-6.51***
ELEMENT	*Aqueous speciation*		
Ra	Ra^{2+} Ra^{2+} $RaSO_4(aq)$	Ra^{2+}	$RaSO_4(aq)$ Ra^{2+}
Th	$Th(OH)_4(aq)$	$Th(OH)_4(aq)$	$Th(CO_3)_5^{6-}$ $Th(OH)_4(aq)$
Pa	$PaO_2OH(aq)$	$PaO_2OH(aq)$	$PaO_2OH(aq)$
U	$U(OH)_4(aq)$	$U(OH)_4(aq)$	$UO_2(CO_3)_3^{4-}$ $U(OH)_4(aq)$
Np	$Np(OH)_4(aq)$ $Np(OH)_3CO_3^-$	$Np(OH)_3CO_3^-$ $Np(CO_3)_2^-$ $Np(CO_3)_2^-$ $Np(OH)_3CO_3^-$ $Np(OH)_4(aq)$	$Np(OH)_3CO_3^-$ $Np(OH)_4(aq)$
Pu	$Pu(OH)_4(aq)$ $Pu(OH)_2^+$ $Pu(OH)_2^+$ $Pu(OH)_4(aq)$	$PuCO_3^+$ Pu^{3+}	$Pu(OH)_4(aq)$ $Pu(OH)_4(aq)$ $Pu(OH)_2^+$
Am	$Am(OH)_2^+$ $AmOH^{2+}$ $AmCO_3^+$	$AmCO_3^+$	$Am(CO_3)_3^{3-}$ $Am(CO_3)^{2-}$
Cm	$CmOH^{2+}$	$CmOH^{2+}$	$CmOH^{2+}$

* pe assuming equilibrium with magnetite (constraint assigned to O_2 fugacity) and hematite (constraint assigned to iron concentration)

7.1 DISCUSSION

In this section we will discuss the reported radionuclide solubility limits, in the light of the evidence from relevant Natural System Studies, as well as the information collected from Spent Fuel Dissolution tests. The data from Natural System studies includes the trace element concentration measurements performed in connection with Natural Analogue studies in Poços de Caldas (Brazil), Cigar Lake (Canada) and El Berrocal (Spain). Data on Pd measurements from the hiperalkaline environment in Oman are also included. Other data that has been introduced in the comparison with Natural Systems include the survey of UK groundwaters and seawater concentrations, as a final reference. The data concerning uranium, fission products and transuranium elements from spent fuel tests have been selected from the previously set of data presented with the following criteria: in principle only data collected in log term synthetic groundwater experiments has been chosen. For uranium, the data selected is the one in nominally anoxic or reducing conditions, to minimise alteration effects of the spent fuel matrix. For the rest of the radionuclides, data in oxic conditions is preferred. This is because we are interested in secondary solubility limits for these radionuclides, and the long term oxic alteration of the spent fuel matrix could in principle favour the maximum release of the nuclides from the matrix.

7.1.1 Ni

We have assumed that under reducing, NiO(s) is the solubility limiting phase. The precipitation of pure Ni(II) sulphides is not assumed due to the competition of iron for the limited sulphide supply. The precipitation of mixed Ni(II)-Fe(II) sulphides is not considered, although these are probably the most realistic phases to control the solubility of Ni(II) under reducing conditions.

The calculated solubilities by assuming the precipitation of NiO(s) are unrealistically high, if compared to the measured Ni(II) concentrations in relevant natural systems. An upper Ni solubility limit of 10^{-6} mole dm^{-3}, would appear to be reasonable if we take into account the data obtained in Poços de Caldas (Brazil), El Berrocal (Spain) and Swiss groundwaters. Berner (1994) has arrived to similar conclusions. The Ni content in groundwaters and sea water ranges from $6 \cdot 10^{-7}$ to 10^{-9} mole·dm^{-3}. See Figure 7-1.

The free Ni^{2+} cation and $NiCO_3(aq)$ are the predominant aqueous species under the conditions of the calculations.

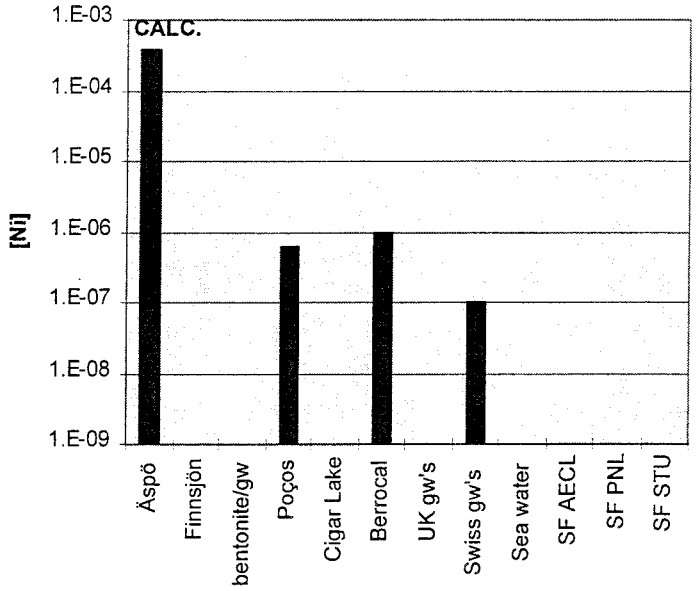

Figure 7-1. Nickel concentrations calculated in this work and measured values in Natural Systems.

7.1.2 Se

As we have already discussed (Section 4), the limiting solid phase for this element is critically dependent on the redox state of the system. Under reducing conditions, the solubility of selenium is limited by the precipitation of selenides, mainly of Fe, Cu and Pb, keeping Se at low concentration levels. Due to similarities of selenide in charge and ionic radius with sulphide, substitution and co-precipitation of these anions can occur (Sellin and Bruno, 1992).

In the range of waters considered in this exercise, the calculated solubilities are not affected by the difference in compositions, ranging between 10^{-8} and 10^{-10} mole·dm^{-3}. This is because all the groundwaters have a reducing redox condition. Otherwise, we have to take into account that under oxidising conditions, solubilities increase. However, even under oxidising conditions, the reported Se levels in UK groundwaters (Edmunds et al., 1989) are in the same range ($1.2 \cdot 10^{-8}$ to $3 \cdot 10^{-10}$ mole·dm^{-3}). See Figure 7-2.

The other effect on selenium solubilities is the concentration of Fe in the groundwaters, in such case, the solubility of the solid phase increases when decreasing the iron concentration.

A realistic solubility limit is expected to be below $6 \cdot 10^{-7}$ mole·dm^{-3} calculated for $FeSe_2$ (Berner, 1994).

The predominant aqueous species is HSe^- in all water compositions studied.

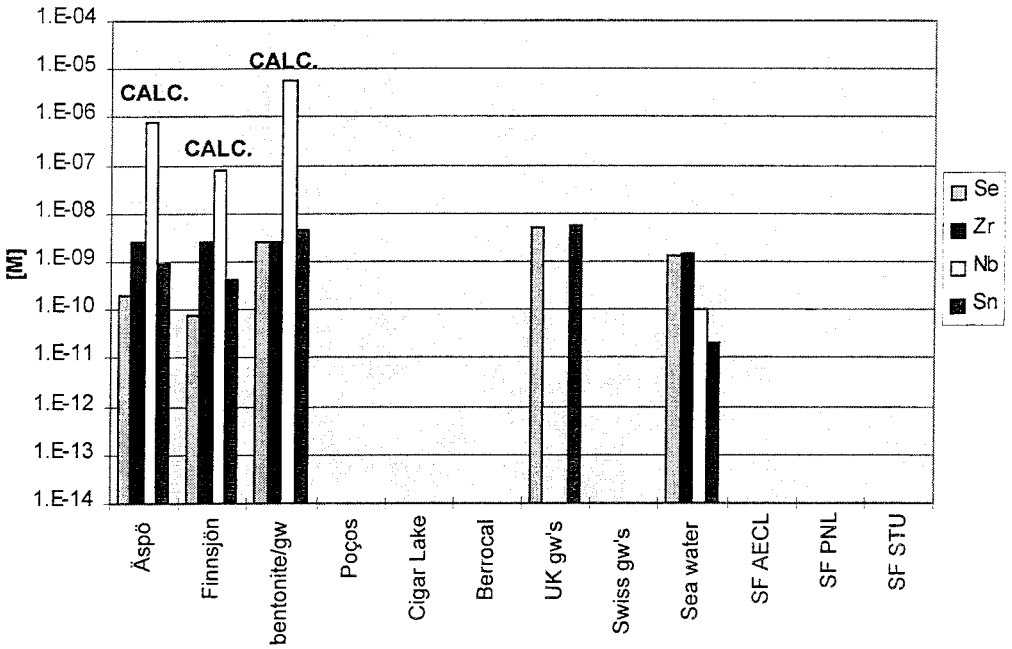

Figure 7-2. Selenium, zirconium, niobium and tin concentrations calculated in this work and reported values from Natural Systems and from spent fuel dissolution experiments.

7.1.3 Sr

The calculated solubility limit for this element under the conditions of the exercise, is imposed by the precipitation of either sulphate or carbonate solid phases. The stability range of these phases is quite close under these conditions, and the precipitation of a particular phase depends on the aqueous $[CO_3^{2-}]/[SO_4^{2-}]$ ratio. In Äspö groundwater (low carbonate content) two solid phases can limit the solubility due to the close solubility values obtained by considering this water composition. Solubility values obtained are 2-8 10^{-4} mole·dm^{-3} for strontianite and celestite, as calculated by using the HARPHRQ code package (Brown et al., 1989). These values are in good agreement with the measured levels at Äspö, $4 \cdot 10^{-4}$ mole·dm^{-3} (SR 95).

The Sr^{2+} free cation is the dominant aqueous species in the waters studied. However, due to the relatively high suphate content of the bentonite pore water considered in this study the predominant aqueous phase becomes the strontium sulphate.

The calculated solubilities decrease when increasing carbonate content in solution due to the stabilisation of the strontianite.

As we will see in a later discussion, the solubility of these phases is highly dependent on the system studied, obtaining solubility values for the same phase ranging from $1 \cdot 10^{-3}$ to $4 \cdot 10^{-4}$ mole·dm^{-3}, depending on the calculation approach.

7.1.4 Zr

ZrO_2 is the solubility limiting solid phase in all calculations. This solid phase, presents different degrees of stability depending on crystallinity, a common thread in many four valent metal oxides. Following the Ostwald rule, we have considered the less crystalline (more soluble) to perform the calculations. Zirconium contents in natural waters is in general much lower than the calculated solubilities, this is mainly because Zr normally resides in very weathering resistant silicates, and it dissolution is kinetically controlled at the source. This fact is normally used in geochemistry to define the background unaltered level in bedrock. Therefore, the calculated Zr concentrations can be considered as a conservative but also a realistic estimate of the behaviour of this element as it is released from the Zircalloy elements (see Figure 7-2).

The dominant aqueous species in all the waters studied is $Zr(OH)_4(aq)$. This complex is expected to be the dominant species in average granitic groundwaters.

7.1.5 Nb

Solubility is limited by the Nb_2O_5 phase, we again have selected the more soluble phase compiled in the databases. The calculated solubilities increase with pH. The changes in solubilities are basically associated to this parameter.

The abundance of niobium in sea water is 10^{-10} mole·dm^{-3}, this concentration is lower than the solubilities obtained from the calculations (see Figure 7-2 or 7-3). There are, to our knowledge, no data available of niobium concentrations in river or ground waters.

The speciation in granitic groundwaters is dominated by NbO_3^- and $Nb(OH)_5(aq)$, depending on the pH of the groundwater considered.

7.1.6 Tc

Under reducing conditions, the solubility limiting solid phase is the hydrous technetium dioxide. The calculated solubilities are not affected by the different water compositions considered. They are of the same order of magnitude than experimental concentrations obtained from long term spent fuel dissolution tests in granitic groundwaters, with the exception of the data reported by PNL, which is higher due to the oxic conditions of the experiments carried out. (see Figure 7-3)

The aqueous speciation is mainly dominated by $TcO(OH)_2$ in the groundwaters under study, however, in the Finnsjön water, dominant aqueous species include also $TcOCO_3(aq)$ and $Tc(OH)_3CO_3^-$, as a consequence of the higher total carbonate content of this water.

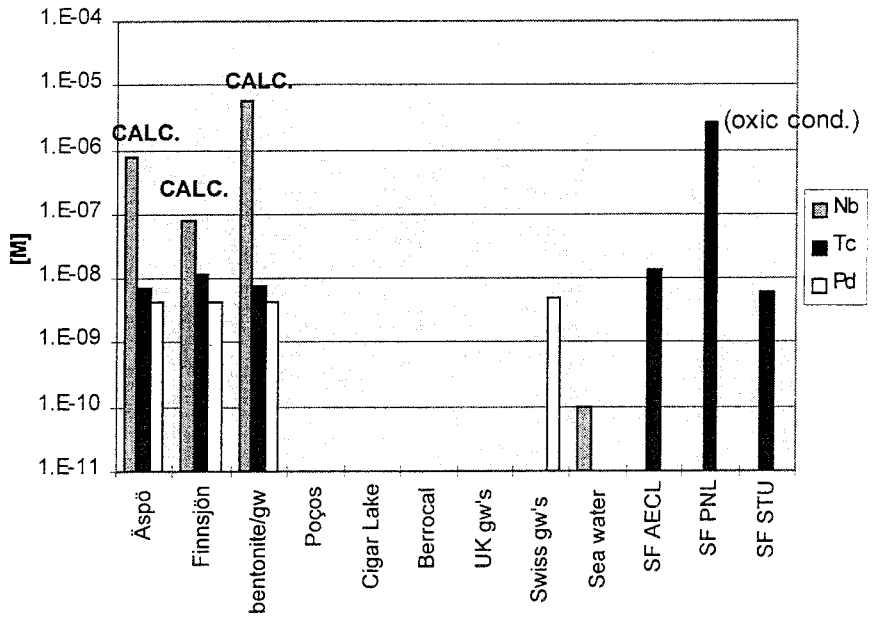

Figure 7-3. Technetium, niobium and palladium concentrations calculated in this work and reported values from Natural Systems and from spent fuel dissolution experiments.

7.1.7 Pd

Palladium oxide is considered the limiting solid phase in the groundwaters studied. The calculated solubilities are not affected by the different water compositions assumed. Several insoluble palladium compounds, i.e., sulphides, elemental palladium can be considered under reducing conditions as solubility limiting solid phases, however, these phases give unrealistically low, due to their low solubility values ($\approx 10^{-27}$ mole·dm^{-3}). The palladium concentrations measured in the hyperalkaline Oman groundwaters ($3\text{-}7 \cdot 10^{-9}$ mole·dm^{-3}) are in good agreement with the solubilities obtained in this work. Sea water levels are in the 10^{-13} mole·dm^{-3} range (see Figure 7-3).

The dominant aqueous complex is in all cases $Pd(OH)_2(aq)$.

7.1.8 Ag

The solubility limiting solid phase considered in these calculations has been the Ag(s). The solubilities obtained are very low and initially we can consider them independent of water composition. However, the calculated solubilities in the Äspö waters are two orders of magnitude higher than in Finnsjön and bentonite waters. This is mainly due to the higher chloride content in Äspö waters.

The calculated solubilities are lower than the concentrations measured in several natural systems (sea and groundwaters) which range between 10^{-12} to 10^{-9} mole·dm^{-3}. Therefore, an upper realistic limit for Ag(I) solubility

would be given by the concentration measured in Poços de Caldas, 10^{-7} mole dm^{-3}. The precipitation of metallic silver is probably hindered by kinetic constrains.

An alternative solubility limiting phase is AgCl(s) which would imply larger solubilities of the order of 10^{-5} mole·dm^{-3} in Äspö groundwater .

The aqueous speciation is dominated basically by chloride complexes and the Ag^{+} free cation, depending on the chloride content.

7.1.9 Sn

Under reducing conditions SnO_2 is the solubility limiting solid phase while the dominant aqueous species are $Sn(OH)_4(aq)$ and $Sn(OH)_5^-$ if we consider the groundwaters studied.

The calculated solubilities increase with pH. The changes in solubilities are basically associated to this parameter.

Calculated solubilities are in good agreement with measured concentrations in several groundwaters, these values ranges between 10^{-10} to·10^{-8} mole·dm^{-3} (see Figure 7-2).

7.1.10 Sm

The solid phase that limits the solubility of this element in all groundwaters studied is the $Sm_2(CO_3)_3$. The formation of mixed hydroxocarbonato solid phase similar to the ones formed by Am(III) has not been reported (Spahiu and Bruno, 1995). Aqueous speciation is mainly dominated by samarium carbonates.

The calculated solubilities are not affected by the different water compositions assumed. Only a slight increase in solubility is calculated by increasing pH.

Samarium contents in different natural waters ranges between 10^{-7} and 10^{-12} mole·dm^{-3} while calculated solubilities are slightly higher than the upper limit given. Measurements of REE in spent fuel dissolution tests are scarce. We have used a datum provided for Eu in leach tests at AECL for comparison. In the overall, the reported solubilities can be considered as conservative. (see Figure 7-4).

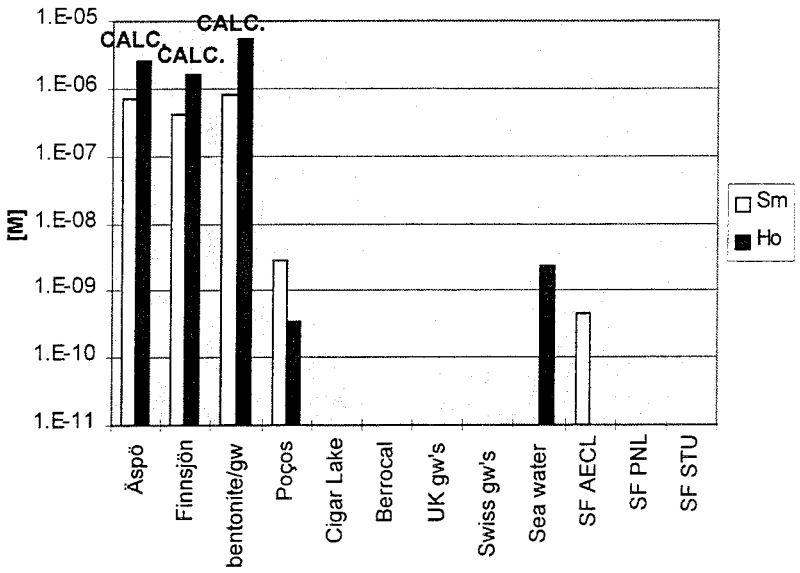

Figure 7-4. Samarium and holmium concentrations calculated in this work and reported from several Natural Systems and from spent fuel dissolution experiments.

7.1.11 Ho

Holmium follows the same behaviour as Samarium. Therefore, the solubility limiting solid phase is $Ho_2(CO_3)_3(s)$, and the dominant aqueous speciation is given by the holmium carbonates.

The calculated solubilities are not affected by the different water compositions assumed. Only a slight increase in solubility is calculated by increasing pH.

Holmium contents in natural waters are low in comparison with calculated solubilities reported. Therefore, the calculated solubility limits have to be considered as conservative (see Figure 7-4).

7.1.12 Ra

The aqueous speciation is dominated by the Ra^{2+} free cation, however, in waters with higher sulphate content, $RaSO_4(aq)$ becomes the dominant aqueous species.

The solubility limiting solid phase in the groundwaters studied is $RaSO_4(s)$. The equilibrium concentrations decrease when increasing pH.

Radium concentrations in natural waters do not exceed 10^{-12} mole·dm^{-3}. The ^{226}Ra measured values in the ore zone at Cigar Lake are two order of magnitude larger than the ones measured in other parts of the system, although they are in the 5 10^{-13} mole·dm^{-3} range. These values are low in comparison with calculated individual solubilities reported in this work.

Radium is usually either source term controlled or co-precipitates with other major cations (Langmuir and Riese, 1985). Reported solubility values by considering its co-precipitation are closer to the measured concentrations in natural waters and could be considered as upper realistic levels to Ra(II) solubility in granitic environments. (see Figure 7-5)

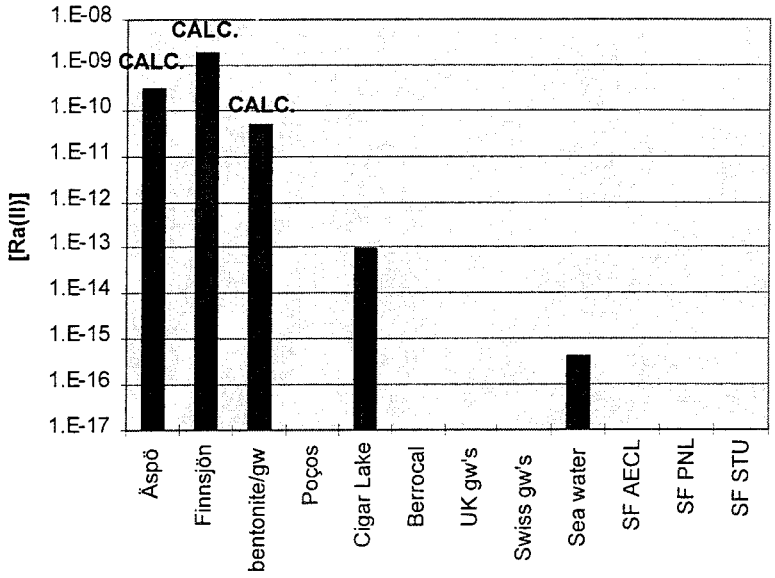

Figure 7-5. Radium solubilities calculated in this work by assuming co-precipitation and reported concentrations measured in Natural Systems.

7.1.13 Th

$Th(OH)_4(am)$ has been taken as the solubility limiting solid phase. The calculated solubilities do not change between the Äspo and Finnsjön waters.

On the other hand, the calculated solubilities increase in the bentonite pore water due to an increase in the carbonate content. This increase is given by the stabilisation of the $Th(CO_3)_5^{6-}$ which causes an increase in the solubility of the solid phase.

The aqueous speciation is dominated by the complex $Th(OH)_4(aq)$ except in the case of the bentonite pore water where the dominant aqueous phase is $Th(CO_3)_5^{6-}$. The rôle of mixed Th(IV)-hydroxo-carbonato complexes (Östhols, 1994) is unclear, as they have not been included in the selected data bases.

Calculated solubilities agree with the value reported by Berner (1994) corresponding to the crystalline ThO_2 phase. The same author obtained a value of $5 \cdot 10^{-7}$ mole·dm^{-3} for the hydrous phase. The difference in the solubility values obtained by this author and the values reported in this work is due to the different thermodynamic data available in the data bases used, as it was previously discussed.

The calculated solubilities are in the range of the reported thorium content in natural systems, including the Natural Analogue sites at Poços de Caldas, Cigar Lake and Berrocal. ($1.75 \cdot 10^{-11}$-$4.3 \cdot 10^{-9}$ mole·dm^{-3}), see Figure 7-6.

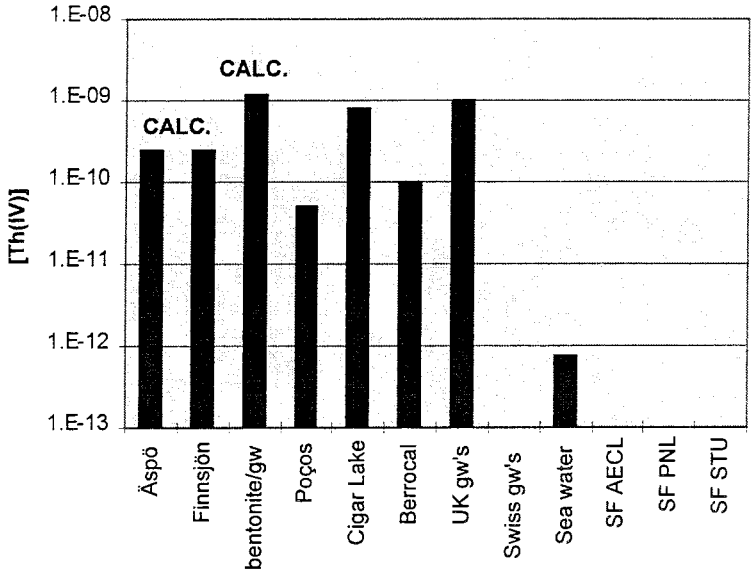

Figure 7-6. Thorium concentrations calculated in this work and measured values in Natural Systems.

7.1.14 Pa

The aqueous speciation is dominated by PaO_2OH, under all the conditions of the calculations.

The solubility limiting solid phase is Pa_2O_5. The calculated solubilities are not affected by the different water compositions assumed. Reported solubilities agree with the calculations previously performed by Bruno and Sellin (1992).

Protactinium is also a trace component in the reprocessed glass matrices with a U:Pa ratio of 10^6. By considering a congruent release of the protactinium with the uranium, and by taking a conservative estimate of the uranium solubility of 10^{-7} mole·dm^{-3}, Berner calculated the dissolved protactinium by obtaining a value of 10^{-13} mole·dm^{-3}. According to this result, calculated solubilities reported in this work can be considered very conservative.

Reported solubilities are higher than protactinium content found in natural waters (10^{-17}-10^{-14} mole·dm^{-3}), see Figure 7-7. However, due to the fact that this is one of the most scarce elements in Earth, source term control in Natural Systems cannot be ruled out.

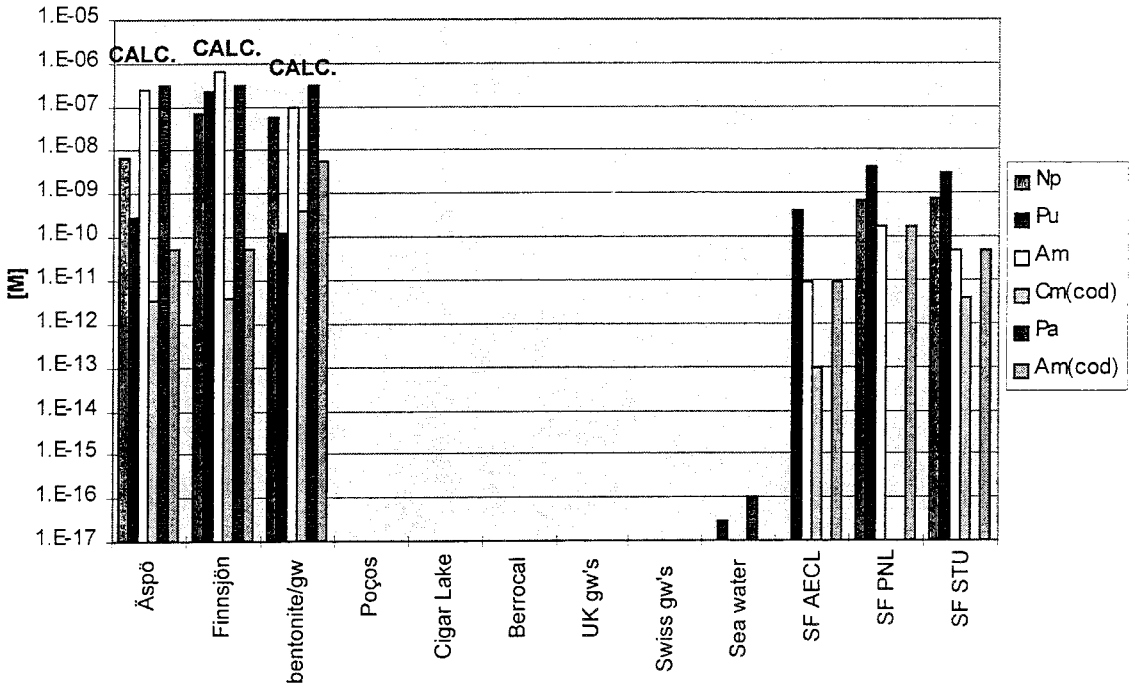

Figure 7-7. Radionuclide solubilities calculated in this work and measured concentrations in spent fuel dissolution experiments.

7.1.15 U

The dominant aqueous speciation is given by the complex $U(OH)_4$ in Äspö and Finnsjön groundwaters. However, in the case of the bentonite pore water, because the composition of this water lies on a higher pH, pe domain, the aqueous speciation is dominated by the uranyl tri-carbonato complex.

The solubility limiting solid phase is UO_2(fuel). In general, there is not a major variation in calculated solubilities within the water compositions assumed.

However, the calculated solubility increases in the bentonite pore water at pe=-3.38, due to the stabilisation of the $UO_2(CO_3)_3^{4-}$.

In order to study the effect of the carbonate content in the solubility of this solid phase, we have calculated the solubility curve depending on the bicarbonate content in water (Figure 7-8). Calculations have been performed by using the bentonite pore water composition, at pH=9.21 and pe=-3.38.

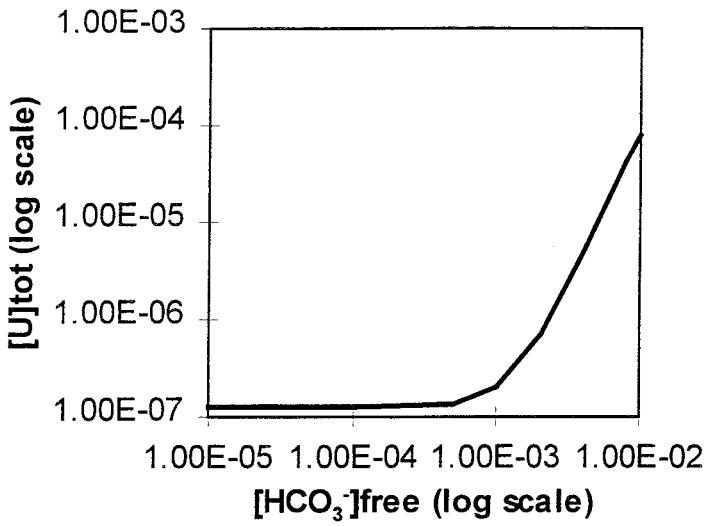

Figure 7-8. Solubility curve of uranium as a function of the free bicarbonate concentration.

As we can see in the graph, solubility markedly raises at a free bicarbonate content of 10^{-3} mole·dm^{-3}.

The reported solubilities are in good agreement with measured uranium concentrations in many natural systems, including Cigar Lake, Poços de Caldas , Stripa and El Berrocal. There is also quite a good agreement with most of the reported uranium concentration measurements from spent fuel dissolution test in granitic groundwaters. The high results form PNL are the exception. (see Figure 7-9). Berner (1994), selected a realistic solubility limit of 10^{-7} mole·dm^{-3} for uranium, see Figure 7-9.

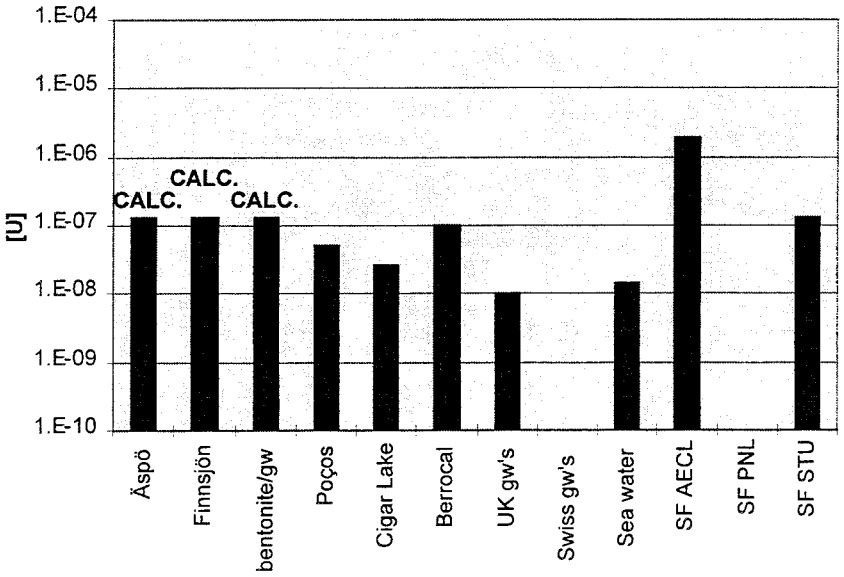

Figure 7-9. Uranium solubilities calculated in this work and reported measured concentrations from Natural Systems and from spent fuel dissolution tests.

7.1.16 Np

The aqueous speciation is dominated by the $Np(OH)_4$ (aq) complex in the Äspö groundwater. However, when the carbonate content increases, as is the case of the Finnsjön and bentonite waters, neptunium carbonates complexes become the dominant aqueous species.

Np as well as Pu and the rest of actinides are expected to be in solid solution with the UO_2 fuel and therefore *a priori* to be mobilized congruently with the oxidative dissolution of the matrix. However, according to experimental results (Forsyth and Werme, 1992), the release of neptunium and plutonium are independent of the uranium release, indicating a secondary solubility control for both phases.

Figure 7-10 illustrates the different Np/U ratio for the inventory of the fuel samples and in solution for two different times (Experimental data extracted from Forsyth and Eklund, 1995). The different ratios in solution with respect the inventory as well as the fact that the solution concentrations remain constant with time indicate a solubility control of the neptunium release.

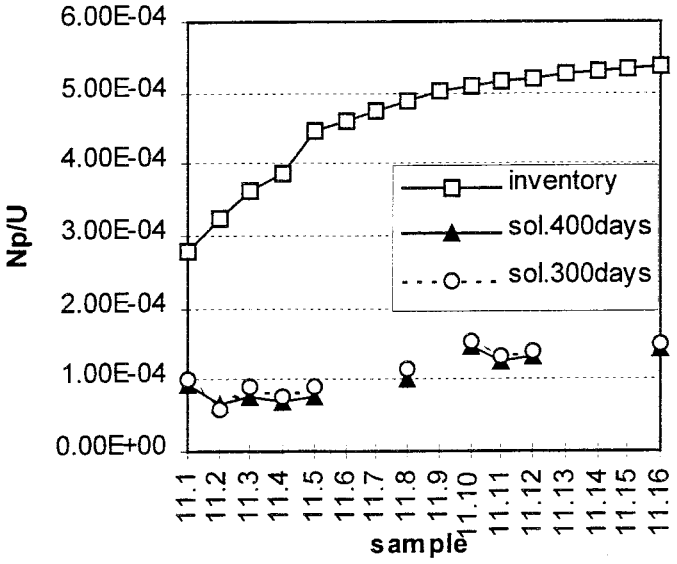

Figure 7-10. Np/U ratios in the inventory and in solution for the experiments of series 11, carried out in Studsvik (Forsyth and Eklund, 1995).

Therefore a solubility control has been considered for neptunium to calculate the expected neptunium concentrations in the groundwaters studied.

Under reducing conditions, $Np(OH)_4(s)$ is the solubility limiting solid phase. The calculated solubilities increase approximately one order of magnitude in Finnsjön and bentonite waters due to the increase in carbonate content. This increase is provided by the stabilisation of carbonate complexes in solution.

The calculated solubilities are of the same order of magnitude or one order of magnitude larger than neptunium concentrations determined from spent fuel leaching tests (see Figure 7-7) Therefore, the calculated values can be taken as realistically conservative.

7.1.17 Pu

The predominant aqueous species are $Pu(OH)_4(aq)$ and $Pu(OH)_2^+$, with the exception of the Finnsjön water where, due to the lower pH, Pu^{3+} becomes the dominant aqueous species.

As for neptunium, a solubility control is expected for this actinide in solution, The solubility is limited by $Pu(OH)_4(am)$, by applying the Ostwald rule to this very dynamic system. Because of the stabilisation of the aqueous Pu(III) species, the solubility increases when decreasing pH and consequently, the higher solubilities have been calculated in Finnsjön waters.

As we can see in Figure 7-11, the solubility of this phase is strongly dependent on the pH under reducing conditions due to the stabilisation of Pu(III) aqueous complexes as previously mentioned.

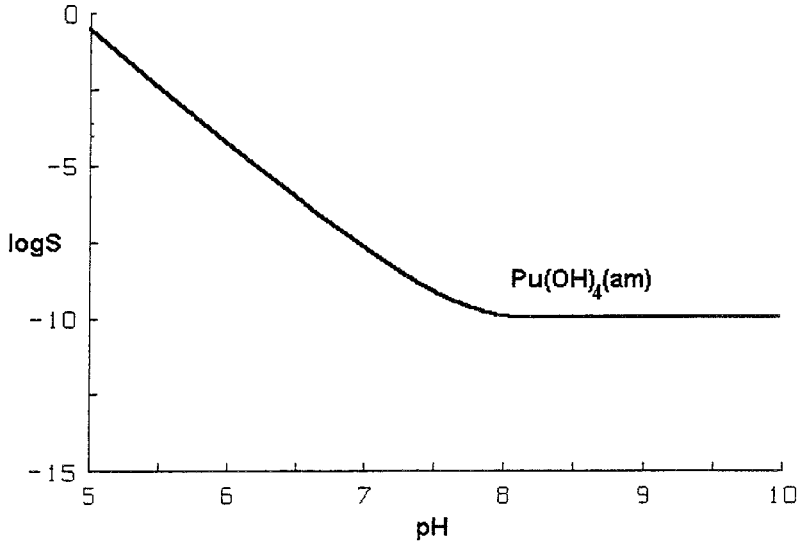

Figure 7-11. Solubility curve of Pu(OH)4(am) as a function of pH (Finnsjön water, pe=-3-38).

Reported solubilities from Finnsjön water are 2 orders of magnitude larger than the measured plutonium concentrations in spent fuel dissolution tests (Werme and Forsyth, 1989). However, calculated solubilities from Äspö and bentonite waters are in the same range than reported solubilities from these spent fuel dissolution tests (see Figure 7-12). Concentrations measured in natural waters are in general lower, probably due to Pu(IV) sorption on particles, or source term limitations.

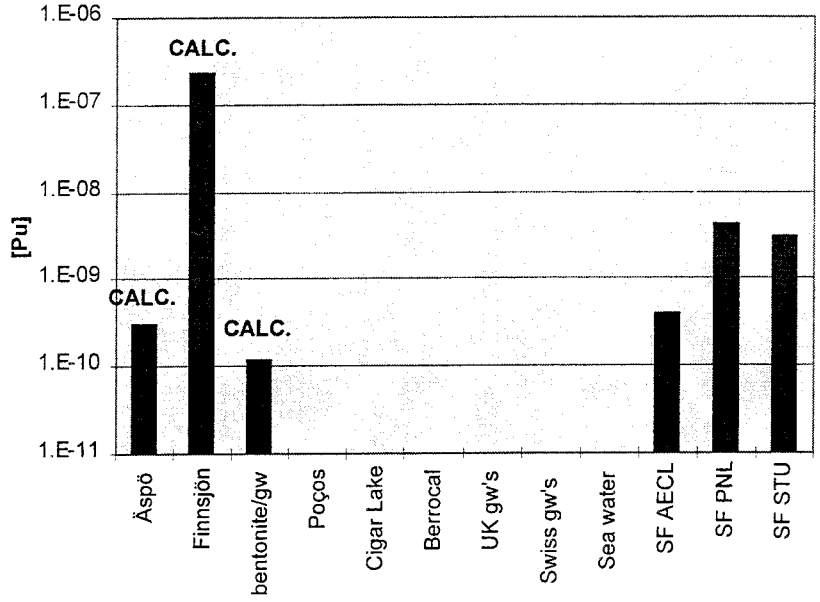

Figure 7-12. Plutonium concentrations calculated in this study and reported values from spent fuel dissolution tests.

7.1.18 Am

Am(III) hydroxides are the predominant aqueous complexes in the Äspö reference water. Americium (III) carbonates become, the dominant aqueous species in the Finnsjön and bentonite waters due to their higher carbonate content.

$AmOHCO_3$ (s) is the solubility limiting phase in all the waters studied. The solubility limiting phase is independent on the different water compositions. However, the solubility of americium increases slightly in the more acidic Finnsjön waters.

There are not reported values of americium content in natural waters. However, measured americium concentrations in spent fuel dissolution experiments are approximately 3 orders of magnitude lower than reported solubilities of this work (see Figure 7-7). This could either be the result of a different solubility limiting phase in the spent fuel leaching tests, or more probably that the release of Am is controlled by the dissolution of the spent fuel matrix. An estimate of the Am(III) levels obtained by assuming the congruent dissolution of Am(III) with the dissolved uranium gives us solubilities in the 10^{-11} mole dm^{-3} range, in satisfactory agreement with the measured concentrations in Spent Fuel leach tests. At any rate, the calculated individual solubilities can be treated as conservative.

7.1.19 Cm

The aqueous speciation is dominated by the complex $Cm(OH)^{2+}$ in all the waters studied.

The solubility limiting solid phase is $CmOHCO_3(s)$. The calculated solubilities decrease when increasing carbonate content, and consequently the lower solubilities are obtained in bentonite pore waters.

The release of Cm(III), similarly to the behaviour of Am(III) will be mainly controlled by the dissolution of the spent fuel matrix. Therefore, we have calculated the expected solubilities by assuming the co-dissolution with the UO_2 matrix. The calculated Cm(III) concentrations fall in the same range as the Cm(III) measured in spent fuel dissolution tests, 10^{-12} mole dm^{-3}, as it can be seen in Figure 7-7.

8 SENSITIVITY ANALYSIS

The sensitivity analysis has been performed in order to study solubility changes associated to the analytical errors in the determination of the main parameters, pH, Eh and bicarbonate content of the water.

The groundwater composition used in these calculations corresponds to the reported in Äspö (SR 95) (Table 7-1). The calculations have been performed by using the same code package as in the case of aqueous and solid speciation. No ionic strengh effects have been considered.

Solubility changes are reported in two ways; 1) as percentages of error associated to the analytical error of each main parameter (Table 8-1) and 2) as the mean standard deviation (Table 8-2).

We have considered a weak influence if percentage of error is lower than 30%. In opposite, a percentage of error higher has been classified as a strong influence. This last case is indicated in bold in Table 7-6.

As a general trend the solubilities of metal oxides and hydroxides studied are not influenced by the analytical error in groundwater compositions. However, there are some elements which are slight influenced by the uncertainties on pH determinations as we can see in Table 8-1. These elements are Ni, Sn, Pu and Am.

Holmium has a larger uncertainty on pH measurements. This influence is associated to the various predominant solid phases as a function of water composition (see solid speciation). The precipitation of holmium hydroxide is also strongly influenced by analytical error on carbonate determination, this is mainly due to the higher stability of the carbonate solid phase with respect the hydroxide. The carbonate solid phase is only slightly influenced by pH and carbonate analytical errors due to its higher stability.

The uncertainty on Eh determinations has a clear effect on the solubility of phases which have a strong redox dependency in the measured Eh range in Äspö: Se, Pd, Ag and also Pu.

Finally, as expected, carbonate solid phases are influenced by the analytical error on the carbonate determination. Because of the interconnection between the carbonate system and pH, the carbonate phases are also dependent on pH variations. However, in general this influence is lower than the influence on carbonate.

Table 8-1. (I). Percentage of error in calculated solubilities associated to the analytical errors in groundwater determinations.

			Parameters					
			pH=8.3±0.1		pe=-5.07±0.4		HCO_3^-= $1.64\cdot10^{-4}\pm8\cdot10^{-5}$	
Element	**Solid Phase**	**Solubility**	**pH-σ**	**pH+σ**	**pe-σ**	**pe+σ**	**HCO_3^-- σ**	**HCO_3^-+σ**
		($mol\cdot dm^{-3}$)	**% of error**					
Ni	NiO	$2.17\cdot10^{-4}$	**32**	**31**			19	16
Se	FeSe	$1.03\cdot10^{-10}$	20	19				
	$FeSe_2$	$7.51\cdot10^{-10}$	20	20	**57**	**60**		
	Se	$1.10\cdot10^{-6}$	20	21	**82**	**84**		
Sr	$SrCO_3$	$4.18\cdot10^{-4}$	21	21			**49**	**32**
	$SrSO_4$	$5.27\cdot10^{-4}$						
Zr	ZrO_2(c)	$2.51\cdot10^{-12}$						
	ZrO_2(am)	$2.51\cdot10^{-9}$						
Nb	Nb_2O_5(ac)	$8.14\cdot10^{-5}$	18	26				
Tc	$TcO_2.xH_2O$	$7.24\cdot10^{-9}$						
Pd	PdO	$4.17\cdot10^{-9}$						
	Pd(m)	$3.98\cdot10^{-29}$	**37**	**37**	**84**	**84**		
Ag	Ag(s)	$3.37\cdot10^{-15}$			**60**	**60**		
	AgCl(s)	$1.26\cdot10^{-5}$						
Sn	SnO_2	$8.16\cdot10^{-10}$	10	11				
Sm	$Sm_2(CO_3)_3$	$1.80\cdot10^{-7}$	9	8			29	15
Ho	$Ho(OH)_3$(am)	$1.82\cdot10^{-5}$	**34**	**32**			**51**	**38**
	$Ho(OH)_3$(c)	$7.63\cdot10^{-8}$	**34**	**33**			**49**	**37**
	$Ho_2(CO_3)_3$	$7.18\cdot10^{-7}$	6	5			24	11
Ra	$RaSO_4$	$1.40\cdot10^{-7}$						
	$RaCO_3$	$4.58\cdot10^{-3}$	20	20			**47**	**32**
	Ra-SO_4-cop	$1.40\cdot10^{-10}$						
	Ra-CO_3-cop	$4.75\cdot10^{-6}$	21	20			**49**	**32**
Th	ThO_2(c)	$7.59\cdot10^{-15}$						
	ThO_2(am)	$4.79\cdot10^{-9}$						
	$Th(OH)_4$(am)	$2.40\cdot10^{-10}$						
Pa	Pa_2O_5	$1.58\cdot10^{-7}$						
U	UO_2(am)	$9.12\cdot10^{-6}$						
	UO_2(fuel)	$1.86\cdot10^{-7}$						
	UO_2(c)	$1.05\cdot10^{-10}$						
Np	NpO_2(c)	$4.36\cdot10^{-18}$					12	10
	$Np(OH)_4$	$6.92\cdot10^{-9}$					12	10
Pu	PuO_2(c)	$4.41\cdot10^{-17}$	18	13	**33**	20	2	2
	$Pu(OH)_4$	$1.57\cdot10^{-10}$	18	13	**33**	20	2	2
Am	$Am(OH)_3$(am)	$6.38\cdot10^{-6}$	28	27			10	9
	$Am(OH)_3$(c)	$1.01\cdot10^{-7}$	28	27			10	10
	$Am(OH)CO_3$	$1.03\cdot10^{-7}$	10	7			**43**	25
Cm	$CmOHCO_3$	$1.02\cdot10^{-8}$	21	20			**49**	**32**
	Cm-copret.	$6.47\cdot10^{-10}$	21	21			**49**	**32**

Bold numbers indicate a % of error greater than 30%.

Table 8-2. (II). Calculated solubilities and standard deviations.

Element	Solid Phase	Solubility (mol·dm-3)	±σ
Ni	NiO	$2.17 \cdot 10^{-4}$	$7.81 \cdot 10^{-5}$
Se	FeSe	$1.03 \cdot 10^{-10}$	$3.16 \cdot 10^{-11}$
	$FeSe_2$	$7.51 \cdot 10^{-10}$	$6.30 \cdot 10^{-10}$
Sr	$SrCO_3$	$4.18 \cdot 10^{-4}$	$2.40 \cdot 10^{-4}$
	$SrSO_4$	$5.27 \cdot 10^{-4}$	
Zr	ZrO_2(am)	$2.51 \cdot 10^{-9}$	
Nb	Nb_2O_5(ac)	$8.14 \cdot 10^{-5}$	$3.08 \cdot 10^{-5}$
Tc	$TcO_2.xH_2O$	$7.24 \cdot 10^{-9}$	$1.41 \cdot 10^{-11}$
Pd	PdO	$4.17 \cdot 10^{-9}$	
Ag	Ag(s)	$3.37 \cdot 10^{-15}$	$5.03 \cdot 10^{-15}$
	AgCl(s)	$1.26 \cdot 10^{-5}$	
Sn	SnO_2	$8.16 \cdot 10^{-10}$	$1.27 \cdot 10^{-10}$
Sm	$Sm_2(CO_3)_3$	$1.80 \cdot 10^{-7}$	$4.52 \cdot 10^{-8}$
Ho	$Ho(OH)_3$(am)	$1.82 \cdot 10^{-5}$	$1.04 \cdot 10^{-5}$
	$Ho_2(CO_3)_3$	$7.18 \cdot 10^{-7}$	$1.36 \cdot 10^{-7}$
Ra	$RaSO_4$	$1.40 \cdot 10^{-7}$	
	$RaCO_3$	$4.58 \cdot 10^{-3}$	$2.52 \cdot 10^{-3}$
	Ra-SO_4-cop	$1.40 \cdot 10^{-10}$	
	Ra-CO_3-cop	$4.75 \cdot 10^{-6}$	$2.74 \cdot 10^{-6}$
Th	$Th(OH)_4$(am)	$2.40 \cdot 10^{-10}$	
Pa	Pa_2O_5	$1.58 \cdot 10^{-7}$	
U	UO_2(fuel)	$1.86 \cdot 10^{-7}$	
Np	$Np(OH)_4$	$6.92 \cdot 10^{-9}$	$1.15 \cdot 10^{-9}$
Pu	$Pu(OH)_4$	$1.57 \cdot 10^{-10}$	$4.04 \cdot 10^{-11}$
Am	$AmOHCO_3$	$1.03 \cdot 10^{-7}$	$4.53 \cdot 10^{-8}$
Cm	$CmOHCO_3$	$1.02 \cdot 10^{-8}$	$5.93 \cdot 10^{-9}$
	Cm-copret.	$6.47 \cdot 10^{-10}$	$3.73 \cdot 10^{-10}$

9 SOLUBILITY LIMITS IN ÄSPÖ, FINNSJÖN AND GIDEÅ GROUNDWATERS

In order to complete the previous solubility calculations presented, we have considered three groundwater compositions corresponding to the three hypothetical sites finally selected by SR97 for the HNLW repository in Sweden. These sites are located in Äspö, Finnsjön and Gideå.

9.1 SELECTED GROUNDWATERS

The groundwater compositions used in the calculations are given in Tables 9-1, 9-2 and 9-3 respectively. These groundwaters have been selected to represent the deep groundwater at the three hypothetical sites used in the performance assessment study SR 97.

The first one is the Äspö groundwater, with a low carbonate and a high chloride and sulphate contents (SR 95). The second one is a typical Finnsjön fresh groundwater, with a high carbonate and a low chloride and sulphate contents and the last one corresponds to the Gideå groundwater with lower carbonate, chloride and sulphate concentrations and with a higher pH with respect the previous ones (Alhbom and Smellie,1989).

Two different redox states have been considered in order to perform the calculations as indicated in Tables 9-1, 9-2 and 9-3.

Table 9-1. Composition of the Äspö water used in the calculations.

Component	Concentration ($mol \cdot dm^{-3}$)
Na	$9.13 \cdot 10^{-2}$
K	$2.05 \cdot 10^{-4}$
Ca	$4.73 \cdot 10^{-2}$
Mg	$1.73 \cdot 10^{-3}$
Fe^{2+}	$4.30 \cdot 10^{-6}$
Mn^{2+}	$5.28 \cdot 10^{-6}$
NH_4^+	$2.14 \cdot 10^{-6}$
H_4SiO_4	$1.46 \cdot 10^{-4}$
HCO_3^- (free)	$1.64 \cdot 10^{-4}$
F^-	$7.89 \cdot 10^{-5}$
Cl^-	$1.81 \cdot 10^{-1}$
Br^-	$5.01 \cdot 10^{-4}$
SO_4^{2-}	$5.83 \cdot 10^{-3}$
HS^-	$4.55 \cdot 10^{-6}$
PO_4^{3-}	$1.61 \cdot 10^{-7}$
NO_3^-	$7.14 \cdot 10^{-7}$
pH	7.7
pe	-5.21/-1.24

Table 9-2. Composition of the Finnsjön water used in the calculations.

Component	Concentration ($mol \cdot dm^{-3}$)
Na	$1.20 \cdot 10^{-2}$
K	$5.13 \cdot 10^{-5}$
Ca	$3.55 \cdot 10^{-3}$
Mg	$6.99 \cdot 10^{-4}$
Fe^{2+}	$3.22 \cdot 10^{-5}$
Mn^{2+}	$2.37 \cdot 10^{-6}$
NH_4^+	$6.43 \cdot 10^{-6}$
H_4SiO_4	$1.99 \cdot 10^{-4}$
HCO_3^- (free)	$4.56 \cdot 10^{-3}$
F^-	$7.89 \cdot 10^{-5}$
Cl^-	$1.56 \cdot 10^{-2}$
SO_4^{2-}	$5.10 \cdot 10^{-4}$
NO_3^-	$1.43 \cdot 10^{-7}$
pH	7.9
pe	-4.23/-1.16

Table 9-3. Composition of the Gideå water used in the calculations.

Component	Concentration ($mol \cdot dm^{-3}$)
Na	$4.57 \cdot 10^{-3}$
K	$5.13 \cdot 10^{-5}$
Ca	$5.25 \cdot 10^{-4}$
Mg	$4.11 \cdot 10^{-5}$
Fe^{2+}	$8.95 \cdot 10^{-7}$
Mn^{2+}	$1.82 \cdot 10^{-7}$
NH_4^+	$7.14 \cdot 10^{-7}$
H_4SiO_4	$1.67 \cdot 10^{-4}$
HCO_3^- (free)	$2.95 \cdot 10^{-4}$
F^-	$1.68 \cdot 10^{-4}$
Cl^-	$5.01 \cdot 10^{-3}$
I^-	$1.10 \cdot 10^{-6}$
SO_4^{2-}	$1.04 \cdot 10^{-6}$
HS^-	$3.03 \cdot 10^{-7}$
PO_4^{3-}	$2.58 \cdot 10^{-7}$
NO_3^-	$6.43 \cdot 10^{-7}$
pH	9.3
pe	-3.41/-1.01

9.2 SOLUBILITY CALCULATIONS

As in the previous section (Section 7), solubility calculations have been performed by using the code EQ3NR (Wolery, 1992). The correction of the ionic strength of the system has been performed by using the b-dot equation (Helgeson, 1969). This approach is used by default by the EQ3NR code. The thermodynamic data base used has been the Nagra/SKB-97-TDB decribed in the next chapter.

As in the previous calculations, the basic principle that the less crystalline metal hydroxide phases are kinetically favoured (Ostwald Principle), and consequently they constitute the initial solubility limiting phases has been assumed.

We have also assumed for radium the possibility that its solubility is limited by co-precipitation with other alkaline-earth-elements, and for curium and americium that their solubilities are limited by co-dissolution from the fuel according to the lower concentrations measured in spent fuel leaching tests. The co-precipitation approach has been also applied in the present calculations for Ni.

pe values have been selected in order to cover pe ranges expected in these groundwaters, the pe boundaries have been used in the calculations.

The results of the solubility calculations as well as the aqueous speciation are given in Tables 9-4 and 9-5 respectively.

Table 9-4. Calculated solubilities and limiting solid phases.

	ÄSPÖ	FINNSJÖN	GIDEÅ
pH	**7.70**	**7.90**	**9.30**
$[HCO_3^-]_{free}$	**$1.64 \cdot 10^{-4}$**	**$4.56 \cdot 10^{-3}$**	**$2.95 \cdot 10^{-4}$**
pe	**-5.21** **-1.24**	**-4.23** **-1.16**	**-3.41** **-1.01**
ELEMENT	*Solubility (mole·dm^{-3}) / Limiting Solid Phase*		
Ni	$1.09 \cdot 10^{-13}$ $1.09 \cdot 10^{-13}$ $NiSiO_3$ $6.12 \cdot 10^{-8}$ $6.87 \cdot 10^{-16}$ $NiFe_2O_4$	$1.51 \cdot 10^{-13}$ $1.51 \cdot 10^{-13}$ $NiSiO_3$ $6.41 \cdot 10^{-13}$ $4.65 \cdot 10^{-19}$ $NiFe_2O_4$	$5.15 \cdot 10^{-16}$ $5.16 \cdot 10^{-16}$ $NiSiO_3$ $1.94 \cdot 10^{-22}$ $1.41 \cdot 10^{-24}$ $NiFe_2O_4$
	$5.15 \cdot 10^{-3}$ $5.15 \cdot 10^{-3}$ NiO	$9.73 \cdot 10^{-3}$ $9.73 \cdot 10^{-3}$ NiO	$2.07 \cdot 10^{-5}$ $2.07 \cdot 10^{-5}$ NiO
Ni-copret $\chi=10^{-3}$	$5.15 \cdot 10^{-6}$ $5.15 \cdot 10^{-6}$ Ni-copret	$9.73 \cdot 10^{-6}$ $9.73 \cdot 10^{-6}$ Ni-copret	$2.07 \cdot 10^{-8}$ $2.07 \cdot 10^{-8}$ Ni-copret
Se	$7.34 \cdot 10^{-10}$ $1.65 \cdot 10^{-13}$ FeSe Se	$3.52 \cdot 10^{-11}$ $5.98 \cdot 10^{-14}$ FeSe Se	$9.80 \cdot 10^{-12}$ $1.27 \cdot 10^{-8}$ $FeSe_2$ Se
Sr	$1.11 \cdot 10^{-3}$ $1.11 \cdot 10^{-3}$ celestite $6.88 \cdot 10^{-3}$ $6.88 \cdot 10^{-3}$ strontianite	$3.09 \cdot 10^{-3}$ $3.09 \cdot 10^{-3}$ celestite $7.14 \cdot 10^{-5}$ $7.14 \cdot 10^{-5}$ strontianite	$3.05 \cdot 10^{-5}$ $3.08 \cdot 10^{-5}$ strontianite
Zr	$2.48 \cdot 10^{-9}$ $2.48 \cdot 10^{-9}$ ZrO_2(am)	$2.51 \cdot 10^{-9}$ $2.51 \cdot 10^{-9}$ ZrO_2(am)	$2.51 \cdot 10^{-9}$ $2.51 \cdot 10^{-9}$ ZrO_2(am)
Nb	$6.08 \cdot 10^{-5}$ $6.08 \cdot 10^{-5}$ Nb_2O_5(ac)	$7.44 \cdot 10^{-5}$ $7.44 \cdot 10^{-5}$ Nb_2O_5(ac)	$1.39 \cdot 10^{-3}$ $1.40 \cdot 10^{-3}$ Nb_2O_5(ac)
Tc	$7.14 \cdot 10^{-9}$ $7.17 \cdot 10^{-9}$ $TcO_2 \cdot xH_2O$	$7.92 \cdot 10^{-9}$ $8.12 \cdot 10^{-9}$ $TcO_2 \cdot xH_2O$	$7.27 \cdot 10^{-9}$ $2.09 \cdot 10^{-4}$ $TcO_2 \cdot xH_2O$
Pd	$4.21 \cdot 10^{-9}$ $4.21 \cdot 10^{-9}$ PdO	$4.17 \cdot 10^{-9}$ $4.17 \cdot 10^{-9}$ PdO	$4.18 \cdot 10^{-9}$ $4.18 \cdot 10^{-9}$ PdO

Table 9-4. Calculated solubilities and limiting solid phases (Cont.).

	ÄSPÖ		FINNSJÖN		GIDEÅ	
pH	**7.70**		**7.90**		**9.30**	
$[HCO_3^-]_{free}$	**$1.64 \cdot 10^{-4}$**		**$4.56 \cdot 10^{-3}$**		**$2.95 \cdot 10^{-4}$**	
pe	**-5.21**	**-1.24**	**-4.23**	**-1.16**	**-3.41**	**-1.01**
ELEMENT	*Solubility (mole·dm^{-3}) / Limiting Solid Phase*					
Ag	$3.88 \cdot 10^{-15}$	$3.63 \cdot 10^{-11}$	$1.21 \cdot 10^{-16}$	$1.43 \cdot 10^{-13}$	$2.16 \cdot 10^{-16}$	$5.41 \cdot 10^{-14}$
	Ag(s)		Ag(s)		Ag(s)	
	$2.96 \cdot 10^{-5}$	$3.02 \cdot 10^{-5}$	$9.39 \cdot 10^{-7}$	$9.39 \cdot 10^{-7}$	$7.12 \cdot 10^{-7}$	$7.12 \cdot 10^{-7}$
	AgCl(s)		AgCl(s)		AgCl(s)	
Sn	$5.52 \cdot 10^{-10}$	$5.52 \cdot 10^{-10}$	$6.03 \cdot 10^{-10}$	$6.03 \cdot 10^{-10}$	$4.68 \cdot 10^{-9}$	$4.69 \cdot 10^{-9}$
	SnO_2		SnO_2		SnO_2	
Sm	$2.13 \cdot 10^{-6}$	$2.13 \cdot 10^{-6}$	$2.69 \cdot 10^{-7}$	$2.69 \cdot 10^{-7}$	$2.91 \cdot 10^{-7}$	$2.91 \cdot 10^{-7}$
	$Sm_2(CO_3)_3$		$Sm_2(CO_3)_3$		$Sm_2(CO_3)_3$	
Ho	$6.27 \cdot 10^{-6}$	$6.27 \cdot 10^{-6}$	$1.52 \cdot 10^{-6}$	$1.52 \cdot 10^{-6}$	$1.97 \cdot 10^{-6}$	$1.97 \cdot 10^{-6}$
	$Ho_2(CO_3)_3$		$Ho_2(CO_3)_3$		$Ho_2(CO_3)_3$	
					$1.68 \cdot 10^{-6}$	$1.68 \cdot 10^{-6}$
					$Ho(OH)_3(am)$	
Ra	$2.86 \cdot 10^{-7}$	$2.86 \cdot 10^{-7}$	$5.02 \cdot 10^{-7}$	$5.03 \cdot 10^{-7}$	$1.20 \cdot 10^{-4}$	$1.22 \cdot 10^{-4}$
	$RaSO_4$		$RaSO_4$		$RaSO_4$	
Ra-copret.	$2.86 \cdot 10^{-10}$	$2.86 \cdot 10^{-10}$	$5.02 \cdot 10^{-10}$	$5.03 \cdot 10^{-10}$	$1.20 \cdot 10^{-7}$	$1.22 \cdot 10^{-7}$
$\chi=10^{-3}$	Ra-copret		Ra-copret		Ra-copret	
Th	$2.40 \cdot 10^{-10}$	$2.40 \cdot 10^{-10}$	$1.17 \cdot 10^{-9}$	$1.17 \cdot 10^{-9}$	$2.40 \cdot 10^{-10}$	$2.40 \cdot 10^{-10}$
	$Th(OH)_4$		$Th(OH)_4$		$Th(OH)_4$	
Pa	$3.16 \cdot 10^{-7}$	$3.16 \cdot 10^{-7}$	$3.16 \cdot 10^{-7}$	$3.16 \cdot 10^{-7}$	$3.16 \cdot 10^{-7}$	$3.16 \cdot 10^{-7}$
	Pa_2O_5		Pa_2O_5		Pa_2O_5	
U	$1.27 \cdot 10^{-7}$	$1.30 \cdot 10^{-7}$	$1.29 \cdot 10^{-7}$	$9.45 \cdot 10^{-6}$	$1.29 \cdot 10^{-7}$	$5.23 \cdot 10^{-5}$
	UO_2(fuel)		UO_2(fuel)		UO_2(fuel)	
	$4.01 \cdot 10^{-10}$	$4.08 \cdot 10^{-10}$	$3.01 \cdot 10^{-10}$	$2.56 \cdot 10^{-8}$	$4.76 \cdot 10^{-10}$	$1.34 \cdot 10^{-7}$
	Coffinite		Coffinite		Coffinite	

Table 9-4. Calculated solubilities and limiting solid phases (Cont.).

	ÄSPÖ		FINNSJÖN		GIDEÅ	
pH	**7.70**		**7.90**		**9.30**	
$[HCO_3^-]_{free}$	**$1.64 \cdot 10^{-4}$**		**$4.56 \cdot 10^{-3}$**		**$2.95 \cdot 10^{-4}$**	
pe	**-5.21**	**-1.24**	**-4.23**	**-1.16**	**-3.41**	**-1.01**
ELEMENT	*Solubility (mole·dm^{-3}) / Limiting Solid Phase*					
Np	$7.00 \cdot 10^{-9}$	$7.01 \cdot 10^{-9}$	$1.05 \cdot 10^{-7}$	$1.04 \cdot 10^{-7}$	$8.39 \cdot 10^{-9}$	$8.47 \cdot 10^{-9}$
	$Np(OH)_4$		$Np(OH)_4$		$Np(OH)_4$	
Pu	$6.56 \cdot 10^{-9}$	$1.04 \cdot 10^{-10}$	$5.35 \cdot 10^{-10}$	$1.04 \cdot 10^{-10}$	$1.03 \cdot 10^{-10}$	$1.03 \cdot 10^{-10}$
	$Pu(OH)_4(am)$		$Pu(OH)_4(am)$		$Pu(OH)_4(am)$	
Am	$6.87 \cdot 10^{-7}$	$6.87 \cdot 10^{-7}$	$9.36 \cdot 10^{-8}$	$9.36 \cdot 10^{-8}$	$4.89 \cdot 10^{-8}$	$4.91 \cdot 10^{-8}$
	$AmOHCO_3$		$AmOHCO_3$		$AmOHCO_3$	
Am-codiss.	$5.49 \cdot 10^{-11}$	$5.62 \cdot 10^{-11}$	$5.57 \cdot 10^{-11}$	$4.08 \cdot 10^{-9}$	$5.57 \cdot 10^{-11}$	$2.26 \cdot 10^{-8}$
$\chi = 4.32 \cdot 10^{-4}$	Am-codiss.		Am-codiss.		Am-codiss.	
Cm	$2.22 \cdot 10^{-7}$	$2.21 \cdot 10^{-7}$	$2.02 \cdot 10^{-9}$	$2.02 \cdot 10^{-9}$	$9.01 \cdot 10^{-10}$	$9.11 \cdot 10^{-10}$
	$CmOHCO_3$		$CmOHCO_3$		$CmOHCO_3$	
Cm-codiss.	$3.66 \cdot 10^{-12}$	$3.74 \cdot 10^{-12}$	$3.71 \cdot 10^{-12}$	$2.72 \cdot 10^{-10}$	$3.72 \cdot 10^{-12}$	$1.51 \cdot 10^{-9}$
$\chi = 2.88 \cdot 10^{-5}$	Cm-codiss.		Cm-codiss.		Cm-codiss.	

Table 9-5. Aqueous speciation.

	ÄSPÖ	FINNSJÖN	GIDEÅ
pH	**7.70**	**7.90**	**9.3**
$[HCO_3^-]_{free}$	**$1.64 \cdot 10^{-4}$**	**$4.56 \cdot 10^{-3}$**	**$2.95 \cdot 10^{-4}$**
pe	**-5.21 -1.24**	**-4.23 -1.16**	**-3.41 -1.01**
ELEMENT	*Aqueous speciation (%)*		
Ni	Ni^{2+} (74) $NiCl^+$ (10) $NiHCO_3^+$ (5)	$NiCO_3$(aq) (41) $NiHCO_3^+$ (26) $Ni(CO_3)_2^{2-}$ (24) Ni^{2+} (8)	$NiCO_3$(aq) (52) $Ni(CO_3)_2^{2-}$ (40) Ni^{2+} (5)
Se	HSe^- (100)	HSe^- (100)	HSe^- (100) SeO_3^{2-} (91) $HSeO_3^-$ (9)
Sr	Sr^{2+} (91) $SrSO_4$(aq) (9)	Sr^{2+} (92)	Sr^{2+} (99)
Zr	$Zr(OH)_4$(aq) (100)	$Zr(OH)_4$(aq) (100)	$Zr(OH)_4$(aq) (100)
Nb	NbO_3^- (74) $Nb(OH)_5$(aq) (26)	NbO_3^- (79) $Nb(OH)_5$(aq) (21)	NbO_3^- (99)
Tc	$TcO(OH)_2$(aq) (95)	$TcO(OH)_2$(aq) (86)	$TcO(OH)_2$(aq) (94) TcO_4^- (100)
Pd	$Pd(OH)_2$(aq) (99)	$Pd(OH)_2$(aq) (100)	$Pd(OH)_2$(aq) (100)
Ag	$AgCl_3^{2-}$(46) $AgCl_4^{3-}$ (33) $AgCl_2^-$ (20)	$AgCl_2^-$ (53) AgCl(aq) (39) $AgCl_3^{2-}$ (6)	AgCl(aq) (49) $AgCl_2^-$ (21) AgI (20) Ag^+ (6)
Sn	$Sn(OH)_4$(aq) (76) $Sn(OH)_5^-$ (24)	$Sn(OH)_4$(aq) (70) $Sn(OH)_5^-$ (30)	$Sn(OH)_5^-$ (91) $Sn(OH)_4$(aq) (9)
Sm	$SmCO_3^+$ (43) Sm^{3+} (39) $SmSO_4^+$ (7)	$Sm(CO_3)_2^-$ (59) $SmCO_3^+$ (40)	$Sm(CO_3)_2^-$ (67) $SmCO_3^+$ (27)

Table 9-5. Aqueous speciation (Cont.).

	ÄSPÖ	FINNSJÖN	GIDEÅ
pH	**7.70**	**7.90**	**9.30**
$[HCO_3^-]_{free}$	**$1.64 \cdot 10^{-4}$**	**$4.56 \cdot 10^{-3}$**	**$2.95 \cdot 10^{-4}$**
pe	**-5.21 -1.24**	**-4.23 -1.16**	**-3.41 -1.01**
ELEMENT	*Aqueous speciation (%)*		
Ho	$HoCO_3^+$ (52) Ho^{3+} (30) HoF^{2+} (5)	$Ho(CO_3)_2^-$ (74) $HoCO_3^+$ (25)	$Ho(CO_3)_2^-$ (70) $HoCO_3^+$ (14) $Ho(OH)_3(aq)$ (12)
Ra	Ra^{2+} (86) $RaSO_4(aq)$ (11)	Ra^{2+} (92) $RaSO_4(aq)$ (6)	Ra^{2+} (99)
Th	$Th(OH)_4(aq)$ (100)	$Th(HPO_4)_3^{2-}$ (79) $Th(OH)_4(aq)$ (20)	$Th(OH)_4(aq)$ (100)
Pa	$PaO_2OH(aq)$ (100)	$PaO_2OH(aq)$ (100)	$PaO_2OH(aq)$ (100)
U	$U(OH)_4(aq)$ (100)	$U(OH)_4(aq)$ (100) $UO_2(CO_3)_3^{4-}$ (81) $UO_2(CO_3)_2^{2-}$ (18)	$U(OH)_4(aq)$ (100) $UO_2(CO_3)_3^{4-}$ (55) $(UO_2)_3(OH)_7^-$ (27) $UO_2(CO_3)_2^{2-}$ (15)
Np	$Np(OH)_4(aq)$ (75) $Np(OH)_3CO_3^-$ (25)	$Np(HPO_4)_5^{6-}$ (50) $Np(OH)_3CO_3^-$ (44) $Np(OH)_4(aq)$ (5)	$Np(OH)_4(aq)$ (62) $Np(OH)_3CO_3^-$ (35)
Pu	Pu^{3+} (58) $Pu(OH)_4(aq)$ (99) $Pu(OH)_2^+$ (21) $PuOH^{2+}$ (11) $PuCO_3^+$ (8)	$PuCO_3^+$ (66) $Pu(OH)_4(aq)$ (100) $Pu(OH)_4(aq)$ (19) $Pu(OH)_2^+$ (9)	$Pu(OH)_4(aq)$ (100)
Am	$AmOH^{2+}$ (47) $Am(OH)_2^+$ (17) $AmCO_3^+$ (16) $AmSO_4^+$ (5) Am^{3+} (5)	$AmCO_3^+$ (63) $Am(CO_3)_2^-$ (29)	$Am(OH)_2^+$ (88)
Cm	$CmOH^{2+}$ (99)	$CmOH^{2+}$ (99)	$CmOH^{2+}$ (100)

9.3 DISCUSSION OF THE RESULTS OBTAINED

In this section we will discuss the reported radionuclide solubility limits. A comparison of the results obtained depending on the groundwater composition will be done as well as with the solubility calculations performed in the previous sections.

9.3.1 Ni

We have initially assumed that under reducing conditions NiO(s) is the solubility limiting phase. However, the calculated solubilities are unrealistically high, if compared to the measured Ni(II) concentrations in relevant natural systems. Most probably, Ni(II) is associated with Fe(III)-oxyhydroxides, as indicated by recent natural systems observations (Zielinski et al., 1983). Therefore, in the present calculations, we have also assumed the co-precipitation of Ni with Fe(III)-oxyhydroxides, obtaining more realistic solubility values for this radionuclide.

As in the previous calculations the precipitation of pure Ni(II) sulphides is not assumed due to the competition of iron for the limited sulphide supply.

The precipitation of $NiSiO_3$(s) and trevorite ($NiFe_2O_4$(s)) have been also considered in the present calculations, although these phases do not control the solubility of Ni(II) at low temperatures. However, experimental results showed the precipitation of trevorite at temperatures around 60°C (Duro, personnal communication).

The free Ni^{2+} cation and $NiCO_3$(aq) are the predominant aqueous species under the conditions of the calculations.

9.3.2 Se

As we have discussed in the previous sections, the limiting solid phase for this element is critically dependent on the redox state of the system. Under the most reducing conditions, the solubility of selenium is limited by the precipitation of selenides, keeping Se at low concentration levels. By considering a higher pe (Table 9-4) the limiting solid phase will be Se(s). This phase also keeps this element at low concentration levels, with the exception of the Gideå groundwater, in such case, the solubility obtained is $1.27 \cdot 10^{-8}$ mole·dm^{-3}.

The predominant aqueous species is HSe^- in all water compositions studied. However, by assuming the highest pe measured in the Gideå groundwater, SeO_3^{2-} becomes the predominant aqueous phase with the corresponding increase in solubility.

The calculated solubilities depend mainly on the pe of the system and they are not affected by the difference in groundwater compositions. These solubilities are in the same range than the ones obtained in the previous calculations.

9.3.3 Sr

The calculated solubility limit for this element is imposed by the precipitation of either sulphate or carbonate solid phases. The precipitation of a particular phase depends on the aqueous $[CO_3^{2-}]/[SO_4^{2-}]$ ratio.

The calculated solubilities decrease when increasing carbonate content in solution due to the stabilisation of strontianite (Table 9-4).

The Sr^{2+} free cation is the dominant aqueous species in the waters studied.

As previously indicated the solubility of these phases is highly dependent on the system studied, obtaining solubility values for the same phase ranging from $1 \cdot 10^{-3}$ to $3 \cdot 10^{-4}$ mole·dm^{-3} (Äspö groundwater), depending on the calculation approach. The solubility of celestite calculated by using the HALTAFALL based INPUT/SED/PREDOM code package developed by Puigdomènech (1983) and by considering the Äspö groundwater has been $2.78 \cdot 10^{-4}$ mole·dm^{-3}. This concentration is in good agreement with the measured strontium concentration in this groundwater, $3.99 \cdot 10^{-4}$ mole·dm^{-3}.

9.3.4 Zr

ZrO_2(am) is the solubility limiting solid phase in all calculations. We have considered the less crystalline phase to perform the calculations according to the Ostwald rule. The calculated Zr concentrations are in the same range as in the previous calculations. The calculated solubilities are the same independently on the composition of the groundwater.

The dominant aqueous species in all the waters studied is $Zr(OH)_4$(aq). This complex is expected to be the dominant species in average granitic groundwaters.

9.3.5 Nb

Solubility is limited by the Nb_2O_5(ac) phase, we have selected the more soluble phase compiled in the databases. The calculated solubilities increase with pH. The changes in solubilities are basically associated to this parameter.

Calculated Nb concentrations are in the same range than the values obtained in the previous calculations.

The speciation in the groundwaters studied is dominated by NbO_3^-.

9.3.6 Tc

The solubility limiting solid phase is the hydrous technetium dioxide. The calculated solubilities are not affected by the different water compositions considered. They are of the same order of magnitude than solubilities obtained in the previous calculations.

The aqueous speciation is mainly dominated by $TcO(OH)_2(aq)$ in the groundwaters under study.

In the present calculations we have obtained a high solubility value when we have calculated the solubility of this phase by considering the more alkaline Gideå groundwater at the highest pe (pe=-1.01). Under these conditions, the dominant aqueous species is TcO_4^-, this change in the aqueous speciation implies a higher solubility of this solid phase. We have observed the same behaviour for Se.

Figure 9-1 illustrates the increase in the solubility of $TcO_2 \cdot xH_2O(s)$ when increasing the pe of the system and depending on the pH considered.

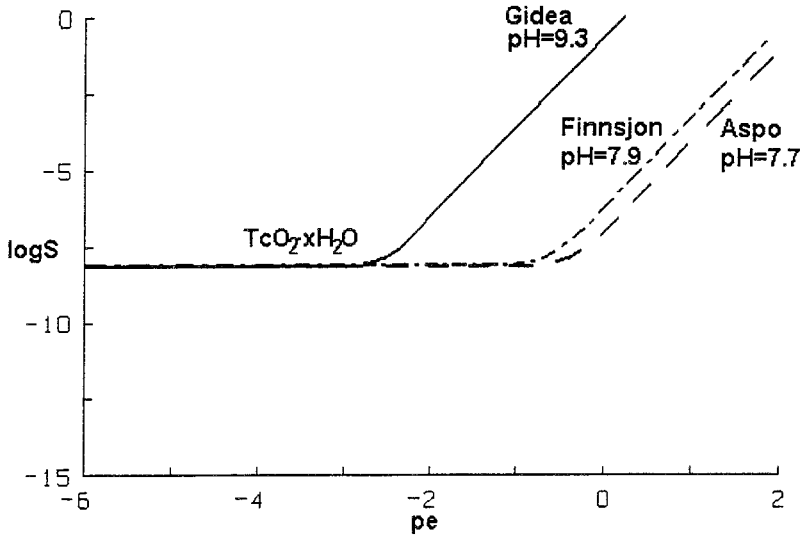

Figure 9-1. Solubility curve of $TcO_2 \cdot xH_2O(s)$ as a function of pe.

9.3.7 Pd

Palladium oxide is considered the limiting solid phase in the groundwaters studied. The calculated solubilities are not affected by the different water compositions assumed. The palladium concentrations calculated agree with the solubilities obtained in the previous section (Section 7).

The dominant aqueous complex is in all cases $Pd(OH)_2(aq)$.

9.3.8 Ag

The solubility limiting solid phase initially considered in these calculations has been the Ag(s). The solubilities obtained are very low and they depend basically on both the redox conditions and the pH of the groundwaters studied.

In addition, another may be more realistic solubility limiting phase has been considered in these calculations, AgCl(s). This solid phase implies larger solubilities of the order of 10^{-5} mole·dm^{-3} in Äspö groundwaters and 10^{-7} mole·dm^{-3} in Finnsjön and Gideå groundwaters. This solubility range is in good agreement with the concentration measured in Poços de Caldas, 10^{-7} mole·dm^{-3}.

The calculated solubilities in the Äspö waters are two orders of magnitude higher than in Finnsjön and Gideå waters. This is mainly due to the higher chloride content in Äspö groundwater which stabilise the aqueous chloride complexes in solution with respect the other ones.

The aqueous speciation is dominated by chloride complexes, depending on the chloride content of the groundwaters.

9.3.9 Sn

SnO_2(s) is the solubility limiting solid phase and the dominant aqueous species are $Sn(OH)_4$(aq) and $Sn(OH)_5^-$ if we consider the groundwaters studied.

The calculated solubilities increase with pH. The changes in solubilities are basically associated to this parameter.

Calculated solubilities are in good agreement with the calculations performed in the previous section.

9.3.10 Sm

The solid phase that limits the solubility of this element in all groundwaters studied is the $Sm_2(CO_3)_3$(s). Aqueous speciation is dominated by samarium carbonates.

The main parameters which affect the calculated solubilities are both the pH and the carbonate content of the groundwaters studied. A slight increase in solubility is observed by increasing pH (see Finnsjön and Gideå in Table 9-4).

The calculated solubility obtained in Äspö groundwater is one order of magnitude higher than in Finnsjön and Gideå groundwaters. This higher solubility is given by the different aqueous speciation as we can see in Table 9-5. The predominance of the different carbonate complexes will depend on both the pH and the carbonate concentration in groundwaters.

Reported solubilities are in the same range than calculations performed in section 7.

9.3.11 Ho

Holmium follows the same behaviour as Samarium. The solubility limiting solid phase is $Ho_2(CO_3)_3(s)$, and the dominant aqueous speciation is given by the holmium carbonates.

$Ho(OH)_3(am)$ has been also considered as limiting solid phase in Gideå groundwater since the stability of this phase is very close to the stability of $Ho_2(CO_3)_3(s)$ under these conditions as we can see in Table 9-4.

As in the case of samarium, a slight increase in solubility is calculated by increasing pH in Finnsjön and Gideå groundwaters. The higher solubility calculated in Äspö groundwater is given by the different aqueous speciation as we can see in Table 9-5.

Reported solubilities are in the same range than calculations performed in the previous section.

9.3.12 Ra

The solubility limiting solid phase in the groundwaters studied is $RaSO_4(s)$ and the aqueous speciation is dominated by the Ra^{2+} free cation. The main parameter which affects the solubility of this solid phase is the sulphate content in groundwaters. Equilibrium concentration in Gideå groundwater is higher than in Äspö and Finnsjön groundwaters due to its lower sulphate content with respect the other ones.

Reported solubility values by considering its co-precipitation are closer to the measured concentrations in natural waters and can be considered as upper realistic levels to Ra(II) solubility in granitic environments.

9.3.13 Th

$Th(OH)_4(am)$ has been taken as the solubility limiting solid phase. The calculated solubilities do not change between the Äspo and Gideå waters.

On the other hand, the calculated solubilities increase in the Finnsjön groundwater due to the phosphate content. This increase is given by the stabilisation of the $Th(HPO_4)_3^{2-}$ which causes an increase in the solubility of the solid phase.

The aqueous speciation in the other cases is dominated by the complex $Th(OH)_4(aq)$.

The calculated solubility in Äspö groundwater is the same as in the previous results. However, in the Finnsjön groundwater, the solubility has increased with respect the previous calcualtions due to the higher pH of this water.

The higher pH is the responsible of the predominance in solution of the phosphate complex in the present calculations with respect the previous ones as we can see by comparing the aqueous speciation in both cases.

9.3.14 Pa

The solubility limiting solid phase is $Pa_2O_5(s)$. The calculated solubilities are not affected by the different water compositions assumed. Reported solubilities agree with the calculations previously performed.

The aqueous speciation is dominated by $PaO_2OH(aq)$, under all the conditions of the calculations.

9.3.15 U

The solubility limiting solid phase considered in these calculations is UO_2(fuel), (see section 4.20). By comparing the results obtained for the most reducing pe in the three water compositions assumed, we can see that there is not a variation in calculated solubilities. The dominant aqueous speciation in such cases is given by the complex $U(OH)_4(aq)$.

The reported solubilities are in good agreement with the solubility calculations previously performed. These concentrations also agree with measured uranium concentrations in many natural systems and with reported uranium concentrations measured in spent fuel dissolution tests as it was discussed in the previous sections.

On the other hand calculated solubilities increase if we consider a higher pe in the system (Table 9-4). This increase is due to the stabilisation of the uranyl carbonate complexes, as we can see in the aqueous speciation (Table 9-5). Both carbonate content and pH in the range of pe considered ($-1.24<pe<-1.01$) and for the three water compositions assumed, lead to an stabilisation of uranium (VI) in solution.

Finally, coffinite has been also considered as the limiting solid phase in the present calculations. Reported solubilities are low if we compare with measured concentrations in natural systems. However, the solubility calculated in Gideå groundwater ($4.76 \cdot 10^{-10}$ mole·dm^{-3}) agree quite well with the measured uranium concentration in this groundwater ($8.40 \cdot 10^{-10}$ mole·dm^{-3}), this could be an indication that this phase may limit the solubility of uranium in this system, taking into account its reducing environment. Nevertheless, the thermodynamics and kinetics of the coffinitation of UO_2 are largely unknown at low temperatures.

9.3.16 Np

$Np(OH)_4(s)$ is the solubility limiting solid phase. The calculated solubilities increase approximately one order of magnitude in Finnsjön groundwater due

to the higher phosphate content in solution with respect the other groundwaters assumed. This increase is provided by the stabilisation of the $Np(HPO_4)_5^{6-}$ complex in solution (Lemire and Garisto, 1989), although we have some reservations about the stability of this comlex.

The aqueous speciation is dominated by the $Np(OH)_4(aq)$ complex in the Äspö and Gideå groundwaters.

The calculated solubilities are of the same order of magnitude or one order of magnitude larger than neptunium concentrations determined from spent fuel leaching tests as we have discussed in the previous sections.

9.3.17 Pu

The solubility is limited by $Pu(OH)_4(am)$, by applying the Ostwald rule for all the groundwaters and redox conditions assumed. Because of the stabilisation of the aqueous Pu(III) species, the solubility increases when decreasing pe and pH. Consequently, the higher solubilities have been calculated in Äspö and Finnsjön waters, with the lower pe assumed.

This effect can be observed in the aqueous speciation (Table 9-5) where we can see that in both cases Pu(III) species are the dominant aqueous complexes in solution. The predominant aqueous species in the rest of cases assumed is $Pu(OH)_4(aq)$.

Calculated solubilities are in the same range than reported solubilities from Äspö and bentonite waters calculated in the calculations presented in previous sections.

9.3.18 Am

$AmOHCO_3(s)$ is the solubility limiting phase in all the waters studied. The solubility limiting phase is independent on the different water compositions. However, its solubility slightly increases when decreasing pH.

Am(III) hydroxides are the predominant aqueous complexes in the Äspö and Gideå reference waters. Americium (III) carbonates become the dominant aqueous species in the Finnsjön groundwater due to its higher carbonate content.

As it was discussed in previous sections, these concentrations are approximately 3 orders of magnitude higher than reported solubilities from spent fuel dissolution experiments. Therefore, as in the previous work, we have assumed a congruent dissolution of americium with the dissolved uranium, giving solubilities in the 10^{-11} mole·dm^{-3} range (Table 9-4), in satisfactory agreement with the measured concentrations in spent fuel dissolution tests.

9.3.19 Cm

The solubility limiting solid phase is $CmOHCO_3(s)$. The calculated solubilities increase when decreasing carbonate content and pH, consequently the higher solubilities are obtained in Äspö groundwater.

The aqueous speciation is dominated by the complex $Cm(OH)^{2+}$ in all the waters studied.

The release of curium, in analogy to americium will be mainly controlled by the dissolution of the spent fuel matrix. Therefore, we have calculated as in the previous section the expected solubilities by assuming the co-dissolution with the UO_2 matrix. The calculated curium concentrations fall in the same range as the concentrations measured in spent fuel dissolution tests, 10^{-12} mole·dm^{-3}.

9.4 CONCLUSIONS RELATED TO THE RESULTS IN SR 97 SITES

The calculated solubilities of the radionuclides taken in this section by considering the Äspö and the Finnsjön groundwaters are, in general, in the same range than reported solubilities in the previous sections.

However, some variations have been observed by taking into account the composition of the selected Finnsjön groundwater, mainly due to the highest pH considered in the present calculations with respect the previous ones.

The higher pH taken, with the effect of a higher phosphate content in comparison with the rest of the groundwaters selected, has given an stabilisation of Th and Np phosphate aqueous complexes with the consequent increase in the solubility of the limiting solid phases, with respect the previous calculations.

The pH and the carbonate content in groundwaters are the main parameters of groundwater compositions affecting the solubility of the radionuclides, such is the case of Ni, Sr, Nb, Sn, Sm, Ho, Am and Cm.

Some redox sensitive radionuclides have also given different solubilities depending on the pe assumed in the calculations.

For selenium, different solubilities have been calculated depending on the solubility limiting solid phase assumed. The solid phases have been selected taking into account their different predominance as a function of the pe of the system.

On the other hand, the aqueous speciation depends on the pe of the system for some redox sensitive radionuclides, such is the case of U and Pu.

Uranium increases its solubility when assuming the higher pe of the system in the calculations, due to the predominance of U(VI)-carbonate complexes in solution. Plutonium increases its solubility when the lower pe is assumed due to the predominance of Pu(III) complexes in solution.

Sr solubility is very sensitive to the calculation approach used. Reported solubilities in the Äspö groundwater are in good agreement with measured Sr concentrations in the same groundwater.

The application of the co-precipitation/co-dissolution approaches for Ra, Am and Cm, has given more realistic values, by comparing their concentrations in natural systems and spent fuel dissolution experiments.

10 THERMODYNAMIC DATABASE

The original thermodynamic data used has been taken from the NTB91-17 and 91-18 databases, plus iron minerals and magnesite. Uranium data from Puigdomenech & Bruno (1988); plutonium data from Puigdomenech & Bruno (1991); technetium data from Puigdomenech & Bruno (1995); REE data from Spahiu & Bruno (1995) and neptunium data from Spahiu (1996). However, some modifications have been done, after checking the thermodynamic databases available (Hatches v.7.0) and according to a review exercise of the concerning literature (Baes and Mesmer, 1976, Lemire and Garisto, 1989, Puigdomènech and Bruno, 1991, Grenthe et al., 1992, Eriksen et al., 1993, Östhols, 1994, Silva et al., 1995, Spahiu and Bruno,1995). We have called this database as Nagra/SKB-97-TDB.

10.1 NICKEL

The thermodynamic database selected for this element in the calculations has been the NTB91-17.

10.2 SELENIUM

We have selected also the NTB91-17 thermodynamic database which is in agreement with the Hatches v.7.0 (Cross and Ewart, 1989). However, due to the lack of some thermodynamic data, mainly solid phases, with respect the Hatches database, the NTB91-17 has been extended by including the following solid phases:

$FeSe + 4H_2O = SeO_4^{2-} + Fe^{2+} + 8H^+ + 8e^-$ logK=-88.2 10-1 (Mills, 1974)

$FeSe_2 + 8H_2O = 2SeO_4^{2-} + Fe^{2+} + 16H^+ + 14e^-$ logK=-178.8 10-2 (Baeyens and McKinley, 1989)

10.3 STRONTIUM

As in the previous cases, the thermodynamic database used in the calculations has been the NTB91-17. However, the strontium phosphate aqueous complex has been added to this database. The logK value has been

extracted from the Hatches v.7.0 database (Cross and Ewart, 1989). The reaction is:

$SrPO_4^- + H^+ = Sr^{2+} + HPO_4^{2-}$ logK=8.17 10-3 (Benson and Teague, 1980)

10.4 ZIRCONIUM

We have taken the NTB91-17 database in these calculations. However, we have included the data for ZrO_2(am) selected from the Hatches v.7.0. This amorphous solid phase has been included in the database to perform the solubility calculations, since the solubility limiting solid phase has been taken according to the Ostwald's step rule as we have seen in the previous section.

The dissociation reaction of ZrO_2(am) with the corresponding logarithm of the solubility constant taken is as follows:

$ZrO_2(am) + 4H^+ = Zr^{4+} + 2H_2O$ logK=1.1 10-4 (Cross et al., 1992)

10.5 NIOBIUM

The thermodynamic database considered in these calculations has been the NTB91-17 database. However, as in the case of zirconium, we have selected the reported "active" Nb_2O_5 solid phase from Baes and Mesmer (1976) in contrast to the more stable one, as the solubility limiting solid phase. Therefore, this solid phase has been included in the database used in this work.

The dissociation reaction of Nb_2O_5(ac) with the corresponding logarithm of the solubility constant taken is:

$Nb_2O_5(ac) + H_2O = 2NbO_3^- + 2H^+$ logK=-24.4 10-5

10.6 TECHNETIUM

The thermodynamic database used in the calculations is the NTB91-17. In addition, recent thermodynamic data determined by Eriksen and co-workers (Eriksen et al., 1993) have been compared and/or included in the NTB91-17 database.

The thermodynamic data included in our database have been:

$TcO(OH)HCO_3(aq) + H^+ = TcO^{2+} + HCO_3^- + H_2O$ logK=-5.34 10-6

$TcO(OH)_2HCO_3^- + 2H^+ = TcO^{2+} + HCO_3^- + 2H_2O$ logK=2.92 10-7

10.7 PALLADIUM

The NTB91-17 has been the thermodynamic database used in the calculations.

10.8 SILVER

The thermodynamic database used in the calculations has been the Hatches v.7.0. (Cross and Ewart, 1989). The thermodynamic data used have been included in the database in order to perform the solubility calculations since no thermodynamic data of this metal was available in this database.

The aqueous complexes and solid phases included have been: AgOH(aq), $Ag(OH)_2^-$, $Ag(OH)_3^{2-}$, $Ag(OH)_4^{3-}$, AgCl(aq), $AgCl_2^-$, $AgCl_3^{2-}$, $AgCl_4^{3-}$, $AgNO_3$(aq), AgI(aq), AgI_2^-, AgI_3^{2-}, Ag(s), AgCl(s) and Ag_2S(s).

10.9 TIN

The thermodynamic database used has been the NTB91-17. However, four hydroxo- Sn(IV) complexes have been added to this database due to the lack of this data. The selected data have been extracted from Baes and Mesmer (1976). The thermodynamic data added to our database are:

$SnOH^{3+} + H^+ + 2e^- = Sn^{2+} + H_2O$ logK=4.68 10-8

$Sn(OH)_2^{2+} + 2H^+ + 2e^- = Sn^{2+} + 2H_2O$ logK=4.62 10-9

$Sn(OH)_3^+ + 3H^+ + 2e^- = Sn^{2+} + 3H_2O$ logK=4.89 10-10

$Sn(OH)4(aq) + 4H^+ + 2e^- = Sn^{2+} + 4H_2O$ logK=6.11 10-11

10.10 SAMARIUM

The REE-TDB (Spahiu and Bruno, 1995) thermodynamic database has been used in the calculations.

10.11 HOLMIUM

REE-TDB (Spahiu and Bruno,1995) is the thermodynamic database used in these calculations.

10.12 RADIUM

The thermodynamic data have been selected from the Hatches v.7.0 (Cross and Ewart, 1989). These data have been included in the NTB91-17 database to perform the solubility calculations since no thermodynamic data were available in this database.

The aqueous complexes and solid phases included have been: $RaOH^+$, $RaSO_4(aq)$, $RaCl^+$, $RaCO_3(aq)$, $RaHCO_3^+$, $RaPO_4^-$, $RaSO_4(s)$, $RaCO_3(s)$ and $RaCl_2 \cdot 2H_2O(s)$.

10.13 THORIUM

The thermodynamic data used in these calculations have been selected combining the NTB91-17 database for the aqueous species, and the Hatches v.7.0 (Cross and Ewart, 1989) for the solid phases including the modifications presented below. In addition, thermodynamic data for phosphate complexes have been selected from recent experimental work (Östhols, 1994).

The thorium database has undergone a substantial revision, particularly for the stability of Th(IV) oxide and hydroxide solid phases.

As it is shown in the next table (Table 10-1), solubility constants disagree substantially between the values reported in the EQ3/6NTB and in the Hatches v.7.0 databases.

Table 10-1. Solubility constants reported for Th(IV) oxide and hydroxide solid phases.

$logK_{s0}$	EQ3/6NTB	HATCHES v.7.0
$Th(OH)_4(c)+4H^+ \Rightarrow Th^{4+}+4H_2O$	13.8	11.3
$Th(OH)_4(am)+4H^+ \Rightarrow Th^{4+}+4H_2O$		9.4
$ThO_2(c)+4H^+ \Rightarrow Th^{4+}+2H_2O$		1.8
$ThO_2(am)+4H^+ \Rightarrow Th^{4+}+2H_2O$	6.3	7.6

Bruno and Duro (1995) observed in a previous work that solubility constants selected in the Hatches v.7.0 for $Th(OH)_4(c)$ and $Th(OH)_4(am)$ gave unrealistically high solubilities. These data came from the Critical Stability Constants (1964). However, by considering the value of $logK_{s0}=6.3$ taken from the compilation of Baes and Mesmer (1976), these authors observed that this new value gave estimates of the thorium solubility, which were in good agreement with measured dissolved Th(IV) in natural analogue sites like Cigar lake, El Berrocal and Poços de Caldas.

Therefore, according to the results obtained in their work, we have considered the formation of $Th(OH)_4(am)$ with a value of $logK_{s0}=6.3$. The crystalline phase has been included in the database used, but its formation is restrained invoking the Ostwald's step rule.

Finally, the modifications on the NTB91-17 database have been the addition of four thorium aqueous complexes, three phosphate complexes and one carbonate complex, and the inclusion of three solid phases. The reactions considered with the corresponding logK values and the source are given in the following table (Table 10-2).

Table 10-2. Dissociation reactions for thorium aqueous complexes and solid phases.

Reaction	logK	Source
$Th(CO_3)_5^{6-}+5H^+=Th^{4+}+HCO_3^-$	16.5	Cross and Ewart, 1989
$Th(H_2PO_4)_2^{2+}=Th^{4+}+2HPO_4^{2-}+2H^+$	-24.4	Östhols, 1994
$Th(H_2PO_4)_4(aq)=Th^{4+}+4HPO_4^{2-}+4H^+$	-40.8	Östhols, 1994
$Th(OH)_4PO_4^{3-}+5H^+=Th^{4+}+HPO_4^{2-}+4H_2O$	27.25	Östhols, 1994
$Th(OH)_4(s)+4H^+=Th^{4+}+4H_2O$	6.3	Baes and Mesmer, 1976
$ThO_2(c)+4H^+=Th^{4+}+2H_2O$	1.8	Cross and Ewart, 1989
$ThO_2(am)+4H^+=Th^{4+}+2H_2O$	7.6	Cross and Ewart, 1989

10.14 PROTACTINIUM

Hatches v.7.0 (Cross and Ewart, 1989) has been selected as the thermodynamic database for the calculations, due to the lack of thermodynamic data available in the NTB91-17 database.

The aqueous complexes and solid phases included have been: $PaOH^{3+}$, $Pa(OH)_2^{2+}$, $Pa(OH)_3^{+}$, $PaO(OH)^{2+}$, $PaO_2(OH)(aq)$, $Pa_2O_5(s)$ and $PaO_2(s)$.

10.15 URANIUM

Thermodynamic database has been selected from the SKBU database (Bruno and Puigdomènech., 1989). The thermodynamic constants of the aqueous complexes and solid phases taken in the calculations agree with the NEA-TDB (Grenthe et al., 1992).

The solubility constant for the UO_2(fuel) solid phase has been changed with a value of logK=-1.6 according to the experimental work of Bruno et al. (1986).

10.16 NEPTUNIUM

The selected database for this element is based on the compilation of Lemire and Garisto (1989). However, in addition, we have incorporated recently determined thermodynamic data from Eriksen and co-workers (Eriksen et al., 1993). These new data includes:

$Np(CO_3)_2^- + 2H^+ = Np^{4+} + 2HCO_3^- + e^-$ logK=-4.67 10-12

$Np(OH)_3CO_3^- + 4H^+ = Np^{4+} + HCO_3^- + 3H_2O$ logK=6.5 10-13

The aqueous complex $Np(OH)_5^-$ has been removed from the database according to the results which were obtained in the previous sections.

A mistake has been found in the logK value of the complex $(NpO_2)_3(CO_3)_6^{6-}$.

The dissociation reaction given by the database is:

$(NpO_2)_3(CO_3)_6^{6-} + 12H^+ = 3Np^{4+} + 1.5O_2 + 6HCO_3^- + 3H_2O$ 10-14

with a logK=-84.77. However, this value is erroneous since it corresponds to the dissociation reaction written as a function of carbonate. Therefore, the new value according to the definition of the dissociation reaction (10-14) is logK=-22.79.

10.17 PLUTONIUM

The thermodynamic database used in the calculations is in agreement with a previous compilation performed by Puigdomènech and Bruno (1991).

The stability constant of the $PuCO_3^+$ aqueous complex has been taken from the Hatches v.7.0 with a value of logK=-3.83 (Allard, 1982) for the following reaction:

$$Pu^{3+} + HCO_3^- = PuCO_3^+ + H^+ \qquad 10\text{-}15$$

This change has been done according to the analysis of the data and later discussion performed in the previous sections.

10.18 AMERICIUM

The thermodynamic database selected for the solubility calculations has been extracted from the NEA Compilation (Silva et al., 1995). Therefore, the thermodynamic data included in the database have been updated according to this compilation.

A new phosphate aqueous complex, $AmHPO_4^+$ has been added to the database since it is included in the NEA Compilation as selected data. On the other hand, the hydroxo-carbonate aqueous complexes have been extracted from the original NTB91-17 database since these species have not been selected by this compilation.

In addition, three solid phases have been added to the database also extracted as selected data from the NEA Compilation, $Am(OH)_3(am)$, $Am_2(CO_3)_3(c)$ and $AmOHCO_3(c)$.

10.19 CURIUM

The thermodynamic database used for this element has been the Hatches v.7.0 (Cross and Ewart, 1989). Due to the lack of thermodynamic data for this radionuclide in the NTB91-17 database, the main aqueous complexes and solid phases have been included in this database for the solubility calculations previously performed. The species included have been: $CmOH^{2+}$, $CmCl^{2+}$, $CmCl_2^+$, CmF^{2+}, CmF_2^+, $CmF_3(aq)$, $CmSO_4^+$, $Cm(SO_4)_2^-$, $CmNO_3^{2+}$, $Cm(NO_3)_2^+$, $Cm(OH)_3(s)$, $CmOHCO_3(s)$ and $CmO_2(s)$.

11 UNCERTAINTIES ASSOCIATED TO CALCULATED SOLUBILITIES

In this section we will focus our discussion on the uncertainties associated to the data generated previously.

Radionuclide solubilities calculated previously can be considered upper bounds but realistic values, on the source term in the Performance Assessment exercise. These statements are based in two facts.

Firstly the solid phases selected as solubility-controlling phases of the different radionuclides have been well-defined thermodynamically. Thermodynamic databases have been checked and updated with a recent selection of the thermodynamic data for critical radionuclides, U, Pu, Np, Tc and REE's.

Secondly the solubilities have been calculated and selected from a conservative point of view. In this sense, these values have been compared with spent fuel dissolution data obtained from leaching tests in laboratories and in the cases where such experimental data are lacking, solubilities have been constrained by measured concentrations of these radionuclides in natural systems. This point has been extensively discussed in the previous sections.

A sensitivity analysis has been previously performed (Section 8) in order to determine the uncertainties associated to the analytical errors in groundwater determinations of the main aqueous ligands. At present, the uncertainties associated to the main parameters of groundwater composition, i.e. pH and carbonate content, will be extensively treated as well as the uncertainties associated to the redox conditions and the temperature of the system.

11.1 DEPENDENCIES ON OTHER PARAMETERS

According to the previous results, solubilities change in a more and less degree depending mainly on groundwater composition. This variability has been extensively discussed for each radionuclide.

Taking into account the previous results, we have considered mainly three groundwater parameters which influence in a major extent the solubilities. These parameters are Eh, pH and carbonate content in water. In addition, temperature has been also considered to study its influence on the solubilities of the different radionuclides.

Therefore, changes in solubilities for the main radionuclides as a function of these parameters have been studied, in order to determine how these parameters can influence the solubilities of the different radionuclides. For this purpose a sensitivity analysis has been carried out.

The reference water used in these calculations corresponds to the Äspö groundwater composition (Table 9-1). The calculations have been performed by using the EQ3NR code package (Wolery, 1992) as before.

Solubilities have been calculated by varying the value of one of the main parameters, i.e. pH, and by keeping the other parameters fixed for each run, according to the Äspö groundwater composition. By this procedure, we have treated the different parameters as no dependent variables.

To perform the sensitivity analysis we have chosen an interval of values for each parameter. The selected intervals include the values found in a major extent in typical granitic groundwaters, therefore, the ranges studied have been:

- pH from 7 to 9. The pH of the Äspö groundwater was 7.7.

- Total carbonate content in groundwater from 10^{-4} to $5 \cdot 10^{-3}$ mole·dm^{-3}. The total carbonate content of the Äspö groundwater was $2.19 \cdot 10^{-4}$ mole·dm^{-3}.

- Reducing environment, pe from Äspö groundwater (pe=-5.21) until pe=-1. We have not taken into consideration oxidising conditions since most of the granitic environments are reducing.

- Temperature between 15 and 60°C. Previous calculations were performed at room temperature, 25°C.

In addition, calculations have been also performed by equilibrating solid phases with the Gideå groundwater previously equilibrated with bentonite (Bruno et al., 1997). The resulting water composition is given in Table 11-1. As we can see in this table, the pH is 1.7 logarithmic units larger than the higher pH taken in the interval considered for this parameter, carbonate content and pe are also larger and lower respectively than the limits taken in the intervals considered in this work. The high pH and carbonate content of this water is mainly given by equilibrium with calcite (Bruno et al., 1997), the low calcium content of the Gideå groundwater leads to a major dissolution of this mineral.

As we mentioned before, the intervals taken in the sensitivity analysis include typical granitic groundwater compositions without considering any previous interaction with a barrier of the repository system designed for the spent nuclear fuel. However, these calculations have been carried out in order to obtain solubilities according to the expected groundwater which will enter into contact with the spent fuel in the repository system. Therefore, these solubilities have been taken as a limit of the solubility values expected in the repository system.

Table 11-1. Water composition obtained by equilibrating Gideå groundwater with bentonite (from Bruno et al., 1997).

Component	Concentration (mole·dm^{-3})
Ca	$7.40 \cdot 10^{-6}$
Mg	$4.00 \cdot 10^{-6}$
Na	$2.35 \cdot 10^{-2}$
K	$1.67 \cdot 10^{-5}$
Fe	$1.54 \cdot 10^{-6}$
SO_4^{2-}	$1.56 \cdot 10^{-6}$
Cl	$5.00 \cdot 10^{-3}$
CO_3^{2-}(tot.)	$9.18 \cdot 10^{-3}$
pH	10.7
pe	-7.5

We have selected one limiting solid phase for each radionuclide to perform the sensitivity analysis. This selection has been based on the results previously obtained.

Only pure solid phases have been taken into consideration, co-precipitation and co-dissolution approaches have not been used, despite for some radionuclides, i.e. Am, Cm, Ni, Ra, we have considered that these processes could limit their concentration in the selected groundwaters. However, the uncertainties associated to the solubilities obtained by these processes can be easily and directly calculated. For this reason, in the present work, we have considered pure solid phases from the most conservative point of view.

In this sense, we have also taken non crystalline solid phases for some radionuclides, i.e. Nb, Np, Pu, Th, U, Zr although the effect of the crystallinity has also an important influence on the solubility of the different solid phases considered. This effect has been studied previously where we have compared the solubilities obtained for some radionuclides by considering crystalline and non crystalline solid phases (Table 8-1). However, according to the Ostwald rule, we have calculated the solubility of the kinetically favoured solid phases, obtaining higher solubilities than the ones calculated by considering crystalline phases, but more realistic values by comparing with radionuclide concentrations measured in natural systems and in spent fuel leaching experiments as it has been previously dicussed.

In addition, in the case of selenium, the limiting solid phase varies depending on the pe of the system (Section 4-4), in such case, we have taken the predominant one under Äspö groundwater conditions, consequently, FeSe(s) has been chosen. The radionuclides studied as well as the selected solid phases are given in Table 11-2.

Table 11-2. Radionuclides and selected solid phases to perform the sensitivity analysis.

Radionuclide	Solid Phase	Radionuclide	Solid Phase
Ag	AgCl	Ra	$RaSO_4$
Am	$AmOHCO_3$	Se	FeSe
Cm	$CmOHCO_3$	Sm	$Sm_2(CO_3)_3$
Ho	$Ho_2(CO_3)_3$	Sn	SnO_2
Nb	Nb_2O_5(ac)	Sr	$SrCO_3$
Ni	NiO	Tc	$TcO_2 \cdot xH_2O$
Np	$Np(OH)_4$	Th	$Th(OH)_4$
Pa	Pa_2O_5	U	UO_2(f)
Pd	PdO	Zr	ZrO_2(am)
Pu	$Pu(OH)_4$		

The results obtained are given later, solubility changes are reported as percentage of variation with respect the calculated solubility, associated to the new value considered for each influencing parameter. The analytical formula applied has been:

$$\text{if } s'<s \qquad \left(1-\frac{s'}{s}\right)\times 100 = \% \qquad \text{11-1}$$

$$\text{if } s'>s \qquad \left(1-\frac{s}{s'}\right)\times 100 = \%$$

where s is the solubility obtained from the reference groundwater and s' is the new solubility calculated by changing the value of one influencing parameter.

The results are given in Table 11-3 for pH uncertainties, in Table 11-4 for carbonate uncertainties, in Table 11-5 for pe uncertainties and in Table 11-6 for temperature uncertainties.The total standard deviation is also included in these tables.

11.2 INFLUENCE OF pH

Table 11-3 shows the percentages of variation in the calculated solubilities associated to the different pH taken in the sensitivity analysis.

As a general trend, the solubilities of metal carbonates and hydroxo-carbonates are largely influenced by pH, this fact is reasonable due to the interconnection between the carbonate system and the pH. However, there are also other radionuclides which are influenced by this parameter, Nb, Ni, Se and Pu. Their variability is mainly due to the different predominant aqueous speciation depending on the pH studied.

In general, a slight influence is observed for oxides and hydroxides, this fact is due to the narrow range of pH variation (basic range) considered in this analysis.

Table 11-3. Percentages of variation and standard deviation in calculated solubilities associated to pH.

	pH			
	7	8	9	
Radionuclide		**% of variation**		σ
Ag	12	1	2	$2.57 \cdot 10^{-6}$
Am	90	46	67	$3.84 \cdot 10^{-6}$
Cm	86	50	92	$9.11 \cdot 10^{-7}$
Ho	89	41	60	$3.14 \cdot 10^{-5}$
Nb	59	42	93	$4.93 \cdot 10^{-4}$
Ni	96	74	100	$7.58 \cdot 10^{-2}$
Np	2	0	9	$4.18 \cdot 10^{-10}$
Pa	0	0	0	$1.15 \cdot 10^{-9}$
Pd	19	1	1	$8.86 \cdot 10^{-10}$
Pu	100	87	98	$1.70 \cdot 10^{-6}$
Ra	28	3	6	$7.63 \cdot 10^{-8}$
Se	82	50	94	$2.23 \cdot 10^{-9}$
Sm	91	46	78	$1.30 \cdot 10^{-5}$
Sn	19	19	82	$1.45 \cdot 10^{-9}$
Sr	85	50	92	$2.44 \cdot 10^{-2}$
Tc	1	0	1	$5.13 \cdot 10^{-11}$
Th	4	0	0	$5.77 \cdot 10^{-12}$
U	0	0	0	
Zr	0	0	0	$5.77 \cdot 10^{-12}$

11.3 INFLUENCE OF TOTAL CARBONATE

In Table 11-4 , we have shown the percentages of variation of the calculated solubilities associated to the different total carbonate contents assumed in the sensitivity analysis.

As expected, carbonate and hydroxo carbonate solid phases are in a major extent influenced by total carbonate content in groundwater.

Other radionuclides are slightly influenced by this parameter, Ni, Np, Pu and Th, the major variation in solubilities is obtained with the highest total carbonate content in groundwater, this is mainly due to the predominance of carbonate aqueous complexes in solution.

Table 11-4. Percentages of variation and standard deviation in calculated solubilities associated to total carbonate content.

	Total carbonate (mole·dm^{-3})			
	$1.00 \cdot 10^{-4}$	$1.00 \cdot 10^{-3}$	$5.00 \cdot 10^{-3}$	
Radionuclide		**% of variation**		σ
Ag	3	2	2	$8.96 \cdot 10^{-7}$
Am	54	66	77	$7.63 \cdot 10^{-7}$
Cm	59	79	96	$3.04 \cdot 10^{-7}$
Ho	61	66	75	$8.26 \cdot 10^{-6}$
Nb	1	0	0	$3.46 \cdot 10^{-7}$
Ni	2	10	39	$1.72 \cdot 10^{-3}$
Np	15	51	89	$3.01 \cdot 10^{-8}$
Pa	0	0	0	$5.02 \cdot 10^{-15}$
Pd	0	0	0	
Pu	2	21	63	$6.26 \cdot 10^{-9}$
Ra	9	5	6	$2.75 \cdot 10^{-8}$
Se	2	1	11	$4.67 \cdot 10^{-11}$
Sm	64	72	85	$3.26 \cdot 10^{-6}$
Sn	0	0	0	$1.15 \cdot 10^{-12}$
Sr	59	79	96	$8.83 \cdot 10^{-3}$
Tc	0	2	11	$4.78 \cdot 10^{-10}$
Th	0	1	33	$6.67 \cdot 10^{-11}$
U	0	0	0	
Zr	0	0	0	

11.4 INFLUENCE OF pE

The uncertainty on redox potential of the system has only an effect on the solubility of phases which are redox sensitive, Np, Pu, Se, Tc, U.

As we can see in Table 11-5, the percentage of variation as a function of the different pe assumed in the system is only important in the case of Pu. This radionuclide has a large influence on the pe, although the range of pe considered is reductant, since the predominant aqueous species depend in a large extent on this parameter.

Table 11-5. Percentages of variation and standard deviation in calculated solubilities associated to pe.

	pe		
	-3	-1	
Radionuclide	**% of variation**		σ
Np	0	1	$4.24 \cdot 10^{-11}$
Pu	98	98	$3.04 \cdot 10^{-11}$
Se	0	0	$7.07 \cdot 10^{-13}$
Tc	0	2	$7.78 \cdot 10^{-11}$
U	0	5	$4.95 \cdot 10^{-9}$

11.5 INFLUENCE OF TEMPERATURE

The influence of the temperature on calculated solubilities has been studied only for ten radionuclides, see Table 11-6, which thermodynamic data as a function of several temperatures was available.

In general, it has been observed a large variation on calculated solubilities as a function of this parameter, the different influence observed is basically due to the dependence of the solubility constants and association constants for the solid phases and predominant aqueous complexes respectively on the temperature.

Table 11-6. Percentages of variation and standard deviation in calculated solubilities associated to the temperature.

	T (°C)		
	15	**60**	
Radionuclide	**% of variation**		σ
Ni	27	59	$3.31 \cdot 10^{-3}$
Pd	16	41	$2.70 \cdot 10^{-9}$
Pu	69	79	$1.43 \cdot 10^{-8}$
Ra	46	84	$1.26 \cdot 10^{-6}$
Se	11	56	$6.14 \cdot 10^{-10}$
Sn	74	100	$9.97 \cdot 10^{-6}$
Sr	16	46	$3.03 \cdot 10^{-3}$
Tc	45	84	$2.94 \cdot 10^{-8}$
Th	15	33	$8.49 \cdot 10^{-11}$
U	28	83	$1.10 \cdot 10^{-7}$

11.6 INFLUENCE OF pH/CARBONATE VARIABILITY

As we have seen in the previous sub-sections (11-2 and 11-3), pH and carbonate content in the reference groundwater have been treated as no dependent variables. However, as we know, these two parameters are interconnected. In a granitic environment, carbonate content in groundwater will be limited by equilibrium with calcite. Consequently, last calculations of the sensitivity analysis have been performed by changing the pH, and by considering the reference groundwater with a carbonate content given by equilibrium with calcite. Figure 11-1 shows the solubility curve of calcite as a function of pH, taking a total calcium concentration equal to $4.73 \cdot 10^{-2}$ mole·dm^{-3} which corresponds to the calcium concentration determined in Äspö groundwater.

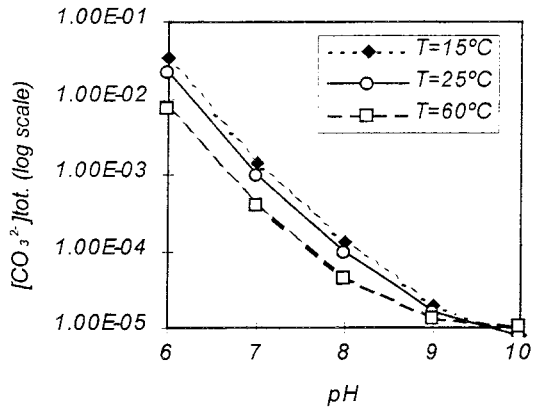

Figure 11-1. Solubility curve of calcite ($CaCO_3(s)$) as a function of pH, [Ca]=$4.73 \cdot 10^{-2}$ mole·dm^{-3}.

The solubility results obtained for each radionuclide are given in the next sub-section.

11.7 RANGES OF SOLUBILITIES

As we have seen in the previous tables (Tables 11-2 to 11-6), radionuclide solubilities have different variations depending on the main parameters considered. In some cases, only an small change in a determined parameter, i.e. pH change of 0.3 logarithmic units can vary the solubility of a determined solid phase, i.e. strontianite ($SrCO_3(s)$) until 50%. Consequently, it is very difficult to give an interval for each parameter for which the punctual solubility data previously reported is valid.

However, it is possible to give a range of solubilities for each radionuclide, as a function of the interval of values taken for the main parameters, these ranges of validity are given in the next table (Table 11-7). A short discussion about the ranges considered for each radionuclide is also given.

The ranges of solubilities shown in the table also include solubilities taken by equilibrating solid phases with Gideå/bentonite water composition. Only in two cases, silver and radium, the intervals given in Table 11-7 do not include solubilities calculated with Gideå/bentonite water since the variation obtained for both radionuclides is due to other components of the system, chloride and sulphate respectively.

Table 11-7. Ranges of calculated solubilities depending on the intervals considered for the influencing parameters; pH between 7 and 9, total carbonate content ranging from 10^{-4} to $5 \cdot 10^{-3}$ mole·dm^{-3}, and equilibrated with calcite, pe of the system (pe=-5.21) until -1 and temperature between 15 and 60°C.

	log[Rn] (mole·dm^{-3})			log[Rn] (mole·dm^{-3})	
Radionuclide	**from**	**to**	**Radionuclide**	**from**	**to**
Ag	-4.53	-4.47	Ra	-6.79	-5.71
Am	-6.89	-5.16	Se	-10.39	-8.39
Cm	-10.93	-5.79	Sm	-6.48	-4.63
Ho	-5.80	-4.24	Sn	-9.84	-4.85
Nb	-4.61	-1.41	Sr	-6.24	-1.35
Ni	-4.88	-0.88	Tc	-8.40	-7.34
Np	-8.27	-7.21	Th	-9.79	-9.31
Pa	-6.50	-6.50	U	-7.66	-6.75
Pd	-8.43	-8.11	Zr	-8.61	-8.60
Pu	-10.00	-5.53			

11.7.1 Silver

Only a slight variation on the solubility of AgCl(s) has been observed as a function of pH and total carbonate content in groundwater (Figure 11-2). This variation is mainly due to small differences in the percentage of predominant aqueous species in solution.

In the previous work, Ag(s) was considered as the limiting solid phase of this radionuclide from a very conservative point of view. According to the solubilities obtained, ranging between $1 \cdot 10^{-16}$ and $3 \cdot 10^{-11}$ mole·dm^{-3}, the solubility of this solid phase depends basically on both the pH and the redox conditions of the system.

The solubility obtained by equilibrating the solid phase with the Gideå/bentonite water is around two orders of magnitude lower than the one obtained by equilibrium with the reference groundwater. This difference is due to the highest chloride content in the reference groundwater with respect the Gideå/bentonite water. The different concentration of chloride implies a different aqueous speciation. The formation of tri- and tetra-chloride aqueous complexes in the Äspö groundwater produces a lower concentration of the chloride anion with the consequent silver concentration increase in solution.

The range of concentrations assumed in Table 11-7 for this radionuclide does not include the lower solubility obtained by equilibrium with Gideå/bentonite water, since in that case, solubility variation is due to chloride content, which is a different component of the main influencing parameters assumed in the sensitivity analysis.

Figure 11-3 shows AgCl(s) solubility variations due to changes in pH, when carbonate content is given by equilibrium with calcite. As we can see,

solubilities are in the same range than previous calculations performed by considering all parameters as no dependent variables.

The interval of solubilities calculated in the sensitivity analysis can be considered negligible in the PA exercise, therefore, we may consider an individual solubility value independently of the variation in the influencing parameters taken in this sensitivity analysis.

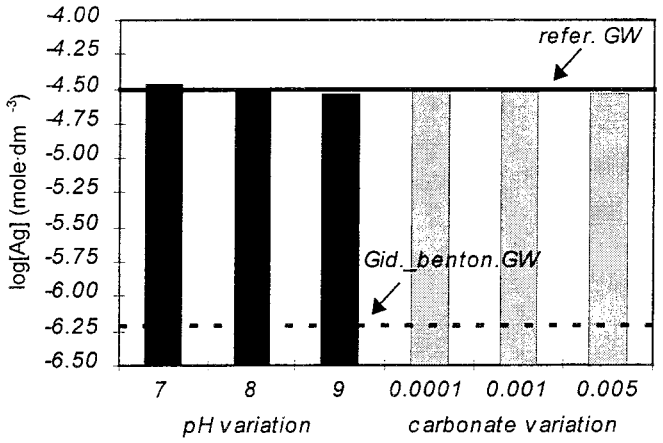

Figure 11-2. Solubility of AgCl(s) as a function of pH and total carbonate content respectively. Solid and dashed lines perform the calculated solubilities of this solid phase equilibrated with the reference groundwater and the Gideå/bentonite water respectively.

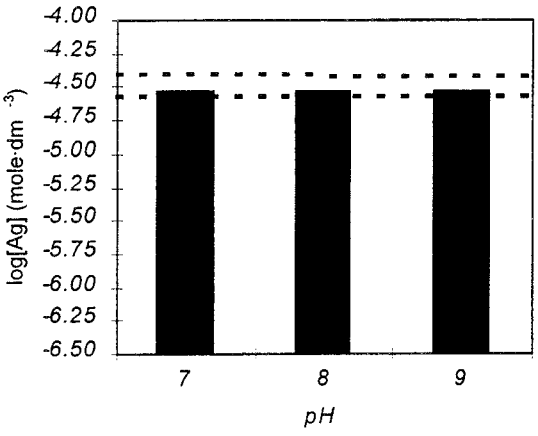

Figure 11-3. Solubility of AgCl(s) as a function of pH, total carbonate content given by equilibrium with calcite. Dashed lines give the interval of solubilities calculated in the sensitivity analysis.

11.7.2 Americium

The solubility of $AmOHCO_3(s)$ solid phase decreases when increasing both pH and total carbonate content in groundwater (Figure 11-4). This is due to the stabilisation of this solid phase in basic and carbonated waters.

Figure 11-5 shows $AmOHCO_3(s)$ solubility variations due to changes in pH, when carbonate content is given by equilibrium with calcite. In these calculations, the higher the pH, the lower the carbonate content (Figure 1-1), consequently, we can observe two different trends in the solubility of this solid phase when increasing pH, depending on the relative weight of each parameter (pH and carbonate concentration) on the solubility of this solid phase. However, the solubilities are in the same range than previous calculations performed by considering all parameters as no dependent variables.

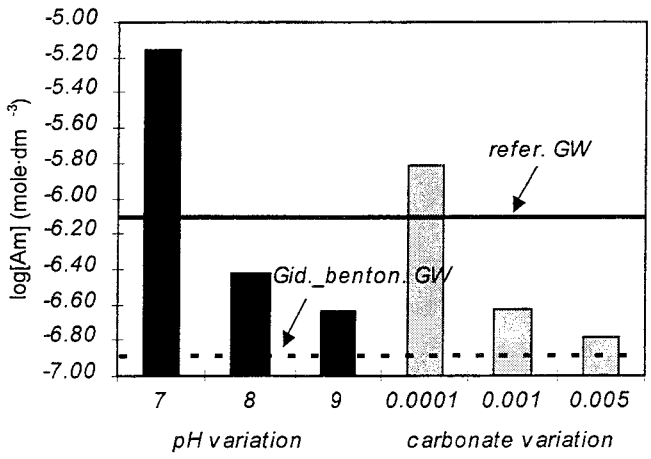

Figure 11-4. Solubility of $AmOHCO_3(s)$ as a function of pH and total carbonate content respectively. Solid and dashed lines show the calculated solubilities of this solid phase equilibrated with the reference groundwater and the Gideå/bentonite water respectively.

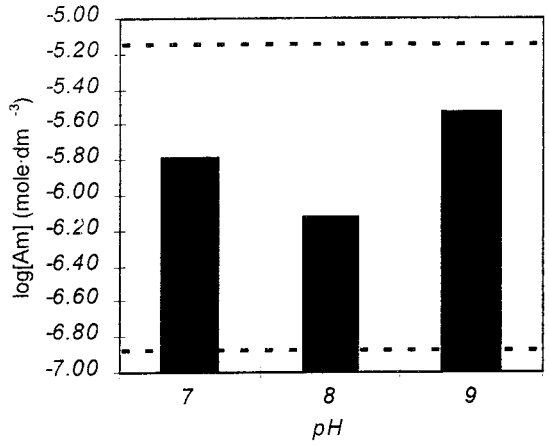

Figure 11-5. Solubility of $AmOHCO_3(s)$ as a function of pH, total carbonate content given by equilibrium with calcite. Dashed lines give the interval of solubilities calculated in the sensitivity analysis.

Solubility changes as a function of both pH and carbonate content variations are approximately 1.5 orders of magnitude. Consequently a range of solubilities may be taken into consideration in the PA exercise (Table 11-7).

11.7.3 Curium

As in the previous case, the solubility of $CmOHCO_3(s)$ solid phase decreases when increasing both pH and total carbonate content in groundwater (Figure 11-6). This is also due to the stabilisation of this solid phase in basic and carbonated waters.

As it is shown in Figure 11-6, dashed line, the solubility of this solid phase decreases four orders of magnitude in equilibrium with Gideå/bentonite water, this is due to the sum of two effects, the highest pH and carbonate content considered in this water. The same effect has been observed in the previous case, for americium.

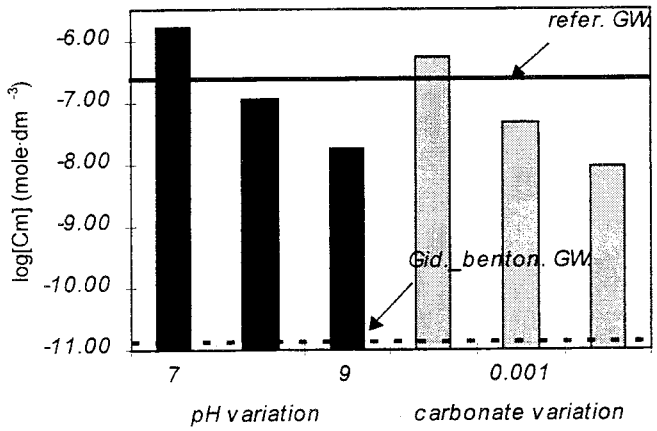

Figure 11-6. Solubility of $CmOHCO_3(s)$ as a function of pH and total carbonate content variations. Solid and dashed lines perform the calculated solubilities of this solid phase equilibrated with the reference groundwater and the Gideå/bentonite water respectively.

Figure 11-7 shows $CmOHCO_3(s)$ solubility variations due to changes in pH, when carbonate content is given by equilibrium with calcite. The same effect as in the case of americium has been observed in these calculations. However, in that case, only an slight solubility change has been observed depending on the pH taken.

Solubilities are in the same range than previous calculations performed by considering all parameters as no dependent variables.

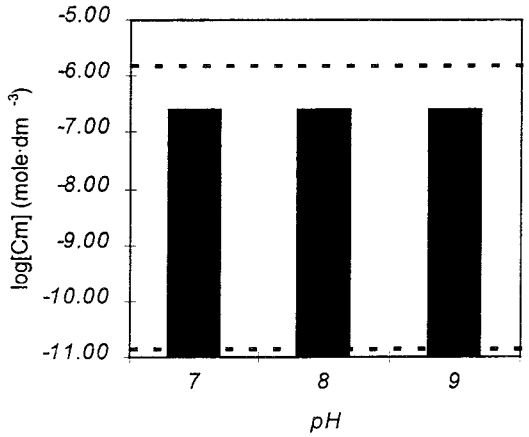

Figure 11-7. Solubility of $CmOHCO_3(s)$ as a function of pH, total carbonate content given by equilibrium with calcite. Dashed lines show the interval of solubilities calculated in the sensitivity analysis.

Solubility changes due to the influencing parameters, pH and total carbonate content, are approximately 5 orders of magnitude. Consequently, as in the case of americium, a range of solubilities may be taken into consideration in the PA exercise (Table 11-7).

11.7.4 Holmium

As we can see in Figure 11-8, the solubility of $Ho_2(CO_3)_3(s)$ is affected by both pH and total carbonate content in groundwater. The calculated solubilities follow the same behaviour as americium and curium, therefore, the solubility of this solid phase decreases when increasing both influencing parameters. This is mainly due to the stabilisation of this solid phase in carbonated waters.

Holmium-carbonate complexes become the predominant aqueous species when increasing pH or carbonate concentration in groundwater, these species are less stable than the free cation in solution, this implies an stabilisation of the solid phase with the consequent solubility decrease.

On the other hand, a highest solubility has been calculated by equilibrating this solid phase with Gideå/bentonite water (dashed line, Figure, 11-8). This fact is because of the stabilisation of hydroxo-aqueous complexes, $Ho(OH)_3(aq)$ when increasing pH with the consequent increase in the solubility.

In Figure 11-9, we can see the effect of pH increase on the $Ho_2(CO_3)_3(s)$ solubility, when carbonate content is given by equilibrium with calcite. The higher the pH, the lower the total carbonate content in the system. In such case, the solubility of this solid phase increases with pH, the opposite trend than in Figure 11-8. This behaviour is given by the stabilisation of different aqueous species in solution; at pH 7 (high carbonate concentration), carbonate aqueous species are predominant, at pH 9 (low carbonate concentration), hydroxo aqueous species become the predominant ones, with the consequent solubility increase.

Despite the different trend observed in the last calculations, these solubilities are in the same range than previous calculations performed by considering all parameters as no dependent variables.

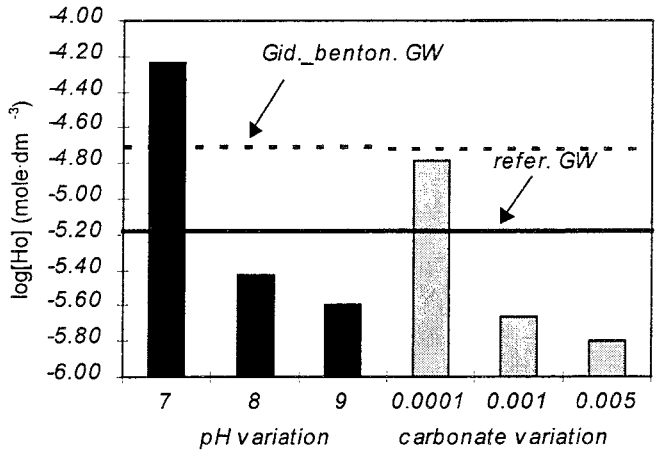

Figure 11-8. Solubility of $Ho_2(CO_3)_3(s)$ as a function of pH and total carbonate content variations. Solid and dashed lines plot the calculated solubilities of this solid phase equilibrated with the reference groundwater and the Gideå/bentonite water respectively.

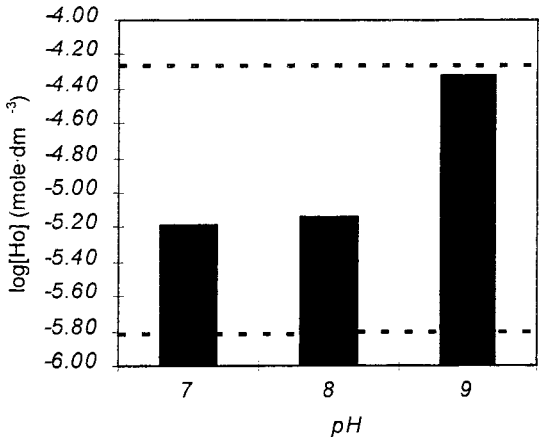

Figure 11-9. Solubility of $Ho_2(CO_3)_3(s)$ as a function of pH, total carbonate content given by equilibrium with calcite. Dashed lines show the interval of solubilities calculated in the sensitivity analysis.

As it is shown in the previous figures, solubility changes due to the influencing parameters considered in this exercise are approximately 1.5 orders of magnitude. Consequently, the range of solubilities given in Table 11-7 for this radionuclide may be taken in the PA exercise.

11.7.5 Niobium

As it was expected, $Nb_2O_5(ac)$ is only affected by changes in pH (Figure 11-10), its solubility increases when increasing pH, due to the destabilisation of this solid phase. Therefore, as it was expected, no variations have been observed in calculated solubilities as a function of pH, when considering the total carbonate content of the system given by equilibrium with calcite.

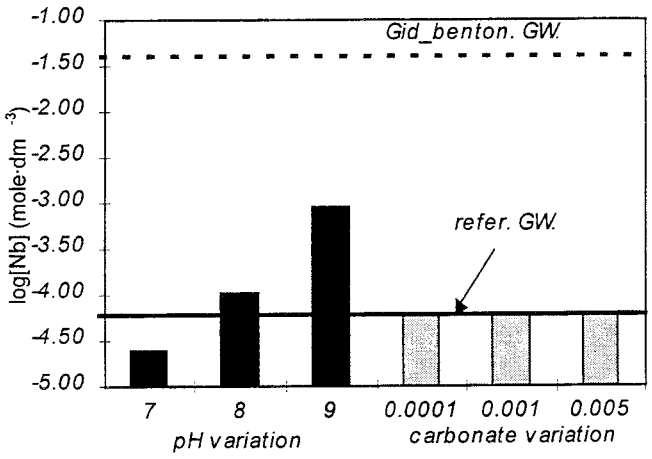

Figure 11-10. Solubility of $Nb_2O_5(ac)$ as a function of pH and total carbonate content changes. Solid and dashed lines perform the calculated solubilities of this solid phase equilibrated with the reference groundwater and the Gideå/bentonite water respectively.

According to this trend, the highest solubility has been calculated in equilibrium with the Gideå/bentonite water, with a pH greater than 10 (Figure 11-10, dashed line).

Solubility changes approximately 3 orders of magnitude in the pH range studied. Consequently, the range of solubilities given in Table 11-7 for this radionuclide may be considered in the PA exercise.

11.7.6 Nickel

As it is shown in Figure 11-11, the parameter which affects in a major extent the solubility of NiO(s) is the pH. Its solubility increases dramatically when decreasing pH due to the destabilisation of the nickel oxide. As we can see, this solid phase is very sensitive to changes in the pH of the system.

On the other hand, only an slight effect has been observed in carbonate concentration and temperature variations of the system.

The solubility obtained by equilibrium of NiO(s) with Gideå/bentonite water is lower than the one calculated by using the reference water. However, the decrease in solubility is not so large as expected according to the pH of this water (pH=10.7). This effect is due to the high carbonate concentration of this water which leads to a destabilisation of the solid phase.

The same behaviour as the one obtained due to pH variation in Figure 11-11 has been observed when increasing the pH of the system, with a carbonate content given by equilibrium with calcite (Figure 11-12). Calculated solubilities are in the range obtained in the previous calculations, where all parameters were considered as no dependent variables.

According to the results obtained, the range of solubilities given in Table 11-7 may be taken for a PA exercise. However, this range can be narrower if we assume lower pH variations in the system (see Figure 11-12).

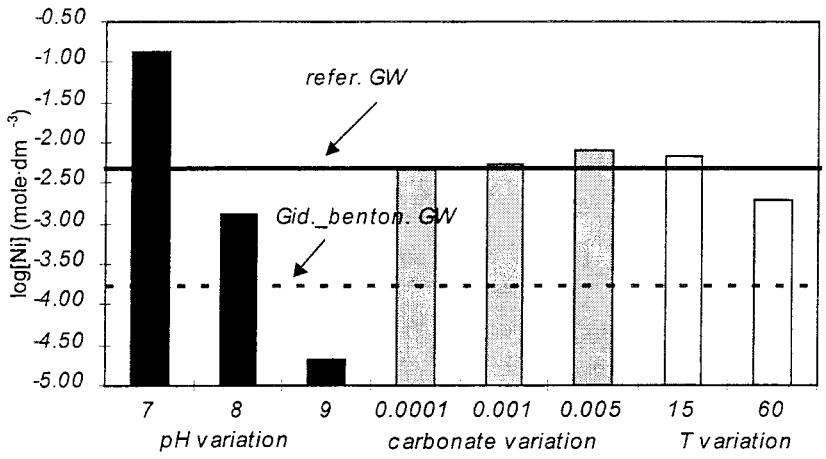

Figure 11-11. Solubility of NiO(s) as a function of pH, total carbonate content and temperature changes. Solid and dashed lines show the calculated solubilities of this solid phase equilibrated with the reference groundwater and the Gideå/bentonite water respectively.

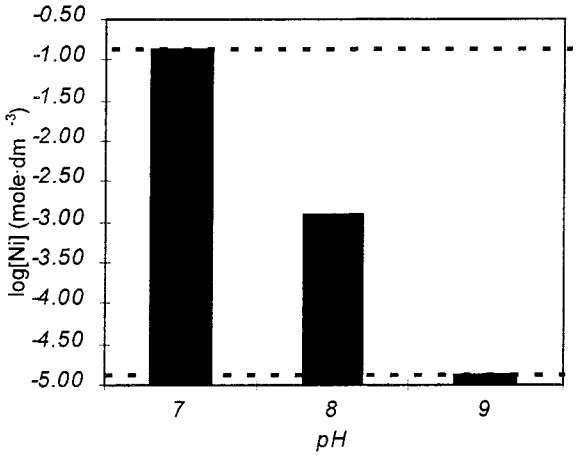

Figure 11-12. Solubility of NiO(s) as a function of pH, total carbonate content given by equilibrium with calcite. Dashed lines show the interval of solubilities calculated in the sensitivity analysis.

11.7.7 Neptunium

As it is shown in Figure 11-13, the solubility of $Np(OH)_4(s)$ is mainly affected by changes in total carbonate content in groundwater. Its solubility arises when increasing the total carbonate concentration of the system, this fact is due to the stabilisation of neptunium-carbonate aqueous complexes.

On the other hand we can also observe an slight decrease in the solubility of this solid phase at the higher pH (pH=9). This is due to the stabilisation of the neptunium hydroxide solid phase when increasing the pH of the system.

This effect has been also observed when equilibrating this solid phase with Gideå/bentonite water (Figure 11-13, dashed line). Despite the highest carbonate content which leads to an increase in the solubility, the highest pH

stabilise the solid phase with the consequent increase in the solubility but not so high as expected due to the influence of carbonate.

The interval of pe considered in the system (Figure 11-13) does not change the solubility of this solid phase. This radionuclide is not redox sensitive to the pe range considered in this exercise.

Solubilities obtained in the last calculations (Figure 11-14) decrease when increasing the pH of the system, this behaviour is due to the lower carbonate content when increasing pH (Figure 11-1) with the consequent stabilisation of the solid phase.

The solubility of this solid phase changes around 1 order of magnitude with the ranges of the influencing parameters taken. Therefore, the range of solubilities given in Table 11-7 may be considered in a PA exercise.

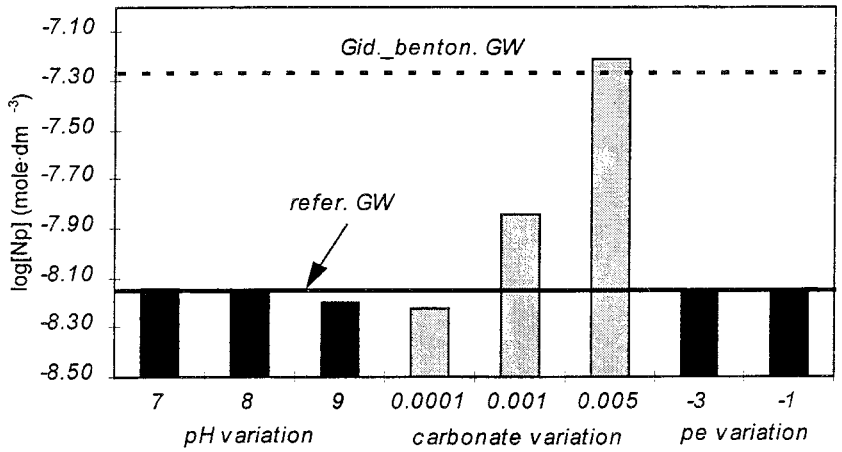

Figure 11-13. Solubility of $Np(OH)_4(s)$ as a function of pH, total carbonate content and pe changes. Solid and dashed lines show the calculated solubilities of this solid phase equilibrated with the reference groundwater and the Gideå/bentonite water respectively.

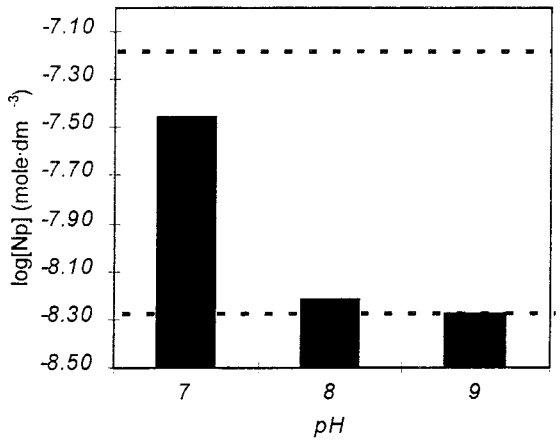

Figure 11-14. Solubility of $Np(OH)_4(s)$ as a function of pH, total carbonate content given by equilibrium with calcite. Dashed lines show the interval of solubilities calculated in the sensitivity analysis.

11.7.8 Protactinium

As it is shown in Figure 11-15, the solubility of $Pa_2O_5(s)$ is not affected by any influencing parameter considered in this exercise. This unvariation includes calculations performed by using Gideå/bentonite water. Therefore, a solubility value may be considered in the PA exercise (solid line in the figure).

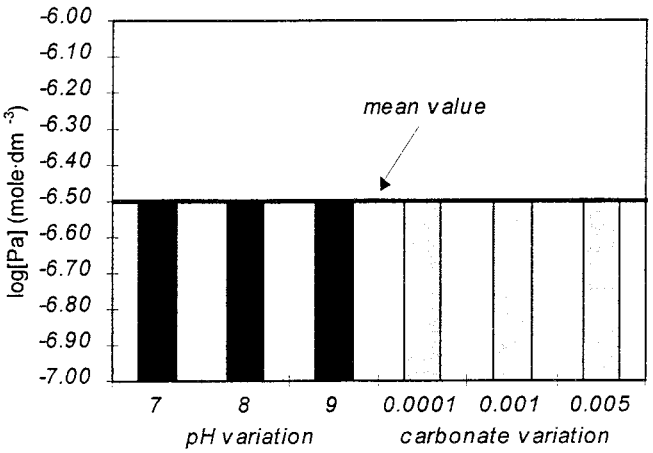

Figure 11-15. Solubility of $Pa_2O_5(s)$ as a function of pH and total carbonate content changes. Solid line gives the mean value.

11.7.9 Palladium

As it is shown in Figure 11-16, the solubility of PdO(s) is slightly affected by the lower pH and the temperature of the system assumed. The solubility increases at lower pH due to the destabilisation of the palladium oxide. On the other hand, the solubility of this solid phase decreases when increasing

the temperature of the system. Total carbonate content does not have any effect on the solubility of this solid phase.

Therefore, as it was expected, no variations have been observed in calculated solubilities as a function of pH, when considering the total carbonate content of the system given by equilibrium with calcite.

Due to the slight solubility changes by influencing parameters, we may take a mean solubility value for this radionuclide which could correspond to the solubility calculated by considering the reference system (Figure 11-16). Therefore, we may consider solubility changes calculated in the sensitivity analysis negligible in the PA exercise.

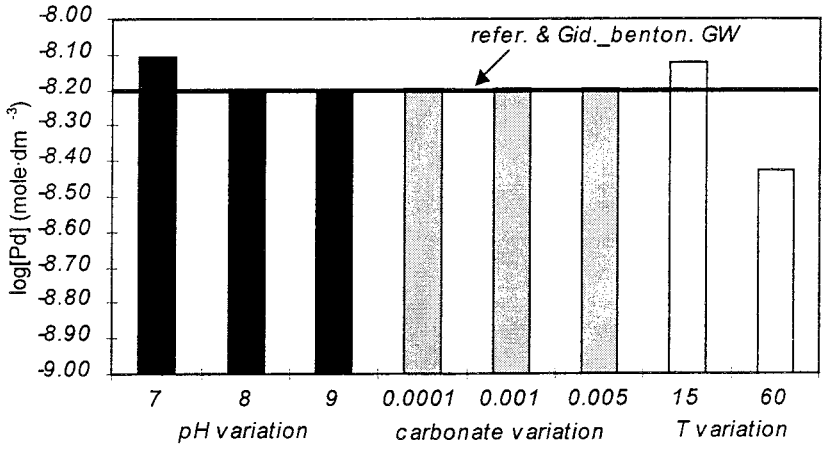

Figure 11-16. Solubility of PdO(s) as a function of pH, total carbonate content and temperature changes. Solid line shows the calculated solubilities of this solid phase equilibrated with the reference groundwater and the Gideå/bentonite water.

11.7.10 Plutonium

The solubility of plutonium hydroxide changes depending on the influencing parameters taken in the sensitivity analysis (Figure 11-17). The solubility of this solid phase is affected in a major extent by changes in the pH and in the pe of the system.

The solubility increases when decreasing either pH or pe of the system, this fact is due to the stabilisation of the aqueous Pu(III) species at lower pH and pe values (Bruno et al., 1997). At higher pH or pe values, aqueous Pu(IV) species become the predominant complexes in solution, with a consequent decrease in the solubility.

Carbonate variations have only an slight effect in the solubility of this solid phase. The solubility increases when increasing carbonate concentration of the system due to the stabilisation of aqueous plutonium-carbonate complexes (Bruno et al., 1997).

The temperature of the system also has an important influence on the solubility of this radionuclide. As it is shown in Figure 11-17, the concentration of this radionuclide in solution decreases with temperature.

Due to the slight influence of the carbonate content on the solubility of this solid phase, the solubilities calculated by assuming equilibrium of the system with calcite (Figure 11-18), are the same as the previous ones calculated by assuming the pH as a no dependent parameter (Figure 11-17).

According to the results obtained in the sensitivity analysis, the range of solubilities given in Table 11-7 may be taken in a PA exercise. However, this range could be narrower if we assume lower pH variations in the system (see Figure 11-18).

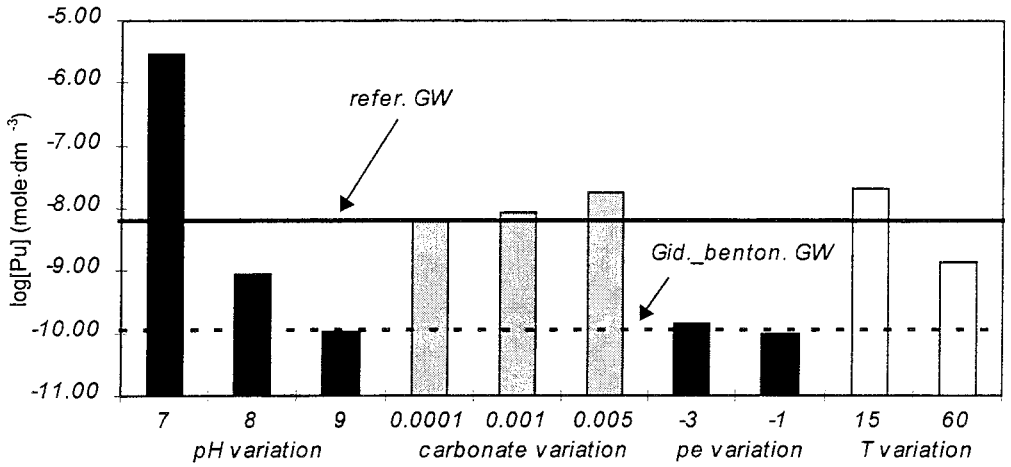

Figure 11-17. Solubility of $Pu(OH)_4(s)$ as a function of all the influencing parameters; pH, total carbonate content, pe and T. Solid and dashed lines show the calculated solubilities of this solid phase equilibrated with the reference groundwater and the Gideå/bentonite water respectively.

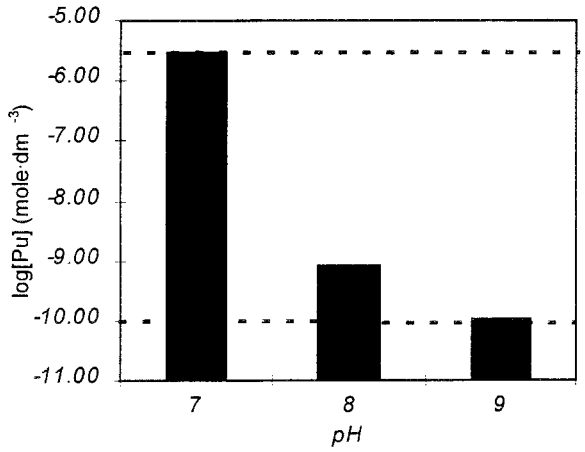

Figure 11-18. Solubility of $Pu(OH)_4(s)$ as a function of pH, total carbonate content given by equilibrium with calcite. Dashed lines show the interval of solubilities calculated in the sensitivity analysis.

11.7.11 Radium

The solubility of $RaSO_4(s)$ slightly increases when decreasing pH or carbonate content parameters. However, the solubility is affected in a major extent by the temperature of the system. A highest increase can be observed when increasing this parameter (Figure 11-19).

The solubility obtained by equilibrating the solid phase with the Gideå/bentonite water is around three orders of magnitude higher than the one obtained by equilibrium with the reference groundwater. This difference is due to the highest sulphate content in the reference groundwater with respect the Gideå/bentonite water.

The range of concentrations assumed in Table 11-7 for this radionuclide does not include the lower solubility obtained by equilibrium with Gideå/bentonite water, since in that case, solubility variation is due to sulphate content, which is a different component of the main influencing parameters assumed in the sensitivity analysis.

Figure 11-20 shows $RaSO_4(s)$ solubility variations due to changes in pH, when carbonate content is given by equilibrium with calcite. As we can see, solubilities are in the same range than previous calculations performed by considering all parameters as no dependent variables.

By neglecting temperature effects, a mean value of the solubility may be considered in a PA exercise, according to the results obtained in this analysis. This solubility may correspond to the solubility calculated in the reference system (solid line in Figure 11-19). However, if temperature effects is considered in the PA exercise, the range of solubilities given in Table 11-7 could be taken.

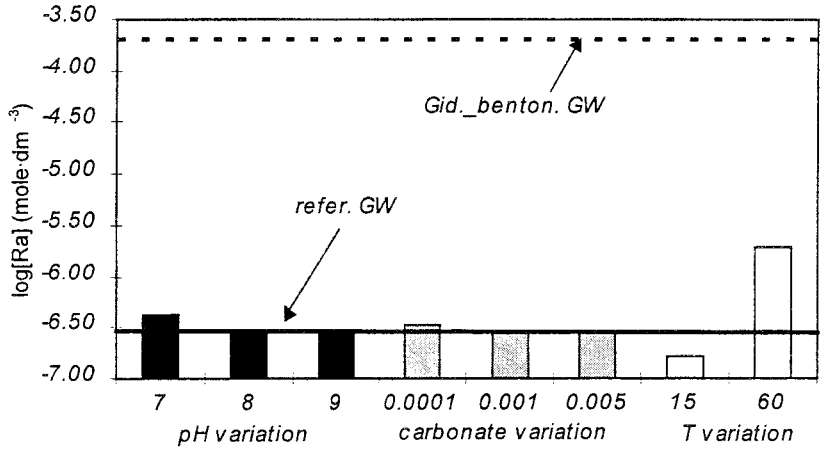

Figure 11-19. Solubility of $RaSO_4(s)$ as a function of pH, total carbonate content and T. Solid and dashed lines show the calculated solubilities of this solid phase equilibrated with the reference groundwater and the Gideå/bentonite water respectively.

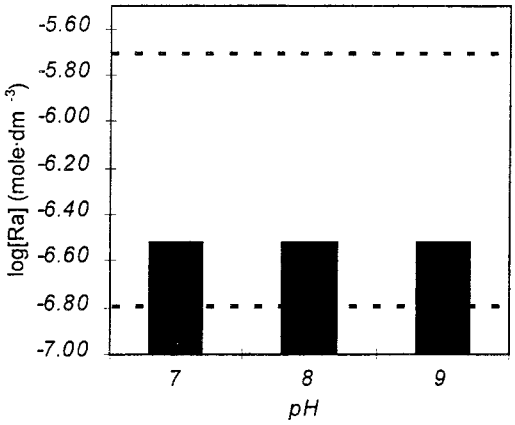

Figure 11-20. Solubility of $RaSO_4(s)$ as a function of pH, total carbonate content given by equilibrium with calcite. Dashed lines show the interval of solubilities calculated in the sensitivity analysis.

11.7.12 Selenium

According to Figure 11-21, the parameter which affects in a major extent the solubility of FeSe(s) is the pH. Its solubility decreases when increasing the pH of the system. The predominant aqueous complex is HSe^-, therefore, the lower the pH the higher the stability of the aqueous species with the consequent increase in the solubility of the solid phase.

According to this trend, the solubility obtained when equilibrating this solid phase with the reference groundwater is higher than when equilibrating with the Gideå/bentonite water.

As it was expected, carbonate concentration does not affect the solubility of this radionuclide. Consequently, no variations have been observed in calculated solubilities as a function of pH, when considering the total carbonate content of the system given by equilibrium with calcite.

The range of pe considered does not affect the solubility of this solid phase despite selenium is a redox sensitive radionuclide, this fact is because aqueous speciation does not change in the range of pe studied.

As it was mentioned before, other solid phases can limit the concentration of this radionuclide in solution at pe around -1. However, we have considered FeSe(s) in all the pe range studied as the limiting solid phase from a conservative point of view.

Finally, only an slight effect has been observed depending on the temperature of the system. The solubility of this radionuclide increases at higher temperatures.

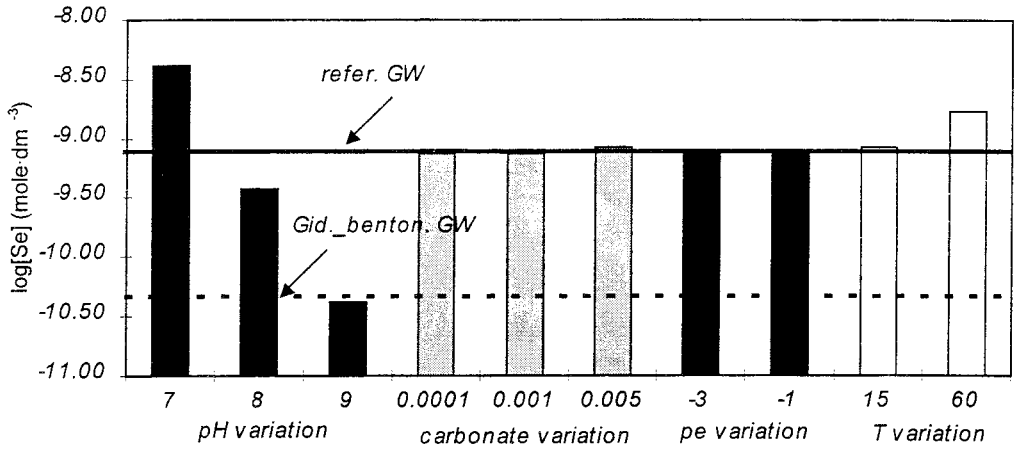

Figure 11-21. Solubility of FeSe(s) as a function of the influencing parameters; pH, total carbonate content, pe and T. Solid and dashed lines show the calculated solubilities of this solid phase equilibrated with the reference groundwater and the Gideå/bentonite water respectively.

As we can see in Table 11-7, according to the sensitivity analysis performed, the solubilities can vary 2 orders of magnitude, therefore, a range of values may be taken in a PA exercise. Although, if the range of pH can be narrower, also a narrow interval of solubilities can be considered.

11.7.13 Samarium

As we can see in Figure 11-22, the solubility of $Sm_2(CO_3)_3(s)$ is affected by both pH and total carbonate content in groundwater. The calculated solubilities follow the same behaviour as holmium, therefore, the solubility of this solid phase decreases when increasing both influencing parameters. This is mainly due to the stabilisation of this solid phase in carbonated waters.

Samarium-carbonate complexes become the predominant aqueous species when increasing pH or carbonate concentration in groundwater, these species are less stable than samarium free cation in solution, this implies an stabilisation of the solid phase with the consequent solubility decrease.

A solubility increase has been observed in equilibrium with Gideå/bentonite water (Figure, 11-22). This fact is because hydroxo-aqueous complexes, $Sm(OH)_3(aq)$, lead to predominant aqueous species when increasing pH with the consequent increase in the solubility.

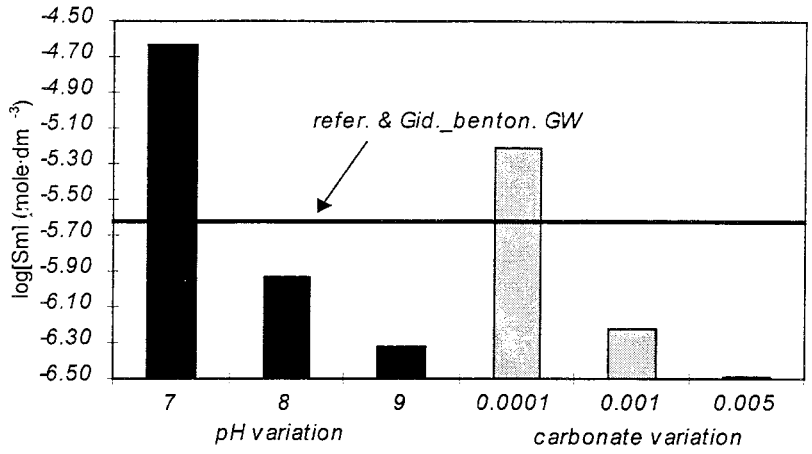

Figure 11-22. Solubility of $Sm_2(CO_3)_3(s)$ as a function of pH and total carbonate content variations. Solid line shows the calculated solubilities of this solid phase equilibrated with the reference groundwater and the Gideå/bentonite water.

In Figure 11-23, we can see the effect of pH increase on the $Sm_2(CO_3)_3(s)$ solubility, when carbonate content is given by equilibrium with calcite. The higher the pH, the lower the total carbonate content in the system. In such case, the solubility of this solid phase increases with pH. This behaviour is given by the stabilisation of different aqueous species in solution; at pH 7 (high carbonate concentration), carbonate aqueous species are predominant, at pH 9 (low carbonate concentration), hydroxo aqueous species become the predominant ones, with the consequent solubility increase.

However, solubilities are in the same range than the ones obtained in the previous calculations when considering pH and carbonate as no dependent variables.

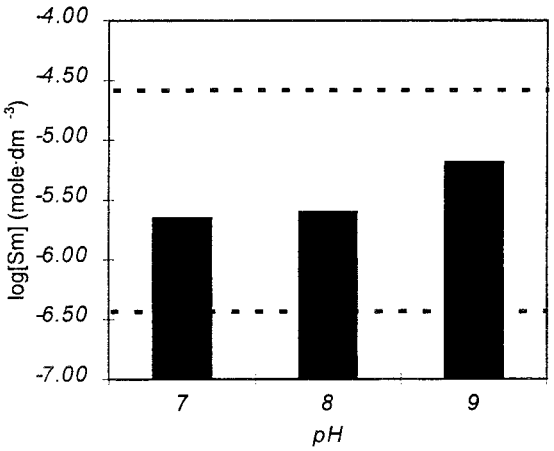

Figure 11-23. Solubility of $Sm_2(CO_3)_3(s)$ as a function of pH, total carbonate content given by equilibrium with calcite. Dashed lines show the interval of solubilities calculated in the sensitivity analysis.

Solubility changes due to the influencing parameters considered in this exercise are approximately 2 orders of magnitude. Consequently, the range of solubilities given in Table 11-7 for this radionuclide may be taken in the PA exercise.

11.7.14 Tin

The parameters studied affect in different extents the solubility of this radionuclide (Figure 11-24).

As expected, carbonate concentration does not affect the solubility of SnO_2(s). On the other hand, the solubility increases when increasing pH, this behaviour is due to the stabilisation of $Sn(OH)_5^-$ aqueous complex in basic solutions. The calculated solubility in equilibrium with Gideå/bentonite water arises due to the highest pH assumed in this system.

Solubility variations due to changes in pH, when carbonate content is given by equilibrium with calcite are the same as solubilities obtained by considering all parameters as no dependent variables.

Temperature is the parameter which affects in a major extent the solubility of this radionuclide. As we can see in Figure 11-24, the solubility increases four orders of magnitude when increasing the temperature of the system.

According to the results obtained, a range of solubilities may be taken for a PA exercise. However, because of the large variation in solubilities due to temperature changes in the system, these values could be neglected because they can be considered unrealistic. This fact is because at highest temperatures, another solid phase, SnS, could limit the solubility of this radionuclide. In such case, a narrower range of solubilities may be taken than the one given in Table 11-7.

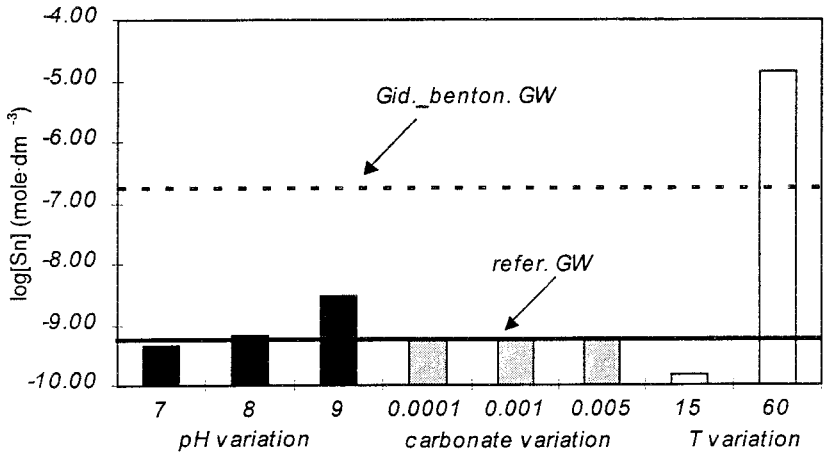

Figure 11-24. Solubility of SnO_2(s) as a function of pH, total carbonate content and temperature variations. Solid and dashed lines show the calculated solubilities of this solid phase equilibrated with the reference groundwater and the Gideå/bentonite water respectively.

11.7.15 Strontium

As it is shown in Figure 11-25, the solubility of strontianite decreases with increasing pH, carbonate content and temperature of the system.

The effect of carbonate concentration on the solubility of strontianite is due to the stabilisation of this solid phase in carbonated waters. Because of the interconnection between the pH and the carbonate system, the effect is the same when increasing pH.

Consequently, the solubility obtained for strontianite in equilibrium with Gideå/bentonite water is the lowest one calculated (dashed line, Figure 11-25) due to the highest pH and carbonate concentration of this system.

On the other hand, a slight variation can be also observed due to temperature changes.

Figure 11-26 shows $SrCO_3(s)$ solubility variations due to changes in pH, when carbonate content is given by equilibrium with calcite. In these calculations, the higher the pH, the lower the carbonate content (Figure 1-1). The effect on the solubility of this solid phase is only an slight solubility variation as a function of the pH as it is shown in the figure.

Solubility changes due to the influencing parameters considered in this exercise are approximately 2 orders of magnitude. Consequently, the range of solubilities given in Table 11-7 for this radionuclide may be taken in the PA exercise.

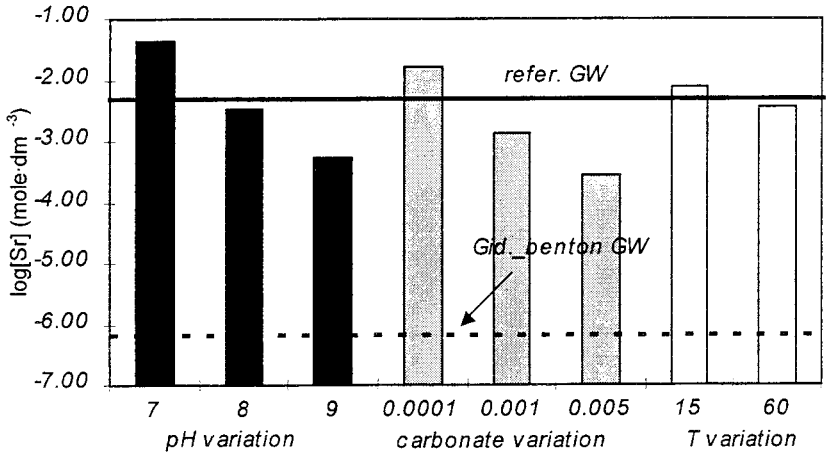

Figure 11-25. Solubility of $SrCO_3(s)$ as a function of pH, total carbonate content and temperature variations. Solid and dashed lines show the calculated solubilities of this solid phase equilibrated with the reference groundwater and the Gideå/bentonite water respectively.

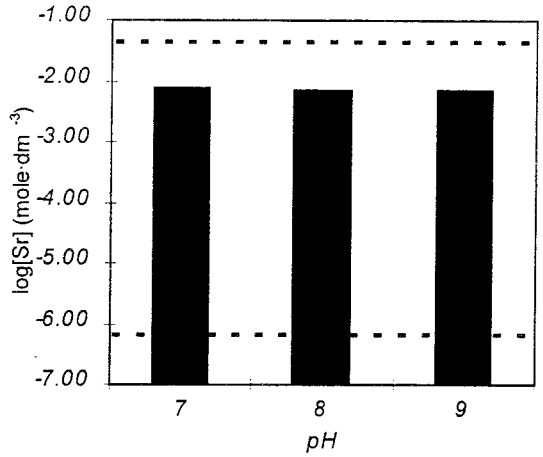

Figure 11-26. Solubility of $SrCO_3(s)$ as a function of pH, total carbonate content given by equilibrium with calcite. Dashed lines show the interval of solubilities calculated in the sensitivity analysis.

11.7.16 Technetium

According to the results obtained (Figure 11-27), the solubility of $TcO_2 \cdot xH_2O$ is mainly affected by temperature changes in the system. The technetium concentration in solution increases when increasing temperature.

As expected, pH does not affect the solubility of this solid phase. Only an slight effect has been observed on carbonate increase, due to the presence of hydroxo-carbonate aqueous species in solution. Consequently, solubility increases when this solid phase is equilibrated with Gideå/bentonite water (dashed line in Figure 11-27).

Although this radionuclide is redox sensitive, in the range of pe studied, this parameter does not have any effect on its solubility. However, according to the results obtained before, in this interval of pe, the solubility of this solid phase increases if a higher pH is considered, this is due to a change in the aqueous speciation, at pH around 9 and pe of -1, TcO_4^- becomes the predominant aqueous species, with a consequent solubility increase (logs=-4.76).

From the sensitivity analysis, we have obtained a solubility change of approximately 1 order of magnitude, this interval is given in Table 11-7. However, if we neglect temperature changes, a mean value for technetium solubility may be considered in a PA exercise. Otherwise, it will be important to take into account that at higher pH and pe values, the solubility will increase dramatically, this last case is not considered in the interval of solubilities given before.

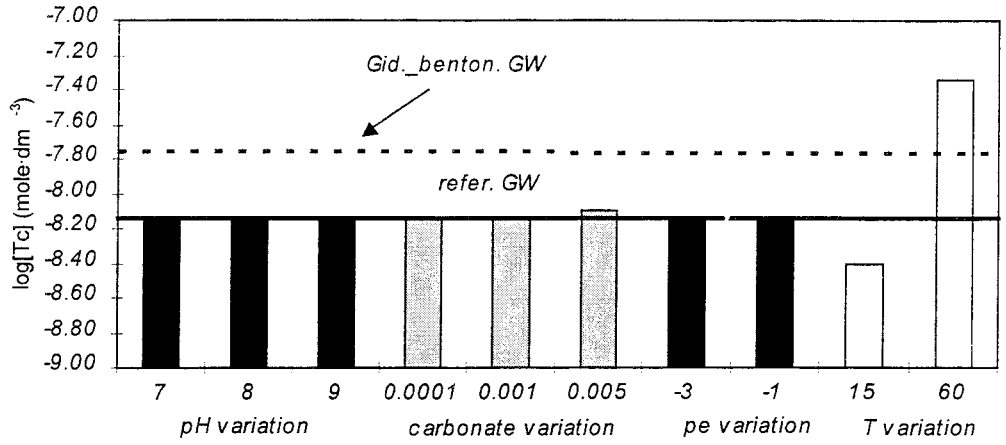

Figure 11-27. Solubility of $TcO_2 \cdot xH_2O(s)$ as a function of pH, total carbonate content, pe and temperature variations. Solid line is the solubility of this solid phase by considering Äspö groundwater composition.

11.7.17 Thorium

Only a slight variation on the solubility of $Th(OH)_4(s)$ has been observed as a function of total carbonate content in groundwater (Figure 11-28). This variation is mainly due to the predominance of Th-carbonate aqueous complexes in solution at high carbonate concentrations.

An slight change on the solubility has been also observed with temperature (Figure 11-28). In that case, solubility decreases when increasing the temperature of the system.

The solubility obtained in equilibrium with the reference groundwater is the same as the one calculated by using the Gideå/bentonite water. The high carbonate concentration of the Gideå/bentonite water could stabilise thorium-carbonate aqueous species in solution like it occurs when changing carbonate content in the sensitivity analysis (Figure 11-28), with the consequent increase in the solubility. However the high pH stabilise hydroxo aqueous complexes and consequently, the solubility does not increase with respect the one calculated by assuming pH and carbonate as no dependent parameters.

In Figure 11-29, we can see the effect of pH increase on the $Th(OH)_4(s)$ solubility, when carbonate content is given by equilibrium with calcite. The higher the pH, the lower the total carbonate content in the system. Consequently, at the lowest pH, the solubility increases, due to the predominance of carbonate aqueous complexes in solution.

As we can see in Figure 11-29 (dashed lines), the range of solubilities obtained from the sensitivity analysis is 0.5 logarithmic units approximately.

However, these variations can be considered negligible in the PA exercise, therefore, we may consider an individual solubility value independently of the variation in the influencing parameters taken in this sensitivity analysis.

This value may be the solubility obtained by using the reference system, solid line in Figure 11-28.

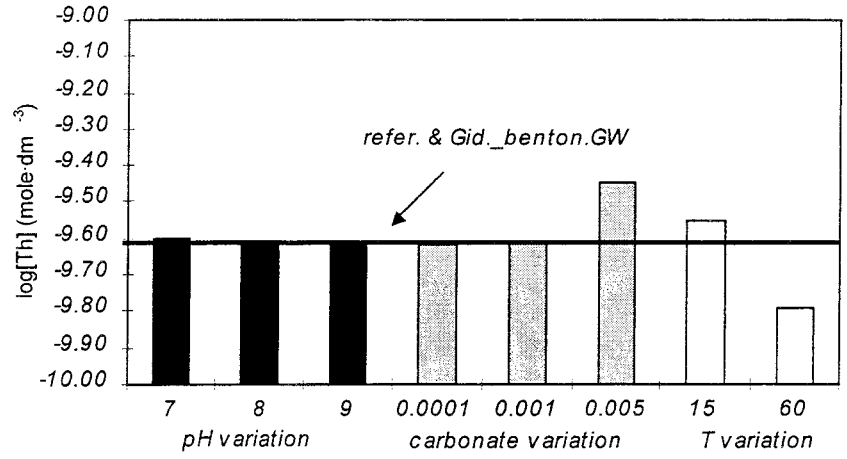

Figure 11-28. Solubility of $Th(OH)_4(s)$ as a function of pH, total carbonate content and temperature variations. Solid line shows the calculated solubilities of this solid phase equilibrated with the reference groundwater and the Gideå/bentonite water.

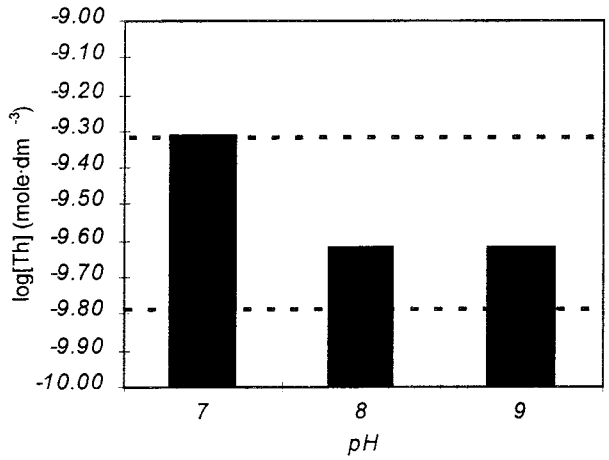

Figure 11-29. Solubility of $ThOH_4(s)$ as a function of pH, total carbonate content given by equilibrium with calcite. Dashed lines show the interval of solubilities calculated in the sensitivity analysis.

11.7.18 Uranium

According to the sensitivity analysis (Figure 11-30), they are not changes in the solubility of UO_2(fuel) as a function of pH, total carbonate concentration and pe of the system; only an slight increase has been observed, at pe=-1. The reason is that we have studied the influence of the different parameters under reducing conditions, therefore, $U(OH)_4(aq)$ is the predominant

aqueous species in solution, consequently, changes in pH and in carbonate concentration do not affect the stability of this complex. The slight increase in the solubility observed at the highest pe taken (pe=-1) is because at this value, a percentage of U(VI) in solution can be found, with a consequent increase in the solubility of the solid phase considered.

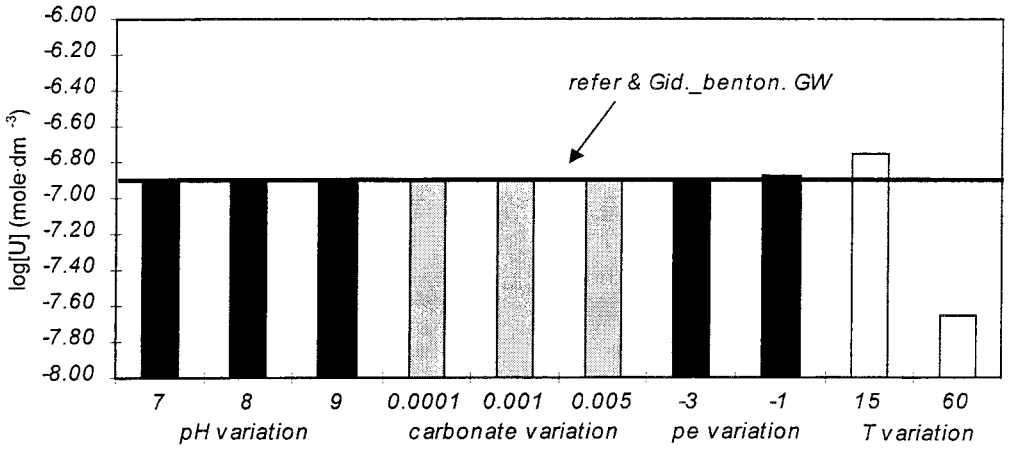

Figure 11-30. Solubility of UO_2(fuel) as a function of pH, total carbonate content, pe and temperature variations. Solid line shows the calculated solubilities of this solid phase equilibrated with the reference groundwater and the Gideå/bentonite water.

On the other hand, the solubility of uranium decreases when increasing the temperature of the system.

From the sensitivity analysis, we have obtained a solubility change of approximately 1 order of magnitude, this interval is given in Table 11-7. However, if we neglect temperature changes, a mean value for uranium solubility may be considered in a PA exercise. This solubility may correspond to the solubility calculated in the reference system (solid line in Figure 11-30).

11.7.19 Zirconium

As it is shown in Figure 11-31, the solubility of ZrO_2(am) is not affected by any influencing parameter considered in this exercise. This unvariation includes calculations performed by using Gideå/bentonite water. Therefore, a solubility value may be considered in the PA exercise (solid line in the figure).

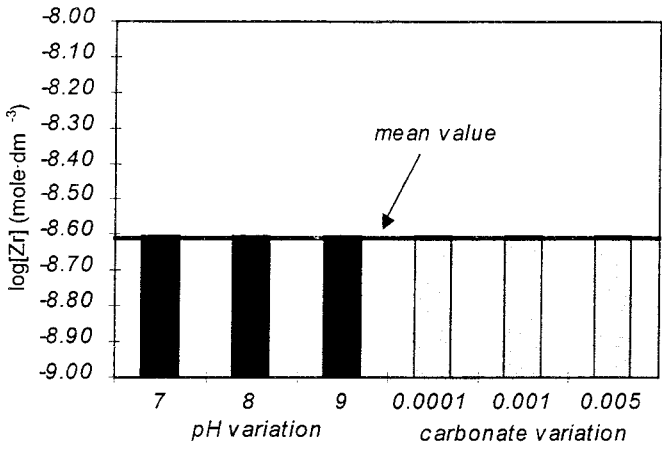

Figure 11-31. Solubility of ZrO_2(am) as a function of pH and total carbonate content changes. Solid line shows the mean value of the solubility.

11.8 CHARACTERISATION OF UNCERTAINTIES

The uncertainties associated with the data can be classified as:

11.8.1 Uncertainties associated with natural variations in site groundwater chemistry

This point has been previously discussed with the sensitivity analysis of the main groundwater parameters performed in the section before.

11.8.2 Conceptual uncertainties of the model used to perform the calculations

EQ3NR is a speciation solubility code for modelling the thermodynamic state of an aqueous solution. It involves an static calculation based on water chemistry and analysis. This kind of models are better used when they are employed to test the degree of disequilibrium of heterogeneous reactions than when they are forced to assume that such reactions are in equilibrium.

This code package has been also verified and validated in some exercises through inter-code comparison studies by different groups, i.e., Chemval Project.

Calculations have been performed by using the b-dot approach (Helgeson, 1969) for the ionic strength correction. This approach is used by default by the EQ3NR code. However, it has been considered sufficiently accurate taking into account the low ionic strength of the groundwaters considered.

A limitation of the model found during calculations has been that a solid phase only can be equilibrated with one component, i.e., we can not equilibrate calcite with calcium and carbonate at the same time, in the same input. This fact is an important constraint to simulate heterogeneous equilibrium in natural systems. To solve this limitation, we can precipitate

calcite until equilibrium with the EQ6 code package, otherwise in such case, pH could not be maintained fix during the calculation.

11.8.3 Uncertainties associated to the thermodynamic data needed to perform the calculations

The uncertainties associated to the thermodynamic data are primarily related to the availability of this information. This work has been previously done (Section 10) with the selection of both the aqueous complexes and the limiting solid phases that were relevant to the conditions of interest.

In this sense, the selection of the solid phases given in Table 11-2 to perform the sensitivity analysis has been based on the results previously obtained.

Nevertheless, a lack of information has been found related to the dependency on temperature of the thermodynamic data. In this sense, temperature dependence has been only available for ten radionuclides, as it has been presented before.

The temperature dependence of $Nb_2O_5(ac)$ solubility constant selected in the previous work was available in the selected database. However, this influence has not been considered in the present study since the temperature dependence on the solubility constant of this solid phase gave a variation of 25 logarithmic units in the solubility constant. Taking into account that the solubility constant is an estimated value (Baes and Mesmer, 1976), we preferred to neglect temperature dependence on these calculations.

Another important source of uncertainty in the solubilities is still associated to the accuracy and consistency of the thermodynamic data available. Evaluating the accuracy of thermodynamic data is a complex task, as evidenced by the NEA/OECD effort in compiling a selected set of consistent thermodynamic data for inorganic aqueous species and solid phases of uranium (Grenthe et al., 1992) and americium (Silva et al., 1995).

Because such evaluations are unavailable for many radionuclides, we could take for the purpose of this work an uncertainty of ± 0.5 logarithmic units in solubility calculations associated to the inaccuracy of thermodynamic data.

12 CONCLUSIONS AND RECOMMENDATIONS

In this section we will attempt to draw some conclusions and recommendations concerning both methodological aspects of the calculations as well as some of the implications from the calculated solubilities.

12.1 METHODOLOGICAL CONCLUSIONS

Concerning the use of the conditional constants approach, the proposed methodology does not substitute the use of computer aided equilibrium calculations. However, the conditional constant calculations give a feeling for the main chemical variables of the system, and hopefully help to minimise the risk of running the codes beyond the helm of reality. These calculations provide an initial insight on the sensitivity of the various radionuclides to the variations in groundwater compositions and the associated analytical uncertainties.

The use of information related to trace element occurrence in Natural Systems, as well as radionuclide concentrations from spent fuel dissolution experiments has proven to be very useful in order to bracket realistic solubility limits for the concerned radionuclides. This approach is highly recommended in any assessment involving trace element solubility limits.

The application of the co-precipitation/co-dissolution approaches for sub-trace elements like Ra, Am and Cm has given more realistic estimates of their solubilities, as compared to their occurrences in Natural Systems and spent fuel dissolution experiments.

The evaluation of the uncertainties associated to the analytical errors in groundwater determinations should be used to encourage better accuracy in the analytical work, as well as to set the limitations arising the establishment of radionuclide solubility limits. As expected, the determination of key master variables (Eh and pH) as well as carbonate concentration, appear to be critical.

12.2 THERMODYNAMIC DATA BASE CONCLUSIONS

The use of the EQ 3 NTB data base as main source of thermodynamic data has been helpful. The data base has proven to be up to date and includes many of the latest compilations done within the NEA-TDB project as well

as the data base work done within the SKB programme. The main amendments and modifications done have been:

- for Th(IV) the stability of the $Th(OH)_4(am)$ phase has been corrected to be compatible with the observations from Natural Systems. The recommended datum from Bases and Mesmer (1976) has been selected.
- for Pu(III), the stability of the $PuCO_3^+$ complex has been corrected, to be compatible with the stability trends observed in other Ac(III) systems.
- for Np(IV) the non-existent $Np(OH)_5^-$ complex has been removed from the data base, to be consistent with the ample evidence from Ac(IV)-hydrolysis studies.

12.3 COMPARISON WITH PREVIOUS EXERCISES

In the case of Ni, the solubilities calculated for Äspö groundwater are in the same range as the ones calculated for SKB91 (Bruno and Sellin, 1992). Berner (1994), gives a high solubility to Ni(II) for the Kristallin-I assessment. The Ni(II) levels calculated are neither consistent with the observed concentrations in groundwaters, nor with the reported association to iron-sulphides in these environments. Therefore, work has to be directed to provide the necessary data and laboratory evidence to pin down the geochemical behaviour of Ni in granitic groundwaters. The Äspö hard-rock laboratory would constitute and excellent site for such an effort.

The calculated Se solubilities in Äspö groundwater are in the 10^{-10} mole·dm^{-3} range, if the formation of Fe-selenides is assumed. These are of the same order of magnitude as the ones proposed in SKB91 for reducing groundwaters. In Kristallin-I the realistic solubilities are assumed to be in the 10^{-8} mole·dm^{-3} range, while conservative values are two orders of magnitude higher. This is another trace element in which we could improve much of our geochemical knowledge by using the Äspö laboratory as test site, particularly at redox interfaces.

For Sr, the calculated solubilities in Äspö groundwaters show an encouraging agreement with the measured Sr concentrations at the site. Sr solubilities have not been previously calculated in the SKB91 or Kristallin-I exercises.

The calculated Zr solubilities are in the range 10^{-9}-10^{-12} mole·dm^{-3} depending on the crystallinity of the $ZrO_2(s)$ phase assumed. Calculated solubilities in SKB 91 (10^{-12} mole·dm^{-3}) fell within this range, while Berner (1994) reported higher solubilities: 10^{-9} mole·dm^{-3} in the realistic case, while a conservative value of $5 \cdot 10^{-7}$ mole·dm^{-3} was given. These large solubilities are hardly expected from Zr(IV) which has a tendency to build very refractory phases.

For Nb(V) the calculated solubilities in the Äspö groundwaters are higher than the ones previously calculated for the SKB91 exercise The values reported for the Kristallin-I exercise are one order of magnitude higher and fall in the 10^{-3} mole·dm^{-3} range. This is obviously due to the effect of increased alkalinity on the calculated solubility. The calculated solubilities are undoubtedly conservative and most probably unrealistic. Nb(V) is another element where we could improved our knowledge by appropriate field experimentation at Äspö.

Tc solubilities are in the same range as the ones calculated for SKB91, under reducing conditions. The reported Tc solubilities for Kristallin-I are one order of magnitude higher for the realistic case, in spite of the fact that they all have been calculated by using the same basic data from Eriksen et al. (1993).

Pd solubilities are three orders of magnitude lower than the ones reported in the SKB 91 exercise. This is because a more crystalline Pd-oxide phase has been used. They fall within the realistic solubility limits proposed by Berner (1994) for the Kristallin-I case, while the 10^{-6} mole·dm^{-3} limit was considered by this author to be conservative. Much could be gained for this element by field experimentation at the Äspö site.

Silver was neither contemplated in the SKB91 exercise nor in the Kristallin-I assessment.

Tin(IV) solubilities are one order of magnitude lower than the ones previously calculated for SKB 91. The proposed Sn(IV) solubilities for Kristallin-I are four orders of magnitude larger, which probably reflect the difference in crystallinity of the selected solid phase. Tin is another candidate for a more detailed study if its solubility behaviour under field conditions.

Samarium and Holmium solubilities are calculated to be lower in the Äspö groundwaters than in previous calculations fro SKB91 or Kristallin-I. This is a case where our improved knowledge on REE geochemistry has narrowed down the uncertainties from previous calculations.

The application of the co-precipitation approach to Ra(II) solubilities has a clear effect on getting these values closer to realistic estimates which are in accordance to observations from Natural Systems. The same approach had been used by Berner (1994) in his solubility calculations for Kristallin-I, obtaining similar values.

The calculated Th(IV) solubilities are identical to the ones previously calculated for SKB91, and in the same range as the realistic estimates for Kristallin-I (Berner, 1994).

The calculated Pa(V) solubilities are the same as the ones already proposed in SKB91. However, Berner (1994) proposed a lower solubility limit based on the assumption of congruent dissolution (co-dissolution) with components of the glass matrix.

Uranium solubilities are in the same range as the ones predicted for SKB91, under reducing conditions. For the Kristallin-I exercise a realistic U solubility limit was estimated in the same range (Berner, 1994), while a conservative value of 10^{-5} mole·dm^{-3} was proposed. The proposed conservative values stems from measurements of the solubility of amorphous UO_2(s) under anoxic conditions (Bruno et al, 1986). We have recently demonstrated that in neutral to alkaline pH values anoxic conditions do not prevent the formation of soluble U(VI) species, and therefore these measurements are not representative of the behaviour of U under reducing conditions.

Np solubilities in Äspö groundwaters are in the 10^{-9} mole dm^{-3} range, in agreement with the previous calculations for reducing waters in SKB91. This is a similar value to the one proposed by Berner (1994) as realistic solubility limit for Kristallin-I.

Pu solubilities in Äspö groundwaters are two orders of magnitude lower than the ones previously proposed for reducing conditions in the SKB91 exercise. This is the result of our improved knowledge on the evolution in crystallinity and solubility of the amorphous Pu(IV) hydroxide. The value proposed by Berner (1994) is two orders of magnitude larger, following our previous estimates.

Individual Am(III) solubilities in Äspö groundwaters are in the 10^{-7} mole·dm^{-3} range, one order of magnitude larger than the ones previously proposed for SKB91. This is a consequence of the difference in carbonate concentration between the two water compositions. Berner (1994) gave a much higher solubility limit, as it is already discussed by the author this was the result of shortcomings of the Am(III) database available at that point. The Am(III) TDB compilation and selection performed later on by the NEA has settled this issue in much firmer grounds (Silva et al., 1995).

The calculation of Am(III) solubility limits by assuming its congruent dissolution with the fuel matrix results in a decreased Am(III) concentration and a better agreement with the observations from spent fuel dissolution tests.

Cm(III) individual solubilities in Äspö groundwaters are in agreement with the realistic values calculated for Kristallin-I (Berner, 1994). The assumption of congruent dissolution with U from the fuel decreases the predicted concentrations and is in better agreement with the measured Cm(III) concentrations in long-term spent fuel dissolution tests.

12.4 UNCERTAINTIES CONCLUSIONS

The variability of the groundwater chemistry; pH and carbonate concentration, and redox conditions and temperature of the system have been considered the main factors affecting the solubilities. In this sense, a

sensitivity analysis has been performed in order to study solubility changes as a function of these parameters.

In summary, the following analysis has been carried out for each radionuclide studied:

- Silver: We can consider a solubility value independently of the variability of the influencing parameters.
- Americium: The solubility of this radionuclide changes as a function of both pH and carbonate content approximately 1.5 orders of magnitude.
- Curium: The solubility of this radionuclide changes as a function of both pH and carbonate content approximately 5 orders of magnitude.
- Holmium: The solubility of this element changes as a function of both pH and carbonate content approximately 1.5 orders of magnitude.
- Niobium: Its solubility changes approximately 3 orders of magnitude in the pH range studied. $Nb_2O_5(ac)$ is not affected by changes in carbonate content in groundwater.
- Nickel: The parameter which affects in a major extent its solubility is pH. The solubility changes 4 orders of magnitude.
- Neptunium: The solubility of this radionuclide changes around 1 order of magnitude within the ranges of the influencing parameters taken. Carbonate content is the parameter which affects in a major extent the solubility of $Np(OH)_4(s)$ in the ranges studied.
- Protactinium: Its solubility is not affected by any influencing parameter considered in this exercise.
- Palladium: This solubility is only slightly affected by pH and the temperature of the system. Therefore, a mean solubility value can be considered for this radionuclide.
- Plutonium: pH is the variable which affects in a major extent (around 4 orders of magnitude) the solubility of this radionuclide, by considering the ranges of the different parameters taken in this exercise.
- Radium: It is slightly affected by pH and carbonate content in groundwaters, a larger effect has been observed as a function of the temperature of the system. Therefore, by neglecting temperature variations, a mean value for its solubility could be considered.
- Selenium: pH is the parameter which affects in a major extent its solubility, the interval of pe considered does not affect its solubility. Solubility varies 2 orders of magnitude approximately according to the intervals taken in the sensitivity analysis.
- Samarium: The solubility of this element changes as a function of both pH and carbonate content approximately 2 orders of magnitude.
- Tin: SnO_2 is slightly affected by pH, However, its solubility changes dramatically when increasing the temperature of the system, another solid phase may limit the solubility of this radionuclide at this temperature.
- Strontium: Solubility changes due to the influencing parameters considered, pH, carbonate content and T, are around 2 orders of magnitude.
- Technetium: A solubility variability of 1 order of magnitude has been obtained in the sensitivity analysis mainly due to temperature changes in the system.

- Thorium: Only an slight influence has been observed as a function of the different parameters taken in this analysis, Therefore, a mean solubility value can be considered.
- Uranium: A solubility variability of 1 order of magnitude has been obtained in the sensitivity analysis mainly due to temperature changes in the system. The pe of the system does not affect its solubility since we have only considered reducing conditions.
- Zirconium: This radionuclide is not affected by any influencing parameter considered in this exercise.

13 COMPARISON OF CALCULATED SOLUBILITIES OBTAINED BY USING THE HALTAFALL OR THE EQ3NR CODES

Some minor discrepancies have been observed in the calculated solubilities by using the HALTAFALL or the EQ3NR codes. These differences are mainly due to the effect of the ionic strength correction.

As we have discussed, the aqueous and solid speciation as well as the sensitivity analysis have been performed without taking into account the effect of the ionic strength of the system studied by using the HALTAFALL code (Puigdomènech, 1983). On the other hand, the solubility calculation exercise performed by taking different groundwater compositions has been done by using the EQ3NR (Wolery, 1992) code and by considering the effect of the ionic strength in the system under study.

However, in some cases we have detected some large differences (Table Ap.I) which have been atributed to the different systems considered in each calculation.

The HALTAFALL code is very limited since it only can accept a maximum number of nine components in the system while the EQ3NR code is unlimited.

According to the number of components considered the speciation slightly change due to the different reactions taken in each system. In some cases, the different speciation is reflected with discrepancies in the calculated solubilities of the trace metals studied, by using different codes, i.e. Sr, Nb, Sm and Ho.

Therefore, as a final solubilities, we have taken the values obtained by the EQ3NR code which give us a more complete and exhaustive description of the system under study.

Table 14-1. Comparison of calculated solubilities obtained by using the HALTAFALL and the EQ3NR codes.

Element	Solid Phase	HALTAFALL ($mol \cdot dm^{-3}$)	EQ3NR ($mol \cdot dm^{-3}$)	% difference
Ni	NiO	$2.17 \cdot 10^{-4}$	$3.68 \cdot 10^{-4}$	41
Se	FeSe	$1.03 \cdot 10^{-10}$	$1.97 \cdot 10^{-10}$	48
Sr	strontianite	$4.18 \cdot 10^{-4}$	$1.71 \cdot 10^{-3}$	75
	celestite	$5.27 \cdot 10^{-4}$	$1.13 \cdot 10^{-3}$	53
Zr	ZrO_2(am)	$2.51 \cdot 10^{-9}$	$2.49 \cdot 10^{-9}$	0.8
Nb	Nb_2O_5(ac)	$8.14 \cdot 10^{-5}$	$1.96 \cdot 10^{-4}$	58
Tc	$TcO_2.xH_2O$	$7.24 \cdot 10^{-9}$	$7.14 \cdot 10^{-9}$	1.3
Pd	PdO	$4.17 \cdot 10^{-9}$	$4.15 \cdot 10^{-9}$	0.5
Ag	Ag(s)	$3.37 \cdot 10^{-15}$	$5.28 \cdot 10^{-15}$	36
Sn	SnO_2	$8.16 \cdot 10^{-10}$	$9.48 \cdot 10^{-10}$	14
Sm	$Sm_2(CO_3)_3$	$1.80 \cdot 10^{-7}$	$7.00 \cdot 10^{-7}$	74
Ho	$Ho_2(CO_3)_3$	$7.18 \cdot 10^{-7}$	$2.48 \cdot 10^{-6}$	71
Ra	$RaSO_4$	$1.40 \cdot 10^{-7}$	$2.95 \cdot 10^{-7}$	52
	Ra-SO_4-cop	$1.40 \cdot 10^{-10}$	$2.95 \cdot 10^{-10}$	52
Th	$Th(OH)_4$(am)	$2.40 \cdot 10^{-10}$	$2.40 \cdot 10^{-10}$	
Pa	Pa_2O_5	$1.58 \cdot 10^{-7}$	$3.15 \cdot 10^{-7}$	50
U	UO_2(fuel)	$1.86 \cdot 10^{-7}$	$1.27 \cdot 10^{-7}$	32
Np	$Np(OH)_4$	$6.92 \cdot 10^{-9}$	$6.99 \cdot 10^{-9}$	1.0
Pu	$Pu(OH)_4$	$1.51 \cdot 10^{-10}$	$1.86 \cdot 10^{-10}$	19
Am	$AmOHCO_3$	$1.03 \cdot 10^{-7}$	$2.37 \cdot 10^{-7}$	56
Cm	$CmOHCO_3$	$1.02 \cdot 10^{-8}$	$5.52 \cdot 10^{-8}$	81

14 REFERENCES

Ahlbom K. and Smellie J.A.T, 1989. Characterization of fracture zone 2, Finnsjön study site. SKB 89-19.

Alaux-Negrel G, Beaucaire C, Michard G, Toulhoat P, Ouzounian G, 1993. Trace metal behaviour in natural granitic waters. Journal of Contaminant Hydrology 13, 309-325.

Allard B, 1982. Solubilities of actinides in neutral or basic solutions. Actinides in perspective. N.M. Edelstein, Pergamon Press, 553-580.

Anton M.P, Gasco C, Sanchezcabeza J.A, Pujol L, 1994. Geochemical association of plutonium in marine sediments from Palomares (Spain). Radiochimica Acta 66:7, 443-446.

Baes C.F. and Mesmer R.E, 1976. The Hydrolysis of Cations. New York. John Wiley and Sons.

Baeyens B. and McKinley I.G, 1989. A PHREEQE database for Pd, Ni and Se. Nagra technical report 88-28.

Benson L.V. and Teague L.S, 1980. A tabulation of thermodynamic data for chemical reactions involving 58 elements common to radioactive waste package systems. LbL-11448.

Berner U, 1994. Estimates of solubility limits for safety relevant radionuclides. NTB 94-08.

Blanc P-L, 1995. Oklo, Natural Analogue. Final report: Volume 1: Acqueriments of the Natural Analogy Programme. Institut de Protection et de Sureté Nucléaire. Oklo-Final report 1 (SERGD-95/33). Fontenay-aux-Roses.

Bockris J.O.M, Ed., 1977. Environmental Chemistry. New York, Plenum Press.

Brookins D.G, 1988. Eh-pH Diagrams for geochemists. New York. Springer-Verlag Pubs.

Brookins D.G, 1989. Aqueous Geochemistry of Rare Earth Elements. in Geochemistry and Mineralogy of Rare Earth Elements (B.R. Lipin and G.A. McKay, Eds.). Blacksburg. Mineralogical Society of America. Reviews in Mineralogy. Vol. 21.

Brown P.L, Haworth A, Sharland S.M, Tweed C.J, 1991. HARPHRQ: A geochemical speciation program based on PHREEQE. Theoretical studies

Department, Radwaste disposal division B424.2. Hornwall Laboratory, Didcot Oxon OX110RA.

Bruno J, Arcos D, Duro L, 1997. Processes and features affecting the near field hydrochemistry. I. Groundwater-bentonite interaction. QuantiSci Internal Report.

Bruno J, Ayora C, Casas I, Delgado J, Duro L, Gimeno M.J, Goldberg J.E, Linklater C.M, 1996. El Berrocal Project. Blind Predictive Modelling Exercise. Geochemistry Task Group Report TGR-6.

Bruno J, Casas I, Lagerman B, Muñoz M, 1987. The determination of the solubility of amorphous $UO_2(s)$ and the mononuclear hydrolysis constants of uranium (IV) at 25°C. Mater. Res. Soc. Symp. Proceedings MRS Vol. 84, 153-160.

Bruno J, Cross J.E, Eikenberg J, McKinley I.G, Read D, Sandino A, Sellin P, 1992. Testing models of trace element geochemistry at Poços de Caldas. Journal of Geochemical Exploration 45, 451-470.

Bruno J, de Pablo J, Duro L, Figuerola E, 1995. Experimental study and modeling of the U(VI)-$Fe(OH)_3$ surface precipitation-coprecipitation equilibria. Geochimica et Cosmochimica Acta, Vol. 59, No 20, 871-878.

Bruno J, Ferri D, Grenthe I, Salvatore F, 1986. Studies on metal carbonate equilibria. 13. On the solubility of uranium(IV) dioxide, $UO_2(s)$. Acta Chemica Scand. 40, 428-434.

Bruno J, Forsyth R.S, Werme L.O, 1985. Spent UO_2-fuel dissolution. Tentative modelling of experimental apparent solubilities. Mater. Res. Soc. Symp. Proceedings MRS Vol. 44, 413-420.

Bruno J., Casas I, 1994. Spent fuel dissolution modelling. in Final Report of SKB/AECL Cigar Lake Analog Study (J.J. Cramer and J.A.T. Smellie, Eds.). SKB-(AECL). Technical Report TR 94-04 (10851).

Bruno J., Duro L, 1995. El Berrocal Project. BPM Exercise. QuantiSci Internal Report.

Bruno J., Duro L, 1996. Extending the RDC model to the minor components of the spent fuel matrix. Modelling of apparent Pu solubilities from Studsvik leaching experiments. QuantiSci Internal Report.

Bruno J., Puigdomènech I, 1989 Validation of the SKBU1 uranium thermodynamic data base for its use in geochemical calculations with EQ3/6. Mater. Res. Soc. Symp. Proceedings MRS Vol. 127, 887-896.

Bruno J., Sellin P, 1992. Radionuclide solubilities to be used in SKB 91. SKB 92-13.

Byrd J.T, Andreae M.O, 1986. Geochemistry of tin in rivers and estuaries. Geochimica et Cosmochimica Acta 50: 835-845.

Caballero E, Reyes E, Huertas F, Yáñez J, Linares J, 1986. Elementos traza en las bentonitas de Almeria. Boletin Sociedad Española de Mineralogía 9, 63-70.

Calvert S.E. and Piper D.Z, 1984. Geochemistry of ferromanganese nodules from DOMES Site A, northern equatorial Pacific; multiple diagenetic metal sources in the deep sea. Geochimica et Cosmochimica Acta 48, 1913-1928.

Cera E, Savage D, Casas I, Bruno J, 1995. Solubility limits for SKB 95. Solubility limiting solid phases and calculated solubilities. Experiences from natural system studies and the Tracex Data Base. INTERA Internal Report.

Chemval Project, 1991. Application and validation of predictive computer programs describing the chemistry of radionuclides in the geosphere. EUR 13315 EN.

Choppin G.R, Stout B.E, 1989. Actinide behaviour in natural waters. The Science of the Total Environment 83, 203-216.

Copenhaver S.A, Krishnaswami S.L, Turekian K.K, Epler N, Cochran J.K, 1993. Retardation of ^{238}U and ^{232}Th decay chain radionuclides in Long Island and Connecticut aquifers. Geochimica et Cosmochimica Acta 57, 597-603.

Cramer J, Vilks P, Miller H, Bachinski D, 1994. Hydrogeochemistry: Water sampling and analysis. in Final Report of SKB/AECL Cigar Lake Analog Study (J.J. Cramer and J.A.T. Smellie, Eds.). SKB-(AECL). Technical Report TR 94-04 (10851).

Cross J. E, Moreton A.D, Tweed C.J, 1992. Thermodynamic modelling of radioactive waste disposal, assessment of near-field solubility. UK Nirex Ltd. report.

Cross J. E., Ewart F. T, 1989. HATCHES- A Thermodynamic Database Management System. Proceedings of the Conference on Chemistry and Migration Behaviour of Actinides and Fission Products in the Geosphere.

Cutter G.A, 1989. Freshwater systems. in Occurrence and Distribution of Selenium (M. Ihnat, Ed.). CRC Press, Boca Raton, 99, 243-262.

Decarreau B.L, 1985. Partitioning of divalent transition elements between octahedral sheets of trioctahedral smectites and water. Geochimica et Cosmochimica Acta 49, 1537-1544

Dickson B.L, 1985. Radium isotopes in saline seepages, southwestern Yilgarn, Western Australia. Geochimica et Cosmochimica Acta 49, 349-360.

Doerner H.A, Hoskins W.M, 1925. Co-precipitation of radium and barium sulphates. Journal of the American Chemical Society 47, 662-675.

Doyle G.A, Lyons W.B, Miller G.C, Donaldson S.G, 1995. Oxyanion Concentrations in Eastern Sierra Nevada Rivers. 1. Selenium. Applied Geochemistry 10:5, 553-564.

Edmunds W.M, Cook J.M, Kinniburg D.G, Miles D.G, Trafford J.M, 1989. Trace-element occurrence in British groundwaters. British Geological Survey. Research Report SD/89/3. Nottingham.

Edmunds W.M, Cook R.L.F, Miles D.L, Cook J.M, 1987. The origin of saline groundwaters in the Carnmenellis granite (U.K.): further evidence from minor and trace elements. *in* Saline Water and Gases in Crystalline Rocks (P. Fritz and S.K. Frape, Eds.). Geological Association of Canada Special Paper 33, pp 127-143.

Elderfield H, Upstill-Goddard R, Sholkovitz E.R, 1990. The rare earth elements in rivers, estuaries, and coastal seas and their significance to the composition of ocean waters. Geochimica et Cosmochimica Acta 54, 971-991.

Elderfield H., Greaves M.J, 1989. The rare earth elements in seawater. Nature 296:5854, 214-219.

Elkin E.M, 1982. Selenium and selenium compounds. In Encyclopaedia of Chemical Technology Volume 20, John Wiley & Sons, New York.

Eriksen T.E, Ndalamba P, Cui D, Bruno J, Caceci M, Spahiu K, 1993. Solubility of the redox-sensitive radionuclides ^{99}Tc and ^{237}Np under reducing conditions in neutral to alkaline solutions. Effect of carbonate. SKB 93-18.

Eriksen T.E, Ndalamba P, Cui D, Bruno J, Caceci M, Spahiu K, 1993. Solubility of the redox-sensitive radionuclides ^{99}Tc and ^{237}Np under reducing conditions in neutral to alkaline solutions. Effect of carbonate. SKB Technical Report TR 93-18.

Fabryka-Martin J, Curtis D.B, Dixon P, Rokop D, Roensch F, Aguilar R, Attrep M, 1994. Nuclear reaction product geochemistry: Natural nuclear products in the Cigar Lake deposit. in Final Report of SKB/AECL Cigar Lake Analog Study (J.J. Cramer and J.A.T. Smellie, Eds.). SKB-(AECL). Technical Report TR 94-04 (10851).

Finch R.J, Ewing R.C, 1991. Uraninite alteration in an oxidising environment and its relevance to the disposal of spent nuclear fuel. SKB Technical Report TR 91-15.

Forsyth R, Eklund U-B, 1995. Spent nuclear fuel corrosion: The application of ICP-MS to direct actinide analysis. SKB Technical Report 95-04 (1995) pp 18.

Forsyth R.S, Werme L.O, 1992. Spent fuel corrosion and dissolution. Journal of Nuclear Materials 190, 3-19.

Forsyth R.S, Werme L.O, Bruno J, 1986. The corrosion of spent UO_2 fuel in synthetic groundwater. Journal of Nuclear Materials 138, 1-15.

Fukai R, Yokoyama Y, 1982. Natural Radionuclides in the Environment. *in* The Hanbook of Environmental Chemistry. The Natural Environment and the Biogeo-chemical Cycles (O. Hutzinger, Ed.). Springer-Verlag Berlin Heidelberg. Vol. 1.

Gauthier-Lafaye F, 1995. Oklo, Analogues naturels. Rapport final: Volume 2: Les Réacteurs de Fission et les Systèmes Géochimiques. 2ème partie: Géologie des réacteurs, études des épontes et des transferts anciens. Institut de Protection et de Sureté Nucléaire. Oklo-Rapport final 2-2. Strasbourg.

Golightly J.P, 1981. Nickeliferous laterite deposits. Economic Geology 75th Anniversary Volume. 710-735.

Gómez P, Turrero M.J, Martínez B, Melón A, Gimeno M.J, Peña J, Mingarro M, Rodríguez V, Gordienko F, Hernández A, Crespo M.T, Ivanovich M, Reyes E, Caballero E, Plata A, Fernández J.M, 1995. Hydrogeochemical study of El Berrocal site. CIEMAT. Task Group Report 4 EB-CIEMAT (95) 35. Madrid.

Gosselin D.C, Smith M.R, Lepel E.A, Laul J.C, 1992. Rare earth elements in chloride-rich groundwater, Palo Duro Basin, Texas, USA. Geochimica et Cosmochimica Acta 56, 1495-1505.

Grambow B, Loida A, Dressler P, Geckeis H, Gago J, Casas I, de Pablo J, Giménez J, Torrero M.E, 1996. Long Term Safety of Radioactive Waste Disposal: Chemical Reaction of Fabricated and High Burnup Spent UO_2 Fuel with Saline Brines. Final Report FZK 5702 pp 174.

Grauch R.I, 1989. Rare Earth Elements in Metamorphic Rocks. in Geochemistry and Mineralogy of Rare Earth Elements (B.R. Lipin and G.A. McKay, Eds.). Blacksburg. Mineralogical Society of America. Reviews in Mineralogy. Vol. 21.

Gray W.J, 1987. Comparison of uranium release from spent fuel and unirradiated UO_2 in salt brine. Scientific Basis for Nuclear Waste Management X, 84, 141.

Gray W.J, 1988. Salt Repository Project. Effect of surface oxidation α-radiolysis and salt brine composition on the spent fuel and UO_2 leaching performance. PNL/SRP-6689UC-70.

Grenthe I, Fuger J, Konings R.J.M, Lemire R.J, Muller A.B, Nguyen-Trung C, Wanner H, 1992. Chemical Thermodynamics Vol.1. Chemical Thermodynamics of Uranium. NEA. (Wanner and Forest ed.) Elsevier.

Guenther R.J, Blahnik d.E, Campbell T.K, 1989. Detailed characterization of LWR fuel rods for the U.S. civilian radioactive waste

management program. Mater. Res. Soc. Symp. Proceedings MRS Vol. 127, 325-336.

Helgeson H.C, 1969. Thermodynamics of hydrothermal systems at elevated temperatures and pressures. American Journal of Science Vol. 267, 729-804.

Howard J.H, 1977. Geochemistry of selenium: formation of ferroselite and selenium behaviour in the vicinity of oxidising sulphide and uranium deposits. Geochimica et Cosmochimica Acta 41, 1665-1678.

Humphris S.E. and Thompson G, 1978. Trace element mobility during hydrothermal alteration of oceanic basalts. Geochimica et Cosmochimica Acta 42, 127-136.

Ikeda N, 1955. Determination of minute quantities of tin in hot spring waters. Nippon Kagaku Zassi 76, 1011.

Kraemer T.F, Kharaka Y.K, 1986. Uranium geochemistry in geopressures-geothermal aquifers of the U.S. Gulf Coast. Geochimica et Cosmochimica Acta 50, 1233-1238.

Kraemer T.F, Reid D.F, 1984. The occurrence and behaviour of radium in saline formation water of the U.S. Gulf Coast region. Isotope Geoscience 2, 153-174.

Krauskopf K.B, 1967. Introduction to Geochemistry. McGraw-Hill, New York.

Krishnaswami S, Graustein W.C, Turekian K.K, 1982. Radium, thorium and radioactive lead isotopes in groundwaters: applications to the in situ determination of absorption-desorption rate constants and retardation factors. Water Resources Research 18, 1633-1675.

Langmuir D, Herman J.S, 1980. The mobility of thorium in natural waters at low temperatures. Geochimica et Cosmochimica Acta 44, 1753-1766.

Langmuir D, Melchior D, 1985. The goechemistry of Ca, Sr, Ba and Ra sulfates in some deep brines from the Palo Duro Basin, Texas. Geochimica et Cosmochimica Acta 49, 2423-2432.

Langmuir D, Riese A.C, 1985. The thermodynamic properties of radium. Geochimica et Cosmochimica Acta 49, 673-680.

Laul J.C, Smith M.R, Hubbard N, 1985a. $^{234}U/^{230}Th$ ratio as an indicator of redox state, and U, Th and Ra behaviour in briney aquifers. Mater. Res. Soc. Symp. Proceedings MRS Vol. 44, 475-482.

Laul J.C, Smith M.R, Hubbard N, 1985b. Behaviour of natural uranium, thorium and radium isotopes in the Wolfcamp brine aquifers, Palo Duro Basin, Texas. Materials Research Society Proceedings 44, 475-482.

Lemire R.J, Garisto F, 1989. The solubility of U, Np, Pu, Th and Tc in a geological disposal vault of used nuclear fuel. AECL-10009.

Lemire R.J, Garisto F, 1989. The solubility of U, Np, Pu, Th and Tc in a geological disposal vault of used nuclear fuel. AECL-10009.

Lin S, Popp R.K, 1984. Solubility and complexing of Ni in the system $NiO-H_2O-HCl$. Geochimica et Cosmochimica Acta 48, 2713-2722.

Lloyd J.W, Heathcote J.A, 1985. Natural inorganic hydrochemestry in relation to groundwater. An Introduction. Oxford. Oxford University Press.

MacKenzie A.B, Scott R.D, Linsalata P, Miekeley N, Osmond J.K, Curtis D.B, 1991. Natural radionuclide and stable element studies of rock samples from the Osamu Utsumi mine and Morro do Ferro analogue study sizes, Poços de Caldas, Brazil. SKB. Poços de Caldas Report 7.

Mariano A.N, 1989. Economic Geology of Rare Earth Elements. in Geochemistry and Mineralogy of Rare Earth Elements (B.R. Lipin and G.A. McKay, Eds.). Blacksburg. Mineralogical Society of America. Reviews in Mineralogy. Vol. 21.

Mazor E, 1962. Radon and radium content of some Israeli water sources and a hypothesis on underground reservoirs of brines, oils and gases in the Rift valley. Geochimica et Cosmochimica Acta 26, 706-786.

McKelvey B.A, Orians K.J, 1993. Dissolved zirconium in the North Pacific Ocean. Geochimica et Cosmochimica Acta 57, 3801-3805.

McKibben M.A, Williams A.E, Hall G.E.M, 1990. Solubility and transport of platinum-group elements and Au in saline hydrothermal fluids: constraints from geothermal brine data. Economic Geology 85, 1926-1934.

McKinley I.G, Bath A.H, Berner U, Cave M, Neil C, 1988. Results of the Oman analogue study. Radiochimica Acta 44/45, 311-316.

McLennan S.M, 1989. Rare Earth Elements in Sedimentary Rocks: Influence of Provenance and Sedimentary Processes. *in* Geochemistry and Mineralogy of Rare Earth Elements (B.R. Lipin and G.A. McKay, Eds.). Blacksburg. Mineralogical Society of America. Reviews in Mineralogy. Vol. 21.

Michard A, 1989. Rare earth element systematics in hydrothermal fluids. Geochimica et Cosmochimica Acta 53, 745-750.

Michard A, Beaucaire C, Michard G, 1987. Uranium and rare-earth elements in CO2-rich waters from Vals-les-Bains (France). Geochimica et Cosmochimica Acta 51, 901-909.

Michel J, Moore W.S, 1980. ^{228}Ra and ^{226}Ra content of groundwater in Fall Line aquifers. Health Physics 38, 663-671.

Miekeley N, Coutinho de Jesus C, Porto da Silveira C.L, Linsalata P, Morse R, Osmond J.K, 1991. Natural series radionuclide and rare-earth element geochemistry of waters from the Osamu Utsumi mine and Morro do Ferro analogue study sizes, Poços de Caldas, Brazil. SKB. Poços de Caldas Report 8.

Miller W.M, Smith G.M, Towler P.A, Savage D, 1994. Natural elemental mass movement in the vicinity of the Äspö Hard Rock Laboratory. Intera Information Technologies IG3427-2. Melton.

Mills K.C, 1974. Thermodynamic data for inorganic sulphides, selenides and tellurides. London Butterworths.

Möller P, Dulski P, Szacki W, Malow G, Riedel E, 1988. Substitution of tin in cassiterite by tantalum, niobium, tungsten, iron and manganese. Geochimica et Cosmochimica Acta 52, 1497-1503.

Nordstrom D.K, Smellie J.A.T, Wolf M, 1991. Chemical and isotopic composition of groundwaters and their seasonal variability at the Osamu Utsumi and Morro do Ferro analogue study sizes, Poços de Caldas, Brazil. SKB. Poços de Caldas Report 6.

Östhols E, 1994. Some processes affecting the mobility of thorium in natural ground waters. TITRA-OOK-1038.

Oudin E. and Cocherie A, 1988. Fish debris record the hydrothermal activity in the Atlantis Ii deep sediments (Red Sea). Geochimica et Cosmochimica Acta 52, 177-184.

Paige C.R, Kornicker W.A, Hileman O.E, Snodgrass W.J, 1993. Study of the dynamic equilibrium in the $BaSO_4$ and $PbSO_4$/aqueous solution systems using $^{133}Ba^{2+}$ and $^{210}Pb^{2+}$ as radiotracers. Geochimica et Cosmochimica Acta 57, 4435-4444.

Pearson F.J. Jr, Berner U, 1991. Nagra Thermochemical Data Base I. Core Data. Technical Report 91-17.

Pearson F.J. Jr, Berner U, Hummel W, 1992. Nagra Thermochemical Data Base II. Supplemental Data 05/92. Technical Report 91-18.

Pentcheva E, 1965. The distribution of rare and dispersed elements in Bulgarian saline underground waters. Compt. Rend. Acad. Bulgare Sci. 18, 149.

Pérez del Villar L, De la Cruz B, Pardillo J, Cózar J.S, Pelayo M, Marín C, Rivas P, 1995. Lithogeochemical characterization and evolutive model of the El Berrocal site: Analogies with a HLRWR. CIEMAT. Topical Report 2. Madrid.

Puigdomènech I, 1983. Input, sed and predom computer programs drawing equilibrium diagrams TITRA-OOK-3010. RIT, Stockholm.

Puigdomènech I, Bruno J, 1988. Modelling uranium solubilities in aqueous solutions: Validation of a thermodynamic data base for the EQ3/6 geochemical codes. SKB 88-21.

Puigdomènech I, Bruno J, 1991. Plutonium solubilities. SKB Technical Report TR 91-04.

Puigdomènech I, Bruno J, 1995. A thermodynamic database for Tc to calculate equilibrium solubilities at temperatures up to 300°C. SKB Technical Report TR 95-09.

Rai D, Ryan J.L, 1982. Crystallinity and solubility of Pu(IV) oxide and hydrous oxide in aged aqueous suspensions. Radiochimica Acta.

Rai D, Swanson J.L, 1981. Properties of plutonium (IV) polymer of environmental importance. Nuclear Technology Vol. 54, 107-112.

Raymond L.A, 1995. Petrology - The Study of Igneous, Sedimentary, and Metamorphic Rocks. Wm. C. Brown Publishers.

Ringbom A, 1963. Complexation in Analytical Chemistry. John Wiley & Sons.

Rittenhouse G, Fulton R.B, Grabowski R.J, Bernard J.L, 1969. Minor elements in oilfield waters. Chemical Geology 4, 189.

Salvi S, Williams-Jones A.E, 1990. The role of hydrothermal processes in the granite-hosted Zr, Y, REE deposit at Strange Lake, Quebec/Labrador: evidence from fluid inclusions. Geochimica et Cosmochimica Acta 54, 2403-2418.

Santschi P.H, Bajo C, Mantovani M, Orciuolo D, Cranston R.E. Bruno J, 1988. Uranium in pore waters from North Atlantic (GME and Southern Nares Abyssal Plain) sediments. Nature Vol. 331, (6152) 155-157.

Sebesta F, Sedlacek J, John J, Sandrik R, 1981. Behaviour of radium and barium in a system including uranium mine waste waters and adjacent surface waters. Environmental Science and Technology 15, 71-75.

Seyfried W.E, Bischoff J.L, 1981. Experimental seawater-basalt interaction at 300 ° C and 500 bars: chemical exchange, secondary mineral formation and implications for the transport of heavy metals. Geochimica et Cosmochimica Acta 45, 135-147.

Seyfried W.E, Dibble W.E, 1980. Seawater-peridotite interaction at 300 ° C and 500 bars: implications for the origin of oceanic serpentinites. Geochimica et Cosmochimica Acta 44, 309-321.

Shanbhag P.M, Morse J.W, 1982. Americium Interaction with Calcite and Aragonite Surfaces in Seawater. Geochimica et Cosmochimica Acta 46, 241-246.

Short S.A, Lowson R.T, 1988. 234U/238U and 230Th/234U activity ratios in the colloidal phases of aquifers in lateritic weathered zones. Geochimica et Cosmochimica Acta 52, 2555-2563.

Sillén L.G, Martell A.E, 1964. Stability constants of metal-ion complexes. Special publication nr 17. The Chemical Society, Burlington House, W1V OBN.

Sillén L.G, Martell A.E, 1971. Stability constants of metal-ion complexes. Special publication nr 25. Supplement nr 1 to Special Publication nr 17. The Chemical Society, Burlington House, W1V OBN.

Silva R.J, Bidoglio G, Rand M.H, Robouch P.B, Wanner H, Puigdomènech I, 1995. Chemical Thermodynamics Vol.2. Chemical Thermodynamics of Americium. NEA. Elsevier.

Siu K.W.M, Berman S.S, 1989. The marine environment. *in* Occurrence and Distribution of Selenium (M. Ihnat, Ed.). CRC Press, Boca Raton, pp 263-293.

Smedley P.L, 1991. The geochemistry or rare earth elements in groundwater from the Carnmenellis area, southwest England. Geochimica et Cosmochimica Acta 55, 2767-2779.

Smellie J, Cramer J, Mac.Kenzie A, 1994. Mineralogy and Lithogeochemistry: Geochemical and isotopic features of the host sandstones and clay halo. *in* Final Report of SKB/AECL Cigar Lake Analog Study (J.J. Cramer and J.A.T. Smellie, Eds.). SKB-(AECL). TR 94-04 (10851).

Spahiu K. and Bruno J, 1995. A selected thermodynamic database for REE to be used in HLNW performance assessment exercises. SKB Technical Report TR 95-35.

Spalding R.F, DrulinerA.D, Whitside L.S, Struempler A.W, 1984. Uranium geochemistry in groundwater from Tertiary sediments. Geochimica et Cosmochimica Acta 48, 2679-2692.

SR 95, 1995. Template for safety reports with descriptive example. SKB Technical Report TR 96-05.

Stroes-Gascoyne S, 1992. Trends in the short-term release of fission products and actinides to aqueous solution from used CANDU fuels at elevated temperatures. Journal of Nuclear Materials 190, 87.

Stumm W, Morgan J.J, 1996. Aquatic chemistry: chemical equilibria and rates in natural waters. New York. John Wiley & Sons.

Sturchio N.C, Bohlke J.K, Markun F.J, 1993. Radium isotope geochemistry of thermal waters, Yellowstone National park, USA. Geochimica et Cosmochimica Acta 57, 1203-1214.

Suter D, 1991. Chemistry of the redox sensitive elements; Literature review. NTB 91-32.

Sverjensky D.A, 1984. Europium redox equilibria in aqueous solution. Earth and Planetary Science Letters 67, 70-78.

Tait J.C, Stroes-Gascoyne S, Hocking W.H, Duclos A.M, Porth R.J, Wilkin D.L, 1991. Dissolution Behavior of used CANDU fuel under disposal conditions. Scientific Basis for Nuclear Waste Management XIV, 212, 189.

Turner D.R, Whitfield M, Dickson A.G, 1981. The equilibrium speciation of dissolved components in freshwater and seawater at 25°C and 1 atm pressure. Geochimica et Cosmochimica Acta 45, 855-881.

Velde B, 1988. Experimental pseudomorphism of talc and serpentine in (Ni, Mg)Cl_2 aqueous solutions. Geochimica et Cosmochimica Acta 52, 415-424.

Wanner H, Wersin P, Sierro N, 1992. Thermodynamic modelling of bentonite-groundwater interaction and implications for near field chemistry in a repository for spent fuel. SKB 92-37.

Weast R.C, Ed, 1975. Handbook of Geochemistry and Physics. Cleveland, CRC-Press Inc.

Wedepohl K.H, 1978. Handbook of Geochemistry II-3. Springer-Verlag, Berlin.

Werme L.O, Forsyth R. S, 1989. The SKB spent fuel corrosion programme. Status report 1988. SKB Technical Report TR 89-14.

Whitfield M, Turner D.R, 1987. The role of particles in regulating the composition of seawater. *in* Aquatic Surface Chemistry: Chemical Processes at the Particle-Water Interface (W. Stumm, Ed.). New York. J. Wiley and sons. Environmental Science and Technology.

Wilson C.N, 1990a. Results from NNWSI series 2 bare fuel dissolution tests. Pacific Northwest Laboratory, Report PNL-7169, UC-802.

Wilson C.N, 1990b. Results from NNWSI series 3 spent fuel dissolution tests. Pacific Northwest Laboratory, Report PNL-7170, UC-802.

Wilson C.N, 1991. Results from long-term dissolution tests using oxidized spent fuel. Scientific Basis for Nuclear Waste Management XIV, 212, 197.

Wilson C.N, Bruton C.J, 1989. Am. Cream. Soc. Annual Meeting, Indianapolis, Indiana.

Wilson C.N, Shaw H.F, 1987. Experimental study of the dissolution of spent fuel at 85°C in natural groundwater. Mater. Res. Soc. Symp. Proceedings MRS Vol. , 84, 123.

Wolery T.J, 1992. EQ3NR, A computer program for geochemical aqueous speciation-solubility calculations: Theoretical manual, user's guide, and related documentation (Version 7.0). LLNL.

Wollenberg H.A, 1975. Radioactivity of geothermal systems. In Second U.N. Symposium on the Development and Use of Geothermal Resources, San Francisco, Lawrence Berkeley Laboratory, University of California, 1283-1292.

Zielinski R.A, Bloch S, Walker T.R, 1983. The mobility and distribution of heavy metals during the formation of first cycle red beds. Econ.Geol. 78, 1574-1589.

Zukin J.G, Hammond D.E, Ku T-L, Elders W.A, 1987. Uranium-thorium series radionuclides in brines and reservoir rocks from two deep geothermal boreholes in the Salton Sea geothermal field, southeastern California. Geochimica et Cosmochimica Acta 51, 2719-2731.

List of SKB reports

Annual Reports

1977-78
TR 121
KBS Technical Reports 1 – 120
Summaries
Stockholm, May 1979

1979
TR 79-28
The KBS Annual Report 1979
KBS Technical Reports 79-01 – 79-27
Summaries
Stockholm, March 1980

1980
TR 80-26
The KBS Annual Report 1980
KBS Technical Reports 80-01 – 80-25
Summaries
Stockholm, March 1981

1981
TR 81-17
The KBS Annual Report 1981
KBS Technical Reports 81-01 – 81-16
Summaries
Stockholm, April 1982

1982
TR 82-28
The KBS Annual Report 1982
KBS Technical Reports 82-01 – 82-27
Summaries
Stockholm, July 1983

1983
TR 83-77
The KBS Annual Report 1983
KBS Technical Reports 83-01 – 83-76
Summaries
Stockholm, June 1984

1984
TR 85-01
Annual Research and Development Report 1984
Including Summaries of Technical Reports Issued during 1984. (Technical Reports 84-01 – 84-19)
Stockholm, June 1985

1985
TR 85-20
Annual Research and Development Report 1985
Including Summaries of Technical Reports Issued during 1985. (Technical Reports 85-01 – 85-19)
Stockholm, May 1986

1986
TR 86-31
SKB Annual Report 1986
Including Summaries of Technical Reports Issued during 1986
Stockholm, May 1987

1987
TR 87-33
SKB Annual Report 1987
Including Summaries of Technical Reports Issued during 1987
Stockholm, May 1988

1988
TR 88-32
SKB Annual Report 1988
Including Summaries of Technical Reports Issued during 1988
Stockholm, May 1989

1989
TR 89-40
SKB Annual Report 1989
Including Summaries of Technical Reports Issued during 1989
Stockholm, May 1990

1990
TR 90-46
SKB Annual Report 1990
Including Summaries of Technical Reports Issued during 1990
Stockholm, May 1991

1991
TR 91-64
SKB Annual Report 1991
Including Summaries of Technical Reports Issued during 1991
Stockholm, April 1992

1992
TR 92-46
SKB Annual Report 1992
Including Summaries of Technical Reports Issued during 1992
Stockholm, May 1993

1993
TR 93-34
SKB Annual Report 1993
Including Summaries of Technical Reports Issued during 1993
Stockholm, May 1994

1994

TR 94-33

SKB Annual Report 1994

Including Summaries of Technical Reports Issued during 1994

Stockholm, May 1995

1995

TR 95-37

SKB Annual Report 1995

Including Summaries of Technical Reports Issued during 1995

Stockholm, May 1996

1996

TR 96-25

SKB Annual Report 1996

Including Summaries of Technical Reports Issued during 1996

Stockholm, May 1997

List of SKB Technical Reports 1997

TR 97-01

Retention mechanisms and the flow wetted surface – implications for safety analysis

Mark Elert

Kemakta Konsult AB

February 1997

TR 97-02

Äspö HRL – Geoscientific evaluation 1997/1. Overview of site characterization 1986–1995

Roy Stanfors[1], Mikael Erlström[2], Ingemar Markström[3]

[1] RS Consulting, Lund

[2] SGU, Lund

[3] Sydkraft Konsult, Malmö

March 1997

TR 97-03

Äspö HRL – Geoscientific evaluation 1997/2. Results from pre-investigations and detailed site characterization. Summary report

Ingvar Rhén (ed.)[1], Göran Bäckblom (ed.)[2], Gunnar Gustafson[3], Roy Stanfors[4], Peter Wikberg[2]

[1] VBB Viak, Göteborg

[2] SKB, Stockholm

[3] VBB Viak/CTH, Göteborg

[4] RS Consulting, Lund

May 1997

TR 97-04

Äspö HRL – Geoscientific evaluation 1997/3. Results from pre-investigations and detailed site characterization. Comparison of predictions and observations. Geology and mechanical stability

Roy Stanfors[1], Pär Olsson[2], Håkan Stille[3]

[1] RS Consulting, Lund

[2] Skanska, Stockholm

[3] KTH, Stockholm

May 1997

TR 97-05

Äspö HRL – Geoscientific evaluation 1997/4. Results from pre-investigations and detailed site characterization. Comparison of predictions and observations. Hydrogeology, groundwater chemistry and transport of solutes

Ingvar Rhén[1], Gunnar Gustafson[2], Peter Wikberg[3]

[1] VBB Viak, Göteborg

[2] VBB Viak/CTH, Göteborg

[3] SKB, Stockholm

June 1997

TR 97-06

Äspö HRL – Geoscientific evaluation 1997/5. Models based on site characterization 1986–1995

Ingvar Rhén (ed.)[1], Gunnar Gustafson[2], Roy Stanfors[3], Peter Wikberg[4]

[1] VBB Viak, Göteborg

[2] VBB Viak/CTH, Göteborg

[3] RS Consulting, Lund

[4] SKB, Stockholm

October 1997

TR 97-07

A methodology to estimate earthquake effects on fractures intersecting canister holes

Paul La Pointe, Peter Wallmann, Andrew Thomas, Sven Follin

Golder Associates Inc.

March 1997

TR 97-08

Äspö Hard Rock Laboratory Annual Report 1996

SKB

April 1997

TR 97-09

A regional analysis of groundwater flow and salinity distribution in the Äspö area

Urban Svensson

Computer-aided Fluid Engineering AB

May 1997

TR 97-10
On the flow of groundwater in closed tunnels. Generic hydrogeological modelling of nuclear waste repository, SFL 3–5
Johan G Holmén
Uppsala University/Golder Associates AB
June 1997

TR 97-11
Analysis of radioactive corrosion test specimens by means of ICP-MS. Comparison with earlier methods
R S Forsyth
Forsyth Consulting
July 1997

TR 97-12
Diffusion and sorption properties of radionuclides in compacted bentonite
Ji-Wei Yu, Ivars Neretnieks
Dept. of Chemical Engineering and Technology, Chemical Engineering, Royal Institute of Technology, Stockholm, Sweden
July 1997

TR 97-13
Spent nuclear fuel – how dangerous is it? A report from the project "Description of risk"
Allan Hedin
Swedish Nuclear Fuel and Waste Management Co,
Stockholm, Sweden
March 1997

TR 97-14
Water exchange estimates derived from forcing for the hydraulically coupled basins surrounding Äspö island and adjacent coastal water
Anders Engqvist
A & I Engqvist Konsult HB, Vaxholm, Sweden
August 1997

TR 97-15
Dissolution studies of synthetic soddyite and uranophane
Ignasi Casas[1], Isabel Pérez[1], Elena Torrero[1], Jordi Bruno[2], Esther Cera[2], Lara Duro[2]
[1] Dept. of Chemical Engineering, UPC
[2] QuantiSci SL
September 1997

TR 97-16
Groundwater flow through a natural fracture. Flow experiments and numerical modelling
Erik Larsson
Dept. of Geology, Chalmers University of Technology, Göteborg, Sweden
September 1997

TR 97-17
A site scale analysis of groundwater flow and salinity distribution in the Äspö area
Urban Svensson
Computer-aided Fluid Engineering AB
October 1997

TR 97-18
Release of segregated nuclides from spent fuel
L H Johnson, J C Tait
AECL, Whiteshell Laboratories, Pinawa, Manitoba, Canada
October 1997

TR 97-19
Assessment of a spent fuel disposal canister. Assessment studies for a copper canister with cast steel inner component
Alex E Bond, Andrew R Hoch, Gareth D Jones, Aleks J Tomczyk, Richard M Wiggin, William J Worraker
AEA Technology, Harwell, UK
May 1997

TR 97-20
Diffusion data in granite Recommended values
Yvonne Ohlsson, Ivars Neretnieks
Department of Chemical Engineering and Technology, Chemical Engineering, Royal Institute of Technology, Stockholm, Sweden
October 1997

TR 97-21
Investigation of the large scale regional hydrogeological situation at Ceberg
Anders Boghammar[1], Bertil Grundfelt[1], Lee Hartley[2]
[1] Kemakta Konsult AB, Sweden
[2] AEA Technology, UK
November 1997

TR 97-22
Investigations of subterranean microorganisms and their importance for performance assessment of radioactive waste disposal. Results and conclusions achieved during the period 1995 to 1997
Karsten Pedersen
Göteborg University, Institute of Cell and Molecular Biology, Dept. of General and Marine Microbiology, Göteborg, Sweden
November 1997

TR 97-23
Summary of hydrogeologic conditions at Aberg, Beberg and Ceberg
Douglas Walker[1], Ingvar Rhén[2], Ioana Gurban[1]
[1] INTERA KB
[2] VBB Viak
October 1997

TR 97-24
Characterization of the excavation disturbance caused by boring of the experimental full scale deposition holes in the Research Tunnel at Olkiluoto
Jorma Autio
Saanio & Riekkola Oy, Helsinki, Finland
September 1997

TR 97-25
The SKB Spent Fuel Corrosion Programme.
An evaluation of results from the experimental programme performed in the Studsvik Hot Cell Laboratory
Roy Forsyth
Forsyth Consulting
December 1997

TR 97-26
Thermoelastic stress due to a rectangular heat source in a semi-infinite medium. Application for the KBS-3 repository
Thomas Probert, Johan Claesson
Depts. of Mathematical Physics and Building Physics, Lund University, Sweden
April 1997

TR 97-27
Temperature field due to time-dependent heat sources in a large rectangular grid. Application for the KBS-3 repository
Thomas Probert, Johan Claesson
Depts. of Mathematical Physics and Building Physics, Lund University, Sweden
April 1997

TR 97-28
A mathematical model of past, present and future shore level displacement in Fennoscandia
Tore Påsse
Sveriges geologiska undersökning, Göteborg
Sweden
December 1997

TR 97-29
Regional characterization of hydraulic properties of rock using well test data
David Wladis, Patrik Jönsson, Thomas Wallroth
Department of Geology, Chalmers University of Technology, Göteborg, Sweden
November 1997

TR 97-30
ZEDEX - A study of damage and disturbance from tunnel excavation by blasting and tunnel boring
Simon Emsley[1], Olle Olsson[2], Leif Stenberg[2], Hans-Joachim Alheid[3], Stephen Falls[4]
[1] Golder Associates, Maidenhead, United Kingdom
[2] Swedish Nuclear Fuel and Waste Management Co., Figeholm, Sweden
[3] Federal Institute for Geosciences and Natural Resources, Hannover, Germany
[4] Queens University, Kingston, Ontario, Canada
December 1997

TR 97-31
Bentonite swelling pressure in strong NaCl solutions. Correlation between model calculations and experimentally determined data
Ola Karnland
Clay Technology, Lund, Sweden
December 1997

TR 97-32
Cement / bentonite interaction. Results from 16 month laboratory tests
Ola Karnland
Clay Technology AB, Lund, Sweden
December 1997